SLCO Influx Transporters and Variability in the Disposition of Antiretroviral Drugs

Thesis submitted in accordance with the requirements of the University of Liverpool for the degree of Doctor of Philosophy

By

Wai San Kwan

June 2009

I declare that this thesis is the result of my own work. The material contained within the thesis has not been presented, either wholly or in part, for any other degree or qualification.

Wai San Kwan

This research was carried out in the

Liverpool HIV Pharmacology Group

Department of Pharmacology and Therapeutics

The University of Liverpool, UK

Table of Contents

Acknowledgements

There are many people, without whom this PhD thesis would not have been possible. Firstly, I would like to thank my supervisors Drs. Andrew Owen, Saye Khoo and Professor David Back for giving me the opportunity to study for this PhD, and for their guidance and continual support during my project. I would like to thank Dr. Owen in particular for organising collaborations for the oocyte work to take place, and for his patience reading this thesis. I am grateful to, and would like to thank my sponsor, Tibotec, who funded the project and Janssen-Cilag for the opportunity to visit their site.

I would like to thank Dr. Becky Chandler for teaching me about the fundamentals of drug transporter research, and Dr. Ruben Hartkoorn for his help during our venture into cloning. I would also like to thank Deidre Egan, Dr. Neill Liptrott, Kirsty Leake and the rest of the Liverpool HIV Pharmacology Group who provided me with useful scientific advice and interesting lunchtime conversations. I would also like to thank the Molecular and Biochemical Parasitology group at Liverpool School of Tropical Medicine for accommodating me in the office and in the lab, particularly Dr. Salcedo-Sora for his invaluable knowledge in oocyte manipulation. I am also grateful to Susan Beveridge and Darren Moss, who helped me on several occasions with regards to the oocyte work.

I am grateful to my family, who have been very encouraging towards my work, and also the Jeffs family, who have been very kind to me during my time on the Wirral. Lastly, I want to thank Aron, who offered a shoulder to cry on when things didn't go so well, but was also the person who shared my achievements when things did go well.

Abbreviations list

AAG	α_1-acid-glycoprotein
ABC	ATP-binding cassette family
ADME	aborption, distribution, metabolism and excretion
AIDS	Acquired immunodeficiency syndrome
BSA	bovine serum albumin
CA	capsid protein
CAR	cellular accumulation ratio
CAR	constitutive androstane receptor
cDNA	complementary DNA
(m, μ, n) Ci	(milli, micro, nano) curies
CO_2	carbon dioxide
CYP	cytochrome P450
DAPY	diarylpyridine
DMEM	Dulbecco's modified Eagles medium
DMSO	dimethyl sulphoxide
DNA	deoxyribonucleic acid
dNTP	deoxynucleoside triphosphate
dpm	decays per minute
DRV	darunavir
E3S	estrone-3-sulphate
EDTA	ethylenediaminetetraacetic acid
EFV	efavirenz
FDA	Food and Drugs Administration (US)
FITC	fluorescein isothiocynate
FCS	foetal calf serum

FXR	farnesoid X receptor
GAPDH	glyceraldehyde 3-phosphate dehydrogenase
(m, μ, n, p) g	(milli, micro, nano, pico) grams
gp	glycoprotein
h	hour
HAART	highly active antiretroviral therapy
HBSS	Hank's balanced salt solution
HIV	human immunodeficiency virus
HSA	human serum albumin
Hsp	heat shock protein
IN	integrase
(m, μ, n) l	(milli, micro, nano) litres
LB	Luria broth
LPV	lopinavir
(m, μ, n) M	(milli, micro, nano) molar
MA	matrix protein
$MgCl_2$	magnesium chloride
mins	minutes
(m, μ, n, p) mol	(milli, micro, nano, pico) moles
mRNA	messenger RNA
MTT	3-(4,5-Dimethylthiazol-2-yl)-2,5-diphenyltetrazolium bromide
NC	nucleocapsid protein
NNRTI	non-nucleoside reverse transcriptase inhibitor
NR	nuclear receptor
NRTI	nucleoside reverse transcriptase inhibitor
NVP	nevirapine
PBMC	peripheral blood mononuclear cell

PBS	phosphate buffered saline
PCR	polymerase chain reaction
PE	phycoerythrin
PGE2	prostaglandin E2
PI	protease inhibitor
PS	penicillin and streptomycin
PXR	pregnane X receptor
RNA	ribonucleic acid
RNAi	RNA interference
rpm	revolutions per minute
RT	reverse transcriptase
RXR	retinoid X receptor
s	seconds
s.d.	standard deviation
SDS	sodium lauryl sulphate
siRNA	small interfering RNA
SLC	solute carrier family
SLCO	solute carrier organic anion transporting family
SNP	single nucleotide polymorphism
SOC	super optimal broth with catabolite repression
SQV	saquinavir
TBE	tris-borate EDTA
TDM	therapeutic drug monitoring

Publications

Hartkoorn R*, **Kwan W***, Shallcross V, Chaikan A, Liptrott N, Egan D, Salcedo-Sora J, Gibbons S, Bray P, Back D, Khoo S, Owen A. "HIV protease inhibitors are substrates for SLCO1A2, SLCO1B1 and SLCO1B3 and lopinavir plasma concentrations are influenced by the SLCO1B1 polymorphisms" (in submission)

Kwan W, Janneh O, Hartkoorn R, Chandler B, Khoo S, Back D, Owen A (2009). "Intracellular 'boosting' of darunavir using known transport inhibitors in primary PBMC", Br J Clin Pharmacol (in press)

*Joint first authors

Communications

Kwan W, Moss D, Hartkoorn R, Salcedo E, Bray P, Khoo S, Back D, Owen A. Determining the substrate specificity of SLCO1B3 for antiretroviral drugs using a *X. laevis* model. BPS Winter Meeting 2008, Brighton, UK, 16-18th December 2008

Kwan W, Hartkoorn R, Salcedo E, Bray P, Khoo S, Back D, Owen A. Determining the substrate specificities of SLCO1A2 and SLCO1B1 for antiretroviral drugs. 9th International Workshop on Clinical Pharmacology of HIV Therapy, New Orleans, USA, 7-9th April 2008

Shallcross V, Hartkoorn R, Egan D, **Kwan W**, Khoo S, Back D, Owen A. Influence of SLCO1B1 521T>C polymorphism on lopinavir plasma concentrations from the Liverpool TDM registry. 9th International Workshop on Clinical Pharmacology of HIV Therapy, New Orleans, USA, 7-9th April 2008

Kwan W, Hartkoorn R, Salcedo E, Khoo S, Back D, Owen A. Determining the substrate specificity of SLCO1A2 for antiretroviral drugs using a *X. laevis* model. BPS Winter Meeting 2007, Brighton, UK, 17-18th December 2007

Kwan W, Hartkoorn R, Khoo S, Back D, Owen A. Assessing transport of anti-retroviral drugs by OATP transporters using a Xenopus *laevis* oocyte expression system. DMDG Open Meeting 2007, Cambridge, UK, 17-19th September 2007

Kwan W, Chandler B, Holmes R, Hoetelmans R, Sekar V, Owen A, Khoo S, Back D. Influence of drug efflux transporters on cellular accumulation of darunavir (TMC114). 7th International Workshop on Clinical Pharmacology of HIV Therapy, Lisbon, Portugal, 20-22nd April 2008

Chandler B, Holmes R, Janneh O, **Kwan W**, Owen A, Khoo S, Back D. Interactions between efavirenz and cellular efflux transporters. AIDS 2006 - XVI International AIDS Conference, Toronto, Canada, 13-18th August 2006

Abstract

There are many factors which contribute to the clinical outcome of antiretroviral therapy, including inter- and intra-individual variability in pharmacokinetics and drug-drug interactions. Drug transporters and metabolism enzymes are known to influence pharmacokinetics of many xenobiotics and hence the role of drug transporters, both efflux and influx, on intracellular accumulation in different *in vitro* models was explored. Further, the impact of polymorphisms in SLCO transporters on the pharmacokinetics of the protease inhibitor (PI) lopinavir was observed.

Using the CEM and MDCKII cell line models darunavir, a PI, was a substrate of ABCB1, whilst rilpivirine, a non-nucleoside reverse transcriptase inhibitor (NNRTI), was not a substrate of ABCB1, but intracellular accumulation was influenced by the presence of human serum albumin (HSA).

To assess antiretrovirals as potential substrates for SLCO transporters, these transporters were first isolated and cloned, followed by subcloning into an expression vector for use in the X. *laevis* model. Using this model, PIs were identified as substrates for SLCO1A2, 1B1 and 1B3; whereas, of the NNRTIs, only rilpivirine was a substrate in the absence of HSA.

Single nucleotide polymorphisms (SNPs) in SLCO transporters were determined in the Liverpool therapeutic drug monitoring (TDM) cohort to observe associations with plasma concentration. Of the SNPs tested, SLCO1B1 521T>C was significantly associated with an increase in plasma concentrations of lopinavir. Other factors such as weight and co-administered PI were also significantly associated with lopinavir plasma concentrations.

To determine whether knockdown of individual transporters would impact on the cellular transport of SLCO1A2, SLCO1B1, SLCO1B3 and SLCO3A1 against basal levels of expression of various other transporters, SLCOs were knocked-down using siRNA; however, due to the low levels of expression of SLCOs in cell lines, the results were inconclusive.

Antiretrovirals have been characterised for efflux transporters, particularly ABCB1, but with the recent identification of SLCOs, many xenobiotics have yet to be characterised for these transporters. This thesis has found PIs to be substrates for SLCOs and has implicated a role for these transporters in the variability of plasma concentrations seen in a HIV+ population.

Chapter 1

General Introduction

1. Introduction

1.1 HIV epidemiology

The human immunodeficiency virus (HIV) was first characterised over twenty years ago (Barre-Sinoussi *et al.* 1983) and is a major epidemic in the world today. HIV is a complex retrovirus, part of the family Retroviridae and the lentivirus genus, with two distinct strains, HIV-1 and HIV-2 (Clavel *et al.* 1986). HIV-1 has a high transmission rate and high virulence and is an epidemic around the world. HIV-2 is localised to West Africa and has a lower transmission rate and lower virulence than HIV-1 (Berry *et al.* 1998). HIV is transmitted by contact with body fluids from infected to uninfected individuals. Transmission occurs by sexual contact, contaminated blood or equipment (Jaffe *et al.* 1983), from mother to child during pregnancy (Sprecher *et al.* 1986) and breast feeding (Thiry *et al.* 1985). It can remain asymptomatic for many years, making infection management difficult.

In 2007, UNAIDS reported an estimate of 33 million people world-wide living with HIV, with around 2.7 million people being newly infected with the virus. It is affecting both developed and developing countries, but 22 million people infected with HIV live in Sub-Saharan Africa (www.unaids.org). HIV infections progress to acquired immunodeficiency syndrome (AIDS) and leads to an increased risk of opportunistic infections and subsequent mortality. With the increasing treatments available for people infected with HIV, we are now dealing with a chronic disease in the West, with people living longer, having fewer opportunistic infections and the time taken for progression to AIDS being increased (Lee *et al.* 2001; Wong *et al.* 2004).

1.2 Structure and genome of HIV

HIV-1 is a spherical virus containing two copies of single stranded, positive sense RNA enclosed in a conical capsid composed of 2000 copies of the capsid protein, p24. The RNA is bound in a complex with the nucleocapsid proteins, p7 and essential enzymes for viral replication and development, reverse transcriptase (RT) and integrase (IN). This core structure is surrounded by a matrix consisting of viral protein, p17 and a viral envelope containing phospholipids obtained during viral budding from the host cell and viral glycoproteins, transmembrane envelope protein (gp41, TM) and surface envelope protein (gp120, SU) (Freed 2001). The structure of the virus is illustrated in Fig. 1.

The HIV genome encodes 9 genes, of which 3 are structural and 6 are regulatory (also called "accessory" or "auxillery") proteins (Fig. 2). The 3 structural genes are polymerase (*Pol*), group-specific antigen (*Gag*) and envelop glycoproteins (*Env*) and the 6 regulatory genes are viral infectivity factor (*Vif*), viral protein R (*Vpr*), viral protein U (*Vpu*), negative factor (*Nef*), trans-activator of transcription (*Tat*) and regulator of virion (*Rev*). Cleavage of *Pol* produces protease (PR), RT and IN, whereas *Gag* produces matrix proteins (MA), capsid proteins (CA), nucleocapsid proteins (NC) and p6 and is performed by viral PR. *Env* is processed by host cellular machinery in the Golgi apparatus and in the endoplastic reticulum to produce gp120 and gp41. The regulatory genes are important as they increase the infectivity of the virus and co-ordinate the progression of the virus life cycle, the assembly and release of the virus, but they are not required for virus replication (Freed 2001; Seelamgari *et al.* 2004).

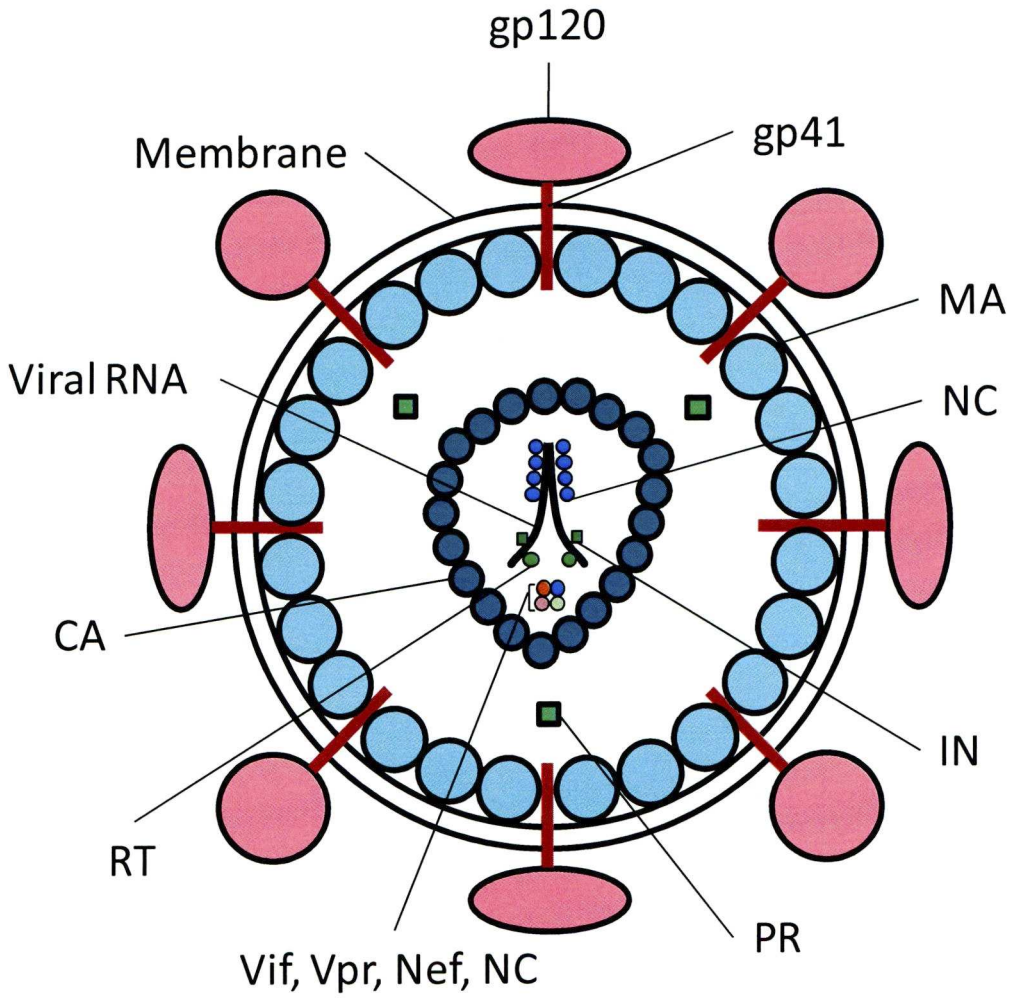

gp120:	glycoprotein 120
gp41:	glycoprotein 41
MA:	viral matrix
NC:	nucleocapsid (p7)
IN:	integrase
PR:	protease
Vif:	viral infectivity factor
Vpr:	viral protein r
Nef:	negative factor
RT:	reverse transcriptase
CA:	capsid

Fig. 1. Diagrammatic representation of the structure of a HIV-1 virion (modified from Robinson, 2002).

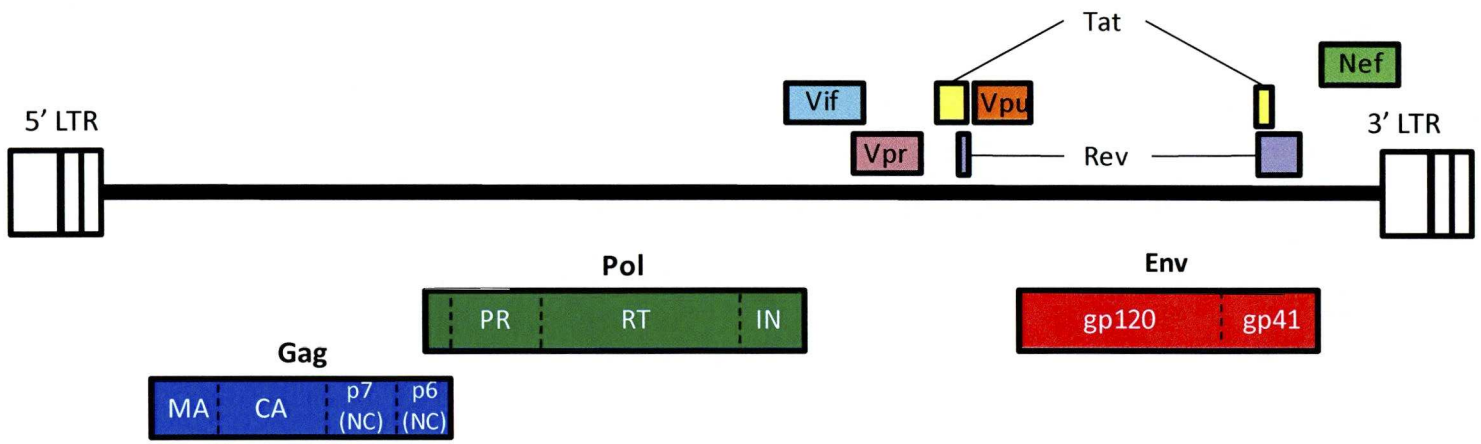

Fig. 2. Organisation of the HIV-1 genome (modified from Bansal, 2008)

1.3 The HIV life cycle

HIV-1 targets circulating CD4+ T cells and macrophages for replication. The virion enters the host cell by utilising glycoprotein gp120, found on the viral envelope as gp41/gp120 trimers, to bind co-receptors CCR5 or CXCR4 on the cell membrane. Following co-receptor binding, gp120 dissociates from gp41, changing the conformation of gp41 to allow fusion of the viral envelope with the cell membrane (Wain-Hobson 1996; Berger *et al.* 1999; Seelamgari *et al.* 2004). This releases the viral core into the host cell cytoplasm where uncoating of the viral core and dissociation of the MA proteins occurs. Meanwhile, reverse transcription of single stranded viral RNA to linear, double stranded viral DNA is achieved by using HIV-1 RT (Freed 2001). Following transcription, the viral DNA forms pre-integration complexes (PICs), which are imported into the nucleus. Nuclear transport enables HIV-1 to infect non-dividing cells, a characteristic of the lentivirus genus. Viral integrase primarily processes the viral DNA and the host DNA to allow integration of viral DNA into the host genome (Gallay *et al.* 1997) and also facilitates nuclear import of pro-viral DNA (Hearps and Jans 2006).

HIV-1 is transcribed using host transcription factors and viral Tat protein. The Tat protein recruits transcription factors to the transcription activation responsive element region (TAR) to form the Tat/TAR complex, which is essential for HIV-1 transcription. The newly transcribed HIV-1 mRNA is spliced by host cellular splicing machinery and produces Tat, Rev and Nef proteins. When the amount of Rev produced reaches a threshold, HIV-1 mRNA production shifts from being multiply spliced to singly spliced and unspliced transcripts. Rev binds to the rev response element found in the singly

spliced and unspliced mRNA and exports the transcripts into the cytoplasm for translation of viral proteins (Nielsen *et al.* 2005).

Singly spliced transcripts produce Env, Vif, Vpr and Vpu proteins, whereas unspliced transcripts produce Gag and Gag-Pol proteins and contain the viral genome. The viral genome is packaged and undergoes virus budding, regulated by Vpu and Vif. Vpu mediates the release of the virus at the cell membrane and the release of Env from the endoplasmic reticulum and allows further processing of Env into gp41 and gp120 (Freed 2001; Seelamgari *et al.* 2004). Vif mediates the processing of Gag by PR and also prevents APOBEC3G (apolipoprotein B mRNA-editing enzyme, catalytic polypeptide-like 3G) from deaminating its DNA:RNA hybrids and interfering with Pol (Sheehy *et al.* 2002). Vpr arrests the cell cycle prior to cell division and Nef downregulates host CD4. Gag is cleaved by PR to produce CA, MA and NC particles, which are assembled in the cell membrane. Following budding, the virus undergoes maturation where Gag-Pol is cleaved by PR and produces IN, RT and PR. After maturation, the virus is ready to infect (Freed 2001).

1.4 Viral tropism

There are two tropic strains of HIV-1, CCR5 (R5) and CXCR4 (X4), depending on which co-receptor they utilise for cell entry; some viruses are dual tropic (R5X4), which can utilise either co-receptor (Berger *et al.* 1999). Other human receptors have been shown to be utilised to a lesser extent by HIV, but R5 and X4 receptor usage is by all strains of HIV (Berger *et al.* 1999). The majority of primary infections are by R5 tropic strains with the more virulent X4 tropic strains appearing later in disease progression (Philpott 2003). Individuals who are homozygous for the CCR5 Δ32 genotype express a non-functional, truncated version of CCR5 and are immune from R5 tropic strains (Samson *et al.* 1996). The discovery of the effect of the CCR5 Δ32 genotype on susceptibility of viral infection with no detriments to health supported the development of CCR5 antagonists (Este and Telenti 2007).

1.5 Antiretroviral therapy

There are several classes of drugs used to treat HIV-1, each targeting a different part of the virus life cycle (illustrated in Fig. 3). CCR5 antagonists prevent the virus binding to the CCR5 co-receptors and inhibit entry of the virus into the host cell (Dorr *et al.* 2005), whereas fusion inhibitors inhibit viral gp41 to prevent fusion of the viral envelope with the host cell membrane (Wild *et al.* 1994; Liu *et al.* 2005). Due to tropism in HIV, CCR5 inhibitors are not effective against X4 tropic viruses (Dorr *et al.* 2005) and tropism profiling is recommended prior to commencing CCR5 inhibitors. Non-nucleoside reverse transcriptase inhibitors (NNRTIs) act by inhibiting reverse

transcriptase, whilst nucleoside and nucleotide reverse transcriptase inhibitors (NRTIs, NtRTI) mimic endogenous DNA bases and terminate reverse transcription by binding to the active site of RT (Nielsen *et al.* 2005). Integrase inhibitors prevent the integration of the viral DNA to host DNA and the specific mechanism of action of raltegravir is by strand transfer inhibition (Summa *et al.* 2008). Protease inhibitors (PIs) with the exception of tipranavir (Poveda 2008) are peptidomimetic compounds, which block HIV-1 protease cleavage of Gag and Gag-Pol, disrupting viral assembly (Nielsen *et al.* 2005). The antiretrovirals that are approved and are currently in use in the UK are listed in Table 1. The molecular structures of antiretrovirals which are commonly used in antiretroviral therapy or used in subsequent chapters are illustrated in Fig. 4.

Highly active antiretroviral therapy (HAART) is the standard for administering antiretrovirals, as it has demonstrated good virologic and immunologic response (Autran *et al.* 1997; Chen *et al.* 2007). However, recent studies have found that patients with HIV suppression to <50 copies/ml for at least 6 months can be treated with a simplified regimen (for example monotherapy consisting of boosted lopinavir) and experience no viral rebound (Pulido *et al.* 2008; Bierman *et al.* 2009). All PIs, except nelfinavir, are boosted with low dose ritonavir to increase their half life and bioavailability (Gazzard 2008). This boosting effect was first demonstrated using saquinavir (Merry *et al.* 1997) and was shown to also be effective for boosting of other PIs, such as lopinavir (Kempf *et al.* 1997; von Hentig 2007). For first line therapy in the UK, efavirenz is administered with an optimised background of two NRTIs and for second line therapy, boosted lopinavir, boosted fosamprenavir, boosted atazanavir or boosted saquinavir with two NRTIs is recommended. Nevirapine is used with two NRTIs for patients with

neuropsychological problems or for female patients who wish to become pregnant (Gazzard 2008). For heavily experienced patients with poor virologic response to therapy, boosted darunavir, etravirine, raltegravir or maraviroc with two NRTIs may be used (Gazzard 2008).

Apart from the regimens within HAART, clinicians are also faced with the dilemmas of prescribing concomitant drugs used to treat opportunistic infections which occur in some HIV patients, such as hepatitis (Gazzard 2008), tuberculosis (Moreno *et al.* 2006) and malaria (Skinner-Adams *et al.* 2008). These drugs may have interactions with the drugs used in HAART as many share, induce and/or repress transporters and metabolism enzymes in their absorption and elimination pathways. Rifampicin, an anti-tuberculosis drug, is an example of an inducer of CYP3A4 and increases the metabolism of PIs boosted with ritonavir, resulting in a loss of virologic response and increased risk of emergence of viral mutation (Moreno *et al.* 2006). Similarly, the administration of some drugs which require clearance by CYP3A4 (e.g. some antihistamines, sedatives) with boosted lopinavir has been contraindicated by the U.S. Food and Drugs Administration (FDA) due to competitive inhibition by ritonavir and lopinavir (Qazi *et al.* 2002).

New drugs are also being developed against other viral targets. One example is bevirimat, which is a maturation inhibitor, and acts by binding viral Gag protein to prevent cleavage by protease, thus disrupting the production of viral CA and other structural proteins. Bevirimat is currently in clinical trials to establish its long term efficacy and tolerability (Martin *et al.* 2008). New drugs against existing drug targets such as rilpivirne (NNRTI) and apricitabine (NRTI) are also in development to overcome viruses resistant to current classes of antiretrovirals (De Clercq 2008).

Table 1. List of antiretrovirals licensed for use in the UK.

Reverse transcriptase inhibitors		**Protease inhibitors**	**Entry/Fusion inhibitors**	**Intergrase inhibitors**
Nucleoside/Nucleotide	**Non-nucleoside**			
Zidovudine (ZDV)	Efavirenz (EFV)	Ritonavir (RTV)	Enfuvirtide (T-20)	Raltegravir (RAL)
Lamivudine (3TC)	Nevirapine (NVP)	Saquinavir (SQV)	Maraviroc (MVC)	
Didanosine (ddI)	Etravirine (ETR)	Lopinavir (LPV)		
Stavudine (d4T)		Indinavir (IDV)		
Abacavir (ABC)		Amprenavir (APV)		
Tenofovir (TFV)		Fosamprenavir (FPV)		
Emtricitabine (FTC)		Nelfinavir (NFV)		
		Atazanavir (ATZ)		
		Tipranavir (TPV)		
		Darunavir (DRV)		

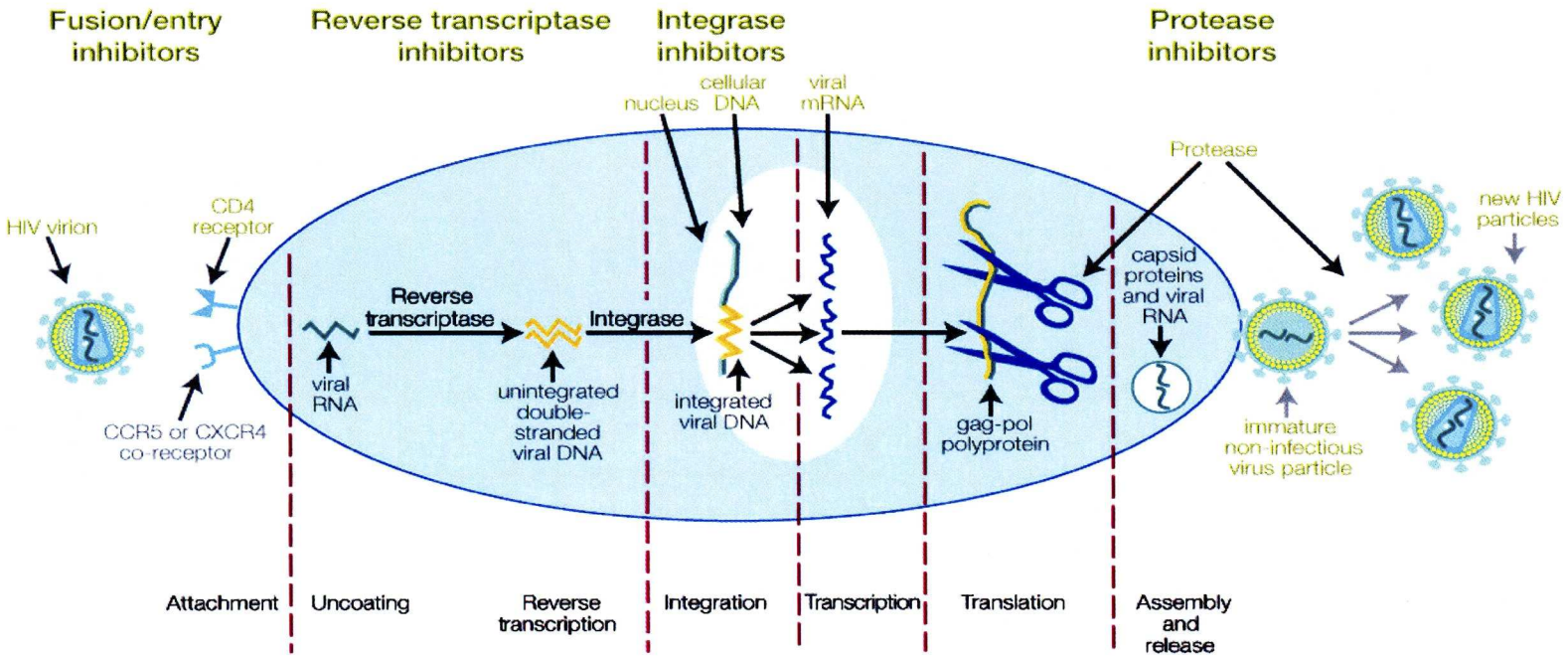

Fig. 3. Site of action of the anti-retroviral drug classes

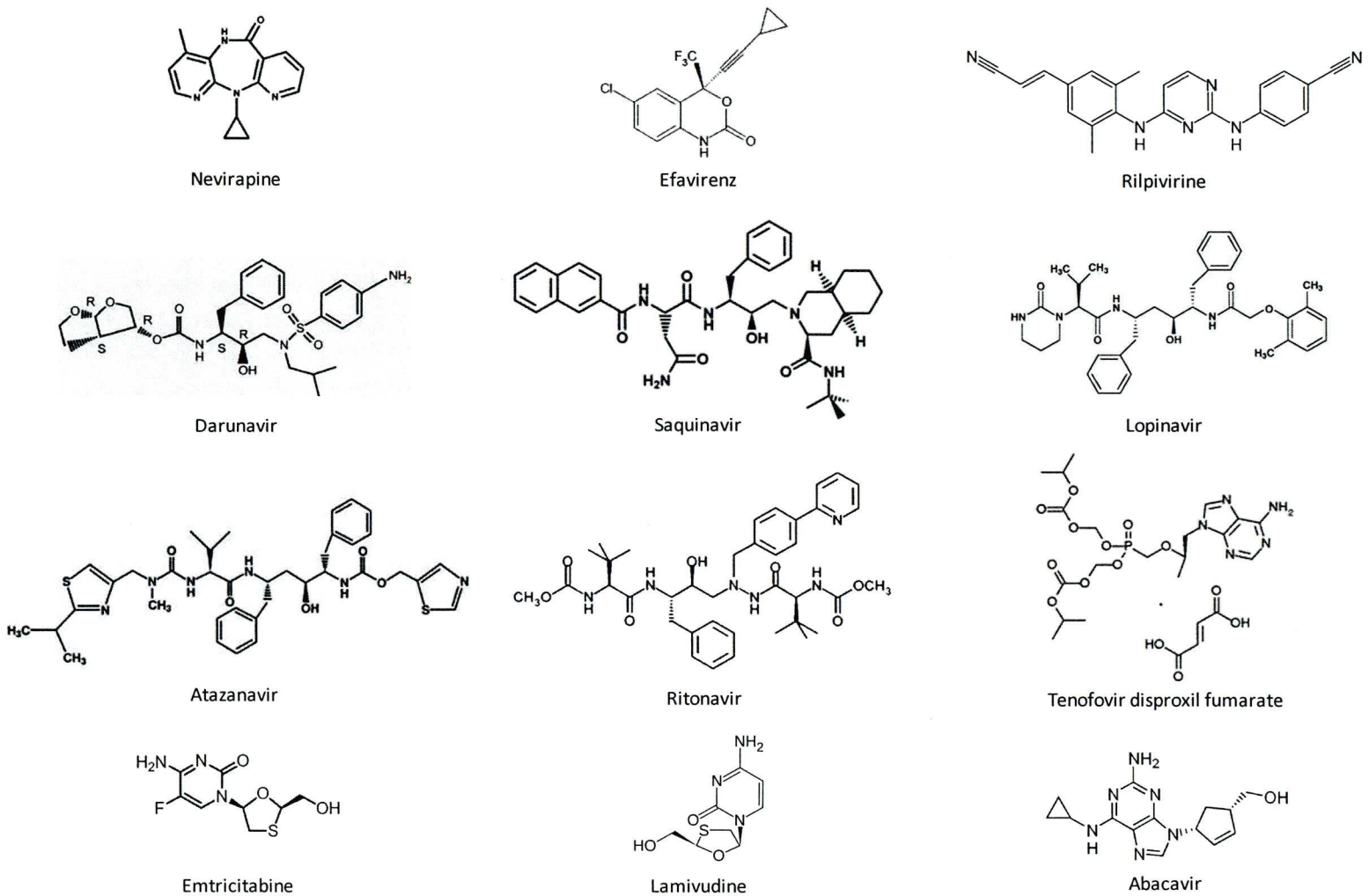

Fig. 4. Structure of commonly prescribed and experimental antiretrovirals

1.6 Therapeutic failure

Failure of therapy can be defined by virologic, immunologic or clinical failure. Virologic failure is defined during treatment as consistent elevations of more than 50 copies/ml of HIV RNA (Hammer *et al.* 2008). Immunologic failure is when CD4 cell counts fall to below 350 cells/μl after 48 weeks of treatment (Gazzard 2008). Clinical failure is a reoccurrence of an opportunistic infection after more than 3 months of therapy (WHO 2007). In patients who are treatment experienced, reaching maximum suppression but not to undetectable levels with clinical and immunological stability is generally acceptable for not changing therapy. Decisions to change regimens are usually based on viral load response (Kalkut 2005).

1.6.1 Viral Resistance

Infected individuals often have a large number of quasispecies, which all differ by a few nucleotides. HIV has a rapid mutation rate due to its use of RNA as its hereditary genetic material, a lack of proof-reading mechanisms in the virus replication pathway and a high genetic recombination rate, which allows it to evade the host immune system and acquire resistance to antiretrovirals (Coffin 1995; Freed 2001).

Viral resistance may occur when the therapeutic concentration of a drug inside host cells is not achieved or maintained. This may be due to pharmacological factors such as active transport of a drug out of cells by drug transporters, which causes low concentrations of the drug at the site of action (Jones *et al.* 2001), or poor patient adherence to drug regimens leading to lowered concentrations of drugs in plasma (hence less inside the

cells) (Groschel *et al.* 1997). If therapeutic concentrations are not maintained, then viral replication may not be suppressed. This creates a selection pressure for drug resistant viruses to dominate the HIV-1 population in the host and render the drug regimen ineffective (Coffin 1995; Wang *et al.* 2000). Another barrier to effective therapy is the existence of anatomical sanctuary sites such as in the central nervous system and the genital tract, and also in cellular sanctuary sites such as CD4 cells and macrophages, where low levels of HIV-1 replication occur and therapeutic drug concentrations are difficult to maintain (Hoetelmans 1998; Geeraert *et al.* 2008).

The difficulty in the eradication of HIV-1 is the viral reservoirs. These reservoirs contain fit, wildtype viruses as well as drug-resistant quasi-species. Viral persistence is mainly caused by infected latent memory CD4+ cells, which have HIV-1 DNA integrated within the host genome, but do not undergo replication or HIV-1 gene expression until re-activation of the host cell, and are not affected by HAART in its latent state (Siliciano *et al.* 2003; Geeraert *et al.* 2008).

Certain antiretroviral regimens have been reserved for patients harbouring HIV-1 with mutations, for example darunavir and etravirine for their potency against HIV-1 strains resistant to first line PIs and NNRTIs respectively. Antiretrovirals in new classes have also been used for experienced patients, for example maraviroc, enfuvirtide and raltegravir because they do not confer cross class resistance and are effective against PI and NNRTI resistant strains (Gazzard 2008). Increasing the doses of the drugs has also been used to treat resistant viruses, but this can also lead to increased risk of drug toxicity and adverse reactions.

1.6.2 Adverse reactions

Adverse effects are common for antiretroviral drugs and are the main reason for discontinuation of a drug regimen and for lack of adherence in patients (Chesney 2000; Applebaum *et al.* 2009). The antiretrovirals are generally well tolerated, but there are a number of adverse effects. These effects vary from mild symptoms such as headaches and fatigue to moderate symptoms such as vomiting and diarrhoea to severe or fatal symptoms such as abacavir hypersensitivity (Staszewski *et al.* 1998; Calmy *et al.* 2007) and lipodystrophy for regimens containing boosted PIs (Carr *et al.* 1998; Calmy *et al.* 2007; Caron *et al.* 2009).

Efavirenz has been associated with neurological related adverse effects (Arendt *et al.* 2007); however, the extent of the adverse reactions varies amongst patients, with a greater number of adverse events and more severe neurotoxicity reported in Black-African patients (Stohr *et al.* 2008). Efavirenz is also not recommended for women who wish to become pregnant as it has been linked to increased incidence of birth defects (Saitoh *et al.* 2005).

Nevirapine is often used as an alternative for efavirenz, especially for patients with a history of neuropsychological disorders (Gazzard 2008); however, patients receiving nevirapine also have a higher risk of idiosyncratic hepatotoxicity compared to patients receiving efavirenz or commonly used boosted PI regimens (Sulkowski *et al.* 2000; Rivero *et al.* 2007).

New antiretroviral drugs are now designed to have better tolerance, better efficacy and fewer incidents of adverse reactions. Research on the pharmacokinetic boosting

compound, GS 9350, which has no metabolic toxicity, adverse effects or antiviral activity, is ongoing by Gilead. This has the potential to replace ritonavir, which often causes poor tolerance in PI containing regimens (Gilead Sciences 2009).

1.7 Drug absorption and distribution

There are many factors which can affect the pharmacokinetics of a drug and determine its efficacy. The bioavailability of an orally administered drug is subject to absorption in the gut and first pass metabolism, which influences the drug concentration in systemic blood circulation and subsequent distribution (Riviere and Papich 2009). The distribution of drug in different tissues is determined by tissue permability, blood flow, perfusion rate, pH and protein binding (Riviere and Papich 2009). Most cells are able to metabolise xenobiotics, but the liver has a major role in the metabolism of a drug. Following metabolism, the drug is excreted via the bile canaliculus or by renal clearance (Riviere and Papich 2009). Renal clearance is affected by glomerular filtration, secretion from the peritubular capillaries to the nephron and reabsorption from the nephron back to the peritubular capillaries (Riviere and Papich 2009).

Intracellular drug concentrations have an impact on the ability of a drug to suppress HIV and may therefore influence the development of resistance and disease progression (Chandler *et al.* 2007). The physiochemical properties of a drug and the overall metabolism and transport of a drug are the main pharmacological factors which can affect intracellular drug concentrations. Intracellular drug accumulation at the site of action, such as CD4 cells and macrophages, affects viral replication. This is different to

intracellular concentrations in organs such as the liver, intestines and kidneys, which influences drug disposition from a whole body perspective. Drug metabolism and transport act in concert to remove toxic endogenous and foreign compounds and this is reflected by their co-ordinated regulation through similar nuclear receptor pathways.

1.7.1 Protein binding

The majority of antiretrovirals are taken orally and are absorbed into the systemic blood circulation via epithelial intestinal cells. There are many plasma serum proteins in systemic blood, including albumin, acid glycoproteins, globulin and lipoproteins. Protein binding of xenobiotics can lower concentrations of unbound (active) drug in systemic blood circulation and in organs (Boffito *et al.* 2003). This can also reduce the accumulation of drugs at their site of action and hence lower their activity (Bilello *et al.* 1996). Antiretrovirals have been shown to bind to plasma proteins with PIs showing generally higher affinities for α1-acid-glycoprotein (AAG) (Bilello *et al.* 1996) and NNRTIs for human serum albumin (HSA) (Boffito *et al.* 2003). HSA is the most abundant plasma protein with efavirenz more than 99% bound and nevirapine more than 60% bound to HSA (Boffito *et al.* 2003). AAG was found to reduce the intracellular concentrations and hence, antiviral activity of saquinavir, ritonavir and indinavir *in vitro* (Jones *et al.* 2001). When bound to plasma proteins, drugs cannot penetrate cell membranes by passive diffusion, but can be transported by active efflux (Boffito *et al.* 2003).

1.7.1 Drug metabolism

Drug metabolism is an enzymatic process involving the biochemical modification of drugs into their metabolites. Some drugs require metabolism to become bio-activated, whereas others are inactivated after metabolism. Metabolism is classified into two types of reactions, phase I and phase II, and the primary objective is to metabolise the compounds into metabolites which are easier to excrete by drug transport or passive permeation (Beers 2006). Phase I may involve oxidation, reduction, hydrolysis, cyclisation or decyclisation and is performed by a range of enzymes including cytochome P450s (CYPs), alcohol dehydrogenase and esterases (Batt *et al.*1994; Beers 2006). Phase II are conjugative reactions such as glucuronidation, glutathione conjugation and sulphation, usually on the metabolites of phase I reactions and are performed by enzymes such as UDP-glucuronosyltransferases (UGTs), glutathione S-transferases (GSTs) and sulfotransferases (Batt *et al.*1994; Danielson 2002; Beers 2006).

CYPs are membrane bound haemoproteins found in mitochondria or the endoplasmic reticulum of cells and perform oxidative reactions (Danielson 2002). These are the main enzymes which are responsible for metabolism of xenobiotic compounds and are expressed in various tissues, but are highly expressed in hepatocytes and enterocytes, i.e. the main sites for drug metabolism (Guengerich *et al.* 1986; Kolars *et al.* 1992). Of the CYP family the main subfamilies of pharmacological interest are CYP1, CYP2, CYP3 and CYP4 (Ferraro and Buono 2005).

Similar to other xenobiotics, antiretrovirals are substrates for metabolic enzymes. For example, the PIs are extensively metabolised by CYP3A4 enzyme (Pal and Mitra 2006).

PIs are commonly co-administered with ritonavir, which is a potent inhibitor of CYP3A4. Inhibition of CYP3A4 increases the half life of the PIs in the body and is required to maintain the therapeutic concentrations of these compounds (Gazzard 2008). Other enzymes important in the metabolism of antiretrovirals include CYP2B6, which metabolises efavirenz (Ward *et al.* 2003) and nevirapine (Erickson *et al.* 1999); UGT1A1, which metabolises raltegravir (Kassahun *et al.* 2007); and CYP2C9, CYP2C18 and CYP2C19, which metabolise etravirine (Seminari *et al.* 2008). The metabolites of the compounds then move out of cells by active transport or passive permeation and are excreted.

1.7.2 Drug transport

Drug transporter proteins modulate the distribution and movement of various drugs and their metabolites by influencing absorption or excretion. Drug transporters impact on the bioavailability and also intracellular drug concentrations of compounds which are substrates (Hoggard and Owen 2003). Drug transporters are broadly classified into two groups, the ATP-binding cassette (ABC) family of efflux transporters and the solute carrier (SLC) family of influx transporters.

The ABC family of transporters are involved in the efflux of endogenous and exogenous compounds and require ATP for active transport. There are currently 48 ABC proteins identified, which are divided into 7 subfamilies (Toyoda *et al.* 2008).

ABCB1 (P-glycoprotein, P-gp) is an extensively researched transporter protein, and was identified due to its ability to cause multi-drug resistance in cancer cells (Juliano and

Ling 1976). It was subsequently found to have broad substrate specificity, transporting various endogenous compounds such as bilirubin, lipids and steroids, and also xenobiotics including anti-cancer, antibiotics and PIs (Janneh *et al.* 2007; Sharom 2008). ABCB1 has a wide tissue distribution from the brain to the liver and the genital tract. It is a 170kDa protein located in cell membranes and is encoded by *ABCB1* (also known as multidrug resistance protein 1, *MDR1*).

ABCB1 expressed in the intestine and liver can affect the bioavailability of substrate drugs by efflux into the gut lumen and bile respectively. ABCB1 at the blood-brain and blood-testes barrier has been shown to reduce drug penetration into these sites (Cordon-Cardo *et al.* 1989), which may allow reservoirs for viral replication to establish (see section 1.6.1). At the cellular level, ABCB1 expression has been demonstrated in lymphocyte subsets including natural killer cells, CD8 and CD4+ cells (Ford *et al.* 2003). Here, drug efflux may serve to decrease drug concentrations at sites vital for the control of HIV replication. ABCB1 shares some substrate specificity with CYP3A4 and many PIs have been found to be substrates of ABCB1 and CYP3A4, suggesting a synergistic effect between metabolism and transport to remove the compound from the body. ABCB1 also shares substrate specificity with the ABCC proteins (multidrug resistance proteins, MRP), which are also efflux transporters (Toyoda *et al.* 2008).

To date, the ABCC subfamily consists of 12 proteins (ABCC1-12), including the cystic fibrosis transmembrane conductance regulator (CFTR, ABCC7) and sulfonylurea receptors (SUR1, ABCC8 and SUR2, ABCC9). They vary in tissue distribution but often share substrate specificity between themselves and with other members of the ABC family (Toyoda *et al.* 2008). ABCC1 (multidrug resistance associated protein 1,

MRP1) has been shown to be expressed ubiquitously, whereas ABCC2 (multidrug resistance associated protein 2, MRP2) is predominantly expressed in liver and kidney cells (Bleasby *et al.* 2006). Of the ABCCs, ABCC1, ABCC2 and ABCG2 (breast cancer resistance protein 1, BCRP1) are more robustly characterised and some PIs are substrates (Huisman *et al.* 2002; Janneh *et al.* 2005; Weiss *et al.* 2007).

Currently, there are 359 influx transporters identified in humans and they are classified under the SLC family of transporters. The SLC subfamilies are described in Table 2. Currently 48 subfamilies have been identified, with the main subfamilies transporting xenobiotics being organic anion transporting polypeptides (OATP; SLC21, SLCO), organic anion and cation transporters (OAT, OCT, OCTN; SLC22), and proton oligopetide co-transporter (PEPT; SLC11) (Koepsell *et al.* 2007; Nigam *et al.* 2007; Hagenbuch and Gui 2008; Sala-Rabanal *et al.* 2008). They vary in tissue distribution and substrate specificity.

Many xenobiotics are substrates of the SLC/SLCOs, including statins, anticancer and antibiotic drugs. SLC22 proteins are mostly expressed in the brain, kidneys and the gastrointestinal tract, and are important in the transport of xenobiotic compounds (Koepsell *et al.* 2007; Nigam *et al.* 2007). SLC15 proteins are expressed in the gastrointestinal tract, at the blood-brain barrier and in glands (Bleasby *et al.* 2006). Antibiotics and antivirals are substrates for this subfamily of proteins and their ability to transport compounds is pH dependent (Sala-Rabanal *et al.* 2008). The SLCOs subfamily has 12 members with varied tissue expression and is listed in Table 3. They are of particular pharmacological interest as they have been identified as transporters of various xenobiotics such as statins (Kopplow *et al.* 2005), anticancer agents (Abe *et al.*

1999), antibiotics (Tamai *et al.* 2000) and antiretrovirals (Su *et al.* 2004). Saquinavir is a substrate of SLCO1A2 (SLC21A3) (Su *et al.* 2004). Aside from the potential ability to manipulate these transporters to enhance drug delivery, some transporters have also been exploited as drug targets, such as glucose transporters (SLC5), neurotransmitter transporters (SLC6), intestinal bile acid transporters (SLC10) and cation-Cl cotransporters (SLC12). Dapagliflozin, an inhibitor of SLC5A2 (SGLT2), was recently developed and is currently undergoing Phase IIb trials to prevent reabsorption of glucose for the treatment of diabetes mellitus (Komoroski *et al.* 2009). SLC6 and SLC12 have been identified as targets for the treatment of neurological and psychiatric diseases, with many commercially available anti-depressants being potent inhibitors of SLC6 transporters (Gether *et al.* 2006; Kahle *et al.* 2008). SLC10 inhibitors have been developed for cholesterol lowering therapy (Geyer *et al.* 2006).

Research into the SLC/SLCO family is rapidly increasing, with more transporters being identified and roles for the better characterised proteins becoming clearer; however, the role of many influx transporters on intracellular drug accumulation and the affect on plasma concentrations of antiretrovirals has not yet been characterised.

Table 2. List of currently approved solute carrier transport families by the HUGO nomenclature committee (modified from an original review by Hediger *et al.* 2002).

HUGO nomenclature	**Solute carrier families**	**Number of members**
SLC 1	High-affinity glutamine and neutral amino acid family	7
SLC2	Facultative GLUT transporter family	14
SLC3	Heavy subunits of the heteromeric amino acid transporter family	2
SLC4	Bicarbonate transporter family	10
SLC5	Sodium glucose cotransporter family	12
SLC6	Sodium- and chloride-dependent neurotransmitter transporter family	19
SLC7	Cationic amino acid transporter/glycoprotein associated amino acid transporter family	14
SLC8	Na^{+}/Ca^{2+} exchanger family	3
SLC9	$Na^{+/}H^{+}$ exchanger family	11
SLC10	Sodium bile salt cotransporter family	7
SLC11	Proton coupled metal ion transporter family	2
SLC12	Electroneutral cation-Cl cotransporter family	9
SLC13	Human Na^{+}-sulphate/carboxylate cotransporter family	5
SLC14	Urea transport family	2
SLC15	Proton oligopeptide cotransporter family	5
SLC16	Monocarboxylate transporter family	14
SLC17	Vesicular glutamate transporter family	8
SLC18	Vesicular amine transporter family	3
SLC19	Folate/thiamine transporter family	3
SLC20	Type-III Na^{+}-phosphate costransporter family	2
SLC21/SLCO	Organic anion transporting family	10
SLC22	Organic cation/anion/zwitterions transporter family	22
SLC23	Na^{+}-dependent ascorbic acid transporter family	4
SLC24	$Na^{+}/(Ca^{2+}$ -$K^{+})$ exchanger family	6
SLC25	Mitochondrial carrier family	43
SLC26	Multifunctional anion exchanger family	11
SLC27	Fatty acid transport protein family	6
SLC28	Na^{+} -coupled nucleoside transport family	3
SLC29	Facultative nucleoside transporter family	4
SLC30	Zinc efflux family	10
SLC31	Copper transporter family	2
SLC32	Vesicular inhibitory amino acid transporter family	1
SLC34	Type-II Na^{+} -phosphate cotransporter family	3

HUGO nomenclature	Solute carrier families	Number of members
SLC35	Nucleoside-sugar transporter family	**23**
SLC36	Proton-coupled amino acid transporter family	**4**
SLC37	Sugar-phosphate/phosphate exchanger family	**4**
SLC38	System A and N, sodium-coupled neutral amino acid transporter family	**11**
SLC39	Metal ion transporter family	**14**
SLC40	Basolateral iron transporter family	**1**
SLC41	MgtE-like magnesium transporter family	**3**
SLC42	Rh ammonium transporter family	**3**
SLC43	Na+ -independent, system-L-like amino acid transporter family	**3**
SLC44	Choline-like transporter	**5**
SLC45	Putative sugar transporter	**4**
SLC46	Heme carrier transporter	**3**
SLC47	Multidrug and toxin extrusion	**2**
SLC48	Heme transporter	**1**

Table 3. The tissue distribution and known substrates of SLCO transporters

Gene symbol	Pseudonym	Endogenous substrates	Xenobiotic substrates	Tissue distribution
SLCO1A2	OATP-A	Bile salts, prostaglandin E2	Fexofenadine	Brain, liver, kidney, lung
SLCO2B1	OATP-B	Prostaglandin E2	Pravastatin	Brain,
SLCO1B1	OATP-C, OATP-2, LST-1	Bilirubin, bile salts, estrone-3-sulphate	Methotrexate, rifampicin, pravastatin	Liver
SLCO1B3	OATP-8, LST-2	Bilirubin, bile salts, estrone-3-sulphate	Methotrexate, rifampicin, digoxin,	Liver
SLCO3A1	OATP-D	Prostaglandins	Benzylpenicillin	Ubiquitous
SLCO4A1	OATP-E	Taurocholate, prostaglandins	?	Lung, muscle
SLCO1C1	OATP-F	Thyroid hormones	?	Brain, testis
SLCO4C1	OATP-H	cAMP	Methotrexate, digoxin	Kidney, liver
SLCO6A1	OATP-I	?	?	Testis
SLCO5A1	OATP-J	?	?	Thymus
SLCO2A1	PGT	Protaglandins, thromboxane	?	Lung

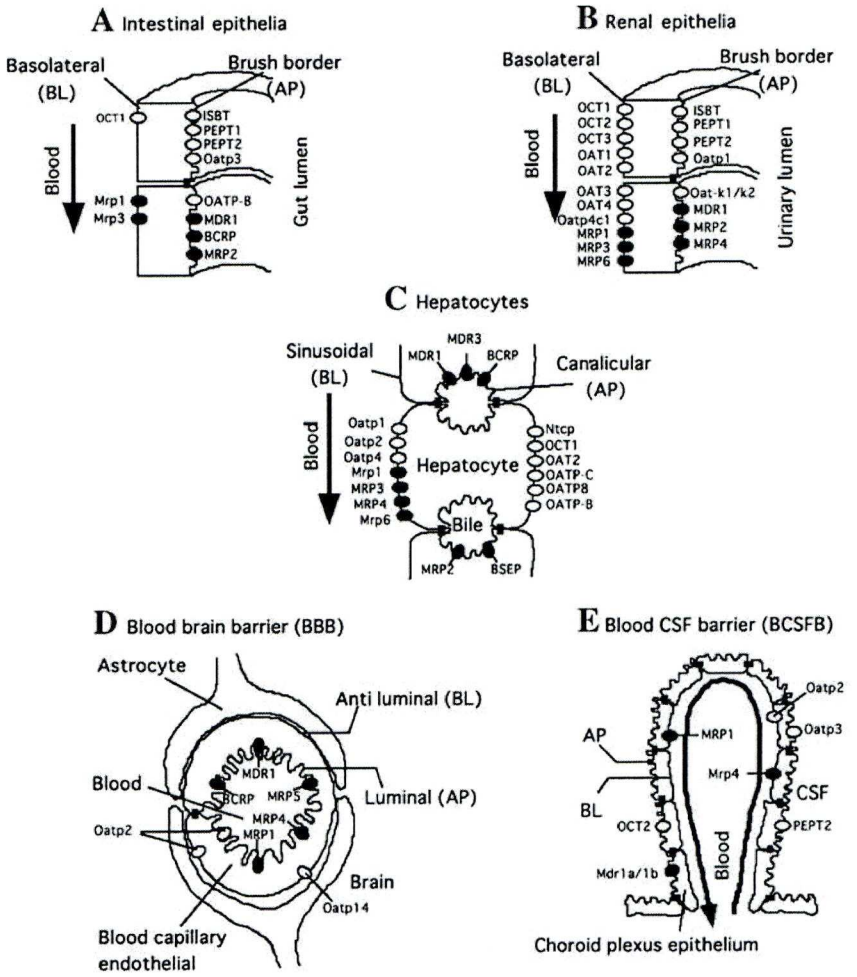

Fig. 3. Distribution and cellular localization of drug transporters in polarized tissues. Intestinal epithelia (A), renal epithelia (B), hepatocytes (C), blood-brain barrier (D), blood-CSF barrier (E) are shown. These tissues are composed of polarized epithelial or endothelial cells with a tight junction structure to limit passive diffusion. Selective expression of particular transporter molecules on the apical or basolateral side determine the net transport of compounds across these monolayers. ABC transporters are indicated by closed circles (modified from Ito et al. 2005).

1.8 Regulation of expression of drug metabolism and transport

The discovery of xenobiotic activated nuclear hormone receptors (NRs) has greatly increased understanding of the regulation of expression of drug metabolism enzymes and transporter proteins. Apart from xenobiotics, NRs can be activated by numerous endogenous compounds such as vitamins, non steroidal hormones and bile salts (Lew *et al.* 2004; Pascussi *et al.* 2008). The activation of NRs triggers a cascade of up- and down-regulation of proteins involved in metabolism and transport to eliminate toxic compounds from the body (Kakizaki *et al.* 2008). When bound to ligands, conformational changes in the nuclear receptors occur and they bind directly to DNA and recruit co-regulators to up-regulate or repress nearby genes. The ability of the NRs to bind DNA classifies them as transcription factors. The NR family is divided by amino acid sequence homology, into 7 subfamilies. Within the NR subfamily 1, the pregame X receptor (PXR, *NR1I2*), the constitutive androstane receptor (CAR, *NR1I3*) and the farnesoid X receptor (FXR, *NR1H4*) have been relatively well characterised and are of pharmacological interest as they are important receptors involved in the regulation of metabolism and transport of xenobiotic compounds (Eloranta *et al.* 2005; Urquhart *et al.* 2007).

The general pathway of activation for NRs within subfamily 1, with the exception of PXR which starts in the nucleus, starts in the cytoplasm as illustrated in Fig. 4. CAR is constitutively active in the absence of a ligand, which is unusual for NRs. CAR is located in the cytoplasm, where it is bound to molecular chaperones and upon activation, disassociates from the chaperones and translocates to the nucleus. NRs can be activated by forming a ligand with a wide variety of endogenous and xenobiotic compounds,

which enter through the cell membrane by passive diffusion or active transport. In the nucleus, histone deacetylase complexes dissociate from the CAR, allowing recruitment of histone acetylases to open up the nucleosome structure to allow access to the DNA and target genes. The ligand-NR forms either a homodimer or a heterodimer with retinoid X receptor (RXR). PXR is located in the nucleus and in the absence of a ligand, is bound to co-repressors. When activated, PXR forms a heterodimer with RXR. The heterodimer complexes bind response elements in promoter and enhancer sections of DNA and upregulate adjacent genes (Urquhart *et al.* 2007).

PXR and CAR have been reported to up-regulate the expression of CYP2B6, CYP3A4, ABCB1, ABCC2 and UGT1A1. FXR has been shown to regulate SLCO1B3 and also CYP3A4 and ABCC2 (Lim and Huang 2008). PXR has also been reported to regulate SLCO1A2 (Meyer zu Schwabedissen *et al.* 2008). Rifampicin and St. John's Wort are examples of xenobiotic activators of PXR and have been shown to induce expression of proteins regulated by PXR, whereas phenobarbital and some statins activate CAR (Kobayashi *et al.* 2005; Lim and Huang 2008). Bile salts are the main activators of FXR (Lim and Huang 2008).

The nuclear receptors share ligands and can auto-regulate as well as regulate each other, as there is a complex cross-talk between their pathways (Lew *et al.* 2004; Pascussi *et al.* 2008). The interplay between metabolism, transporters and their regulators, the nuclear receptors, may cause complex drug-drug interactions (Seden *et al.* 2009, Zhang *et al.* 2006) and alter the pharmacokinetic and pharmacodynamic profiles of drugs, hence treatment with antiretrovirals should be preceded with caution if a patient has been prescribed other drugs or is consuming herbal remedies.

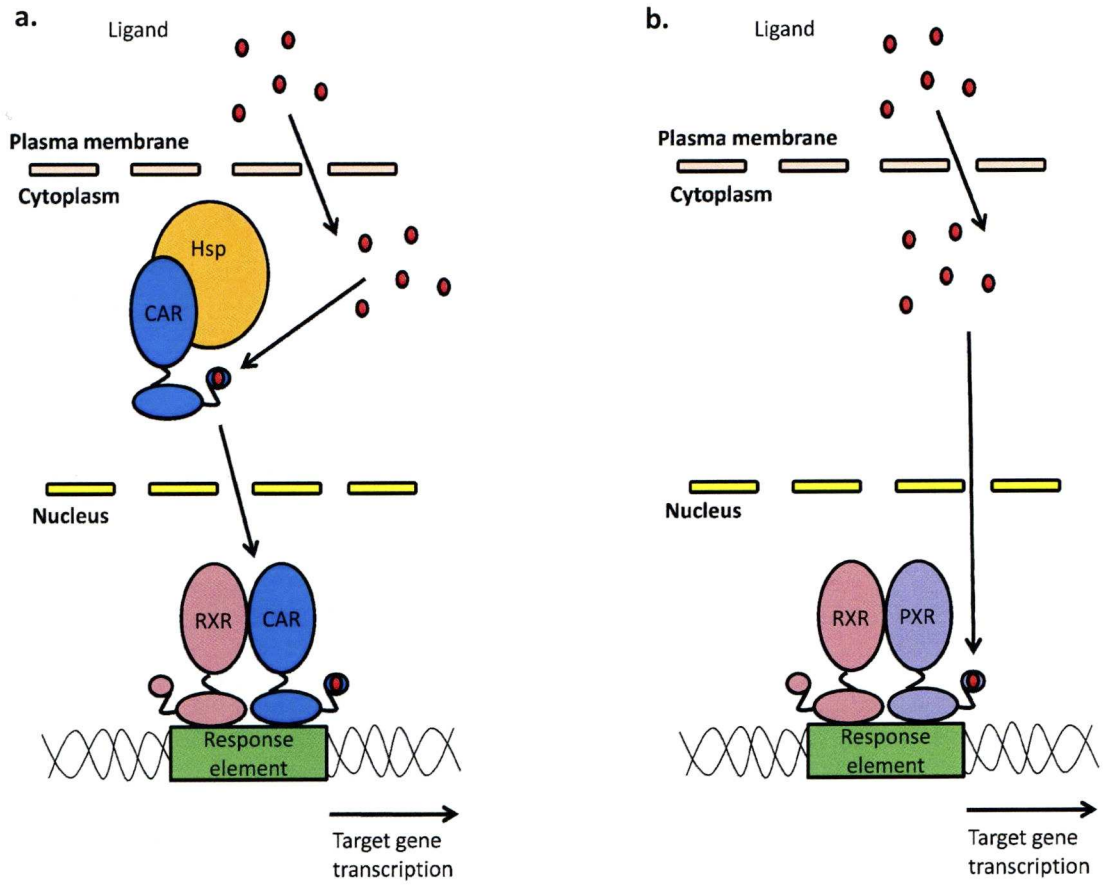

Fig.4. A diagrammatic representation of nuclear receptor activation. Ligands enter the cell by passive diffusion or active transport. **a.** In the cytoplasm, ligands can bind to CAR, causing a conformational change and dissociation from its chaperone (Hsp, heat shock protein). CAR is translocated to the nucleus where it can form a heterodimer with RXR. **b.** Passive diffusion of ligands into the nucleus allows binding of ligands by PXR. PXR forms a heterodimer with RXR.

.

1.9 The influence of pharmacogenetics on antiretroviral therapy

Pharmacogenetics is the study of the effects of genetic polymorphisms on drug response. The main areas of pharmacogenetics include drug metabolism and transporter genes, which have been studied to observe their impact on drug concentrations, and also genes that influence drug safety.

The strongest association in pharmacogenetics related to antiretrovirals is the *HLA-B*5701* genotype and abacavir hypersensitivity (Mallal *et al.* 2002). This has led to testing of patients for the *HLA-B*5701* genotype prior to commencing a regimen containing abacavir and has subsequently lowered the incidence of abacavir hypersensitivity (Mallal *et al.* 2008).

In metabolism, numerous single nucleotide polymorphisms (SNP) and haplotypes have been identified in *CYP2B6*. G516T (rs3745274) and T1459C (rs3211371) were originally described by Lang *et al.* (2001) who saw an association between the presence of these SNPs and reduced hepatic expression and activity of *CYP2B6*. The association between G516T and protein expression and activity was not significant in that study due to the small sample size. However, a study by Haas *et al.* (2005) found significantly higher plasma efavirenz concentrations in homozygotes for the TT genotype, but no change in immunologic or virologic response. T983C (rs28399499) has been more recently described and studies have shown an association between this SNP and increased neurotoxicity in patients administered efavirenz (Wyen *et al.* 2008). The frequency of this genotype is as high as 7.5% among Black-African ethnicities but the allele has not been found in Caucasian populations (Mehlotra *et al.* 2007).

Several *ABCB1* genotypes have been documented and 3 SNPs were noted to be in linkage disequilibrium and may have an effect on protein expression: C1236T (rs1128503), G2677T/A (rs2032582), and C3435T (rs1045642) (Chinn and Kroetz 2007). Of these SNPs, G2677T and C3435T have been more extensively studied, but associations between reduced protein expression and these SNPs individually, as well as these SNPs in conjunction, has yielded conflicting results (Hoffmeyer *et al.* 2000; Kim *et al.* 2001; Sakaeda *et al.* 2003). Associations between increased plasma concentrations and better immunologic response of nelfinavir – an ABCB1 substrate – with *ABCB1* C3435T have also been documented (Fellay *et al.* 2002). However, the associations remain controversial, with some research groups finding no change in drug plasma concentrations of saquinavir, also a ABCB1 substrate (la Porte *et al.* 2007). The unusual aspect of this genotype is that it is a silent mutation, one that does not lead to a change in the amino acid sequence. It has been theorised that this SNP may be in linkage disequilibrium with a functional mutation, or that the silent mutation alters the splicing or the frequency of the splice site of the *ABCB1* gene, thereby altering the amount of functional ABCB1 present on the cell membrane (Kimchi-Sarfaty *et al.* 2007). An additional complication is the inhibitory effect of ritonavir, and since many PIs are co-administered with ritonavir, the effects of SNPs in ABCB1 may be masked.

In peripheral blood mononuclear cells (PBMCs) from healthy volunteers, CXCR4 has been shown to correlate with *ABCB1* mRNA expression and co-localise with ABCB1 in the cell membrane (Owen *et al.* 2004; Chandler *et al.* 2007). This study also found that the *ABCB1* C3435T genotype influences the expression of ABCB1 as well as CXCR4, with CC homozygotes expressing more ABCB1 than CT heterozygotes and TT

homozygotes. The correlation between CXCR4 expression with ABCB1 expression was also observed in a study involving PBMCs from HIV positive patients (Chandler *et al.* 2007). This positive correlation suggests that ABCB1 and CXCR4 are regulated by an overlapping pathway; although, the specific links between the regulations of the two genes have yet to be identified. The implication of this association is that X4 tropic strains may also have increased protection against antiretrovirals with the increased P-gp leading to increased efflux of drug out of the lymphocytes and thereby lowering the intracellular drug concentration below therapeutic levels.

Recently, an association between unboosted atazanavir and the *NR1I2* C63396T (rs2472677) SNP was found (Siccardi *et al.* 2008). TT homozygotes had significantly lower atazanavir trough plasma concentrations than CC homozygotes or CT heterozygotes. This suggests that polymorphisms in *NR1I2* may alter its ability to regulate target genes, including ones which may alter atazanavir concentrations such as metabolising enzymes and transporters. In this study, atazanavir was not administered with ritonavir, which may be the reason for a clearer association than studies examining SNPs with individuals on boosted PI regimens.

For any given drug regimen, there is a large inter-patient variability. Studying genotype and haplotype associations of genes responsible for metabolism, transport, toxicity and the regulators of these genes may lead to better predictors of therapeutic outcome and aid the goal of personalised medicine. In broad terms there are two distinct approaches of identifying novel associations. Firstly, whole genome association studies can be conducted, but there are problems associated with the rigorous corrections that need to be applied for multiple comparisons. Secondly, and relevant to this thesis, basic science

can be applied to characterise the mechanisms involved in drug disposition and thereby identify novel candidate genes for pharmacogenetic association studies.

1.10 Aims of thesis

The aims of this thesis are to determine the factors that can influence cellular drug accumulation. This includes the characterisation of antiretrovirals (PIs and NNRTIs) as potential substrates for drug efflux by using existing models, such as CEM (cultured lymphocytes) and MDCKII (canine kidney cells) cells. Whilst these cells are established models to evaluate substrate affinity for ABC transporters, there are limitations to drug selected (CEM) and transfected (MDCKII) models. The drug selected cells over-express ABC transporters and may also select for and over-express other known and unidentified transporters, whereas transfected cells contain the target genes and other endogenous transporters. Therefore, a new *in vitro* model, the X. *laevis* oocyte expression system was developed.

SLCO transporters were chosen for evaluating influx of antiretrovirals because they were well characterised at the molecular level and have been shown to modulate plasma concentration of various xenobiotics. In addition, lopinavir has been known to have drug-drug interactions with statins in patients, which may be attributed to drug transporters. For evaluation of SLCO transporters using the X. laevis oocytes, clones of the individual transporters were first established. The DNA sequences of the clones were verified and sub-cloned into the pBluescriptII-KSM vector, which contains X. *laevis* β-globin 3' and 5' untranslated regions flanking the multiple cloning site to allow efficient translation of human SLCO genes. SLCO cRNA was generated from the cloned cDNA by *in vitro* transcription for use in the X. *laevis* oocyte model.

The X. *laevis* oocyte model contains few endogenous transporters. Oocytes were injected with SLCO transporters and uptake experiments were conducted to assess antiretrovirals as potential substrates of SLCO influx transporters.

Following the results generated from the X. laevis oocyte model, the effect of genetic polymorphisms in SLCO transporters on the pharmacokinetics of antiretrovirals was explored. Polymorphisms in SLCO transporters have been associated with differences in plasma concentrations of statins and hence are likely to influence plasma concentrations of antiretrovirals. Patient plasma samples from the Liverpool TDM registry were used for examining pharmacogenetic associations due to the availability of a large cohort size, lopinavir plasma concentrations and some population demographic data.

Finally, the effect of SLCO transporter knockdown was observed by using siRNA in human cell lines. The impact of SLCO transporter knockdown was observed by analysing the uptake of a paradigm substrate, estrone-3-sulphate. Cell lines representing liver, intestinal and kidney tissues were used as the distribution of SLCO transporters is tissue specific.

Chapter 2

Evaluating the transport of darunavir and rilpivirine by ABCB1: the impact of protein binding

2.1 Introduction

Darunavir (DRV, TMC114) is a protease inhibitor (PI), which was given FDA approval during 2006. It has potent antiretroviral activity against HIV strains that are resistant to other PIs *in vitro* and has low cytotoxicity *ex vivo* (De Meyer *et al.* 2005) with similar effects also observed in patient trials (Arasteh *et al.* 2005; Lefebvre and Schiffer 2008). The chemical structure of DRV is derived from amprenavir, yet DRV has a higher affinity for HIV protease than amprenavir and other PIs (King *et al.* 2004). This tighter protease binding gives DRV higher antiviral activity and confers a higher genetic barrier to resistance, i.e. viruses are required to harbour multiple mutations at the protease binding sites in order to develop resistance to DRV (King *et al.*, 2004, De Meyer *et al.* 2005).

The antiretroviral activity and cytotoxicity of DRV was assessed by De Meyer *et al.* (2005) in a study testing DRV against drug resistant viruses with different mutations. DRV was found to be non-cytotoxic at 100μM, which was the highest concentration and gave a selectivity index of >20 000 (De Meyer *et al.* 2005).

Rilpivirine is an experimental NNRTI currently in Phase III clinical trials and is a diarylpyrimidine (DAPY) molecule. DAPY molecules are similar to pyrimidine nucleotides used in DNA replication. Rilpivirine has also been demonstrated to have potent antiviral effects against viruses with mutations against the existing NNRTIs, efavirenz (EFV) and nevirapine (NVP) *in vitro* (Mordant *et al.* 2007) and is effective in reducing viral load in treatment naïve patients (Goebel *et al.* 2006).

DRV is a substrate of CYP3A4 and the plasma concentration of DRV is boosted when co-administered with ritonavir (Rittweger and Arasteh 2007). Intracellular drug concentrations of other PIs can be influenced by drug transporters, with ABCB1

being the most extensively researched transporter. The impact of drug transporters on the intracellular accumulation of DRV and rilpivirine has not yet been assessed. PIs and amprenavir – from which the structure of DRV is derived – have been shown to be substrates of ABCB1 whilst NNRTIs have been shown not to be substrates (Janneh *et al.* 2005, Strömer *et al.* 2004). Therefore, we can hypothesise that DRV is also a likely substrate, whereas rilpivirine is unlikely to be a substrate. In addition, protein binding also influences drug plasma concentrations and subsequently, intracellular drug concentrations of antiretrovirals. PIs and NNRTIs have been shown to bind with high affinity to serum proteins α1-acid-glycoprotein (AAG) (Jones *et al.* 2001) and human serum albumin (HSA) respectively (Boehringer-Ingelheim 1999; Bristol-Myers-Squibb 2008). Protein binding is an important factor for intracellular accumulation and with increasing concentrations of AAG, the antiviral activity of PIs decrease (Zhang *et al.* 1999). When bound to protein, antiretrovirals cannot penetrate cellular membranes and cellular accumulation is dependent on active transport (Boffito *et al.* 2003).

The aim of this chapter was to first characterise transport of DRV and rilpivirine by ABCB1 using different *in vitro* models; secondly, to determine whether intracellular concentrations of DRV at its site of action are modifiable by known inhibitors of efflux and influx; and thirdly, to observe whether protein binding alters the intracellular concentrations of rilpivirine.

2.2 Methods

2.2.1 Materials

[^{14}C] DRV (specific activity, 0.21mCi/mmol) and [^{3}H] rilpivirine (specific activity 20mCi/mmol) was provided by Tibotec (Mechelen, Belgium). [^{14}C] EFV (specific activity, 12.7μCi/μmol) was provided by Bristol-Myers-Squibb and [^{3}H] NVP (specific activity, 1.6Ci/mmol) was purchased from Moravek Chemicals (California, USA). Foetal calf serum (FCS) was purchased from Biosera (East Sussex, UK). Tariquidar was a gift from Xenova Group Plc. (Berkshire, UK), GF120918 was obtained from GlaxoSmithKline (Greenford, UK), MK571 and montelukast were gifts from Merck Frosst (Quebec, Canada). Ultima Gold scintillation fluid was purchased from Perkin Elmer (Boston, USA). Primary UIC2 (IgG2A) antibody was purchased from Immunotech (Marseilles, France), primary QCRL (IgG1) antibody was purchased from Calbiochem (Nottingham, UK), ABCB1 isotype control (IgG2A), ABCB1 secondary PE conjugated antibody, ABCC1 isotype control (IgG1) and ABCC1 FITC conjugated secondary antibodies were purchased from Serotec Ltd (Oxford, UK). CellFIX was obtained from Becton Dickinson (Oxford, UK) and all other reagents were purchased from Sigma-Aldrich (Poole, UK). PBMC were isolated from blood buffy coats obtained from the regional blood transfusion centre (Liverpool, UK). CEM (parental), CEM_{VBL100} (ABCB1 over-expressing) and CEM_{E1000} (ABCC1 over-expressing) cells were gifts from Dr. R. Davey, University of Queensland, Australia.

2.2.2 Cell culture

CEM cells are human T-lymphoblastoid cells, from which CEM_{VBL100} and CEM_{E1000} cells are derived. CEM_{VBL100} cells were selected for ABCB1 over-expression by stepwise selection with vinblastine to a final concentration of 100ng/ml, whilst CEM_{E1000} cells were selected for ABCC1 over-expression by stepwise selection with epirubicin up to 1000ng/ml, as described by Davey *et al.* (1996). Cell lines were cultured in RPMI 1640 medium with 10% FCS and incubated at 37.5°C in the presence of 5% CO_2. CEM_{VBL} and CEM_{E1000} were treated routinely with 100ng/ml of vinblastine and 1000ng/ml of epirubicin respectively to maintain their phenotype. Cells were passaged 1:6 every 3-4 days and passaged at least twice in the absence of selecting compound prior to use in experiments.

The MDCKII cell lines are canine kidney derived cells, from which, the MDCKII-ABCB1 cell was generated by transfection with the plasmid containing the ABCB1 gene (Horio *et al.* 1989). The cell lines were cultured with DMEM supplemented with 10% FCS and incubated at 37.5°C with 5% CO_2. MDCKII-ABCB1 was routinely treated with the antibiotic G418 to select for cells containing the ABCB1 plasmid, which also confers resistance to G418.

2.2.3 Verification of ABCB1 and ABCC1 expression by flow cytometry

CEM, CEM_{VBL100}, CEM_{E1000}, MDCKII and MDCKII-ABCBI cells were counted using the NucleoCounter (Chemometec) following the manufacturer's protocol. Each cell line was resuspended in CellFIX (1:10, 2×10^6 cells/ml, 30 mins) and transferred to a 96 well round bottomed plate (100µl, in quadruplicate).

To determine ABCB1 expression, fixed cells were centrifuged (2000rpm, 7 mins), the supernatant was discarded and the cell pellets resuspended in primary mouse anti-human UIC2 antibody or primary mouse anti-human IgG2a isotype control antibodies (2.5µg/ml, room temperature, 1hr). The cells were centrifuged (2000rpm, 7 mins) and washed with Hank's balanced salt solution (HBSS, 200µl) twice and resuspended in secondary goat anti-mouse r-phycoerythrin (PE) conjugated antibody (2.5µg/ml, room temperature, 1hr). The cells were washed twice with HBSS (200µl) before fixing in CellFIX (300µl) and transferral into 5ml plastic test tubes.

For ABCC1, fixed cells were centrifuged (2000rpm, 7 mins), the supernatant was removed and the cells were permeabilised with HBSS (200µl) containing saponin (0.1µg/ml, 4°C, 30 mins). The cells were centrifuged (2000rpm, 7 mins) and resuspended in primary mouse anti-human QCRL1 antibody or primary mouse anti-human IgG1 isotype control antibody (2.5µg/ml in HBSS with saponin, room temperature, 1 hr). The cells were washed twice with HBSS containing saponin (200µl) before resuspension in secondary goat anti-mouse fluorescein isothiocyanate (FITC) conjugated antibody (2.5µg/ml in HBSS with saponin, room temperature, 1 hr). The cells were washed twice with HBSS (200µl) and fixed with CellFIX (300µl) before transferral into 5ml plastic test tubes.

Cells were analysed using the Coulter epics XL-MCL flow cytometer. The target cell population was electronically gated using their forward and side scatter characteristics and fluorescence measured in FL1 and FL2 for ABCC1 (FITC) and ABCB1 (PE) respectively. Arbitrary fluorescence units were calculated by subtraction of the median fluorescence of isotype control incubated cells with that of those incubated with a specific antibody.

2.2.4 Determining the toxicity of darunavir and rilpivirine

The cellular toxicity of DRV was assessed using the MTT (thiazolyl blue tetrazolium bromide) cytotoxicity method (Mosmann *et al.*, 1983). CEM, CEM_{VBL} CEM_{E1000} cells were counted using the NucleoCounter and cells were resuspended in RPMI 1640 media containing 10% FCS, 1×10^6 cells/ml. DRV was serially diluted in RPMI 1640 media containing 10% FCS to give a range of concentrations (100-0.2μM). Drug dilutions (50μl) were added to sterile 96-well plates, which were followed by the addition of CEM, CEM_{VBL} or CEM_{E1000} cells (50μl). The plates were then incubated (3 days, 37.5°C, 5% CO_2). The assays were terminated by adding MTT (20μl, 5mg/ml dissolved in HBSS) to each well. The plates were returned to the incubator (37.5°C, 5% CO_2, 2hrs). Lysis solution (50% v/v dimethylformide in water, 20% w/v lauryl sulphate, 100μl) was added to each well and plates were incubated overnight (37.5°C, 5% CO_2). Plates were analysed using the Genios XFLUOR4 fluorescence plate reader (560nmλ). The cellular toxicity of rilpivirine was performed as above in CEM and CEM_{VBL} cells

2.2.5 Characterising cellular accumulation of darunavir in CEM cell lines

CEM, CEM_{VBL100} and CEM_{E1000} cells were counted using NucleoCounter. The cells were centrifuged (2000rpm, 5 min) and resuspended with RPMI 1640 medium containing 10% FCS (5×10^6 cells/ml). Aliquots of cell suspension (500μl) were incubated (37.5°C, 5% CO_2, 20 mins) with RPMI 1640 (500μl) containing serum and [^{14}C]-DRV (1μM; 0.026μCi/ml). After incubation, the samples were centrifuged (9000rpm, 1 min, 4°C) and the supernatant (100μl) was transferred from each sample to scintillation vials. The remaining supernatant was discarded and the cell pellet was

washed with 1ml of HBSS (9000rpm, 1 min, 4°C). Cell pellets were solubilised with tap water and transferred to scintillation vials. Scintillation fluid (4ml) was added to each vial and the samples were counted.

Following a correction for volume, a comparable value called the cellular accumulation ratio (CAR) was calculated using the following formula:

$$CAR = \frac{\text{Intracellular associated radioactivity}}{\text{Extracellular associated radioactivity}}$$

The volume of a CEM cell was taken as 1pl (Jones *et al.* 2001).

To assess the effects of ABCB1 transport on DRV, the CAR in CEM and CEM_{VBL100} was calculated in the presence or absence of tariquidar (XR9576; ABCB1 inhibitor; 0-1μM concentrations) and in the presence of 10% FCS.

For evaluating ABCC1 transport of DRV, the CAR in CEM, CEM_{VBL} and CEM_{E1000} was calculated in the presence or absence of MK571 (MRP inhibitor, 0-100μM concentrations) and in the presence of 10% FCS.

2.2.6 Characterising transcellular transport of darunavir in MDCKII cell lines

The interactions between ABCB1 and DRV were assessed using the MDCKII and MDCKII-ABCB1 cell lines and tariquidar was used to confirm the role of ABCB1.

Firstly, transwell plate inserts (3μm pore size, 24 mm diameter, Costar) were incubated with DMEM supplemented with 10% FCS MDCKII (30mins, 37°C, 5% CO_2). MDCKII-CTL and MDCKII-ABCB1 cells (1.5×10^6) were suspended in DMEM containing 10% FCS and seeded onto inserts in transwell plates (2ml) and media (2ml) was added to the bottom chamber. The cells were then cultured with

fresh DMEM supplemented with 10% FCS in the apical (top) and basolateral (bottom) chambers each day (3 days, 37°C, 5% CO_2). Confluence was measured by transepithelial resistance (above 150Ω was accepted). The media was aspirated and, in one half of the plate, DMEM containing DRV alone (2ml, 0.063μCi /ml) was added to the basolateral chamber, with DMEM alone (2ml) in the apical chamber. On the other half of the plate, DMEM (2ml) was added to the basolateral chamber and [^{14}C] DRV in DMEM (2ml) was added to the apical chamber. The process was repeated in another plate, where DMEM containing [^{14}C] DRV and tariquidar (1μM) was added to the chambers.

2.2.7 Characterising cellular accumulation of darunavir in PBMCs

PBMCs were isolated from healthy volunteer blood by gradient density centrifugation, using lymphoprep (15ml) and were centrifuged (2000rpm, 30 min). PBMCs were extracted from the solution and washed with HBSS (50ml, 2000rpm, 5 min). The cells were resuspended and cultured overnight in RPMI 1640 media containing 15% FCS in the presence of phytohaemagglutinin (10μg/ml).

Similar procedures as described for cell lines (see above, section 2.6) were used except 1×10^7 cells/ml were used and tissue solubilising solution (50μl, Optisolve: glacial acetic acid: hydrogen peroxide in a 5:5:2.5 ratio) was used with water (100μl) to solubilise the cell pellets. CAR values were calculated as described using the average volume of a PBMC as 0.4pl (Janneh *et al.* 2005). To ascertain the effects of transport proteins present in PBMC on DRV CAR, a range of inhibitors were co-incubated with the cells and [^{14}C] DRV (Table 1).

Table 1. Inhibitors used to characterise drug transporters.

Inhibitor	Action	Referencfes
1 μM tariquidar	Inhibitor of ABCB1, also known to inhibit BCRP	Mistry *et al.* 2001
50 μM MK571	Inhibitor of ABCC1, ABCC2, ABCC3, ABCC4, ABCC7, and influx	Su *et al.* 2004, Leier *et al.* 2000, Klokouzas *et al.* 2003 Ray *et al.* 2006, Chen *et al.* 2003 Letschert *et al.* 2006
100 μM GF120918	Inhibitor of ABCB1 and BCRP	Traunecker *et al.* 1999, Su *et al.* 2004
50 μM dipyridamole	Inhibitor of ABCB1 and ABCC1	Utoguchi. *et al.* 2000, Curtin *et al.* 1999
50 μM frusemide	Inhibitor of ABCC1 and ABCC2	Klokouzas *et al.* 2003 Bakos *et al.* 2000
100 μM estrone-3-sulphate	Inhibits BCRP and influx transporters	Su *et al.*, 2004
50 μM montelukast	Inhibitor of influx transporters SLCO1B3, SLCO1B1 and SLCO2B1	Letschert *et al.* 2006
50 μM verapamil	Non-specific inhibitor of efflux	Pereira *et al.* 1994 Klokouzas *et al.* 2003
50 μM probenecid	Inhibitor of ABCC1, MRP3 and influx transporters	Lucia *et al.* 2005

2.2.8 Inhibition of transport by darunavir

CEM and CEM_{VBL} cells were counted using the NucleoCounter and then cells were resuspended in RPMI 1640 media containing 10% FCS (1×10^6 cells/ml). Vinblastine was serially diluted in RPMI 1640 media containing 10% FCS to give a range of concentrations (2000-10ng/ml). In one set of dilutions, tariquidar (final concentration, 1μM) was added. In another set of dilutions, DRV (final concentration, 25μM) was added. Dilutions without DRV or tariquidar were used as controls. Each of these drug dilutions (50μl) were added to sterile 96-well plates, which were followed by the addition of CEM or CEM_{VBL} cells (50μl). The plates were incubated (3 days, 37.5°C, 5% CO_2). The assays were terminated by adding MTT (20μl, 5mg/ml dissolved in HBSS) to each well and the plates were returned to the incubator (37.5°C, 5% CO_2 2hrs). Lysis solution (100μl) was added to each well and plates were incubated overnight (37.5°C, 5% CO_2). The plates were analysed using the Genios XFLUOR4 fluorescence plate reader (560nm λ).

2.2.9 Characterising cellular accumulation of rilpivirine in CEM cell lines

Rilpivirine transport was assessed using the same methods as for DRV, except cells were incubated in serum free media containing [^{3}H] rilpivirine (140nM; 0.47μCi/ml). The CAR of rilpivirine was also calculated in the same way as for DRV.

2.2.10 Assessing the impact of protein binding on NNRTI transport

PBMCs were isolated from healthy volunteers and counted as described previously. [^{3}H] NVP (1μM; 0.045μCi/ml), [^{14}C] EFV (1μM; 0.23μCi/ml) and [^{3}H] rilpivirine

(1μM; 0.32μCi/ml) were incubated with 5×10^6 cells (37°C, 20mins) in RPMI 1640 media in the absence or presence of protein (10% FCS or 0-60mg/ml HSA). Washing, scintillation counting and analysis of CAR was performed as described for DRV.

2.2.11 Statistical analysis

To analyse the DRV accumulation in each cell line and PBMC, StatsDirect 2.4.5 was used. The Shapiro-Wilk test was used to test for normality of the data. The CEM, CEM_{VBL} and CEM_{E1000} cells in the presence or absence of MK571 or tariquidar data were log transformed and tested for differences using the paired t-test. The paired t-test was also used to assess the PBMC data for differences in accumulation between each inhibitor with the control (no inhibitors).

The toxicity data were tested for normality by Shaprio-Wilk and statistical significance was tested using the paired t-test. The DRV inhibition of transport data were analysed using the GraphPad Prism 3.0 software. Log transformation and non-linear regression analysis was used to obtain EC_{50} concentrations and the paired t-test was used to test for statistical significance.

2.3 Results

2.3.1 ABCB1 and ABCC1 expression in cell lines

Using flow cytometry to quantify relative amounts of protein (median fluorescence – isotype control, relative fluorescence units (RFU)), higher ABCB1 expression was detected in CEM_{VBL} (6.75RFU) than in CEM (0.04RFU, n=2) and CEM_{E1000} cells (0.05RFU, n = 2, Fig. 1a). Similarly, more ABCC1 was expressed by CEM_{E1000} (18.31RFU) than CEM (2.52RFU, n=2) and CEM_{VBL} (1.81RFU, n = 2) cells (Fig. 1b). MDCKII-ABCB1 expressed more ABCB1 (54.16RFU) than in MDCKII parental cells (-0.025RFU, Fig. 1c).

a)

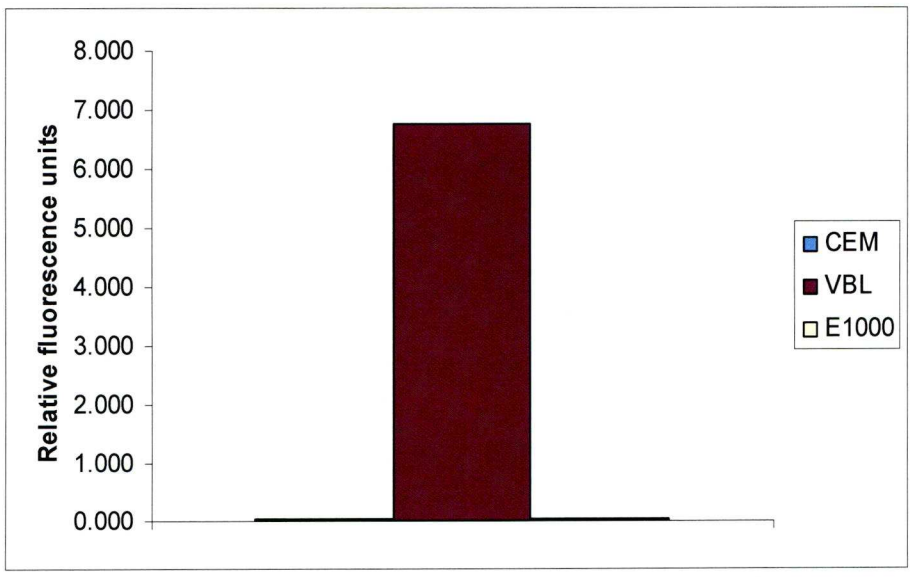

b)

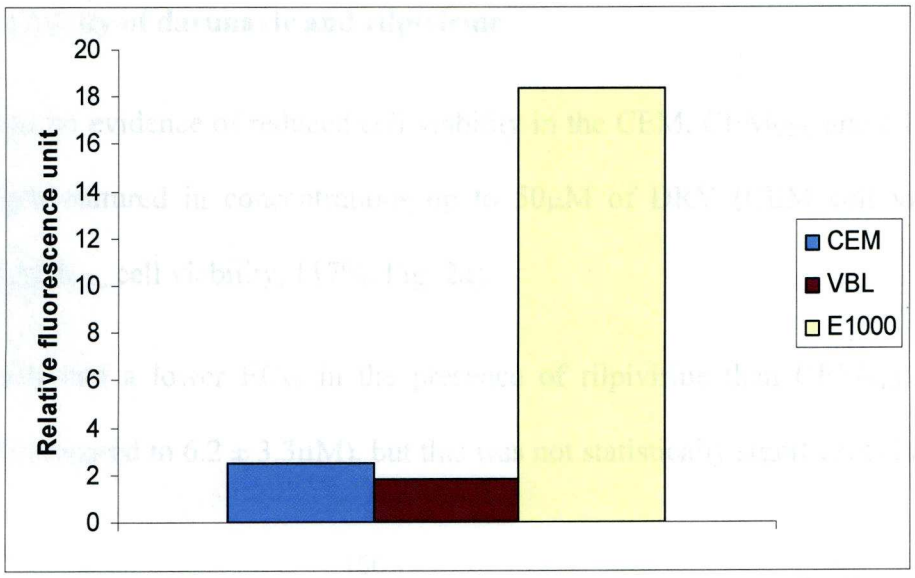

c)

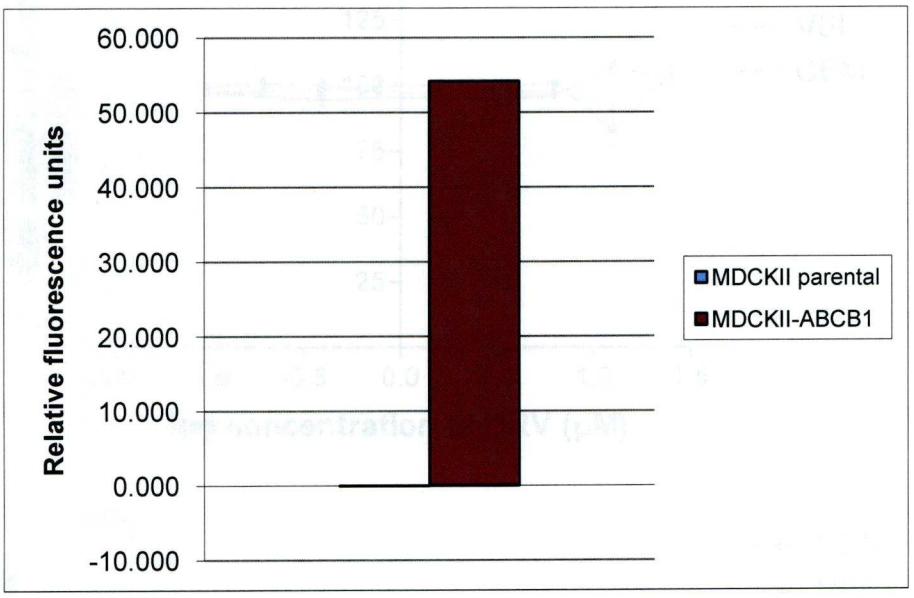

Fig. 1 Relative expression of a) ABCB1 in CEM, CEM_{VBL} and CEM_{E1000} cells (n=2), b) ABCC1 in CEM, CEM_{VBL} and CEM_{E1000} cells (n=2) and c) ABCB1 in MDCKII parental and MDCKII-ABCB1 cells (n=2).

2.3.2 Toxicity of darunavir and rilpivirine

There was no evidence of reduced cell viability in the CEM, CEM_{VBL} and CEM_{E1000} cells when cultured in concentrations up to 50μM of DRV (CEM cell viability, 126%, CEM_{VBL} cell viability, 117%, Fig. 2a).

CEM cells had a lower EC_{50} in the presence of rilpivirine than CEM_{VBL} (3.0 ± 0.64μM compared to 6.2 ± 3.3μM), but this was not statistically significant (Fig. 2b).

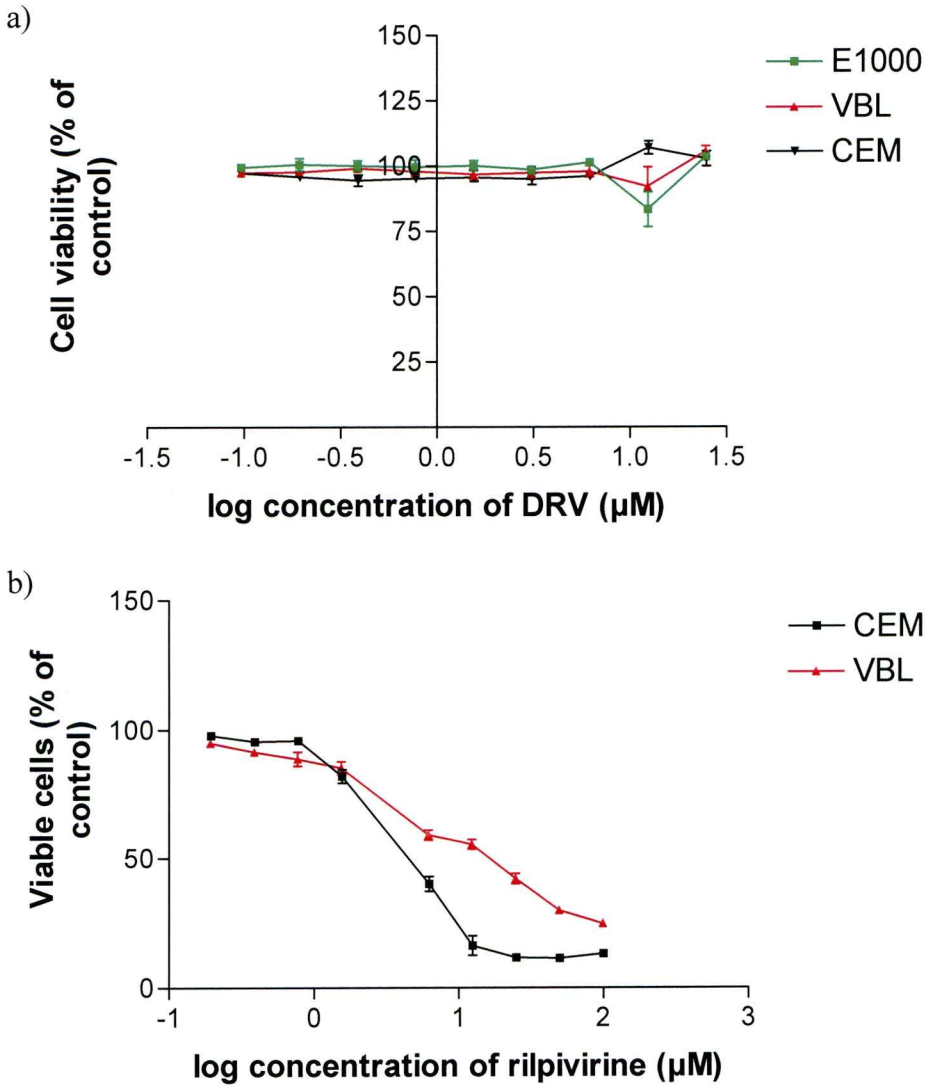

Fig. 2 Toxicity of a) DRV in CEM, CEM_{VBL} and CEM_{E1000} cells (n=4) and b) rilpivirine in CEM and CEM_{VBL} cells (n=4)

2.3.3 Cellular accumulation of darunavir in CEM cell lines

The concentrations of darunavir (1μM) and rilpivirine (140nM) used to assess drug transport were determined by no or low cytotoxicity and drug solubility. The incubation time during cell uptake assays was 20 minutes as this was previously shown to be sufficient for the antiretrovirals (Janneh *et al.* 2005, Janneh *et al.* 2007). The CAR of DRV was significantly higher in CEM cells (mean ± s.d, 5.6 ± 0.7) than in CEM_{VBL} cells (1.4 ± 0.6, $p<0.001$, n=7).

In CEM_{VBL} cells, the CAR was significantly increased in the presence of tariquidar in a concentration dependant manner (Fig. 3a), with significant increases of CAR at 10nM (1.5 ± 0.2, $p<0.05$), 20nM tariquidar (2.9 ± 0.5, $p<0.01$, n=4), 30nM tariquidar (4.6 ± 0.8, $p<0.001$, n=4) and higher concentrations of tariquidar (100nM, 300nM, 1000nM) showing trends towards further increase (4.8, 5.2, 5.2, n=3).

The CAR of DRV was lower in CEM_{E1000} cells (3.6 ± 0.5) compared to CEM cells (5.1 ± 1.0, $p<0.05$, n=6); however, MK571 did not reverse the difference in accumulation significantly (Fig. 3b). In this experiment, there was consistency in the differential accumulation in CEM_{VBL} (0.9 ± 0.06) compared with CEM (5.6 ± 1.0, $p<0.001$, n=6) and the accumulation in CEM_{VBL} was increased by tariquidar (300nM, 5.8 ± 0.4 $p<0.001$, n=6); however, MK571 also significantly increased the mean CAR in CEM_{VBL} cells (5μM, 1.1 ± 0.1, $p<0.001$, 10μM 1.7 ± 0.2, $p<0.001$, n=6).

a)

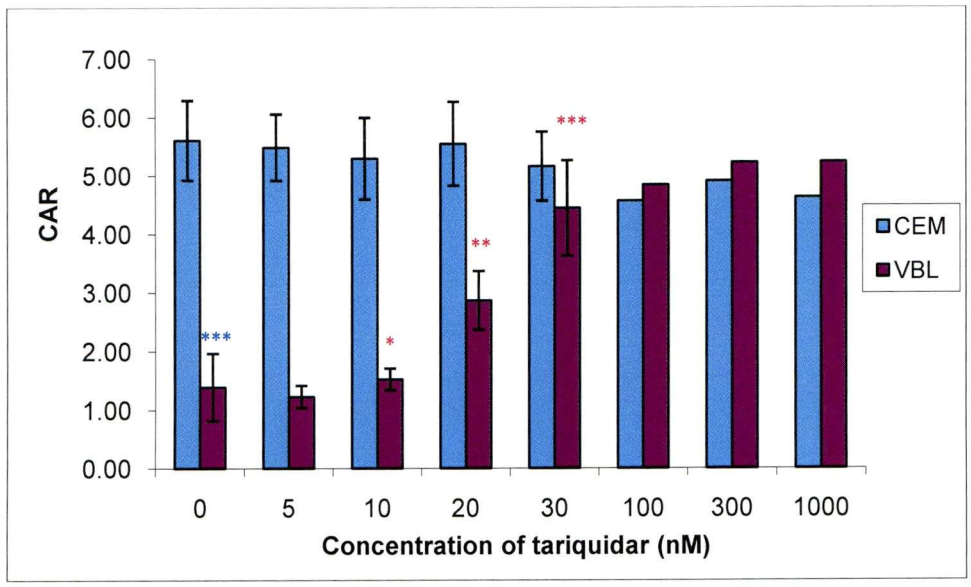

b)

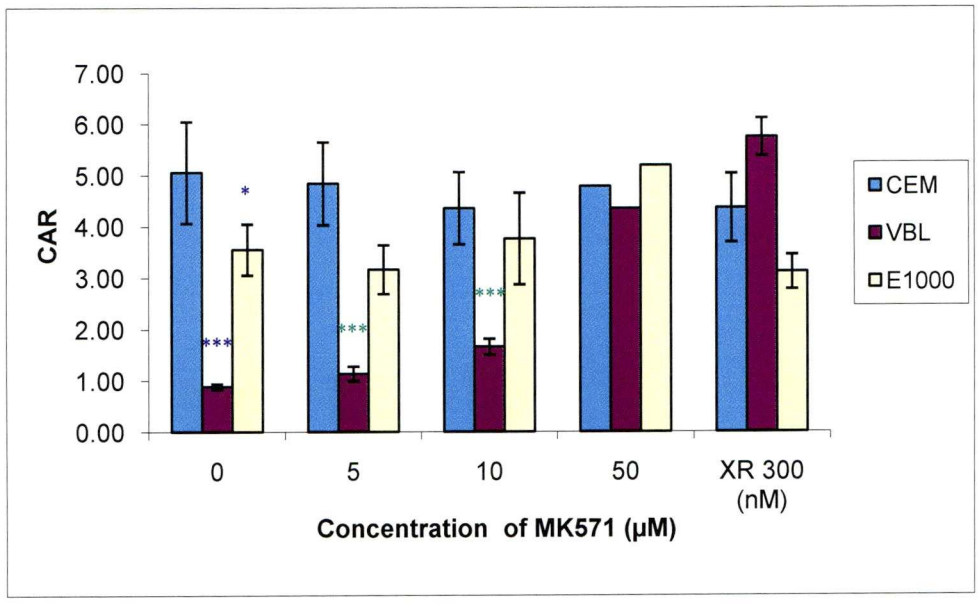

Fig. 3 The effect of a) tariquidar on [C^{14}] DRV CAR in CEM and CEM_{VBL} cell lines and b) MK571 on [C^{14}] DRV CAR in CEM; CEM_{VBL} and CEM_{E1000} cell lines. *** $p<0.001$ (n=7), compared to CEM control. * $p<0.05$ (n=4), ** $p<0.01$ (n=4), *** $p<0.001$ (n=7) compared to CEM_{VBL} control. * $p<0.05$ compared to CEM control (n=6), *** $p<0.001$ compared to CEM control (n=6), *** $p<0.001$ (n=6) compared to CEM_{VBL} control

2.3.4 Transcellular transport of darunavir across MDCKII and MDCKII-ABCB1 cells

Transport of [^{14}C] DRV from the basolateral (BL) chamber to the apical (AP) chamber was observed in the MDCKII-ABCB1 transwell experiments (Fig. 4a). The transcelluar transport was reversed with the addition of tariquidar (Fig. 4b) and minimal transport was observed from the AP to the BL chamber (Fig. 4a and 4b).

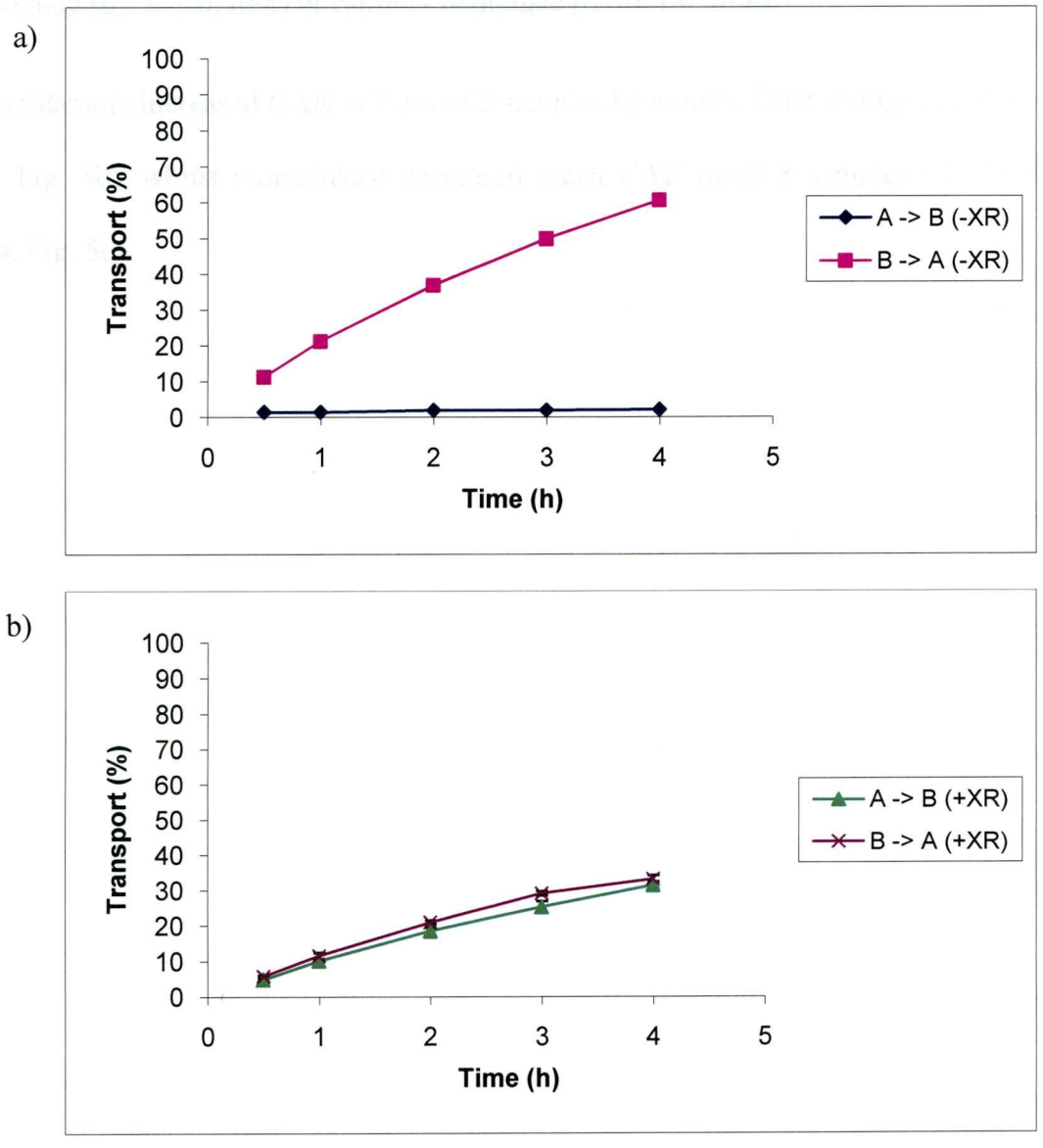

Fig. 4 The transport of [C^{14}] DRV through a MDCKII-ABCB1 monolayer a) in the absence and b) in the presence of tariquidar (n=3).

2.3.5 Cellular accumulation of darunavir in PBMCs

In PBMC, the only inhibitors to lead to a significant change in DRV CAR were dipyridamole (6.9 ± 1.3, $p < 0.01$, n=8) and montelukast (5.7 ± 1.0, $p < 0.01$, n=8) compared to baseline CAR (6.2 ± 1.1, n = 8, Fig. 5a). The mean CAR of DRV was not significantly altered by tariquidar (6.6 ± 1.7, n=8), verapamil (6.5 ± 0.8, n=8), probenecid (6.3 ± 1.2, n=8), MK571 (6.4 ± 1.4, n=8), GF120918 (6.6 ± 1.0, n=4), frusemide (6.1 ± 1.0, n=8) or estrone-3-sulphate (6.0 ± 1.0, n=8).

Dipyridamole increased CAR in 7 out of 8 samples by a mean CAR change (11.8% ± 9.4, Fig. 5b), whilst montelukast decreased mean CAR in all 8 samples (-7.5% ± 5.44, Fig. 5c).

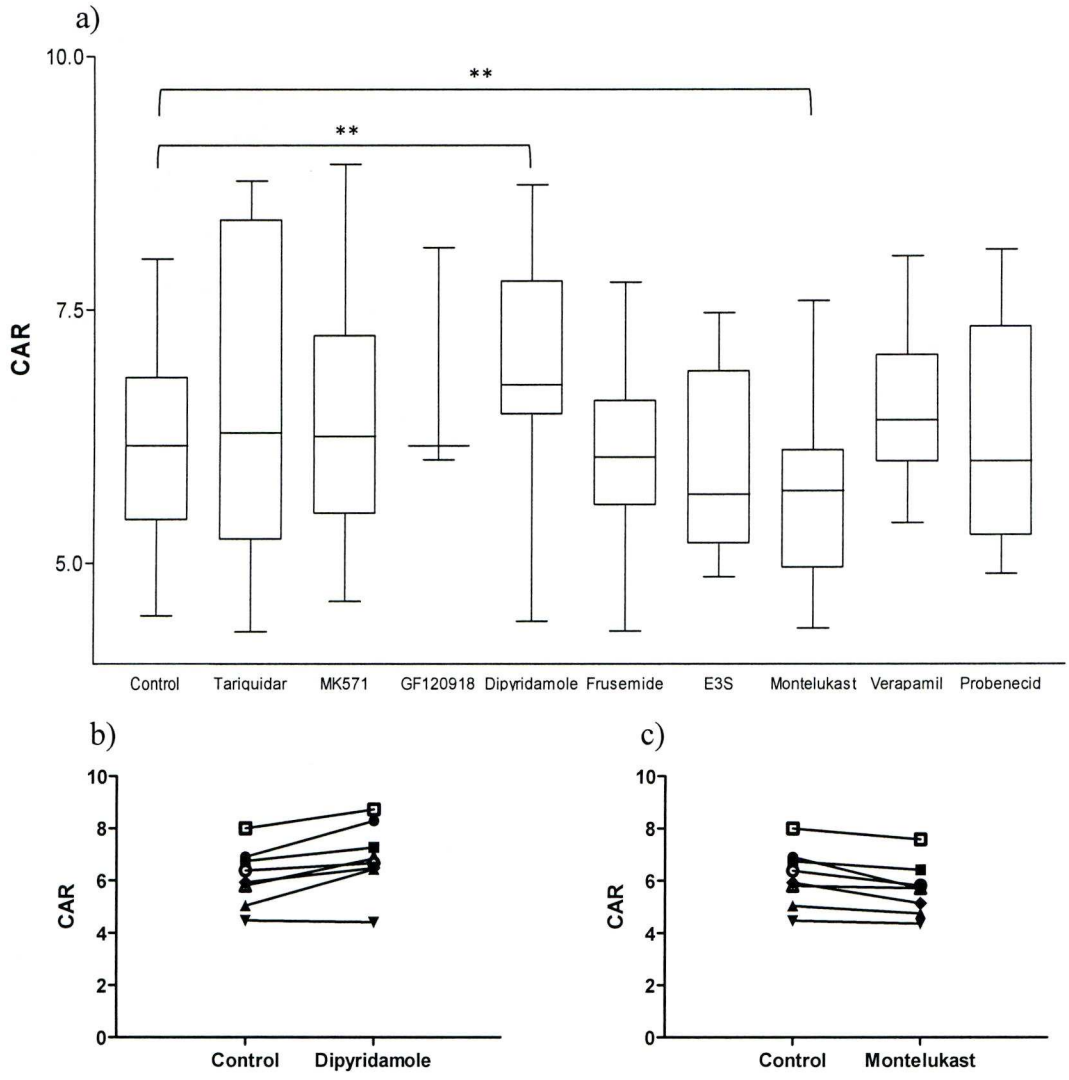

Fig. 5 The effect of a) various inhibitors on the CAR of DRV in PBMC, ** $p<0.01$ b) dipyridamole on the CAR of matched PBMC samples (n=8). c) montelukast on the CAR of matched PBMC samples (n=8).

2.3.6 Inhibition of ABCB1 transport by darunavir

A lower vinblastine EC_{50} was observed in CEM than in CEM_{VBL} cells (0.02 ± 0.01ng/ml, compared to 35.3 ± 9.8ng/ml, $p<0.001$, Fig. 6a). CEM cells cultured in the presence of vinblastine with tariquidar (0.017 ± 0.002ng/ml, Fig. 6b) or DRV (0.004 ± 0.004ng/ml Fig. 6c) had no change in cell viability. Culturing CEM_{VBL} cells in the presence of vinblastine and tariquidar reduced the EC_{50} of the cells (0.45 ± 0.08ng/ml, $p<0.001$, Fig. 6d). When CEM_{VBL} cells are cultured in the presence of vinblastine and DRV, the EC_{50} was reduced (3.50 ± 1.22ng/ml) compared to CEM_{VBL} cells cultured only in vinblastine (35.3 ± 9.8ng/ml, $p<0.001$ Fig. 6e).

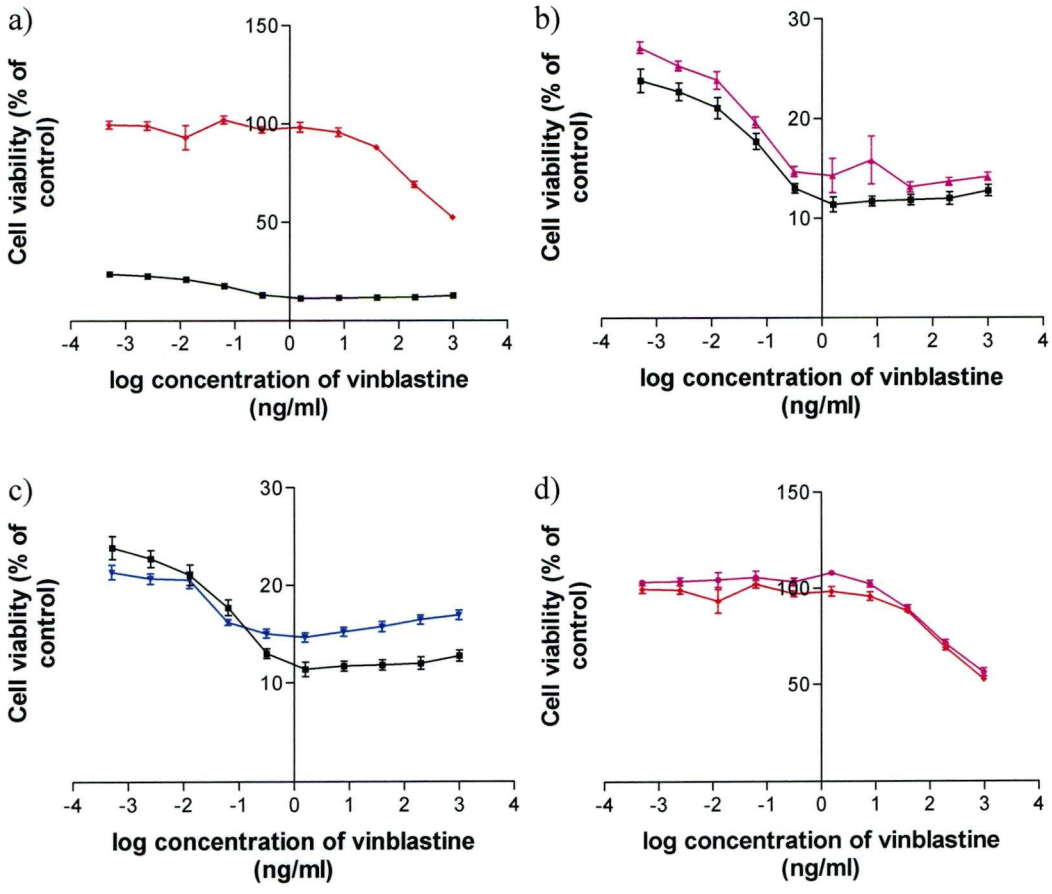

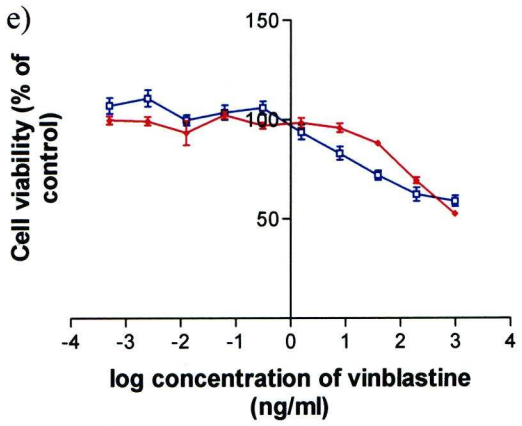

Fig. 6 Toxicity of vinblastine in a) CEM (—■—) and CEM_{VBL} (—•—) cells alone (n=4), b) in CEM cells in the presence and absence of tariquidar (—▲—) (n=4), c) CEM cells in the presence and absence of DRV (—▼—) (n=4), d) CEM_{VBL} cells in the presence of tariquidar (—●—) (n=4) and e) in CEM_{VBL} cells in the presence of DRV (—□—) (n=4).

2.3.7 Cellular accumulation of rilpivirine in CEM cell lines

No significant differences were observed between CEM, CEM_{VBL} and CEM_{E1000} cells and the addition of tariquidar and MK571 had no observable difference in intracellular accumulation of rilpivirine (Fig. 7a and 7b).

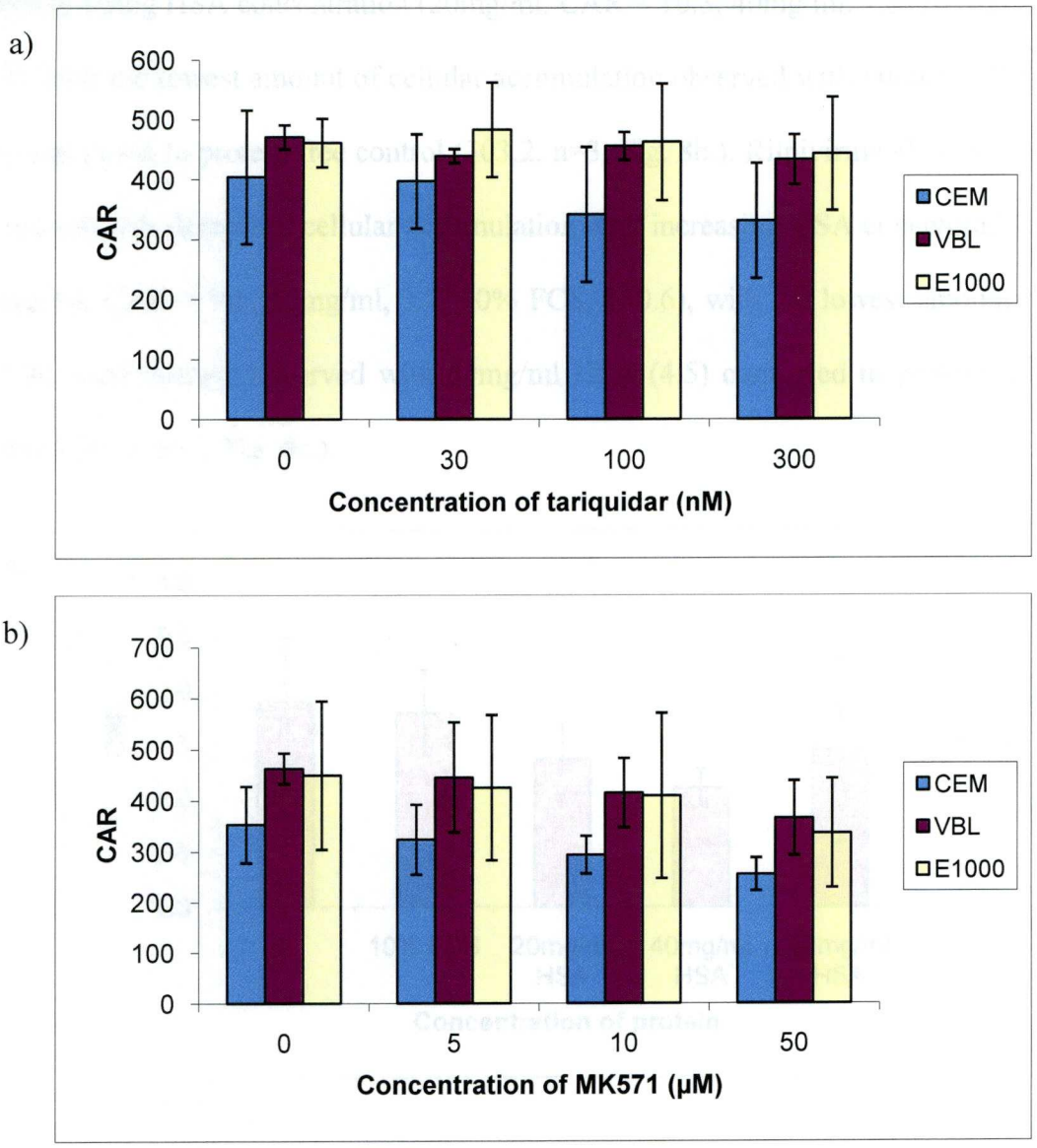

Fig. 7 The effect of a) tariquidar on [H^3] rilpivirine CAR in CEM and CEM_{VBL} cell lines (n=4) and b) MK571 on [H^3] rilpivirine CAR in CEM; CEM_{VBL} and CEM_{E1000} cell lines (n=4).

2.3.8 Impact of protein binding on the transport the of NNRTIs

The CAR of NVP was the least affected by protein, with the highest concentration, 60mg/ml HSA (CAR = 1.5) and 10% FCS (1.8) comparable to protein free control (1.9, n=3, Fig. 8a). EFV showed a trend towards a decrease in cellular accumulation with increasing HSA concentration (20mg/ml, CAR = 10.3, 40mg/ml, 7.3, 10% FCS, 96.3), with the lowest amount of cellular accumulation observed with 60mg/ml HSA (4.9) compared to protein free control (303.2, n=3, Fig. 8b.). Rilpivirine also showed a trend towards decreased cellular accumulation with increasing HSA concentrations (20mg/ml, CAR = 9.1, 40mg/ml, 3.7, 10% FCS, 150.6), with the lowest amount of cellular accumulation observed with 60mg/ml HSA (4.5) compared to protein free control (481.5, n=3, Fig. 8c.).

a)

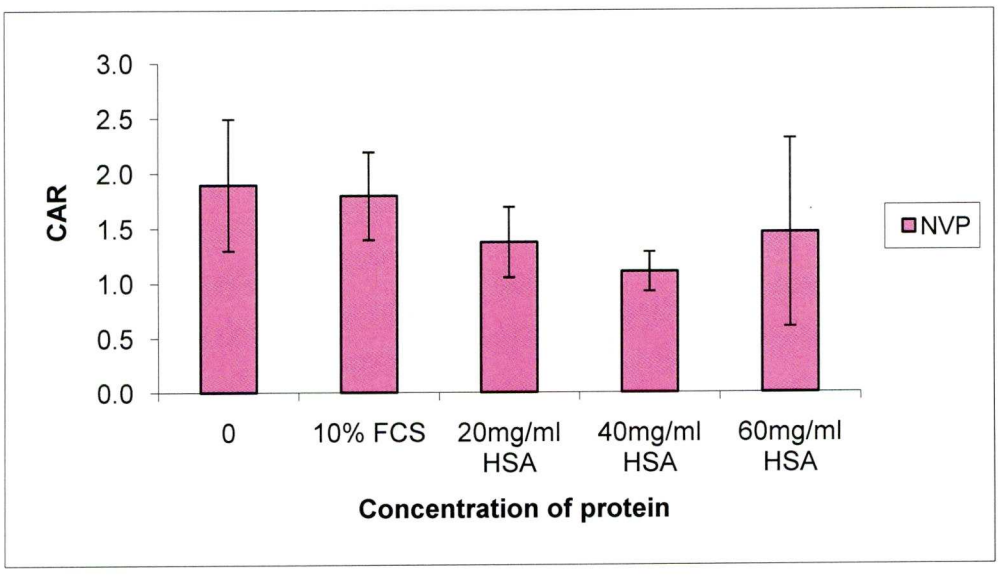

b)

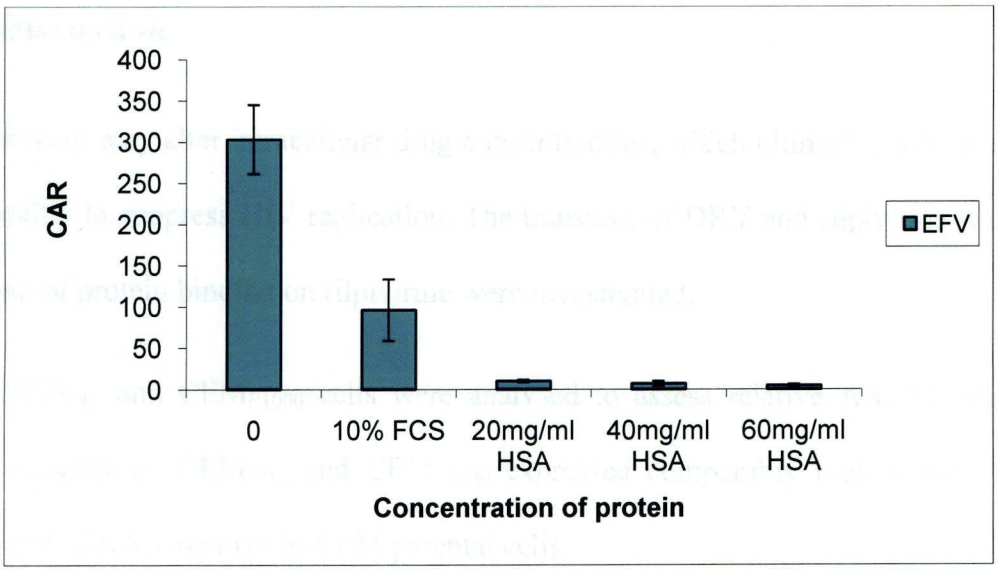

c)

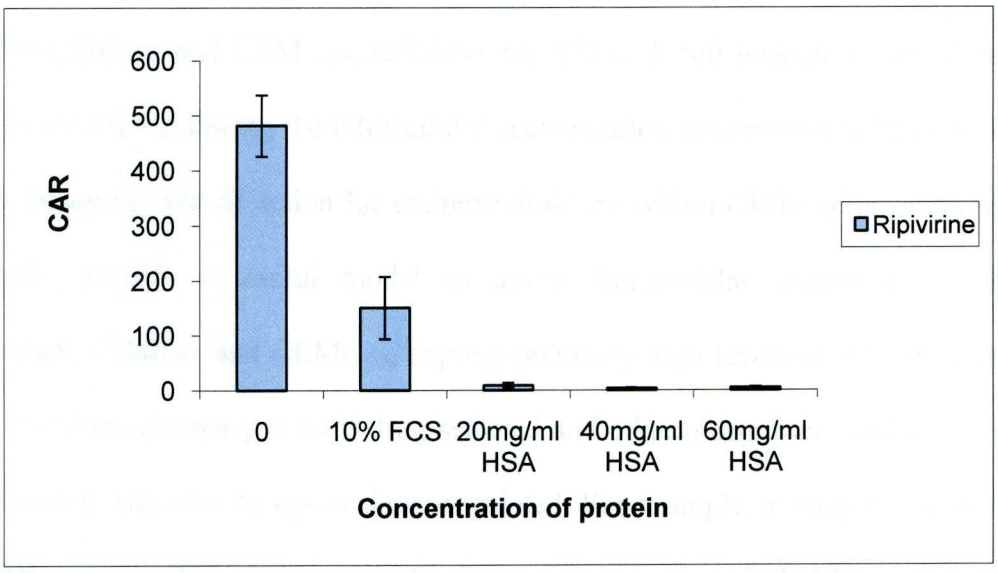

Fig. 8 The CAR of a) [^{3}H] NVP b) [^{14}C] EFV and c) [^{3}H] rilpivirine in the absence or presence of 10% FCS or in varying concentrations of HSA (n=3).

2.4 Discussion

Drug transport may alter intracellular drug concentrations, which ultimately affects a drug's ability to suppress HIV replication. The transport of DRV and rilpivirine and the impact of protein binding on rilpivirine were investigated.

CEM, CEM_{VBL} and CEM_{E1000} cells were analysed to assess relative ABCB1 and ABCC1 expression. CEM_{VBL} and CEM_{E1000} expressed comparably high levels of ABCB1 and ABCC1 relative to CEM parental cells.

The CEM, CEM_{VBL} and CEM_{E1000} cell lines are CD4+ T cell leukaemia cell lines previously used for assessing the intracellular accumulation of xenobiotics (Davey *et al.* 1996). Since the site of action for antiretrovirals are within CD4+ cells, cultured lymphocytes provide a useful model to assess intracellular accumulation of antiretrovirals. CEM_{VBL} and CEM_{E1000} express relatively high levels of ABCB1 and ABCC1, but these phenotypes were drug-selected and other transporters which were not investigated may also be up- or down-regulated. For example, a study by Janneh *et al.* (2008) showed that of the panel of influx transporters tested, PBMCs only had detectable mRNA expression of SLCO3A1. Whilst detectable levels of SLCO3A1 were observed in CEM, CEM_{VBL} and CEM_{E1000} cells, SLCO4A1 was detected in CEM, CEM_{VBL} and CEM_{E1000} cells and SLCO1A2 mRNA was detected only in CEM_{VBL} cells.

The toxicity of DRV was assessed in CEM, CEM_{VBL} and CEM_{E1000} cells, but the highest concentration used (50μM, dictated by solubility) was not toxic in these cells, which was consistent with the lack of toxicity observed by De Meyer *et al.* (2005) in a different cell line.

A significantly lower cellular accumulation of [C^{14}] DRV was observed in CEM_{VBL} cells compared to parental CEM cells, suggesting DRV to be an ABCB1 substrate. This was further supported as the CAR in CEM_{VBL} increased with increasing concentrations of the ABCB1 inhibitor tariquidar and at 30nM, the difference in CAR between CEM and CEM_{VBL} was abrogated. An increase in transport of DRV between MDCKII-ABCB1 basolateral compared to apical chambers in the transwell system was also observed, and this increase was reversed with the addition of 1μM tariquidar. Furthermore, no transport was observed from the apical to the basolateral chamber, which is consistent with other studies which found ABCB1 to be expressed on the basolateral membrane (Horio *et al.* 1989). Both of these uptake models suggest that DRV is a substrate of ABCB1. The CEM uptake model is an established method of assessing transport by ABCB1 and ABCC1 and has been used to demonstrate SQV and LPV as substrates of ABCB1 and ABCC1 (Janneh *et al.* 2005; Janneh *et al.* 2007). The MDCKII uptake model, developed by transfecting ABC transporter genes (Horio *et al.* 1989; Bakos *et al.* 1998), is also an established model for assessing transport. Using this model, SQV has been shown to be a substrate of ABCC1 and ABCC2 (Williams *et al.* 2002) and LPV was confirmed to be a substrate of ABCB1 and ABCC2 (Agarwal *et al.* 2007).

A difference in CAR of DRV between CEM and CEM_{E1000} cells was observed, but this was not reversed by the addition of the inhibitor MK571. This does not confirm nor refute DRV as a substrate of ABCC1 and further evidence will be needed to validate DRV as substrate of ABCC1. DRV CAR in CEM_{VBL} cells also had small increases in the presence of MK571 at any concentration, which suggests that MK571 does not have good specificity for ABCC1.

PBMCs are a mixed population of subsets (primarily CD4+ and CD8+ cells) and during culture, they were incubated with phytohaemogluttin, which activates the cells (Martin-Romero *et al.* 2000). In PBMC, the only change in CAR observed was in the presence of dipyridamole or montelukast. Montelukast significantly lowered CAR of DRV in all of the PBMC samples, which indicates that DRV may be a substrate of influx. This also suggests that influx does have an impact (albeit small) on DRV cellular accumulation *ex vivo*. The ABCB1 inhibitors tariquidar and verapamil did not appear to alter CAR in PBMC samples. This may be due to lower levels of ABCB1 in PBMC compared to CEM_{VBL}, which suggests that ABCB1 may not be a major regulator of intracellular accumulation in PBMC. MK571, the ABCC inhibitor also did not alter cellular accumulation of DRV in PBMC. Dipyridamole is a known inhibitor of multiple transporters (including ABCB1 and ABCC1) and increased 7 out of 8 PBMC samples. This suggests that the inhibition of both ABCB1 and ABCC1 may be required to increase drug accumulation in PBMCs and provides further evidence that DRV may be a substrate of ABCC1 as well as ABCB1 or that dipyridamole inhibits other efflux transporters. In contrast, LPV accumulation in PBMCs increased with the addition of tariquidar (9% increase), MK571 (45% increase), dipyridamole (37% increase) and frusemide (27% increase) (Janneh *et al.* 2007), suggesting a stronger affinity for LPV than DRV by the ABCB1 and ABCC1 transporters. In a separate study by Janneh *et al.* (2005), SQV accumulation in PBMCs also increased with the addition of tarquidar (14% increase), MK571 (39% increase), dipyridamole (45% increase) and frusemide (82% increase), suggesting that there are differences in the transporters involved in intracellular accumulation of different PIs.

CEM_{VBL} cells were more resistant to vinblastine toxicity due to over-expression of ABCB1 on these cells; whereas, CEM cells express much lower levels of ABCB1 and have reduced cell viability when cultured with vinblastine. Tariquidar was used as a positive control against CEM_{VBL} cells as it inhibits ABCB1 and it reduced CEM_{VBL} cell viability in the presence of vinblastine. CEM_{VBL} cell viability was reduced when DRV was included in vinblastine cultures, indicating that DRV is also a competitive inhibitor of ABCB1. CEM cells were cultured with vinblastine and tariquidar or DRV to act as a negative control and to confirm that changes in cell viability are attributable to ABCB1. Neither tariquidar nor DRV altered cell viability of CEM cells cultured with vinblastine.

Rilpivirine is more cytotoxic than DRV and is toxic between 3-6μM when incubated for three days in CEM cells. The concentrations of rilpivirine used to assess intracellular accumulation in PBMCs, CEM, CEM_{VBL} and CEM_{E1000} cells were up to 1μM. This would not be likely to affect the data as the cells were incubated with rilpivirine for 20 mins as opposed to 3 days, which was used to assess toxicity. Rilpivirine does not appear to be a substrate for ABCB1 or ABCC1 using the CEM uptake model. This suggests that these efflux transporters may not be relevant in determining rilpivirine cellular accumulation.

EFV and NVP have been shown to be primarily bound to HSA *in vivo*, with over 99% (Bristol-Myers-Squibb 2008) and 60% (Boehringer-Ingelheim 1999) bound respectively. Concentrations of HSA were chosen to be above (60mg/ml), below (20mg/ml) and within (40mg/ml) the *in vivo* concentration range (30-50g/l). 10% FCS was included as it was used to evaluate DRV and rilpivirine transport. Serum free media was used in these experiments as a protein free control. The effect of protein binding of EFV, NVP and rilpivirine to HSA *in vitro* was investigated. The

order of affinity for protein binding with 10% FCS and HSA is rilpivirine > EFV > NVP. This suggests that rilpivirine is highly bound to albumin. Cellular accumulation experiments to assess ABCB1 function on rilpivirine were performed with the inclusion of 10% FCS in the incubation medium, hence the 10% FCS condition was included to observe the effect of FCS on the cellular accumulation of rilpivirine. Rilpivirine binding to FCS was higher than that of EFV, yet rilpivirine showed higher binding to HSA compared to EFV. This suggests that rilpivirine may have less affinity for other composite proteins in serum compared to EFV. These results are similar to other studies which found higher protein binding by EFV (Almond *et al.* 2005) than by NVP (Almond *et al.* 2005).

In conclusion, this study suggests that DRV is a substrate of ABCB1 *in vitro*, but that the effect of ABCB1 on DRV transport is not as marked in PBMC compared to the cell line models. It is possible that ABCB1 may not be the main transporter altering cellular concentrations of DRV *ex vivo*. However, inhibition of both ABCB1 and ABCC1 appears to have some impact on cellular accumulation of DRV *ex vivo* compared to inhibition of ABCB1 or ABCC1 separately. Whilst ABCB1 alone does not appear to have a strong influence on the intracellular accumulation of DRV, the effect may be observed in other tissues such as the gut, liver and brain where ABCB1 has a more prominent role. For example, DRV may not be very effective against viral reservoirs due to the abundance of ABCB1 at the blood-brain barrier (Choo *et al.* 2000). These findings also support the use of a PI-booster in conjunction with DRV to improve the bioavailability of DRV by lowering the rate of clearance of DRV by ABCB1 (Rittweger and Arasteh 2007). Inhibition of influx transporters also appears to have a modest effect on DRV accumulation in PBMCs, but the effects of individual influx transporters still remain to be elucidated. The impact of individual

transporters is difficult to identify as the use of inhibitors may inhibit unknown, in addition to target transporters. DRV is an inhibitor of ABCB1 efflux, which is likely to be competitive inhibition as it is also a substrate of ABCB1. The interactions between DRV and ABCC1 remain unclear and warrant further investigation; however, it is clear that intracellular concentrations of DRV are, at least in part, the product of complex interactions with multiple transport proteins. Rilpivirine does not appear to be a substrate for ABCB1 or ABCC1 using the CEM model, but the cellular accumulation of rilpivirine is lowered with the inclusion of HSA. This suggests that protein binding may have more impact on the intracellular concentration of rilpivirine than active transport.

Chapter 3

Cloning SLCO transporters

3.1 Introduction

Antiretroviral drugs have been shown to be substrates for efflux transporters, which can affect bioavailability, plasma concentrations, clearance and intracellular concentrations and thereby impact on viral resistance and toxicity. Efflux transporters such as ABCB1 have been extensively studied in relation to pharmacokinetics and drug interactions, but many influx transporters have yet to be characterised.

For studying influx of antiretrovirals, the SLCO sub-family are ideal candidates due to their well characterised protein and molecular structures as well as their implicit roles in the transport of xenobiotics. Members of the SLCO family have been reported to transport bile salts and hormones as well as xenobiotics such as statins (Kopplow *et al.* 2005, Hsiang et al 1999, Hirano et al 2004), anti-cancer (Abe *et al.* 1999, Abe et al 2001) and anti-microbial drugs (Tirona *et al.* 2003, Tamai *et al.* 2000).

SLCO family members include SLCO1B1 and SLCO1B3, which have been identified as major hepatic transporters (Hsiang *et al.* 1999, König et al 2000). SLCO1A2 is expressed in several major organs including the brain, liver and intestines (Bleasby *et al.* 2006, Lee *et al.* 2005). SLCO3A1 has ubiquitous expression including lymphocytes (Bleasy *et al.* 2006, Tamai *et al.* 2000), which is important due to the site of action for antiretrovirals being in CD4+ cells. SLCO2B1 has been identified in various tissues, including the small intestine (Tamai *et al.* 2000), placenta (St-Pierre *et al.* 2002) and heart (Grube *et al.* 2006). SLCO1B1 and SLCO1B3 share over 80% homology, are exclusively expressed in the liver, and have been shown to affect intracellular

concentrations *in vitro* (Hsiang *et al.* 1999) and also plasma concentrations of xenobiotic substrates *in vivo* (Hirano *et al.* 2004, Lau *et al.* 2007). One study suggested that basolaterally expressed SLCO1A2 acted in concert with apically expressed ABCB1 and ABCC1 to excrete saquinaivr (SQV) into bile. This was demonstrated by the transport of SQV in *SLCO1A2* transfected HepG2 cells and X. *laevis* oocytes injected with *SLCO1A2* cRNA (Su *et al.* 2004).

Identification of transporter substrates can help explain drug interactions that alter drug plasma concentrations. For example, rifampicin, which has been shown to be a competitive inhibitor of SLCO1B1 in the X *laevis* oocyte system (Vavricka *et al.* 2002), has subsequently been shown to increase atorvastatin plasma concentrations and affect drug clearance when given as a single dose to healthy volunteers (Lau et al 2007). Several SLCOs have been found to transport various xenobiotics, but many interactions between antiretrovirals and influx transporters have yet to be characterised.

Darunavir is likely to be a substrate of influx transporters because montelukast, which is a known inhibitor of influx reduces the accumulation *ex vivo* (Letschert *et al.* 2006); however, the specific transporters are unknown (discussed in Chapter 2). Many known inhibitors of SLCOs are not specific to individual transporters due to overlap between substrate transporters.

Several approaches have been used for evaluating individual influx transport *in vitro*. These include primary hepatocytes, Xenopus *laevis* oocytes, yeast expression systems and transiently and stably transfected cells (Xia *et al.* 2007). The aim of this chapter was

to clone known SLCOs and develop X *laevis* expression vectors for subsequent determination of whether antiretrovirals are substrates for SLCO1A2, SLCO1B1, SLCO1B3 and SLCO3A1 in Chapter 4.

3.2 Methods

3.2.1 Materials

TaqMan Reverse Transcription Reagents were purchased from Applied Biosystems Inc. (Warrington, UK); Expand High Fidelity PCR System was purchased from Roche Diagnostics (Burgess Hill, UK). (Huntingdon, UK). Cell lines were purchased from ECACC (Salisbury, UK), RPMI 1640 and DMEM media were purchased from Gibco (Invitrogen Ltd, Paisley, UK). Foetal calf serum (FCS) was purchased from Biosera (East Sussex, UK). TRIzol reagent, chloroform, GenElute PCR clean-up kit, GenElute gel extraction kit and isopropanol (Fluka) were purchased from Sigma-Alderich Company Ltd (Poole, UK). TOPO TA cloning kit was purchased from Invitrogen Ltd (Paisley, UK). DH5-α competent E. coli cells, T4 DNA ligase, Antarctic phosphatase, NEB 1kb ladder, NEB 500bp ladder and all restriction enzymes were purchased from New England Biolabs (Hitchen, UK).

pBluescriptII-KSM was a kind gift from WJ Joiner (Yale University, Connecticut, USA) and pSPORT1-*Oatp1-OATP4* (Cattori *et al.* 2000, Huber *et al.* 2006) was a kind gift from Bruce Steiger (Switzerland).

3.2.2 Cloning strategy

The majority of SLCOs were cloned from human cell line mRNA, with *SLCO1A2* cloned from A549, *SLCO1B1* and *SLCO1B3* cloned from Huh7 mRNA. *SLCO3A1* was cloned from a plasmid kindly provided by Dr. Bruno Steiger.

SLCO1A2 was cloned in two fragments, with the introduction of a Kozak consensus sequence prior to the start codon of the gene and BglII restriction sites at the 3' and 5' ends of the gene. *SLCO1A2* fragments were then ligated and cloned into pCRII-TOPO plasmid. *SLCO1B1* and *SLCO1B3* were amplified to include 3' and 5' UTR sections, which were cloned into pCR-II-TOPO. From pCRII-TOPO, *SLCO1B1* and *SLCO1B3* were amplified to contain only the genes and introduce the Kozak consensus. These PCR products were cloned into pCRII-TOPO. *SLCO3A1* was amplified from pSPORT-oatp4-OATPD plasmid and the Kozak consensus was introduced prior to subcloning into pCRII-TOPO. With the SLCO genes in pCRII-TOPO, the sequences were verified by sequencing (GATC Biotech). SLCO genes which contained mutations were converted into wildtype by using site-directed mutagenesis. Once all the SLCOs were confirmed to be wildtype, the genes were subcloned into pBluescriptII-KSM which contains 3' and 5' X. *laevis* β-globin UTR flanking the multiple cloning site. Clones with the correct orientation were selected and inventoried.

The overall cloning strategy is illustrated in Fig. 1.

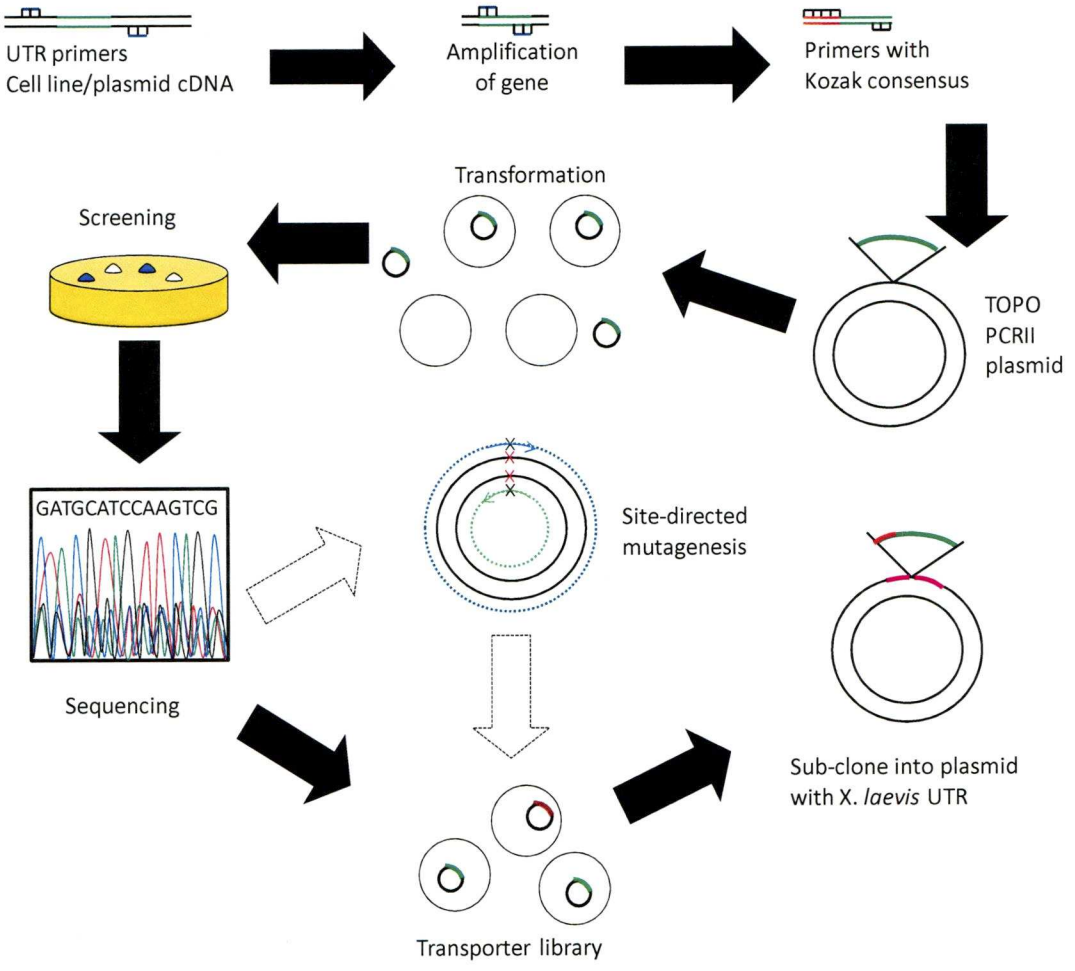

Fig.1 Illustration of the overall cloning strategy of the SLCO transporters

3.2.3 mRNA extraction

The human alveolar basal epithelial cell line A549, and human hepatoma cell line Huh-7 was cultured (DMEM supplemented with 10% foetal calf serum) and used as a source of RNA. TRIzol reagent was used to extract total RNA from A549 cells. A549 cells (1×10^7) were centrifuged (800 × g) to form cell pellets, mixed with TRIzol (1ml) and lysed by a freeze-thaw cycle (-80°C, 20°C). Chloroform (200µl) was added to the mixture and shaken before centrifugation (12000 × g, 15mins). The supernatant was transferred to a new tube and isopropanol (500µl) was added and mixed. The solution was centrifuged (12000 × g, 10mins) and the supernatant was removed. The pellet was washed with 75% ethanol (1ml, 7500 × g, 5mins) and air dried before resuspension in RNase free water (20µl). Quantification of RNA was achieved using a spectrophotometer and samples with an A260:A280 ratio of over 1.70 were deemed to be of suitable purity and stored (-80°C).

3.2.4 Reverse transcription

A549 and Huh7 total RNA was reverse transcribed into cDNA using TaqMan Reverse Transcription Reagents. The reverse transcription reactions were assembled as follows: 10× RT buffer (10µl, final concentration of 1×), 25mM $MgCl_2$ (22µl, final concentration of 5.5mM), 10mM dNTP (20µl, final concentrations of 2mM) 50µM oligo dT primers (5µl, final concentration of 2.5µM), 20U/µl RNase inhibitor (2µl, final concentration of

0.4U), 50U/µl Multiscribe reverse transcriptase (2.5µl, final concentration of 1.25U) and A549/Huh7 mRNA. The reaction was incubated at 25°C for 10min followed by annealing temperature of 48°C, 1h and finally inactivated at 95°C for 5mins using the Applied Biosystems GeneAmp PCR System 9700.

3.2.5 Primer design

Primers were designed based on published sequences of *SLCO1A2* (NM_134431), *SLCO1B1* (AB_026257), *SLCO1B3* (NM_019844) and *SLCO3A1* (NM_013272).

SLCO1A2 primers were designed to amplify the gene in two fragments in a nested PCR reaction to incorporate the Kozak consensus prior to the start codon and BglII restriction sites to flank the gene. This was achieved by using the first 19 bases (5', fragment 1 forward), the last 21 bases (3', fragment 2 reverse) and 20 bases starting from the +973 position (5' → 3', fragment 2 forward) and +1013 (3' → 5', fragment 1 reverse). The product of fragment 1 forward and reverse was predicted to be 993bp and the product of fragment 2 forward and reverse was predicted to be 1020bp. A primer was designed to contain a BglII restriction site and the Kozak consensus (CCACC), followed by the fragment 1 forward sequence. A reverse primer was also designed with the BglII restriction site after the fragment 2 reverse primer.

Suitable primers in the untranslated regions of *SLCO1B1* (-76 and + 15), *SLCO1B3* (-90 and +2088) were identified by using OligoExplorer 1.2. Primers were chosen by their

GC content (approximately 50%), similar annealing temperatures between the forward and the reverse primers and limited mono- and dinucleotide repeats. Two additional forward primers were chosen, one at the start codon of each gene and one with the Kozak consensus added prior to the start codon. For *SLCO3A1*, the forward primer was the Kozak consensus and the first 16bp of the gene and the reverse primer was 23bp from the last base in *SLCO3A1*, i.e. includes the start of the *oatp1* 3' UTR. The primer sequences are presented in Table 1.

Table 1. Primers and templates used to amplify SLCO genes. * These primers contain the BglII restriction site.

Gene	Primers	Sequence (5'→ 3')	Template
SLCO1A2	fragment 1 forward	atgggagaaactgagaaaa	A549 cDNA
	fragment 1 reverse	taacgaatgcattgaactgt	A549 cDNA
	fragment 2 forward	acagttcaatgcattcgtta	A549 cDNA
	fragment 2 reverse	ttacaatttagttttcaattc	A549 cDNA
	Kozak forward*	agatctccaccatgggagaaactgagaaaa	Fragment 1
	BglII reverse*	agatctttacaatttagttttcaattc	Fragment 2
SLCO1B1 UTR -76	UTR forward	ggattctaaatccaggtgattg	Huh7 cDNA
SLCO1B1 UTR +15	UTR reverse	aaacacagaagcagaagtgg	Huh7 cDNA
SLCO1B1	Inner forward	atggaccaaaatcaacatttg	UTR PCR product
SLCO1B1-Kozak	Kozak forward	ccaccatggaccaaaatcaacatttg	UTR PCR product
SLCO1B3-UTR -90	UTR forward	gcattcaaagtcaaggtgatca	Huh7 cDNA
SLCO1B3 UTR +2088	UTR reverse	gttagttggcagcagcattgtc	Huh7 cDNA
SLCO1B3	Inner forward	atggaccaacatcaacatttg	UTR PCR product
SLCO1B3-Kozak	Kozak forward	ccaccatggaccaacatcaacatttg	UTR PCR product
SLCO3A1	Kozak forward	ccaccatgcaggggaagaagc	pSPORT-oatp1-OATP-D
	oatp1 UTR reverse	gcacttcccttcctcggaatcct	pSPORT-oatp1-OATP-D

3.2.6 PCR amplification and ligation of *SLCO1A2*

SLCO1A2 was amplified in two fragments using the Expand High Fidelity PCR System (Roche Applied Science) reagents, the GeneAmp PCR System 9700 (Applied Biosystems) and the Eppendorf Mastercycler gradient (Eppendorf) machines. For both fragments the following reagents were assembled: 10× Expand High Fidelity Buffer with 15mM $MgCl_2$ (5µl, 1× final concentration), 10mM dNTP (4µl, 800nM final concentration), 10µM respective forward primer (1µl, 200nM final concentration), 10µM respective reverse primer (1µl, 200nM final concentration, Table 1.), nuclease-free water (35.75µl), A549 oligo dT cDNA (2.5µl, 10% of cDNA reaction volume) and 3.5U/µl Expand High Fidelity Enzyme Mix (0.75µl, final concentration 2.63U). The PCR conditions were as follows: hot start (94°C for 10s), initial denaturation (94°C for 2mins), 40 cycles of denaturation (94°C for 10s), annealing (59°C/56°C: fragment 1/fragment 2) 30s, elongation (72°C for 1min) and a final elongation (72°C for 7mins).

The amplified fragment 1 and fragment 2 were visualised by agarose gel electrophoresis. The PCR products were loaded into agarose gels (1% w/v in TBE, 0.15µg/ml ethidium bromide) with Sigma λ DNA EcoRI, HindIII digest ladder to mark DNA band sizes and appropriate bands were excised and purified using the GenElute Gel Purification kit. The Kozak consensus and BglII restriction sites were added 5' to the start codon of *SLCO1A2* fragment 1 and a BglII restriction site was added 3' to the stop codon of fragment 2. The PCR was performed using the same reaction mix as the first round of PCR, except the Kozak forward primer was used instead of fragment 1 forward primer and the BglII reverse primer was used instead of fragment 2 reverse primer (Table 1.).

Digestion of *SLCO1A2* fragments were performed with NsiI (NEB) using 10× NEBuffer 3 (5µl, 1× final concentration), *SLCO1A2* fragment 1 (500ng), *SLCO1A2* fragment 2 (500ng), 10U/µl NsiI enzyme (1µl, 0.2U/µl final concentration), nuclease-free water (up to 50µl) and incubated (37°C, 1hr), followed by heat inactivation (80°C, 20mins). *SLCO1A2* fragments were ligated with T4 DNA ligase using 10× T4 DNA ligase Reaction Buffer (2µl, 1× final concentration), *SLCO1A2* fragments 1 and 2 (17µl of digest product) and incubated (10mins, room temperature). The ligation products were visualized and extracted from 1% agarose gel.

3.2.7 PCR amplification of *SLCO1B1*

SLCO1B1 was amplified in full using UTR primers in the Expand High Fidelity System. The following was used to assemble the PCR reaction: 10× Expand High Fidelity Buffer with 15mM MgCl2 (5µl, 1× final concentration), 10mM dNTP (4µl, 800nM final concentration), 10µM respective forward primer (1µl, 200nM final concentration), 10µM respective reverse primer (1µl, 200nM final concentration, Table 1), nuclease-free water (35.75µl), Huh7 oligo dT cDNA (2.5µl, 10% of cDNA reaction volume) and 3.5U/µl Expand High Fidelity Enzyme Mix (0.75µl, final concentration 2.63U).

The PCR conditions were as follows: hot start (94°C for 10s), initial denaturation (94°C for 2mins), 40 cycles of denaturation (94°C for 10s), annealing (62°C for 30s), elongation (72°C for 2mins) and a final elongation (72°C for 7mins). The product was cloned into the pCRII-TOPO plasmid before performing further PCR steps.

The same reagents as above were used except the inner forward primer was used instead of the UTR forward primers and the DNA template used was the *SLCO1B1* with UTR TOPO plasmid. The PCR conditions were the same except for the annealing temperature used (62°C for 30s). The PCR products were visualised on agarose gels (1%) as for *SLCO1A2* and appropriate bands were excised and purified. The Kozak consensus was added to the gel purified products by PCR and replacing the forward primers with Kozak forward primer (Table 1). The reagents and conditions used were the same as the previous PCRs. The final product containing the Kozak consensus was cloned into pCRII-TOPO vector.

3.2.8 PCR amplification of *SLCO1B3*

Amplification of *SLCO1B3* was performed the same as for *SLCO1B1* with the exception of the primers used (Table 1) and the annealing temperature used (68°C for 30s) for amplifying *SLCO1B3*.

3.2.9 PCR amplification of *SLCO3A1*

SLCO3A1 was amplified from the pSPORT1-*oatp1-OATP4* vector using the Expand High Fidelity System. The following was used to assemble the PCR reaction: 10× Expand High Fidelity Buffer with 15mM $MgCl_2$ (5µl, 1× final concentration), 10mM dNTP (4µl, 800nM final concentration), 10µM forward primer (1µl, 200nM final concentration), 10µM reverse primer (1µl, 200nM final concentration, Table 1), 100%

DMSO (1µl, 5% final concentration) nuclease-free water (35.75µl), pSPORT-*oatp1-OATP4* cDNA (2.5µl, 25ng) and 3.5U/µl Expand High Fidelity Enzyme Mix (0.75µl, final concentration 2.63U).

The PCR conditions were as follows: initial denaturation (94°C for 2mins), 25 cycles of denaturation (94°C for 10s), annealing (66°C for 30s), elongation (72°C for 2mins) and a final elongation (72°C for 7mins).

3.2.10 Cloning of SLCO transporters using pCRII-TOPO

Cloning was performed with the pCRII-TOPO cloning kit (Invitrogen, UK). The *SLCO1A2* cloning reaction was assembled with ligated product (15ng), vector (10ng), salt (1.2M NaCl, 0.06M $MgCl_2$, final concentration of 200µM NaCl, 100µM $MgCl_2$) and nuclease free water (up to 6µl) and incubated (10mins, room temperature). The ligation mixture (2µl) was added to a vial of thawed E. coli (50µl) and incubated on ice (10mins). The E. coli was heat shocked (42°C, 30s) and then returned to ice before SOC media was added to the E. coli (200µl) and incubated (37°C, 1hr, orbital shaker, 250rpm). Culture plates were prepared with LB agar (35g/l) containing ampicillin (50µg/ml) and blue-white screening reagent (40µl, IPTG 40mg/ml, X-Gal 40mg/ml in DMSO) was spreaded on the surface of the agar. The E. coli culture was spreaded (100µl per plate) and left to grow (37°C, overnight).

For *SLCO1B1*, *SLCO1B3* and *SLCO3A1*, the cloning reaction was different from that used for the SLCO1A2 as the reaction contained PCR product (10ng) and pCRII-TOPO

vector (10ng) in a 20µl reaction whilst the concentration salt remained the same. The transformation of the E. *coli* was performed in the same way as for *SLCO1A2*.

3.2.11 Clone selection

White colonies were picked and grown in LB containing ampicillin (50µg/ml) and incubated (37°C, overnight). E. *coli* plasmids were extracted using the MiniPrep Plasmid Extraction kit (Sigma-Alderich, UK). Briefly, E. *coli* culture (4ml) was centrifuged (4000rpm, 10mins) and the supernatant was removed. The cell pellet was resuspended with Resuspension Buffer (200µl), lysed with Lysis Buffer (200µl, <5mins) and neutralised with Neutralisation Buffer (300µl). The mixture was centrifuged (13000 × g, 10mins) to pellet cell debris. Spin columns were placed into collection tubes and prepared with Column Prep (500µl, 13000 × g 1min). The flow through was discarded and the supernatant was transferred into the spin columns and centrifuged (13000 × g, 1min). The flow-through was discarded and Wash buffer was added to the spin columns (600µl) and centrifuged (13000 × g). The spin columns were transferred to new collection tubes, molecular grade water (100µl) was added and the columns were centrifuged (13000 × g, 1min). The plasmid DNA was quantified by spectroscopy and verified by restriction digest (Table 2).

3.2.12 Sequencing and analysis

Clones with the predicted digest patterns following agarose gel electrophoresis were chosen and sent to GATC Biotech (Germany) for sequencing and the sequences retrieved were aligned with respective published wild type sequences.

For *SLCO1A2*, a clone identical to NM_134431 was identified. For other transporters, differences between clones and published sequences were observed. Therefore site-directed mutagenesis was performed in order to correct these clones.

3.2.13 Site-directed mutagenesis

SLCO1B1, *SLCO1B3* and *SLCO3A1* clones contained 5, 2 and 6 non synonymous mutations respectively, when compared to their respective wildtype sequences (NM_006446, NM_019844 and NM_013272). They were corrected using the QuikChange Multi Site-Directed Mutagenesis kit (Stratagene).

Primers containing wild type SNPs were designed using Stratagene's QuikChange Primer Design Program, which designs primers to have similar annealing temperatures and GC content (Table 2). Sense strand primers were chosen for *SLCO1B1* and *SLCO1B3* whilst anti-sense primers were chosen for *SLCO3A1*. Primers were dissolved in nuclease free water to make concentrations of 3µM for *SLCO1B1* and *SLCO3A1* whilst concentrations of 6µM were made for *SLCO1B3*. The following reagents were assembled at room temperature: 10× QuikChange buffer (2.5µl, final concentration of 1×), dNTP mix (1µl), QuikSolution (0.25µl), respective plasmid DNA (100ng), primers

(*SLCO1B1/SLCO3A1*: 2µl of each, final concentration of each primer, 240nM, *SLCO1B3*: 2µl of each, final concentration of each primer, 480nM), 2.5U/µl QuikChange Multi enzyme blend (1µl, final concentration of 0.1U/µl) and nuclease free water up to a volume of 25µl. The reaction was cycled through the following parameters, 95°C for 1min, 30 cycles of 95°C for 1min, 55°C for 1min, 65°C for 12mins and hold at 4°C. The template plasmids were digested with DpnI (1µl, final concentration 0.38U/µl, 37°C for 1hr). The XL10-Gold ultracompetent cells were thawed on ice and divided into 45µl aliquots. Three aliquots were treated with β-mercaptoethanol mix (2µl) and incubated on ice (10mins, gently mixed every 2min interval). The DpnI treated *SLCO1B1*, *SLCO1B3* and *SLCO3A1* DNA (1.5µl) was added to the treated XL10-Gold cells and the mixture was incubated (30mins on ice). SOC medium was pre-warmed to 42°C and the cells were heat shocked in a water bath (30s, 42°C) and placed back on ice (2mins). The SOC medium (500µl) was added to the cells and the cells were incubated (37°C, 1hr, shaking 250rpm).

Table 2. Primers used for site-directed mutagenesis

Gene	Mutations	Primers
SLCO1B1	C296T	caaactacatagaccaaagttaattggaatcggttgtttcattatg
	G388A	caggtattctaaagaaactaatatcaattcatcagaaaattcaacatcgac
	C833T	ccattatttcttccataccattctttttcttgccccaaactcc
	G1541A	gtaactggtctccagaacagaaattactcagccca
	C1910T	tgggcttgtcttcaatgttaagagtctcatcacttgttttatatattatattaatttat
SLCO1B3	G334T	ccatgaagaaatgtggtaaagatgtcaaaatacttccagttcc
	A699G	tccaatatccacgtacattttagcaaacagagatcccagtg
SLCO3A1	C253T	ggttcccgatctcgaagctgctagcgatcac
	A604T and T605A	gcacgtggtcgtcgtagtaggagacgccca
	G1690A	agttcagggctgactgtcctgatgaggatgatg
	A1826G	ggcgccttgctccccacagaacgtgct
	G2111A	aaacggactccatgttttcacaccactcatggtct

3.2.14 Subcloning of *SLCO1A2* into pBluescriptII-KSM vector

The pBluescriptII-KSM vector, which contained X. laevis 5' and 3' β-globin UTR, was linearised by BglII (10× NEBuffer 3 (5μl, final concentration 1×), BglII enzyme, (1μl, final concentration 10U), pBluescript-KSM vector (1μg) and nuclease free water (up to 50μl, 37°C, 1hr). This was stabilised by using 1× Antarctic Phosphatase Reaction Buffer (6μl, final concentration 1×), Antarctic phosphatase (1μl, final concentration 5U), p-BluescriptII-KSM vector (1μg), nuclease free water (up to 60μl, incubation at 37°C, 15mins, heat inactivation 65°C, 5mins). *SLCO1A2* was digested from pCRII-TOPO-*SLCO1A2* by BglII, as for pBluescriptII-KSM vector and purified by agarose gel extraction (GenElute Gel Extraction kit, as per manufacturer's protocols). *SLCO1A2* was inserted in between the 5' and the 3' UTR of the pBluescriptII-KSM vector by T4 DNA ligase with a molar ratio of 3:1, *SLCO1A2* insert to p-Bluescript-KSM vector. The ligation product (10ng) was transformed into NEB5-α competent E. coli cells and plated on LB agar containing ampicillin (100μg/ml) and incubated (37°C, overnight). Colonies were picked, grown and plasmids were extracted for digestion according to manufacturer's protocol to verify insert orientation.

3.2.15 Subcloning of *SLCO1B1*, *SLCO1B3* and *SLCO3A1* into pBluescriptII-KSM

The subcloning of *SLCO1B1*, *SLCO1B3* and *SLCO3A1* required the digestion of pBluescriptII-KSM with SpeI, double digestion of *SLCO1B1*, *SLCO1B3* or *SLCO3A1* with SpeI and XbaI and the usage of a 1:1 molar ratio of insert to vector for ligation. pBluescriptII-KSM was digested with SpeI as follows: 10× NEBuffer 2 (5μl, final

concentration 1×), 100× BSA (0.5µl, final concentration 1×), SpeI enzyme (1µl, final concentration 10U), pCRII-TOPO-*SLCO1B1* (1µg) and nuclease free water (up to 50µl, 37°C). SpeI and XbaI digestion of the genes from pCRII-TOPO were performed as for SpeI digestion but with the inclusion of XbaI (1µl XbaI enzyme, final concentration 20U). The genes (DNA mixed with 6× crystal violet loading buffer (100µg/ml crystal violet, 20mM EDTA, 30% glycerol), final concentration 1×) was separated from the TOPO plasmid by crystal violet gel electrophoresis (40µl, crystal violet 2mg/ml, final concentration in 1.6µg/ml, 0.8% agarose gel) and isolated by using the GenElute Gel Extraction kit (as per manufacturer's protocol) and incubated with linear pBluescriptII-KSM (65°C, 5mins). The vector and insert was ligated and transformed in E. *coli* as for *SLCO1A2*.

3.3 Results

3.3.1 Construction of a *SLCO1A2* X. *laevis* oocyte expression vector

Optimisation of *SLCO1A2* showed that fragment 1 and fragment 2 annealing temperatures were optimal at 59°C and 56°C respectively. The products were visualised on agarose gel (1%) and bands were excised and purified using the GenElute Gel Purification kit. *SLCO1A2* with Kozak and BglII restriction sites were amplified from the gel purified products. These products were also visualised on agarose gels (1%), gel purified and ligated. The ligated product was approximately 2000bp.

Digestion of the *SLCO1A2* clone with BglII produced 4 bands, the largest being the full plasmid and the 3 smaller bands being the digest products (Table 3). The digest products were all the expected sizes 1kb, 2kb and 3kb (Fig. 2). The *SLCO1A2* clone sequence was aligned with wild-type (NM_134431) and no mutations were found.

The ligation of BglII digested *SLCO1A2* and BglII digested pBluescriptII-KSM vector produced numerous products. This included the desired product (5234bp) of one copy of *SLCO1A2* in the correct orientation in the pBluescriptII-KSM plasmid (Fig 3).

E. *coli* colonies containing pBluescriptII-KSM-*SLCO1A2* plasmids were verified by BamHI digestion (Table 3, Fig. 3), and one of the clones produced bands with the expected sizes and in the correct orientation. The pBluescriptII-KSM-*SLCO1A2* clone was further digested with BpmI to confirm findings in the BamHI digests. The digestion of a clone with BpmI also showed the expected band sizes (Table 3, Fig. 3).

Table 3. Predicted fragments post restriction digestion of plasmids.

Plasmid	Restriction enzyme	Predicted sizes (base pairs)
pCRII-TOPO-*SLCO1A2*	BglII	993, 2024, 2985
pCRII-TOPO-*SLCO1B1*	BamHI	1886, 4202
	BglII	1718, 4370
	BpmI	2011, 4077
	BstAPI	6088
	HindIII	659, 1294, 4135
pCRII-TOPO-*SLCO1B3*	BamHI	6102
	BglII	1732, 4370
	BpmI	2011, 4091
	BstAPI	1838, 4264
	HindIII	1953, 4149
pCRII-TOPO-*SLCO3A1*	BglII	1117, 5016
	NheI	6133
	BstAPI	1613, 4520
	NcoI	765, 2481, 2887
	StuI	6133
	XcmI	1387, 1690, 3056
pBluescriptII-KSM-*SLCO1A2*	BpmI	2239, 2995
	BamHI	454, 918, 3862
pBluescriptII-KSM-*SLCO1B1*	BpmI	2333, 3046
	NotI	2374, 3005
	BsrDI	174, 575, 1596, 3034
pBluescriptII-KSM-*SLCO1B3*	BpmI	2366, 3046
	NotI	2407, 3005
	BsrD1	174, 805, 835, 1596, 2002
pBluescriptII-KSM-*SLCO3A1*	NotI	3005, 2453

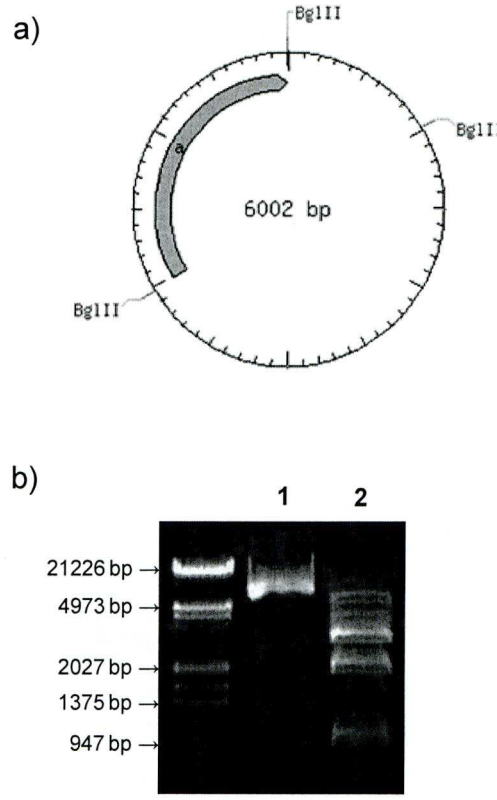

Fig. 2 Verification of TOPO-*SLCO1A2* by BglII restriction digest, a) a diagrammatic representation of TOPO-*SLCO1A2* with BglII restriction sites and b) agarose gel (1%) visualisation of TOPO-*SLCO1A2* clones with Sigma λ DNA EcoRI, HindIII digest ladder.

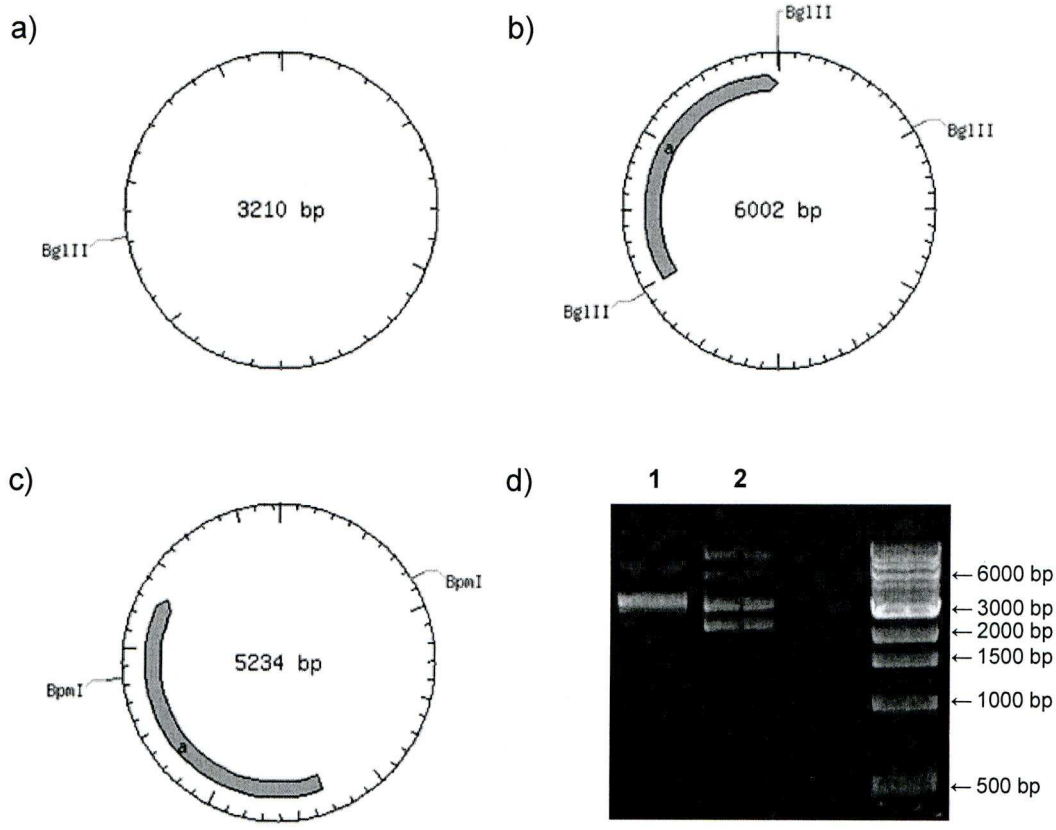

Fig. 3 Diagrammatic representation of *SLCO1A2* subcloning from pCRII-TOPO-*SLCO1A2* into pBluescriptII-KSM a) pBluescriptII-KSM with BglII restriction site, b) pCRII-TOPO-*SLCO1A2* with BglII restriction sites, c) pBluescriptII-KSM-*SLCO1A2* with BpmI restriction sites and d) verification of pBluescriptII-KSM-*SLCO1A2* clones by BpmI digestion visualised on agarose gel (1%) with NEB 1kb ladder.

3.3.2 Construction of a *SLCO1B1* X. *laevis* oocyte expression vector

Preliminary optimisation of *SLCO1B1* with UTR primers by gradient PCR using A549 cDNA showed that the optimal annealing temperature was 62°C. *SLCO1B1* with UTR was successfully amplified from Huh7 cDNA using an annealing temperature of 62°C. Clones of *SLCO1B1* with UTR insert were digested with HindIII and one clone produced the expected digest pattern. Further digests of this clone using BamHI, BglII, BpmI and NsiI also produced expected banding patterns (Table 3).

SLCO1B1 was amplified using inner forward primer and UTR reverse with 62°C annealing temperature. The gel purified PCR product was amplified using Kozak forward primer and UTR reverse primer and an annealing temperature of 62°C. *SLCO1B1* clones containing Kozak consensus were digested with HindIII. All the clones except one clone produced the expected banding patterns. Further digests of one of the *SLCO1B1* clones using BamHI, BglII, BstAPI and HindIII (Table 3) produced the expected banding patterns (Fig. 4).

Alignment of *SLCO1B1* with the published wild-type revealed there were 7 mutations. The non-synonymous mutations were T296C, A388G (published polymorphism, rs2306283), T833C, A1541G and T1910C and the synonymous mutations were C571T and C597T. *SLCO1B1* site-directed mutagenesis clones were sent for sequencing by GATC and alignment of clone sequences with wild-type showed that one clone was successfully reverted to the wild-type sequence. The pBluescriptII-KSM-*SLCO1B1* plasmids were digested with NotI, which produced several plasmids with the expected

band pattern (Table 3). Further digestion of the clone with BpmI and BsrDI also showed the expected band sizes (Table 3, Fig. 5).

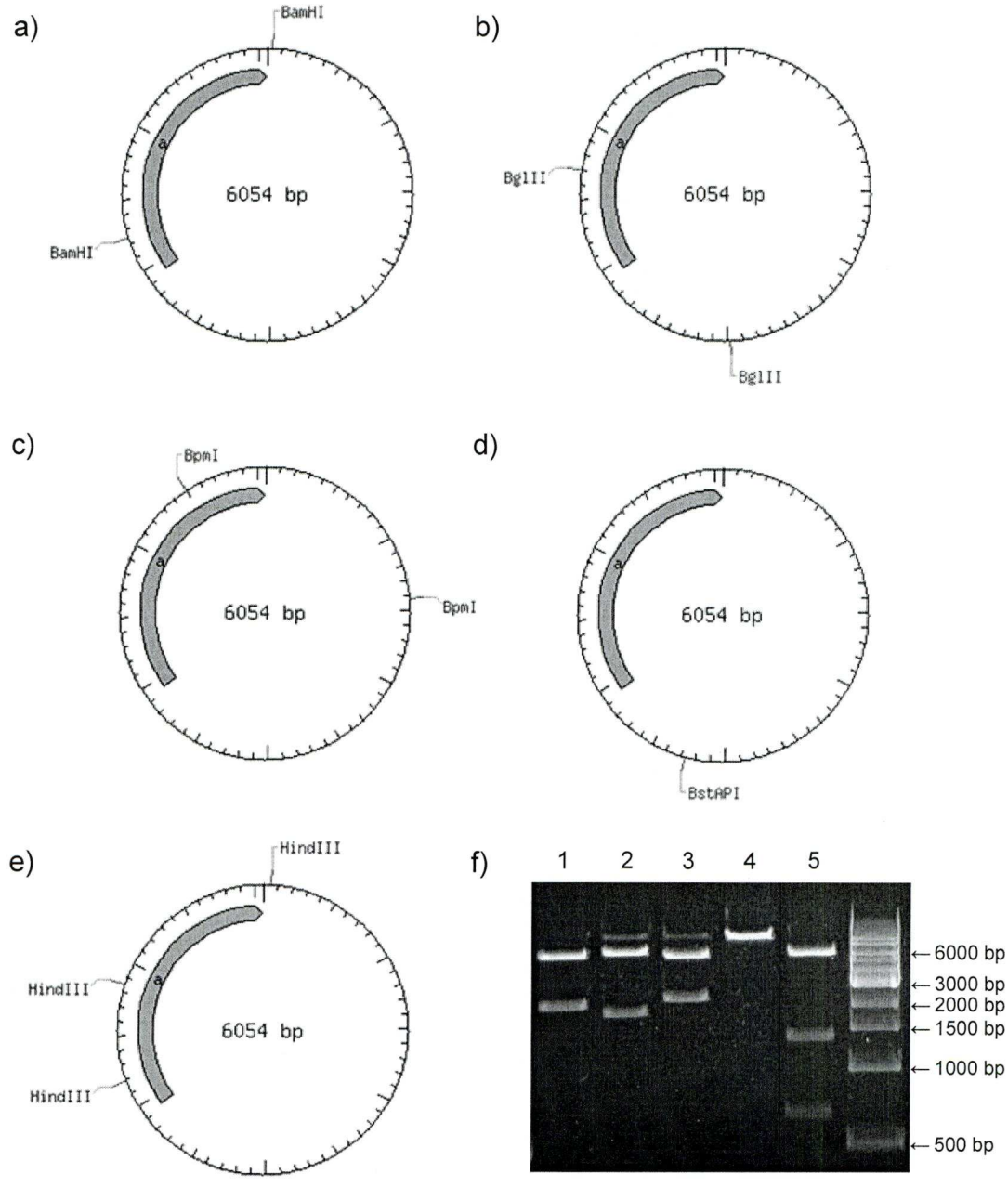

Fig. 4 Verification of TOPO-*SLCO1B1* by BamHI, BglII, BpmI, BstAPI and HindIII restriction digest, a diagrammatic representation of TOPO-*SLCO1B1* with a) BamHI restriction sites, b) BglII restriction sites, c) BpmI restriction sites, d) BstAPI restriction site, e) HindIII restriction sites and f) agarose gel (1%) visualisation of TOPO-*SLCO1B1* clones digested with BamHI (1), BglII (2), BpmI (3), BstAPI (4) and HindIII (5) with NEB 1kb ladder.

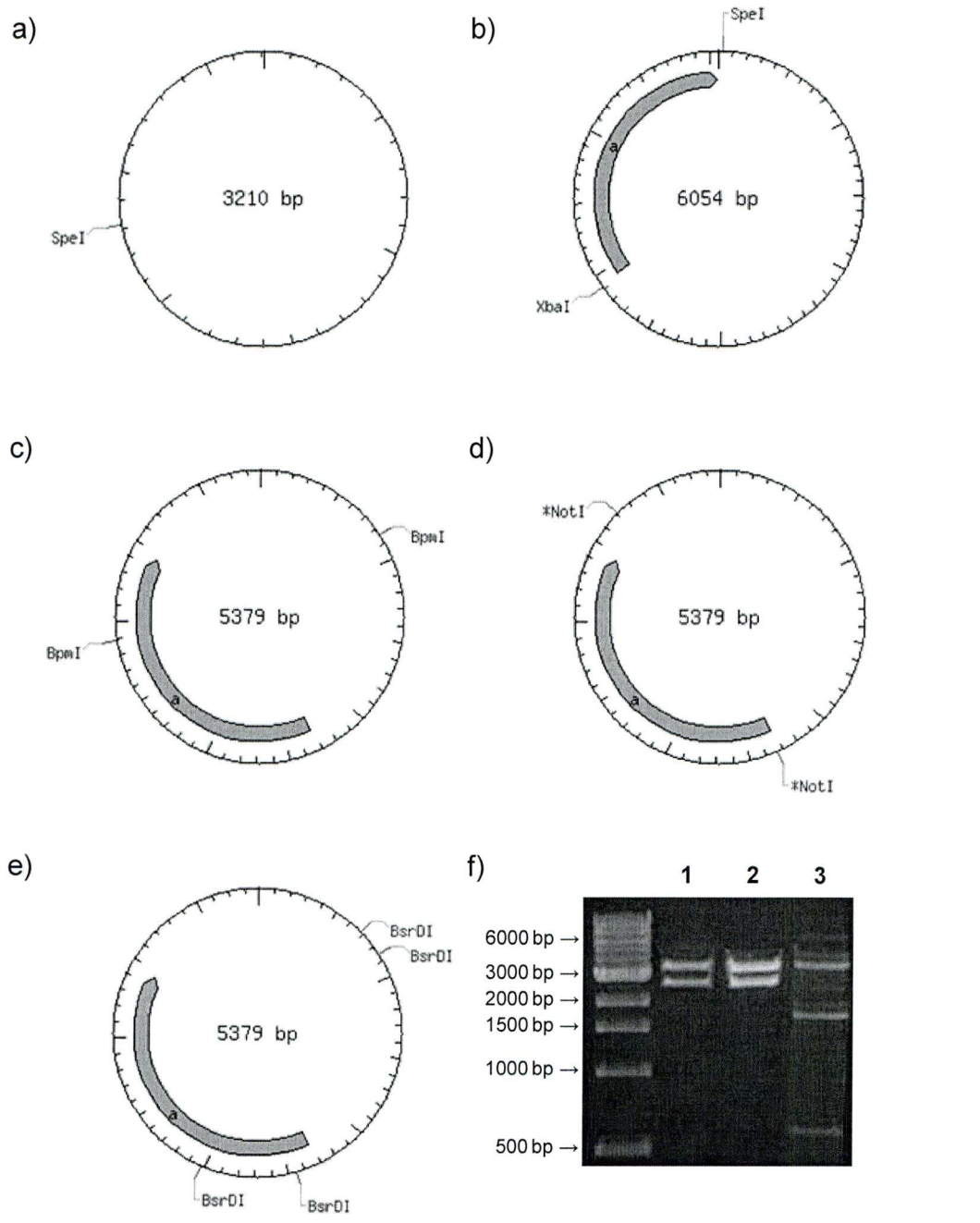

Fig. 5 Diagrammatic representation of *SLCO1B1* subcloning from pCRII-TOPO-*SLCO1B1* into pBluescriptII-KSM a) pBluescriptII-KSM with SpeI restriction site, b) pCRII-TOPO-*SLCO1B1* with SpeI and XbaI restriction sites, c) pBluescriptII-KSM-*SLCO1B1* with BpmI restriction sites, d) pBluescriptII-KSM-*SLCO1B1* with NotI restriction sites, e) pBluescript-KSM-*SLCO1B1* with BsrD1 restriction sites and f) verification of pBluescriptII-KSM-*SLCO1B1* clone by BpmI (1), NotI (2) and BsrDI (3) digestion visualised on agarose gel (1%) with NEB 1kb ladder.

3.3.3 Construction of a *SLCO1B3* X. *laevis* oocyte expression vector

The optimal annealing temperature for *SLCO1B3* amplification from A549 cDNA using UTR forward and reverse primers was 66°C. Amplification of *SLCO1B3* from Huh7 cDNA using UTR forward and reverse primers was successful as a 2000bp band was observed. *SLCO1B3* with UTR clones were digested with HindIII and five clones produced digests with the expected banding patterns (Table 3). Further digests with these clones using BpmI, BglII and BamHI showed that four clones had the expected banding patterns (Table 3).

SLCO1B3 was amplified from Huh7 cDNA using inner forward and UTR reverse primers successfully. *SLCO1B3* amplification using Kozak forward and UTR reverse was successful. *SLCO1B3* clones were verified by HindIII digest and all the clones produced the expected banding pattern. The *SLCO1B3* with Kozak consensus clone was further digested and yielded the expected banding patterns when digested with BamHI, BglII, BpmI, BstAPI and HindIII (Fig. 6). The *SLCO1B3* clone alignment with wild-type sequence showed that the clone contained two non-synonymous mutations, T334G (rs4149117) and G699A (rs7311358), which have been documented (Letschert et al, 2004) and 2 synonymous mutations G33A and A1557G.

Four *SLCO1B3* site-directed mutagenesis clones were sent for sequencing by GATC and alignment of clone sequences with wild-type showed that one clone was successfully reverted to the wild-type sequence. The pBluescriptII-KSM-*SLCO1B3* plasmids were digested with EcoRI and the clone produced the correct banding pattern (Table 3).

Further digests were performed with BglII, BpmI, BsrDI and NcoI (Table 3) for verification (Fig. 7).

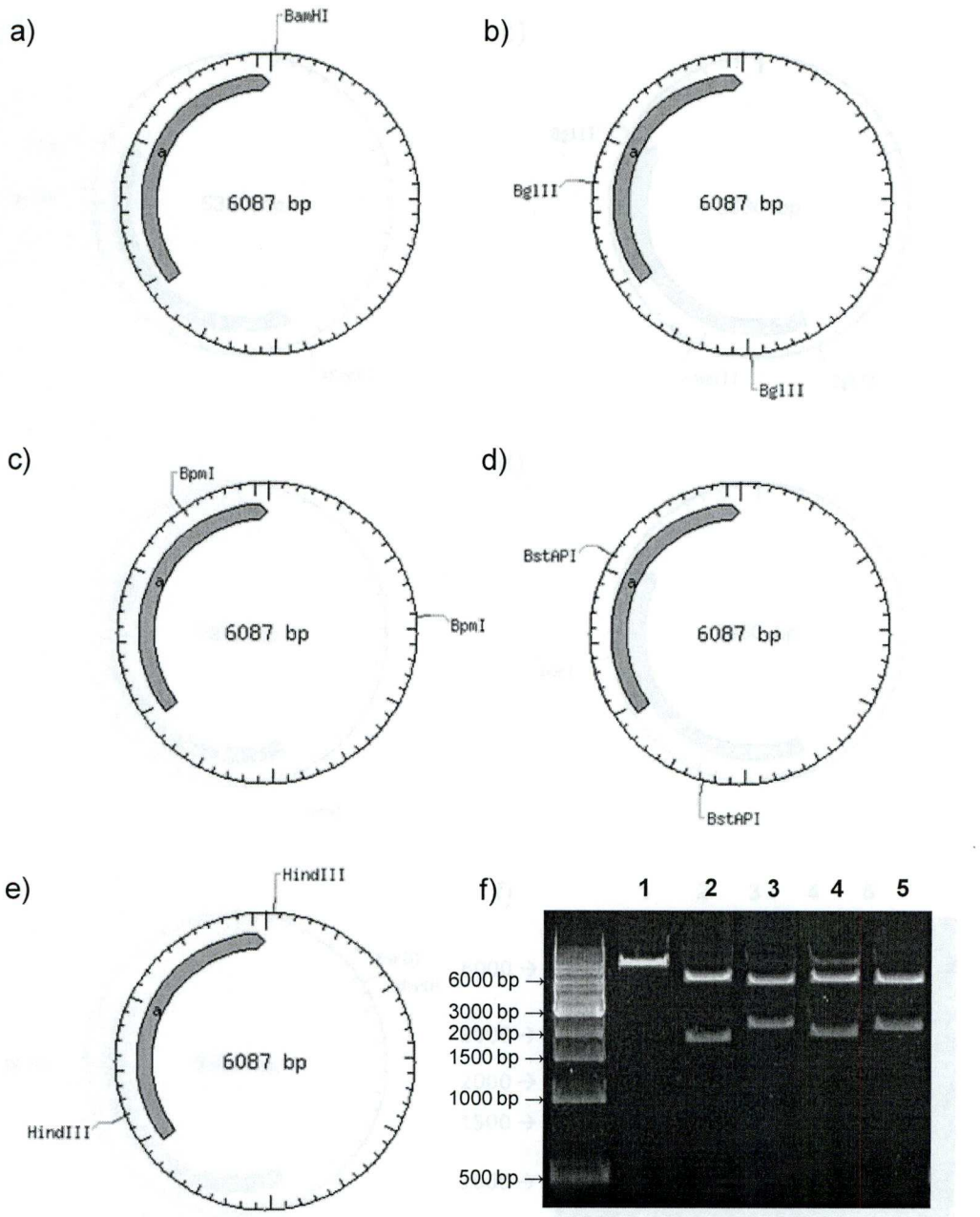

Fig. 6 Verification of TOPO-*SLCO1B3* by BamHI, BglII, BpmI, BstAPI and HindIII restriction digest, a diagrammatic representation of TOPO-*SLCO1B3* with a) BamHI restriction sites, b) BglII restriction sites, c) BpmI restriction sites, d) BstAPI restriction site, e) HindIII restriction sites and f) agarose gel (1%) visualisation of TOPO-*SLCO1B3* clones digested with BamHI (1), BglII (2), BpmI (3), BstAPI (4) and HindIII (5) with NEB 1kb ladder.

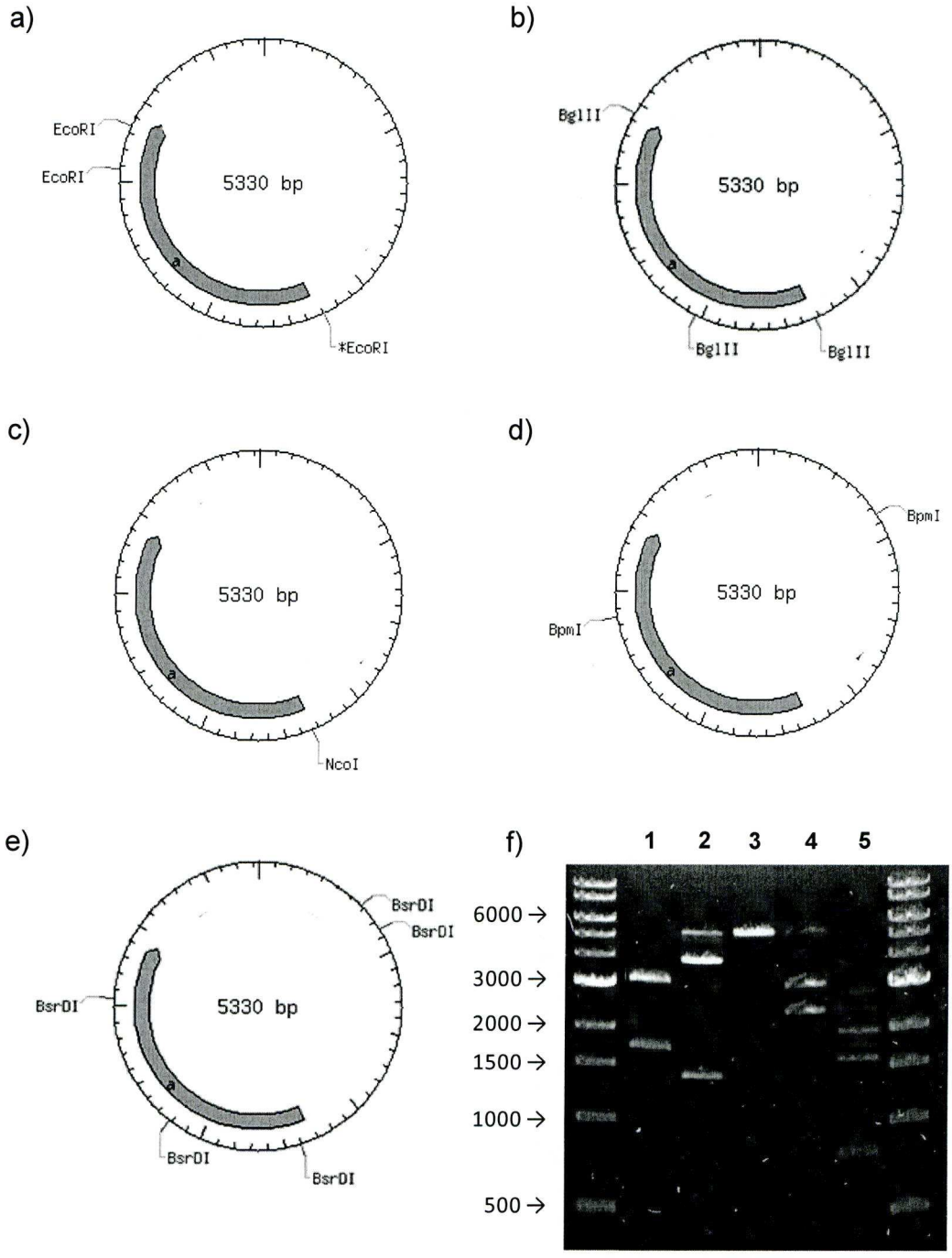

Fig. 7 Diagrammatic representation of pBluescriptII-KSM-*SLCO1B3* restriction digest by a) EcoRI b) BglII, c) NcoI, d) BpmI and e) BsrD1 and f) verification of pBluescriptII-KSM-*SLCO1B3* clone by EcoRI (1), BglII (2), NcoI (3), BpmI (4) and BsrDI (5) digestion visualised on agarose gel (1%) with NEB 1kb ladder.

3.3.4 Construction of a *SLCO3A1* X. *laevis* oocyte expression vector

Preliminary *SLCO3A1* PCRs revealed 66°C as the optimal annealing temperature. *SLCO3A1* was successfully amplified from the pSPORT-*oatp1-OATP4* plasmid using the *SLCO3A1* Kozak forward primer and the *oatp1*-UTR reverse primer when DMSO was used. Subsequent cloning into TOPO was also successful when verified by restriction digest using BglII, NheI, BstAPI, NcoI, StuI and XcmI (Table 3, Fig. 8), followed by sequencing of the clone. Alignment of this clone with wild-type *SLCO3A1* revealed that 6 non synonymous (C253T, A604T, T605A, G1690A, A1826G, G2111A) and 2 synonymous mutations (C361T, C1716T) were present.

After one multi site-directed mutagenesis reaction, eight clones were sent for sequencing, of which seven clones had positions C253T, A1826G and G2111A successfully reverted to wild type. One clone had only positions C253T and G2111A reverted back to wild type. One clone was picked for a repeated multi site-directed mutagenesis reaction but only with primers A604T_T605A and G1690A. Three clones were sent for sequencing and once aligned two clones were revealed to have reverted to wild type at all 6 positions.

The pBluescript-KSM-*SLCO3A1* plasmids were digested with NotI and four clones contained the predicted band sizes (Table 3, Fig. 9). Two clones were selected for sequencing to verify the orientation of the insert and both clones contained the insert in the correct orientation. One of these was stored and used for subsequent applications.

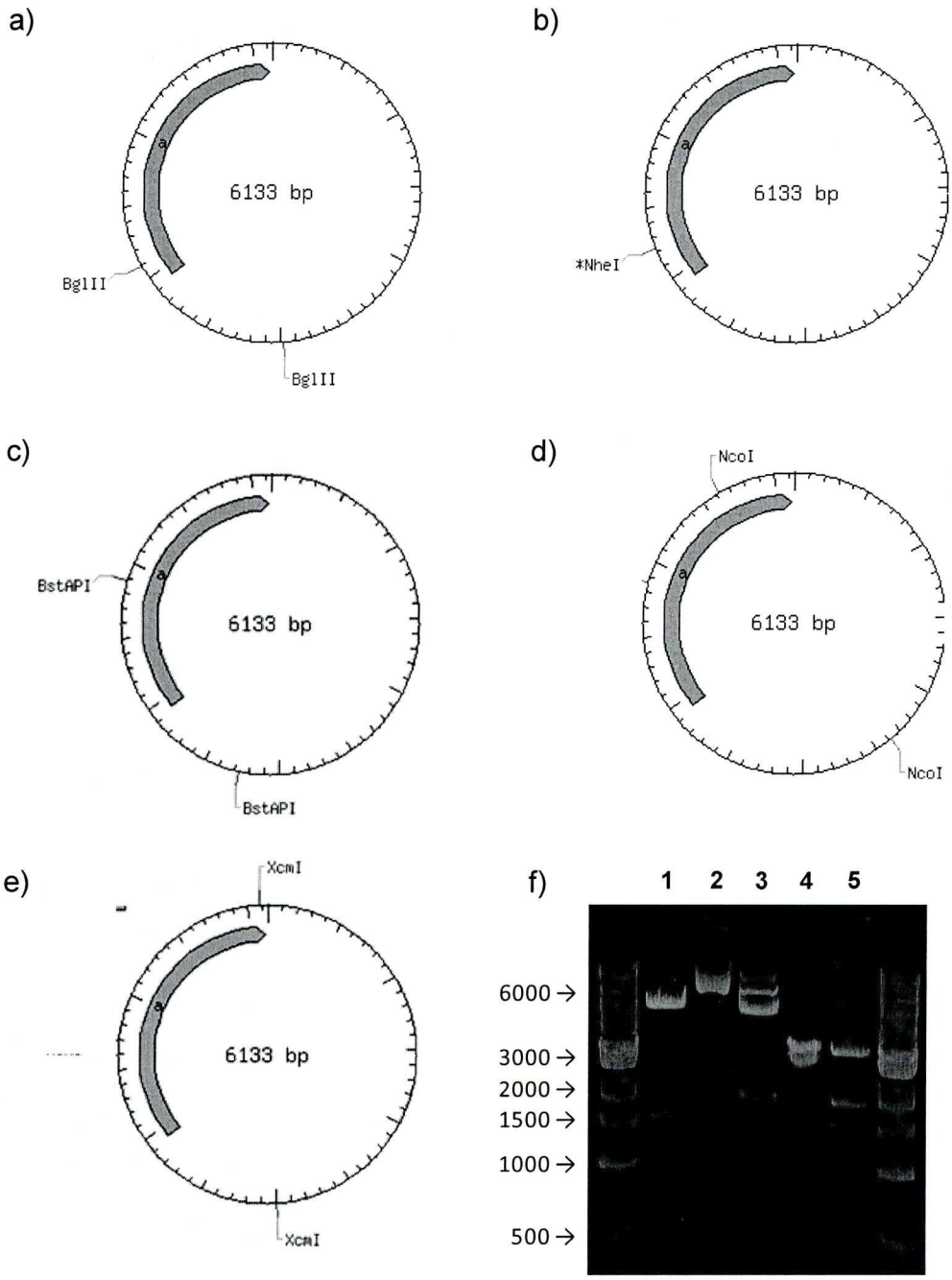

Fig. 8 Verification of TOPO-*SLCO3A1* by restriction digest, a diagrammatic representation of TOPO-*SLCO3A1* with a) BglII restriction sites, b) NheI restriction sites, c) BstAPI restriction sites, d) NcoI restriction site, e) XcmI restriction sites and f) agarose gel (1%) visualisation of TOPO-SLCO3A1 clone 1 digested with BglII (1), NheI (2), BstAPI (3) NcoI (4) and XcmI (5) with NEB 1kb ladder.

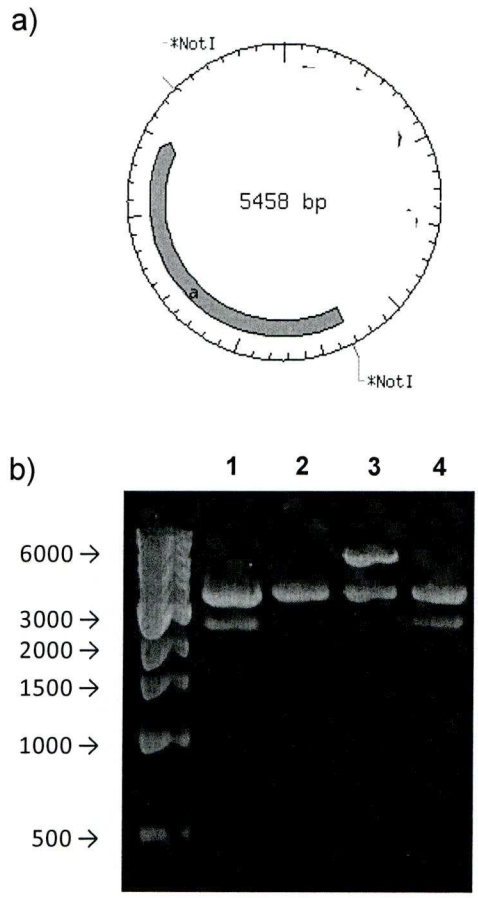

Fig. 9 Verification of pBluescriptII-KSM-*SLCO3A1* a) a diagrammatic representation of pBluescriptII-KSM-*SLCO3A1* with NotI restriction sites, b) visualisation of pBluescriptII-KSM-*SLCO3A1* clones (1 to 4) digestion by NotI on agarose gel (1%) with NEB 1kb ladder.

3.4 Discussion

The transport of many antiretrovirals by efflux transporters has been well defined but antiretrovirals have yet to be characterised as substrates for influx transporters. SLCO transporters have been shown to affect plasma concentration and drug clearance of some xenobiotics and hence it is important to characterise the transport of antiretrovirals by influx transporters. It has been reported that statins are substrates for SLCO1A2, SLCO1B1 and SLCO1B3 (Hirano *et al.* 2004; Fujino *et al.* 2005) and PIs have also been shown to interact with statins and alter their pharmacokinetics (Busti *et al.* 2008; Kiser *et al.* 2008) but these interactions have yet to be linked directly to SLCO transport. SLCO1A2, SLCO1B1, SLCO1B3 and SLCO3A1 are organic anion transporters, with varying tissue distribution. The differences in expressions of these transporters may have the potential to explain variability in the pharmacokinetics and pharmacodynamics of antiretrovirals.

Human genes are available from cDNA libraries, which can be purchased commercially and the advantage of using these libraries is the efficiency of amplification from them. Many SLCOs have been cloned by other research groups using commercially available cDNA libraries (Tamai *et al.* 2000; Kullak-Ublick *et al.* 2001; Huber *et al.* 2007). Alternatively, genes can be cloned from cell lines or primary tissues (Tirona *et al.* 2001) which express the genes of interest and this approach was adopted for this chapter.

Cloning of full length *SLCO1A2* gene from A549 was unsuccessful because we were unable to amplify the correct fragment. Therefore, additional primers were designed to amplify the gene in two fragments. The primers overlap at an NsiI restriction site to allow digestion of the fragments by NsiI and ligation to form the whole *SLCO1A2 gene*.

This method of ligating gene fragments to produce full length cDNA was also utilised by Konya *et al.* (2006), who cloned *ABCB1* by ligating 5 gene fragments. The Kozak consensus (CCACC) and BglII restriction sites were added to the gene, because the Kozak consensus is highly conserved in mammalian genes and greatly improves the initiation of translation of mRNA (Kozak 1987). The Kozak consensus is described as GCCRCCATGG, where ATG is the start codon and with 97% conservation in vertebrates (Kozak 1987). Engineering BglII restriction sites to flank the gene allowed easier recovery from the vector. pCRII-TOPO-*SLCO1A2* was verified by sequencing and no mutations were found. Subcloning of *SLCO1A2* into pBluescriptII-KSM was also successful as shown by a selection of restriction digests.

The pCRII-TOPO vector was used for the initial cloning step due to ease of use. The vector is supplied as a linear plasmid and contains DNA topoisomerase I, which is covalently bonded to 3' T bases of the plasmid to facilitate fast ligation of *Taq* amplified PCR products, as they contain extra A overhangs (Invitrogen 2004). The plasmid has the lacZ operon, which allows blue-white screening of clones. Ampicillin and kanamycin resistance genes are also in the plasmid to allow antibiotic selection of bacterial cultures (Invitrogen 2004). The pCRII plasmid contains dual promoters, T7 and Sp6, which allows *in vitro* transcription without directional cloning (Invitrogen 2004).

The pBluescriptII-KSM vector has 5' and 3' X *laevis* β-globin UTR flanking the multiple cloning site to increase the translational efficiency of the gene of interest and has also been used by other research groups using the X *laevis* expression model (Beck *et al.* 2002; Virkki *et al.* 2002). It also has an ampicillin resistance gene for selection in bacteria cultures and contains the T3 promoter for *in vitro* transcription. Other X laevis

expression vectors have been used by other groups such as the pBSTA plasmid (Very *et al.* 1995) and the pXBG plasmid (Preston *et al.* 1992; Francis *et al.* 2000) which also contains the 3' and 5' X *laevis* β-globin UTR flanking the multiple cloning site.

SLCO1B1 and *SLCO1B3* were cloned from Huh7 (human hepatic cell line) mRNA because amplification from A549 (human lung cell line) was unsuccessful. This may be due to the expression levels of *SLCO1B1* and *SLCO1B3* as these genes have been found to be highly expressed in hepatocytes (Jung *et al.* 2001; Bleasby *et al.* 2006). Nested PCR of *SLCO1B1* and *SLCO1B3* from Huh7 cDNA using UTR primers during the initial round of PCR, followed by a second round of PCR using forward gene primers (comprising of the first 21bps) and UTR reverse primers were unsuccessful. However, amplification of *SLCO1B1* and *SLCO1B3* using UTR primers were successful and these PCR products were cloned into pCRII-TOPO.

SLCO1B1 and *SLCO1B3* genes were successfully amplified using the forward gene primers with UTR reverse primers and the plasmids as templates. All PCR products were gel purified and amplified using UTR forward and UTR reverse primers. The agarose gels used for gel purification were stained with crystal violet instead of ethidium bromide, as crystal violet can be visualised without the use of UV and thus reduces the damage to the DNA (Turgut-Balik *et al.* 2005). Maintaining the integrity of the DNA improves the cloning efficiency and is particularly important with larger PCR products (Turgut-Balik *et al.* 2005). The resulting product was cloned into pCRII-TOPO and verified by sequencing. The second step of amplification, which removes the UTR from the genes, worked well when using the plasmids as templates as opposed to gel purified PCR products. This may be due to higher purity of the template when using mini-prep

extracted plasmids, whilst PCR products from tissues and cell lines may contain non-specific DNA sequences and the gene of interest. Furthermore, gel purification often has lower yields and poorer quality of DNA due to electrophoresis and with ethidium bromide staining in particular, there is increased UV damage.

The site-directed mutagenesis reaction to convert 5 non-synonymous mutations present in *SLCO1B1* and 2 non-synonymous mutations in *SLCO1B3* into the wild-type sequence was successful as verified by sequencing. *SLCO1B1* and *SLCO1B3* clones with the wildtype sequences were subcloned into pBluescriptII-KSM vector.

Cloning of *SLCO3A1* from A549 and Huh7 was unsuccessful. Therefore, the pSPORT1-*oatp1-OATP4* plasmid was used as a template for PCR. Using the standard reaction mixture on a gradient PCR did not yield the correct band, but the inclusion of DMSO into the reaction gave the expected band. The use of DMSO as a PCR additive is common as DMSO has been shown to inhibit secondary structures and self complementarity of DNA and thus improve the efficiency of amplification (Winship 1989; Hube *et al.* 2005). The difficulty in amplification of *SLCO3A1*, which was resolved by the use of DMSO, is likely to be due to the GC-rich regions within the *SLCO3A1* gene. The *SLCO3A1* PCR product was subsequently cloned into pCRII-TOPO and verified by sequencing. Site directed mutagenesis reactions were performed to convert *SLCO3A1* into wildtype, which was verified by sequencing. The clone which contained the *SLCO3A1* wildtype gene was used to subclone *SLCO3A1* into pBluescriptII-KSM.

Cloning is an important process for building transporter cDNA libraries, from which the function of individual transporters can be assessed. There are a number of systems used for assessing functionality of proteins such as stable and transient transfections of cell lines and the X. *laevis* oocyte model, it is the latter model which is used in subsequent studies.

Chapter 4

Assessing the impact of SLCO transporters on the cellular accumulation of antiretrovirals in X. *laevis* oocytes

The impact of SLCOs on antiretroviral accumulation in X. *laevis* oocytes

4.1 Introduction

X. *laevis* oocytes were first used to analyse ion channels and have since been used extensively as a model for functional expression of integral membrane proteins (Sigel, 1990). This model is favoured for evaluating transporters, as oocytes can be micro-injected with extracted mRNA from other cells or synthesised cRNA, and adequate expression of many transporters, including the SLCOs is achieved after 3 days (Mahagita *et al.* 2007; Anderson *et al.* 2008; Markovich 2008). The main advantages of this system over other functional models are low levels of endogenous transporters, expression of most mammalian proteins with a high efficiency (Sigel 1990; Xia *et al.* 2007) and the ease of handling as the oocytes are large cells, approximately 1000nl (Wilhelm *et al.* 2000). This model has been used for characterising interactions between transporters, their substrates and inhibitors, leading to subsequent studies on the effect of relevant polymorphisms (Badagnani et *al.* 2006; Smith *et al.* 2007).

Influx transporters are easier to assess using the X. *laevis* oocytes than efflux transporters, the latter requiring pre-loading of the compound of interest into the oocyte prior to drug transport experiments. There are two main ways to assess the presence of translated protein in injected oocytes, either by analysis of oocyte membrane expression or functional assessment by known radioactive substrates.

Increasing numbers of influx transporters are being identified but antiretrovirals are yet to be characterised for influx transport. Saquinavir (SQV) has been reported to be a substrate of *SLCO1A2* using X. *laevis* oocytes and the transfected HepG2 model (Su *et*

al. 2004). It is important to evaluate antiretrovirals as substrates for influx, as these transporters also have the potential to alter pharmacokinetics of compounds.

The aim of this chapter was to develop a X. *laevis* model for evaluating antiretrovirals as substrates of SLCO transporters. Vectors described in Chapter 3 were used for this analysis. The panel of compounds investigated included SQV, which has been well characterised for several transporters; other commonly used antiretrovirals such as lopinavir (LPV), efavirenz (EFV) and nevirapine (NVP); and more recently licensed or experimental compounds such as darunavir (DRV) and rilpivirine. Since estrone-3-sulphate (E3S) has been reported to be an endogenous substrate for various SLCOs, including SLCO1A2, SLCO1B1 and SLCO1B3 (Tamai *et al.* 2000), and prostaglandin E2 (PGE2) has been shown to be a substrate for SLCO3A1 (Adachi *et al.* 2003; Huber *et al.* 2007), these compounds were included as paradigm control substrates.

4.2 Methods

4.2.1 Materials

T3 and Sp6 mMessage mMachine Transcription kits were purchased from Ambion (Europe) Ltd. (Huntingdon, UK). Ultima Gold scintillation fluid was purchased from Perkin Elmer (Boston, USA). NaCl, HEPES, PS, $CaCNO_3 \cdot 6H_2O$, $CaCl_2 \cdot 6H_2O$ and KCl (Fluka) was purchased from Sigma-Aldrich Company Ltd (Poole, UK). $MgSO_4 \cdot 7H_2O$ was purchased from (BDH) VWR (Leicestershire, UK). Restriction enzymes were purchased from New England Biolabs (Hitchen, UK). Adult female X. *laevis* frogs were purchased from Xenopus Express (Lyon, France).

[^{3}H] E3S (specific activity, 50Ci/mmol) was purchased from American Radiolabeled Company Inc. (Missouri, USA), [^{3}H] PGE2 (specific activity, 184Ci/mmol) was purchased from GE Healthcare (Buckinghamshire, UK), [^{3}H] SQV (specific activity, 1Ci/mmol), [^{3}H] LPV (specific activity, 1Ci/mmol), and [^{3}H] NVP (specific activity, 1.6Ci/mmol) was purchased from Moravek Chemicals (California, USA). [C^{14}] DRV (specific activity, 0.21mCi/mmol) and [^{3}H] rilpivirine (specific activity, 20mCi/mmol) was provided by Tibotec (Mechelen, Belgium) and [^{14}C] EFV (specific activity, 12.7μCi/μmol) was provided by Bristol-Myers-Squibb. pBluescriptII-KSM was a kind gift from WJ Joiner (Yale University, Connecticut, USA).

4.2.2 Experimental strategy for expressing SLCOs

Ovary lobes were extracted from adult female Xenopus *laevis* frogs. Initial experiments (*SLCO1A2*-TOPO, *SLCO1A2*-KSM, *SLCO1B1*-KSM injected oocytes with respective water injected controls) were conducted using oocytes extracted by collagenease treatment and oocytes were incubated for 3 days post injection. The platinum loop extraction method was trialled using *SLCO1B1*-KSM cRNA. *SLCO1B3*-KSM and *SLCO3A1*-KSM injected oocytes were extracted using the platinum loop method and the effect of the number of days post injection was investigated. The overall strategy is illustrated in Fig. 1

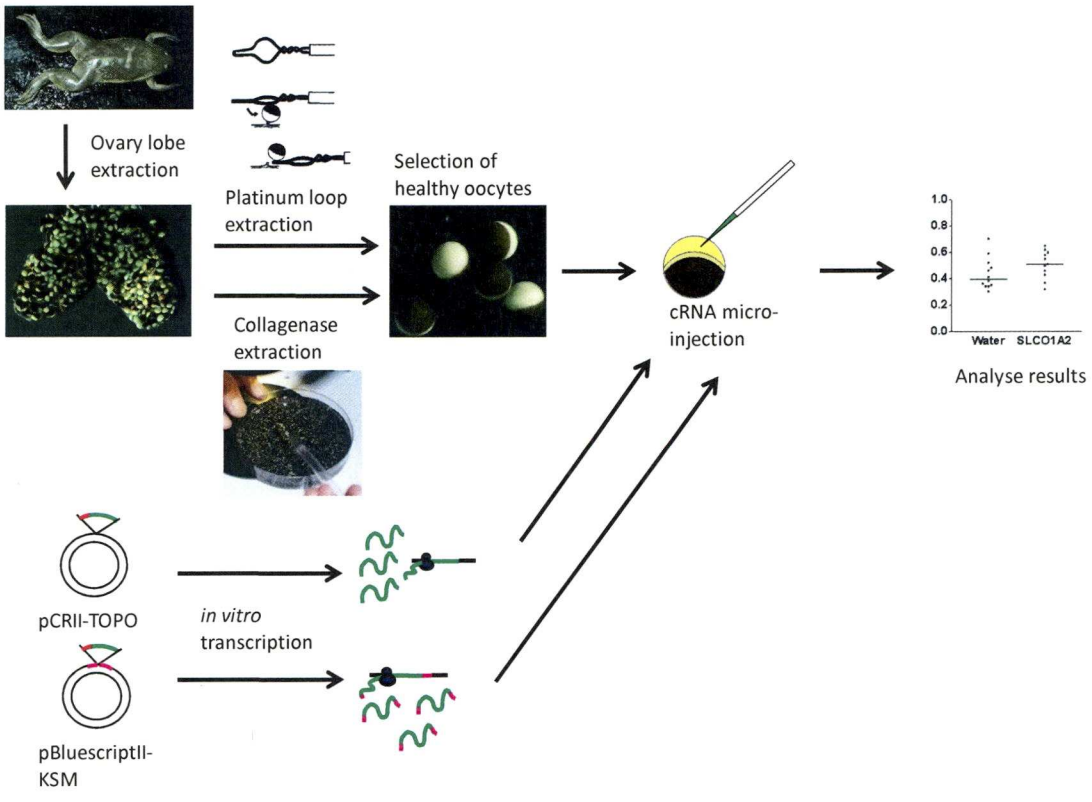

Fig. 1 The experimental strategy for expression of SLCOs in X. *laevis* oocytes.

4.2.3 *In vitro* transcription

The Sp6 mMessage mMachine *in vitro* transcription kit was used to generate *SLCO1A2* cRNA. TOPO-*SLCO1A2* was linearised with PflF1 (1× final concentration of NEBuffer 4, 1× BSA, 0.2U/µl, 1µg DNA, 37°C, 1 hr) and purified using GenElute PCR Clean-Up kit. The linearised DNA was concentrated by LiCl DNA precipitation, 8M LiCl was added to the DNA (final concentration LiCl 800mM, 30mins), precipitated with isopropanol (equal volume, centrifuge 13000 × g, 4°C, 15mins) and washed with absolute ethanol (1ml, centrifuge 13000 × g, 4°C, 15mins). The DNA pellet was solubilised in nuclease free water to a concentration of 1µg/µl. 10X Reaction Buffer (10µl, 1× final concentration, room temperature), 2× NTP/CAP (2µl, 1× final concentration), template DNA (1µg), RNA Polymerase Enzyme Mix (1µl) and nuclease-free water (up to 20µl) were assembled at room temperature and incubated (37°C, 2 hours). The DNase treatment was performed following the incubation (1µl TURBO DNase, 37°C, 15mins). The cRNA was purified by LiCl precipitation. The reaction mix was incubated with nuclease-free water (30µl) and LiCl precipitation solution (30µl, -20°C, 30mins). The mixture was centrifuged (13000 × g, 4°C, 15mins) to pellet the cRNA. The supernatant was removed and the pellet was washed with ethanol (70%, 1ml) and again centrifuged (13000 × g, 4°C, 15mins). The ethanol was removed and the pellet was resuspended in nuclease-free water, quantified with spectrophotometry and diluted to 1µg/µl and stored in aliquots (5µl, -80°C).

The T3 mMessage mMachine *in vitro* transcription kit was used to generate SLCOs with 5' and 3' flanking UTR cRNA from pBluescriptII-KSM. The pBluescriptII-KSM-*SLCO1A2*, pBluescriptII-KSM-*SLCO1B1*, pBluescriptII-KSM-*SLCO1B3* and

pBluescriptII-KSM-*SLCO3A1* plasmids were linearised with SacI (1× final concentration of NEBuffer 1, 1× BSA, 1µg DNA, 37°C, 10mins) and purified using the GenElute PCR Clean-Up kit. The following procedures were the same as using the Sp6 kit except the enzyme mix and reagents used were for T3 transcription.

4.2.4 X. *laevis* maintenance

Adult female X. *laevis* frogs were kept in fresh water and cleaned once a week. Frogs were handled with a net and fed dried frog pellets twice a week. Frogs were sacrificed by an anaesthetic solution (MS222, 5g/l, 45mins).

4.2.5.1 X. *laevis* oocyte isolation by collagenase treatment

Oocytes were isolated by dissection of the abdomen of the frog and excising ovary lobes with forceps into Barth's solution without calcium (NaCl 88mM, KCl 1mM, HEPES 15mM, pH 7.6) containing collagenase (1mg/ml, shaking, 2h). The oocytes were washed twice with Barth's solution without calcium, followed by a wash with Barth's solution containing calcium (NaCl 88mM, KCl 1mM, HEPES 15mM, $CaCNO_3 \cdot 6H_2O$ 0.3mM, $CaCl_2 \cdot 6H_2O$ 41µM, $MgSO_4 \cdot 7H_2O$, 0.82mM, pH 7.6). The cells were incubated (18°C 1h) and healthy stage V-VI oocytes were selected and maintained in Barth's solution with calcium and PS (10µg/ml, 18°C, overnight).

4.2.5.2 X. *laevis* oocyte isolation by platinum loop extraction

Oocytes were isolated by dissection of the abdomen of the frog and excising ovary lobes with forceps into Barth's solution with calcium and PS and individual oocytes were picked using a platinum loop. Healthy stage V-VI cells were selected, placed into fresh Barth's with calcium and PS (10µg/ml) and incubated overnight (18°C).

4.2.6 X. *laevis* microinjection

Needles were made from thin wall glass capillaries (1mm diameter, 102mm length) using the PUL-1 machine (World Precision Instruments). One needle was loaded onto the micro-manipulator and trimmed using forceps. *SLCO1A2*-TOPO (1µg/µl, 7.5µl, TOPO origin) or DEPC treated water (7.5µl) was loaded into the needle by the vacuum pump DA7C (Charles Austen Pumps) and held in the needle using the picopump PV830 (World Precision Instruments) supplied with compressed air. The drop size of the sample was calibrated to one third the size of an oocyte (~50nl). Twenty oocytes were injected per condition and uptake was performed 3 days following injection. *SLCO1A2*-KSM and *SLCO1B1*-KSM cRNA were also injected (as described above) into oocytes isolated by the collagenase treatment.

SLCO1A2-KSM, *SLCO1B1*-KSM, *SLCO1B3*-KSM and *SLCO3A1*-KSM were injected as described, into cells which were isolated with the platinum loop extraction method. These cells were incubated 3-5 days following injection and were treated with collagenase (1mg/ml, shaking, 20mins) 2-3hrs prior to the uptake experiments.

4.2.7 Uptake experiments using X. *laevis* oocytes

Radiolabelled drugs were diluted in Hanks balanced salt solution and oocytes were incubated (room temperature, 1hr, in eppendorfs) with either of the following: [^{3}H] E3S (1μM, 0.33μCi/ml), [^{3}H] SQV (1μM, 0.33μCi/ml), [^{3}H] LPV (1μM, 0.33μCi/ml), [^{14}C] DRV (3μM, 0.60μCi/ml), [^{14}C] EFV (1μM, 0.33μCi/ml), [^{3}H] NVP (1μM, 0.33μCi/ml), or [^{3}H] rilpivirine (3μM, 1.18μCi/ml) in the presence or absence of HSA (HSA, 2%). After incubation, oocytes were transferred into cell strainers and washed with ice cold Hanks balanced solution (3 wells in a 6 well plate) and individual oocytes were transferred into scintillation vials. Scintillation fluid was added to the vials and radioactivity was counted by liquid scintillation spectroscopy (Packard 1900CA Tri-Carb Liquid Scintillation Analyser).

SLCO1A2/1B1/1B3/3A1 with X. *laevis* β-globin UTR flanking region cRNA (50nl, 1μg/μl) or DEPC water was injected into oocytes. Uptake was performed using the same compounds and relative concentrations as above and in the presence and absence of human serum albumin (HSA, 2%) in a 24 well plate (<10 oocytes per condition, room temperature, 1hr, 1 well in a 24 well plate, shaking 150rpm). After incubation, oocytes were washed as above, lysed with 10% SDS and scintillation fluid was added. Radioactivity was then counted by liquid scintillation spectroscopy.

The time at which optimal expression was present for *SLCO1B3* and *SLCO3A1* was also explored using *SLCO1B3*-KSM, *SLCO3A1*-KSM and water injected oocytes incubated in [^{3}H] E3S (1μM, 0.33μCi) and for *SLCO3A1*, [^{3}H] PGE2 (0.33 μCi) was also

included. Uptake was performed at 24hr intervals between 3-6 days post-injection of the oocytes. The incubations were carried out as described above.

To test PIs and NNRTIs as potential substrates of *SLCO1B3*, *SLCO1B3*-KSM injected and water injected oocytes uptake of radioactive compounds were observed after 5 days post-injection and the incubations were performed as described for *SLCO1A2*-KSM.

4.2.8 Statistical analysis

Data from oocyte uptake experiments were processed in Microsoft Excel 2007 and statistical analyses were performed using GraphPad Prism 3.0 and StatsDirect 2.4.5. All data was tested for normality using the Shapiro-Wilk test. For *SLCO1A2*-TOPO data, Mann-Whitney U-test was applied to test for significance. For *SLCO1A2*-KSM, *SLCO1B1*-KSM and *SLCO1B3*-KSM, the data was $\log_{10}$-transformed and the paired t-test was used to test for significance.

4.3 Results

4.3.1 SLCO1A2 uptake experiments in the X. *laevis* model

In the absence of HSA, E3S was the only compound with significantly higher accumulation in *SLCO1A2*-TOPO injected oocytes (mean pmol/oocyte ± s.d, where n is 1 oocyte, 0.86 ± 0.27, n=10) compared to water injected oocytes (0.19 ± 0.04, n=13, $p<0.001$, 4.95-fold). In the presence of HSA, E3S accumulation was still higher in *SLCO1A2*-TOPO (0.14 ± 0.04, n=12) injected compared to water injected controls (0.08 ± 0.02, n=8, $p<0.01$, 1.75-fold, Fig. 2). The addition of HSA lowered the amount of radiolabelled compounds in both water and *SLCO1A2*-TOPO injected oocytes but none of the antiretrovirals tested were significantly different between water and *SLCO1A2*-TOPO injected oocytes (Fig. 3-8).

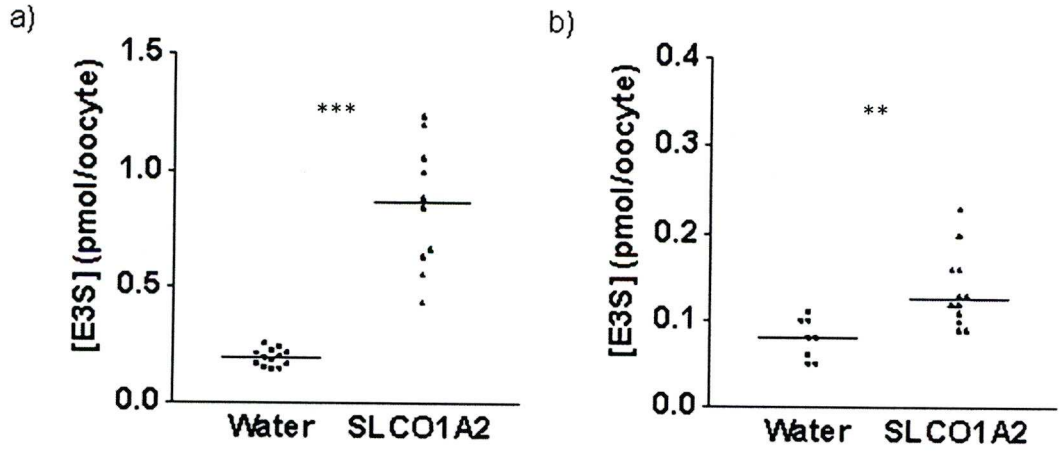

Fig. 2 Water injected and *SLCO1A2*-TOPO injected X. *laevis* oocytes uptake of [^{3}H] E3S in a) the absence and b) the presence of HSA. *** $p < 0.001$, ** $p<0.01$ compared to water injected control, n>8.

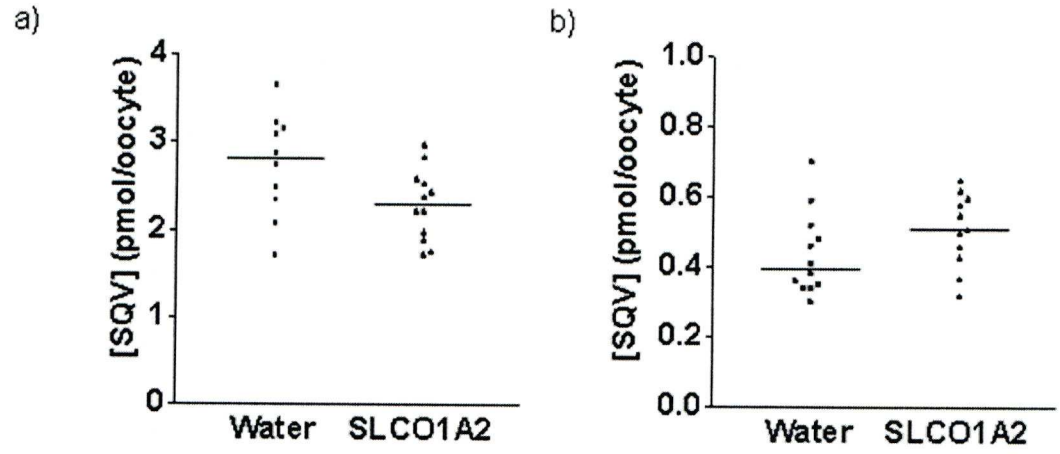

Fig. 3 Water injected and *SLCO1A2*-TOPO injected X. *laevis* oocytes uptake of [^{3}H] SQV in a) the absence and b) the presence of HSA, n>10.

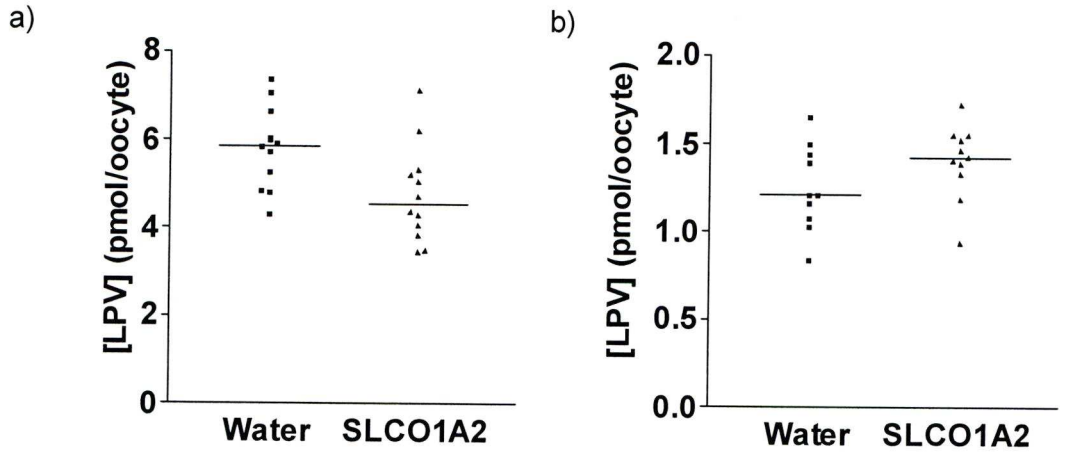

Fig. 4 Water injected and *SLCO1A2*-TOPO injected X. *laevis* oocytes uptake of [^{3}H] LPV in a) the absence and b) the presence of HSA, n>11.

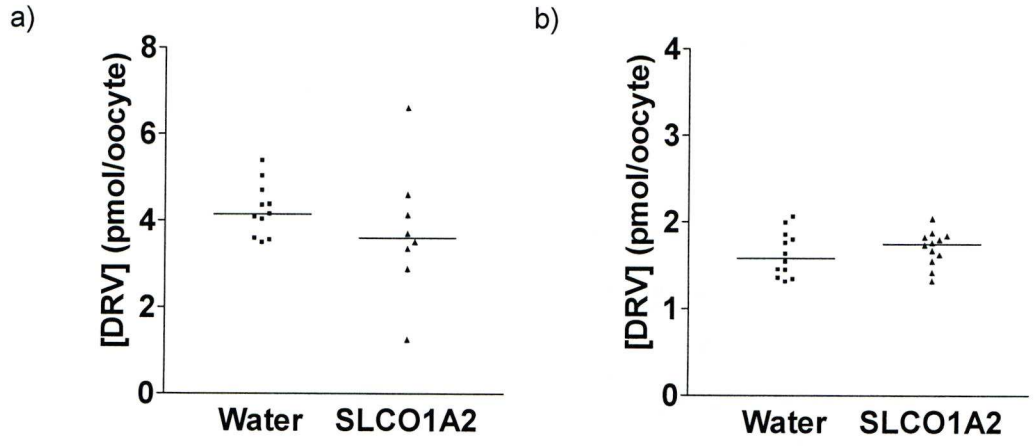

Fig. 5 Water injected and *SLCO1A2*-TOPO injected X. *laevis* oocytes uptake of [^{3}H] DRV in a) the absence and b) the presence of HSA, n>8.

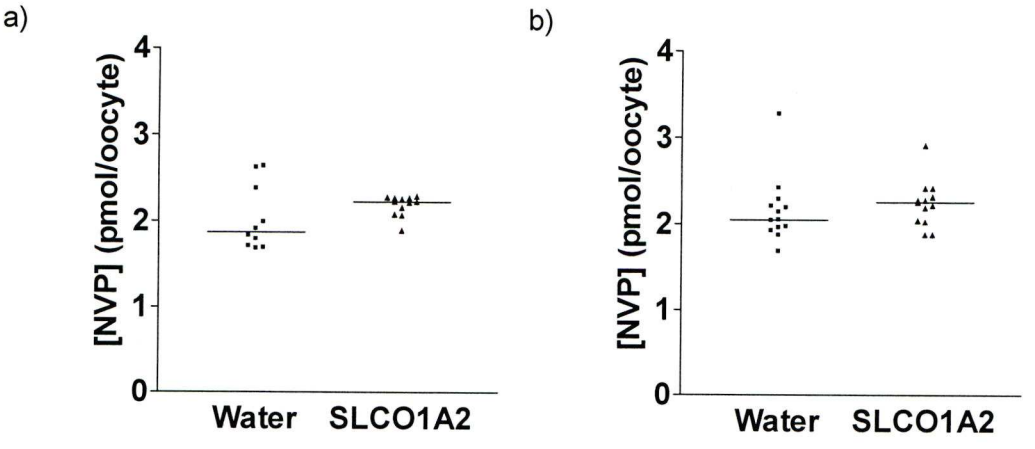

Fig. 6 Water injected and *SLCO1A2*-TOPO injected X. *laevis* oocytes uptake of [^{3}H] NVP in a) the absence and b) the presence of HSA, n>10.

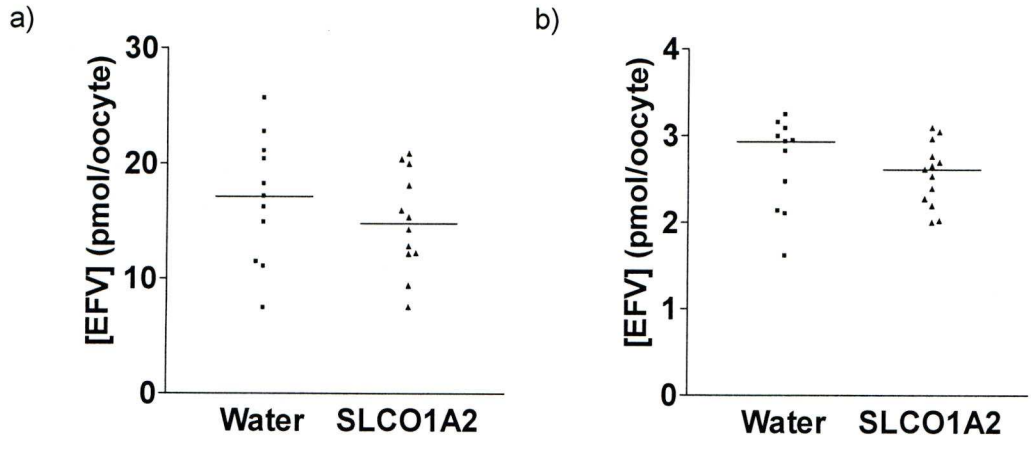

Fig. 7 Water injected and *SLCO1A2*-TOPO injected X. *laevis* oocytes uptake of [^{3}H] EFV in a) the absence and b) the presence of HSA, n>10.

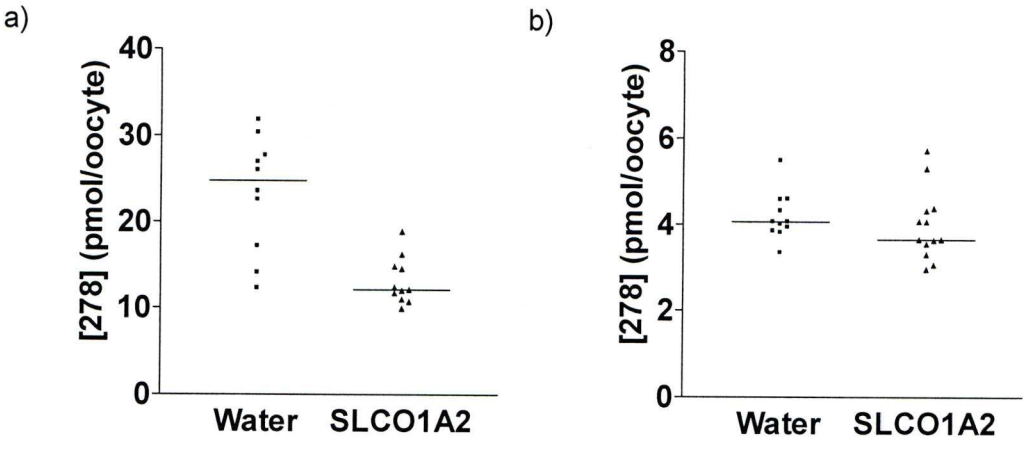

Fig. 8 Water injected and *SLCO1A2*-TOPO injected X. *laevis* oocytes uptake of [^{3}H] rilpivirine (TMC278) in a) the absence and b) the presence of HSA, n>8.

SLCO1A2-KSM (X. *laevis* β-globin UTR flanking region) injected oocytes have significantly increased accumulation of E3S by 3.2-fold (median pmol/oocyte ± s.d, where n is 1 frog, 0.51 ± 0.17, n=4) compared to water (0.16 ± 0.04, n=4, $p<0.05$, 3.21-fold). In the presence of albumin, there was a trend towards increase in accumulation of E3S in *SLCO1A2*-KSM injected oocytes (0.15 ± 0.03 n=4) compared to the water control (0.07 ± 0.01, n=4, $p=0.057$, 1.9-fold). A significant increase in accumulation was also observed for SQV (1.78 ± 0.44, n=4 compared to water 0.94 ± 0.26, n=4, $p<0.05$, 1.9-fold), LPV (4.31 ± 0.72, n=4 compared to water 2.14 ± 0.43, n=4 $p<0.05$, 2.01-fold) and DRV (4.13 ± 0.40, n=4 compared to water 2.12 ± 0.55, n=4, $p<0.05$, 1.95-fold). In the presence of HSA, increased cellular accumulation of SQV (0.64 ± 0.23, n=4, compared to water 0.21 ± 0.06, n=4, $p<0.01$, 3.07-fold), LPV (1.14 ± 0.41, n=4, compared to water 0.66 ± 0.22, n=4, $p<0.05$, 1.73-fold) and DRV (2.14 ± 0.82, n=4, compared to water 0.72 ± 0.18, n=24, $p<0.05$, 2.96-fold) were still observed. There were no significant differences in EFV, NVP or rilpivirine accumulation between water and *SLCO1A2*-KSM injected oocytes in the presence or absence of albumin (Fig. 9 and 10).

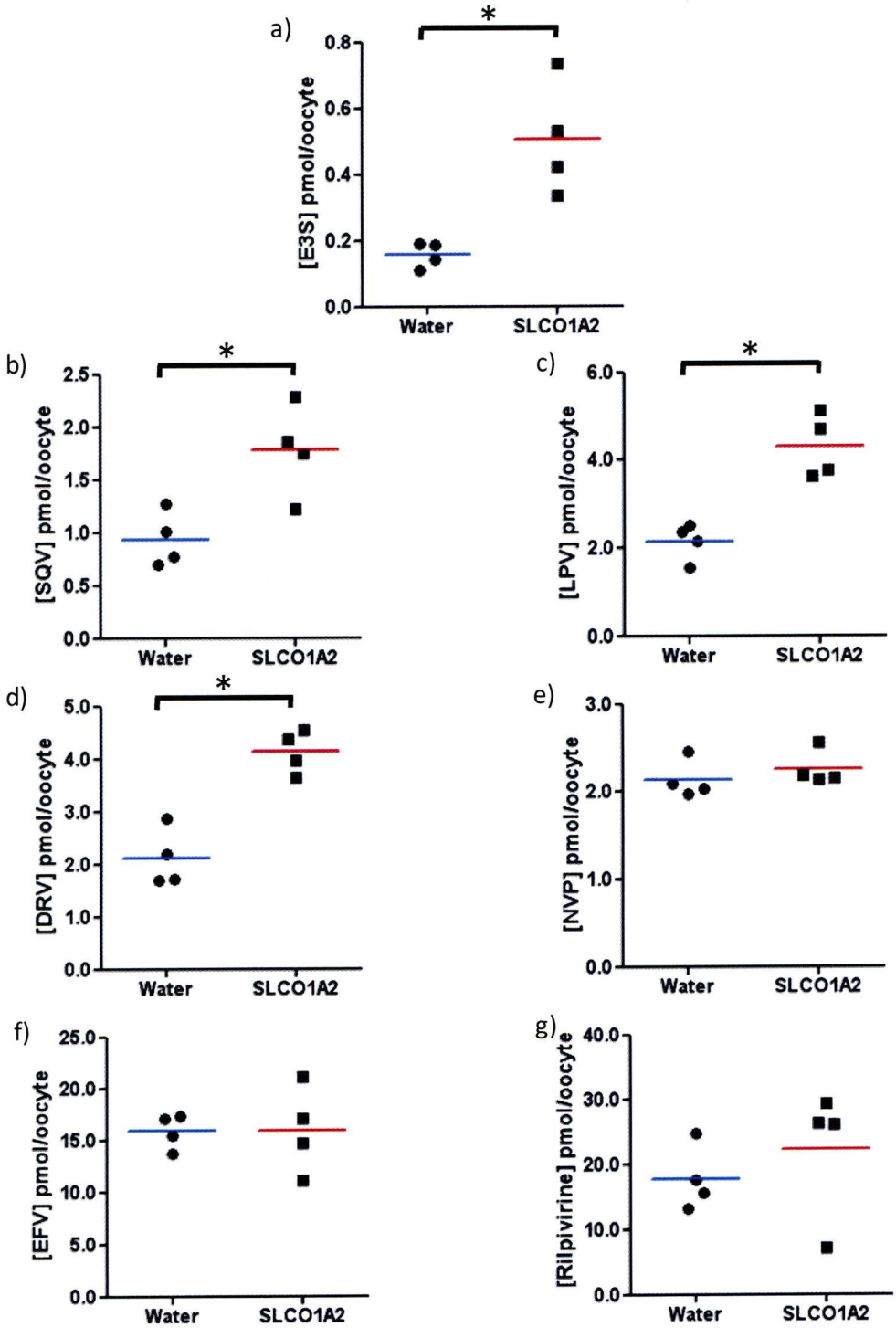

Fig. 9 Water injected and *SLCO1A2*-KSM injected X. *laevis* oocytes uptake of a) [^{3}H] E3S, b) [^{3}H] SQV, c) [^{3}H] LPV, d) [^{14}C] DRV, e) [^{3}H]NVP, f) [^{14}C]EFV and g) [^{3}H] rilpivirine in the absence of HSA (n=4). * $p<0.05$ compared to water injected control.

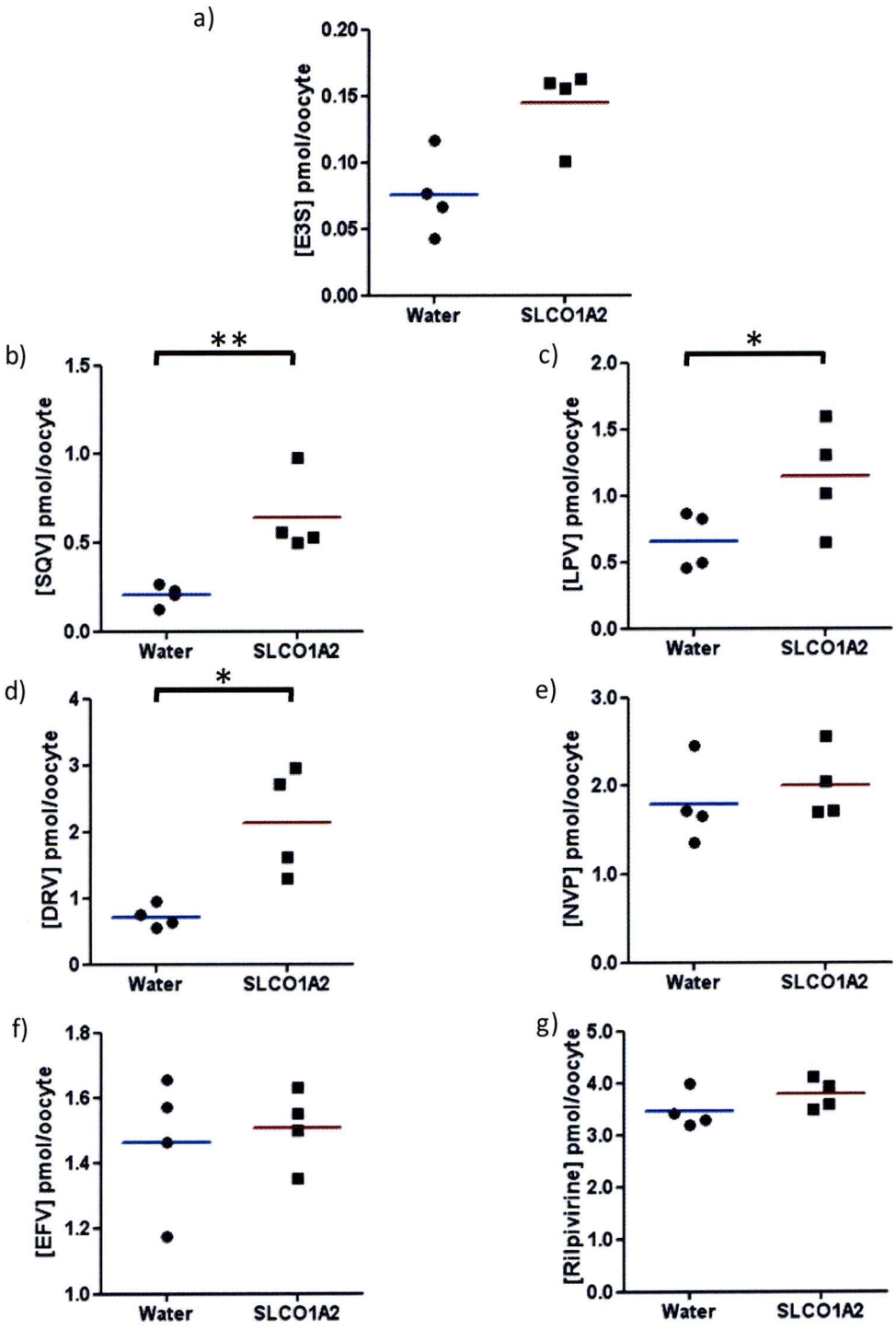

Fig. 10 Water injected and *SLCO1A2*-KSM injected X. *laevis* oocytes uptake of a) [^{3}H] E3S, b) [^{3}H] SQV, c) [^{3}H] LPV, d) [^{14}C] DRV, e) [^{3}H] NVP, f) [^{14}C] EFV and g) [^{3}H] rilpivirine in the presence of HSA (n=4). * $p<0.05$, ** $p<0.01$ compared to water injected control.

4.3.2 SLCO1B1 uptake experiments in the X. *laevis* model

In the absence of HSA, E3S (2.02 ± 0.52, compared to water 0.19 ± 0.05, n=4, $p<0.01$, 10.90-fold), SQV (2.16 ± 0.71, compared to water 1.01 ± 0.21, n=4, $p<0.05$, 2.14-fold), LPV (4.07 ± 0.67, compared to water 2.5 ± 0.36, n=4, $p=0.054$, 1.61-fold), DRV (4.32 ± 0.75, compared to water 2.18 ± 0.40, n=4, $p<0.05$, 1.98-fold) and rilpivirine (24.03 ± 9.11, compared to water 10.67 ± 3.3, n=4, $p=0.05$, 2.25-fold) had significantly increased accumulation in oocytes injected with *SLCO1B1*-KSM compared to water controls (Fig. 9). In the presence of HSA, E3S (0.35 ± 0.15, compared to water 0.1 ± 0.03, n=4, $p<0.05$, 3.55-fold), SQV (0.45 ± 0.05, compared to water 0.27 ± 0.03, n=4, $p<0.01$, 1.65-fold), LPV (1.65 ± 0.60 compared to water 0.82 ± 0.24, n=4, $p<0.05$, 2.02-fold) and DRV (2.85 ± 1.26 compared to water 0.96 ± 0.37, n=4, $p=0.055$, 2.98-fold) had significantly higher accumulation in *SLCO1B1*-KSM injected oocytes compared to water controls. No difference in accumulation was observed in *SLCO1B1*-KSM injected oocytes and water injected oocytes incubated with rilpivirine. No significant increases in cellular accumulation were observed between *SLCO1B1*-KSM and water injected oocytes incubated with NVP or EFV in the presence or absence of HSA (Fig. 11 and 12).

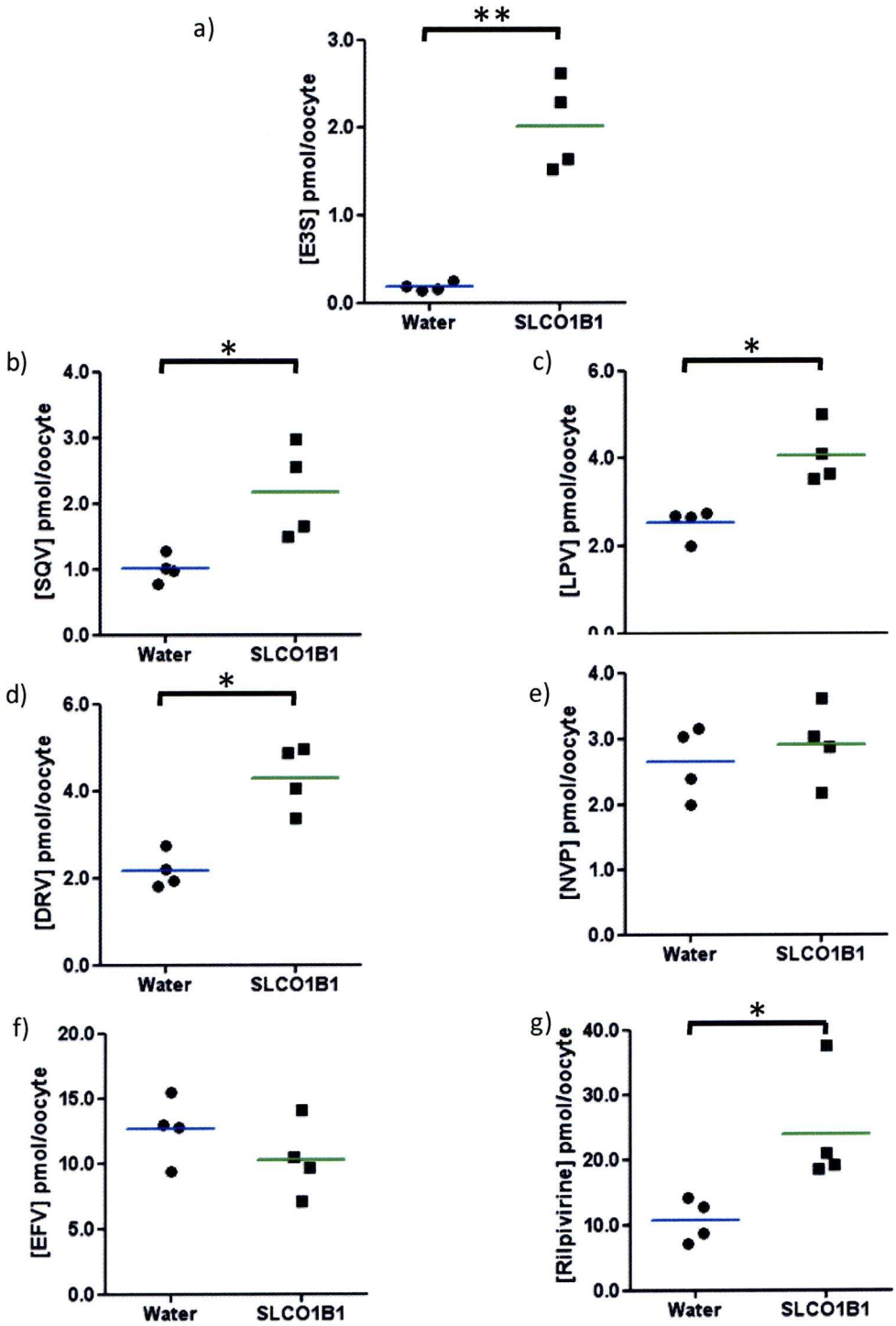

Fig. 11 Water injected and *SLCO1B1*-KSM injected X. *laevis* oocytes uptake of a) [^{3}H] E3S, b) [^{3}H] SQV, c) [^{3}H] LPV, d) [^{14}C] DRV, e) [^{3}H] NVP, f) [^{14}C] EFV and g) [^{3}H] rilpivirine in the absence of HSA (n=4). ** $p<0.01$, * $p\leq0.05$ compared to water injected control.

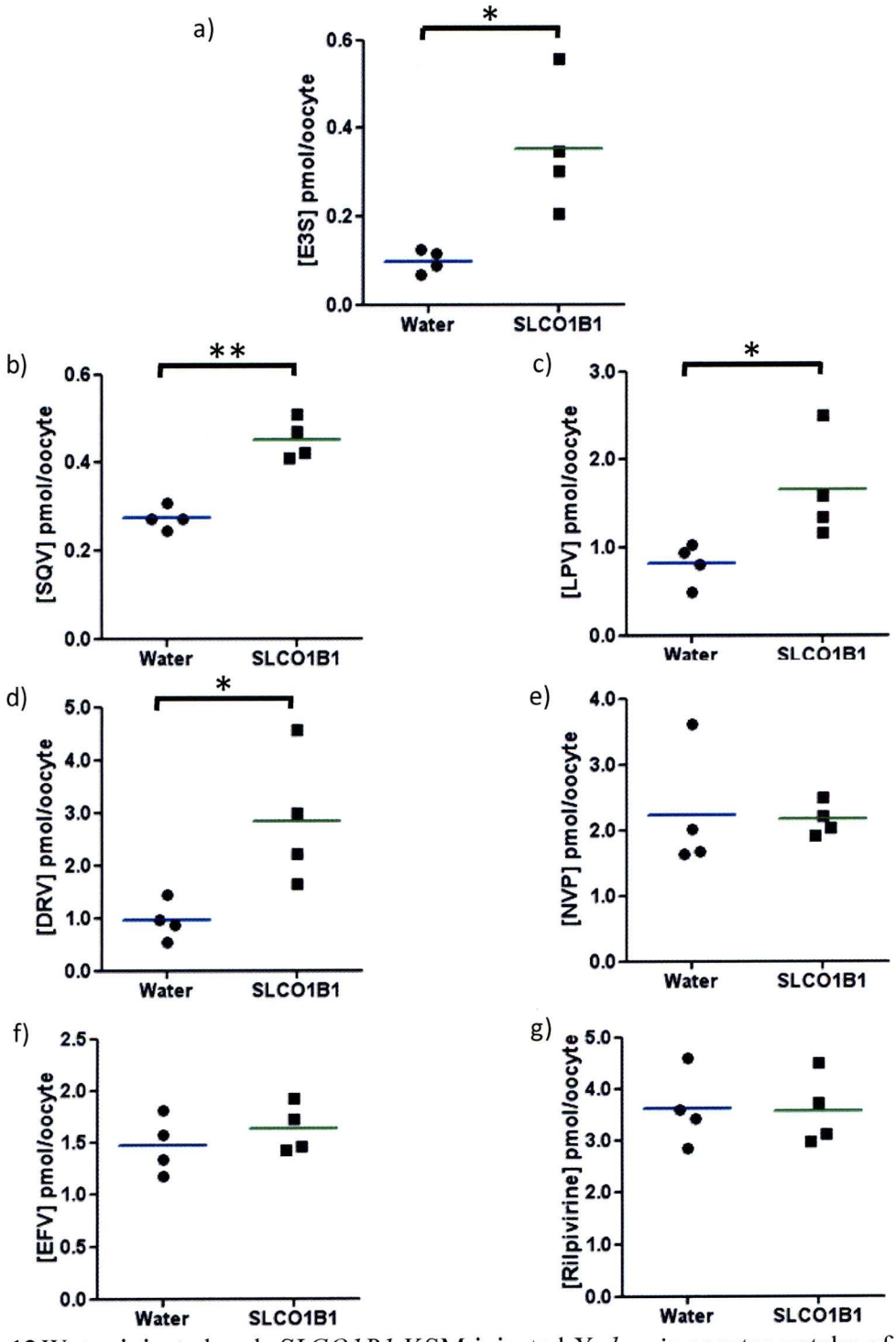

Fig. 12 Water injected and *SLCO1B1*-KSM injected X. *laevis* oocytes uptake of a) [^{3}H] E3S, b) [^{3}H] SQV, c) [^{3}H] LPV, d) [^{14}C] DRV, e) [^{3}H] NVP, f) [^{14}C] EFV and g) [^{3}H] rilpivirine in the presence of HSA (n=4). ** $p<0.001$, * $p<0.05$ compared to water injected control.

When collagenase extracted oocytes were compared to loop extracted oocytes, both methods showed comparable fold increases in accumulation of E3S compared to their respective water injected controls (collagenase fold increase of 20.22, platinum loop fold increase of 13.26, Fig. 13). PGE2 also showed increased accumulation in *SLCO1B1*-KSM injected oocytes compared to water injected control using both extraction methods (collagenase fold increase of 1.54, platinum loop fold increase of 3.07).

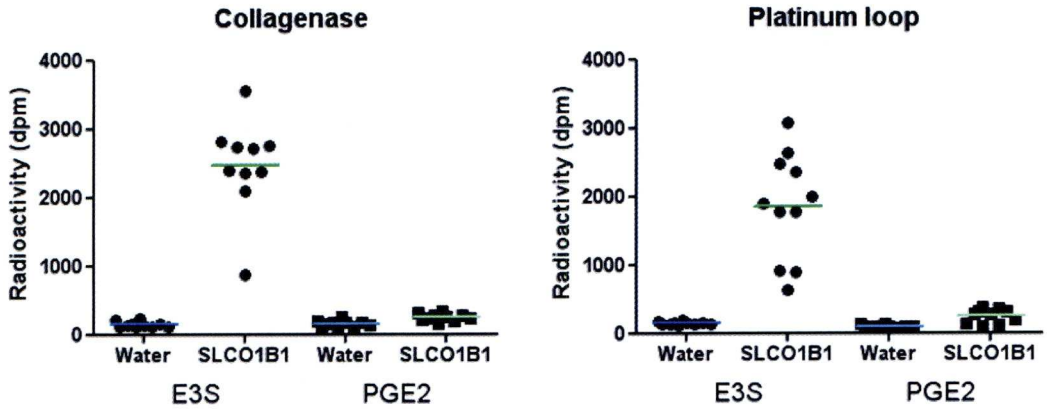

Fig. 13 Water injected and *SLCO1B1*-KSM injected X. *laevis* oocytes uptake of [^{3}H] E3S and [^{3}H] PGE2, comparing oocytes extracted by platinum loop and by collagenase treatment (n=1).

4.3.3 SLCO1B3 uptake experiments in the X. *laevis* model

Following three day incubation, in the presence or absence of HSA, neither the positive controls E3S nor the antiretrovirals (Fig. 14) showed increased accumulation in *SLCO1B3*-KSM injected oocytes versus controls. During the 6 days incubation with functional experiments carried out at 24hr intervals, E3S showed increased accumulation in *SLCO1B3*-KSM injected oocytes versus controls at day 4 (fold increase 1.64×), day 5 (fold increase 2.04×) and day 6 (fold increase 1.57×, Fig 15). Using oocytes which were incubated 5 days post-injection, E3S showed a trend towards increase in *SLCO1B3*-KSM injected oocytes (mean pmol/oocyte ± s.d., 0.50 ± 0.20, p=0.059) compared to water injected control (0.21 ± 0.01, 2.38-fold, n=4). The accumulation of SQV was significantly increased in *SLCO1B3*-KSM injected cells (2.17 ± 0.61) compared to water injected cells (1.62 ± 0.45, 1.34-fold, $p<0.05$, n=4) and rilpivirine also exhibited significantly increased accumulation in *SLCO1B3*-KSM injected cells (37.00 ± 12.43) compared to water control (16.18 ± 3.54, 2.29-fold, $p<0.05$, n=4). DRV showed a trend towards increase (*SLCO1B3*-KSM injected 5.41 compare to water injected control 3.29, 1.64-fold, n=1, Fig. 16) and none of the other antiretrovirals showed statistically significant increases in cellular accumulation.

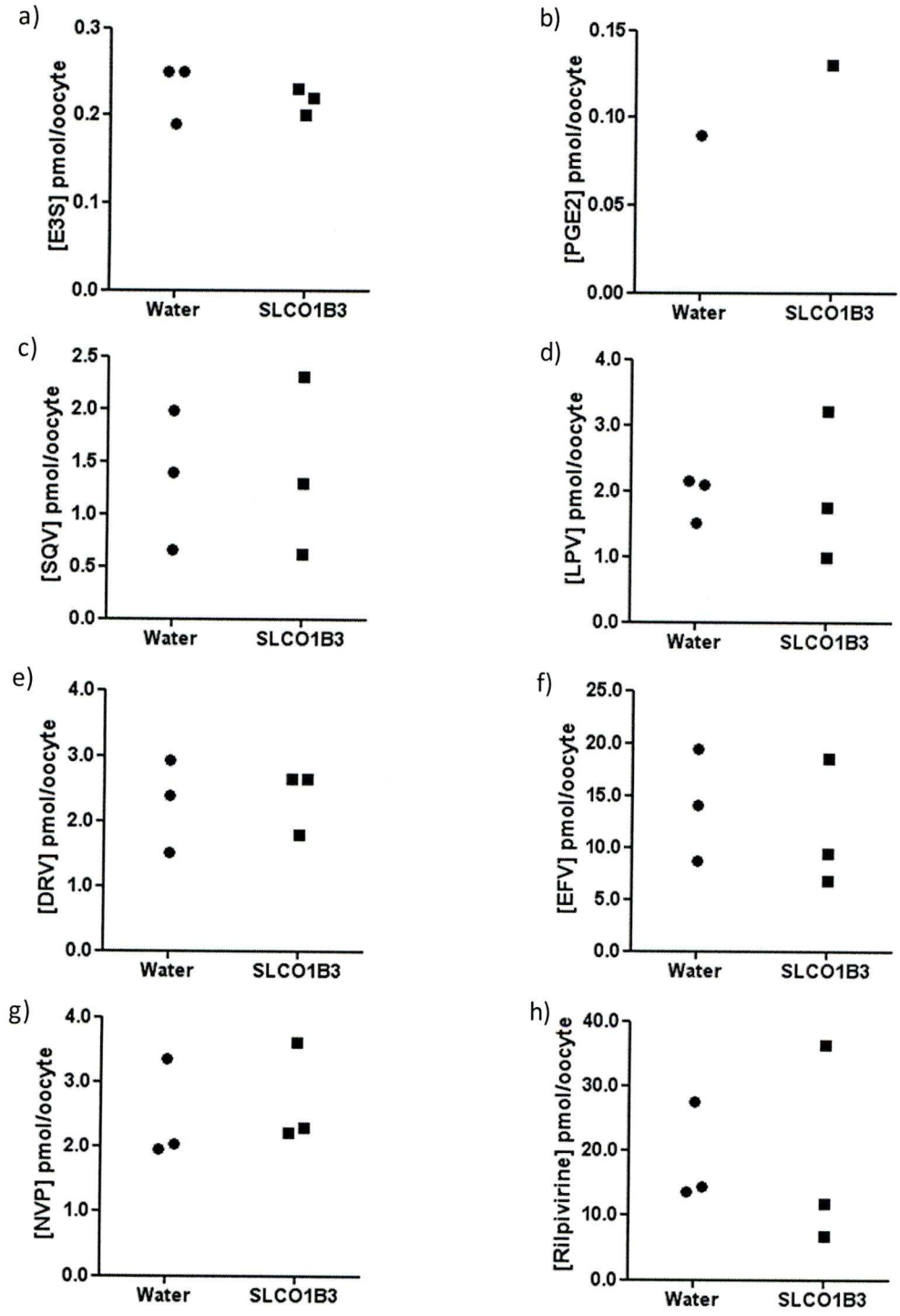

Fig. 14 Water injected and pBluescriptII-KSM-*SLCO1B3* injected X. *laevis* oocytes 3 day post-injection uptake of a) [^{3}H] E3S (n=3), b) [^{3}H] PGE2 (n=2), c) [^{3}H] SQV (n=3), d) [^{3}H] LPV (n=3), e) [^{14}C] DRV (n=3), f) [^{3}H] NVP (n=3), g) [^{14}C] EFV (n=3) and h) [^{3}H] rilpivirine (n=3) in the absence of HSA. * $p<0.05$ compared to water injected control.

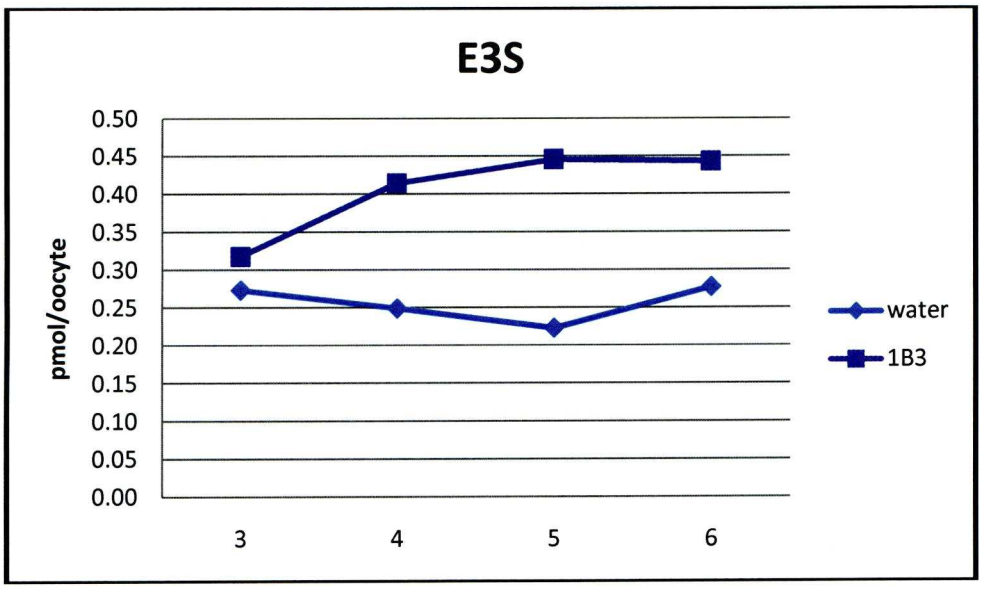

Fig. 15 The accumulation of [^{3}H] E3S in *SLCO1B3*-KSM injected compared to water injected oocytes between 3-6 days post injection (n=1).

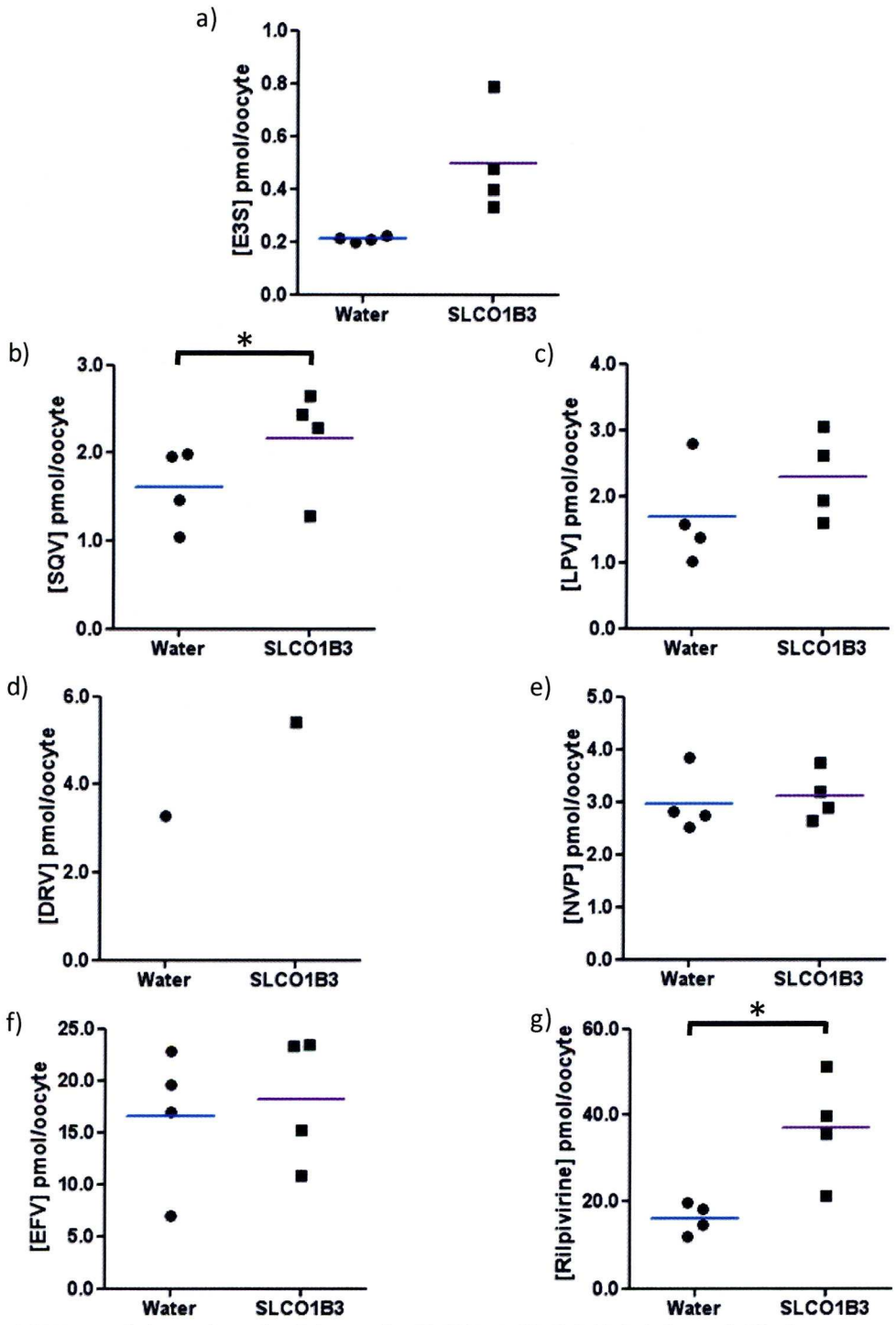

Fig. 16 Water injected and pBluescriptII-KSM-*SLCO1B3* injected X. *laevis* oocytes 5 days post-injection uptake of a) [^{3}H] E3S (n=4), b) [^{3}H] SQV (n=4), c) [^{3}H] LPV (n=4), d) [^{14}C] DRV (n=1), e) [^{3}H] NVP (n=4), f) [^{14}C] EFV (n=4) and g) [^{3}H] rilpivirine (n=4) in the absence of HSA. * $p<0.05$ compared to water injected control.

4.3.4 SLCO3A1 uptake experiments in the X. *laevis* model

Following three day incubation and in the presence or absence of HSA, neither E3S nor PGE2 (Fig. 17) showed increased accumulation in *SLCO3A1* injected oocytes versus controls. No increases in cellular accumulation were observed for any of the antiretrovirals. During the 6 days incubation with functional experiments carried out at 24hr intervals, neither E3S nor PGE2 showed increased accumulation in *SLCO3A1* injected oocytes versus controls for *SLCO3A1* at any of the time points taken (Fig. 18 and 19).

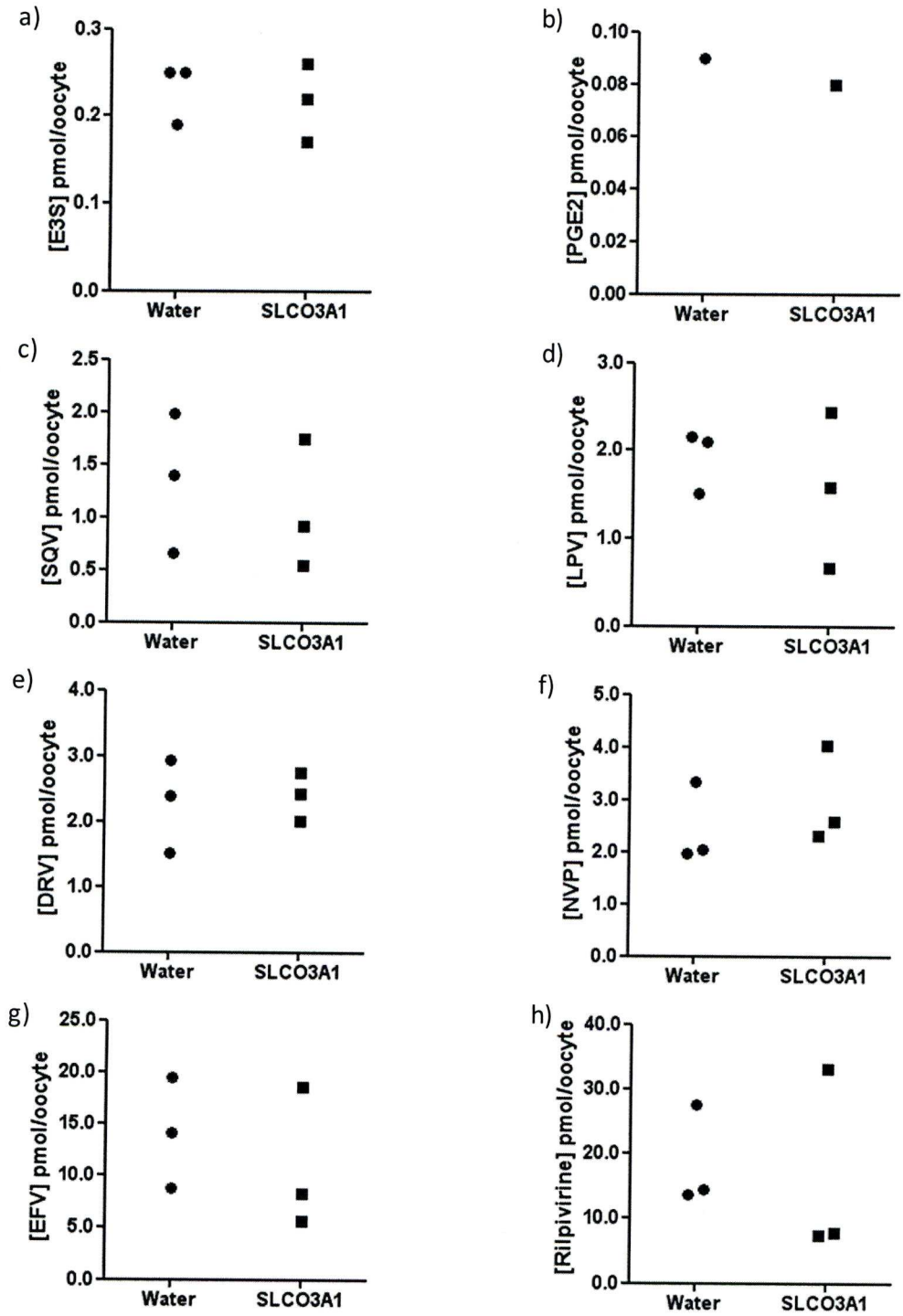

Fig. 17 Water injected and pBluescriptII-KSM-*SLCO3A1* injected X. *laevis* oocytes 3 day post-injection uptake of a) [^{3}H] E3S (n=3), b) [^{3}H] PGE2 (n=2), c) [^{3}H] SQV (n=3), d) [^{3}H] LPV (n=3), e) [^{14}C] DRV (n=3), f) [^{3}H] NVP (n=3), g) [^{14}C] EFV (n=3) and h) [^{3}H] rilpivirine (n=3) in the absence of HSA.

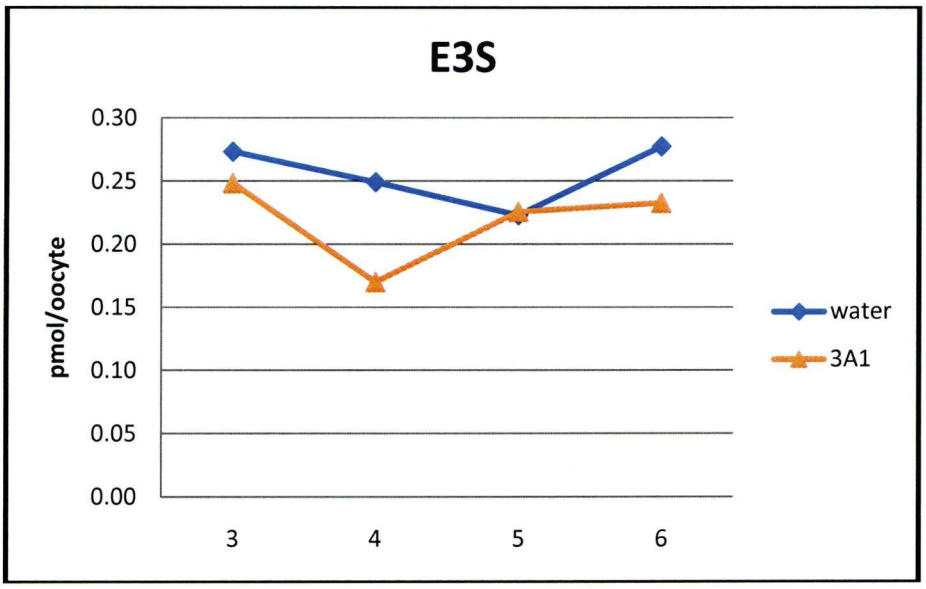

Fig. 18 The accumulation of [^{3}H] E3S in *SLCO3A1*-KSM injected compared to water injected oocytes between 3-6 days post injection (n=1).

Fig. 19 The accumulation of [^{3}H] PGE2 in *SLCO3A1*-KSM injected compared to water injected oocytes between 3-6 days post injection (n=1).

Table. 1 Summary of substrate specificity of SLCO transporters for antiretrovirals

Substrates	SLCO1A2			SLCO1B1			SLCO1B3 (5 days)		
	Water	SLCO1A2-KSM	P-value	Water	SLCO1B1-KSM	P-value	Water	SLCO1B3-KSM	P-value
E3S	**0.16 ± 0.04**	**0.51 ± 0.17**	**p<0.05**	**0.19 ± 0.05**	**2.02 ± 0.52**	**P<0.01**	0.21 ± 0.01	0.50 ± 0.20	NS
E3S (with HSA)	**0.08 ± 0.03**	**0.15 ± 0.03**	**p<0.05**	**0.10 ± 0.03**	**0.35 ± 0.15**	**p<0.05**	-	-	-
SQV	**0.94 ± 0.26**	**1.78 ± 0.44**	**p<0.01**	**1.01 ± 0.21**	**2.16 ± 0.71**	**p<0.05**	**1.62 ± 0.45**	**2.17 ± 0.61**	**p<0.05**
SQV (with HSA)	**0.21 ± 0.06**	**0.64 ± 0.23**	**p<0.05**	**0.27 ± 0.03**	**0.45 ± 0.05**	**p<0.01**	-	-	-
LPV	**2.14 ± 0.43**	**4.31 ± 0.72**	**p<0.05**	**2.53 ± 0.36**	**4.07 ± 0.67**	**p<0.05**	1.69 ± 0.78	2.30 ± 0.66	NS
LPV (with HSA)	**0.66 ± 0.22**	**1.14 ± 0.41**	**p<0.05**	**0.82 ± 0.24**	**1.65 ± 0.59**	**p<0.05**	-	-	-
DRV	**2.12 ± 0.55**	**4.13 ± 0.40**	**p<0.05**	**2.18 ± 0.40**	**4.32 ± 0.75**	**p<0.05**	3.29	5.41	-
DRV (with HSA)	**0.72 ± 0.18**	**2.14 ± 0.82**	**p<0.05**	**1.00 ± 0.37**	**2.85 ± 1.26**	**p<0.05**	-	-	-
NVP	2.14 ± 0.55	2.26 ± 0.20	NS	2.65 ± 0.54	2.92 ± 0.59	NS	2.98 ± 0.59	3.12 ± 0.47	NS
NVP (with HSA)	1.80 ± 0.47	2.01 ± 0.40	NS	2.23 ± 0.93	2.17 ± 0.26	NS	-	-	NS
EFV	15.9 ± 1.70	16.0 ±4.17	NS	12.6 ± 2.49	10.3 ± 2.90	NS	16.6 ± 6.84	18.21 ± 6.21	NS
EFV (with HSA)	1.46 ± 0.21	1.51 ± 0.12	NS	1.47 ± 0.28	1.63 ± 0.24	NS	-	-	NS
Rilpivirine	17.7 ± 5.00	22.6 ± 10.1	NS	**10.7 ± 3.29**	**24.0 ± 9.11**	**p<0.05**	**16.2 ± 3.54**	**37.0 ± 12.4**	**p<0.05**
Rilpivirine (with HSA)	3.48 ± 0.37	3.78 ± 0.29	NS	3.61 ± 0.73	3.57 ± 0.69	NS	-	-	NS

4.4 Discussion

The transport of many antiretrovirals by efflux transporters has been well defined, but antiretrovirals have yet to be characterised by influx transporters. SLCO transporters have been shown to affect plasma concentration and drug clearance of some xenobiotics and hence it is important to characterise the transport of antiretrovirals.

Uptake experiments using *SLCO1A2*-TOPO cRNA did not show any of the antiretrovirals tested as substrates, but E3S accumulation was higher in *SLCO1A2*-TOPO injected compared to water injected oocytes. In experiments where the *SLCO1A2* gene with X. *laevis* 5'and 3' flanking UTR were used, E3S and the PIs appear to be substrates with higher accumulation in *SLCO1A2*-KSM injected compared to water injected oocytes. The difference in accumulation between *SLCO1A2*-TOPO and *SLCO1A2*-KSM experiments may be due to the level of *SLCO1A2* expression in injected oocytes. The low expression of *SLCO1A2*-TOPO injected oocytes still showed increased accumulation of E3S compared to water injected oocytes, which may be due to a strong affinity for E3S and relatively lower affinity for the PIs. The use of plasmids containing 3' and 5' X. *laevis* β-globin UTR to generate cRNA for X. *laevis* oocyte uptake experiments is common (Preston *et al.* 1992; Francis *et al.* 2000; Virkki *et al.* 2002) due to the increase in translational efficiency of the gene of interest by up to 300-fold (Falcone and Andrews 1991). Subcloning *SLCO1A2* into the pBluescriptII-KSM vector improved the transport by *SLCO1A2* in the oocytes, which suggests that future cloning of transporters should involve subcloning into this vector. The NNRTIs did not appear to be substrates of *SLCO1A2* with or without the 5' and 3' UTR or in the presence or absence of HSA.

HSA reduced the accumulation in both water and *SLCO1A2*-KSM injected oocytes but the PIs still accumulated more in *SLCO1A2*-KSM injected compared to water injected oocytes. A reduction in accumulation with the addition of HSA was observed due to the protein binding properties of the antiretrovirals, which vary between the drugs (for binding to plasma proteins, SQV: 98% (Roche 2007), LPV: 98-99% (Abbott 2008), DRV: ~95% (Tibotec 2006), EFV: >99% (Bristol-Myers-Squibb 2008), NVP ~60% (Boehringer-Ingelheim 1999)). PIs have higher binding affinities to α1-acid-glycoprotein, but they also bind to HSA, which is the most abundant plasma protein (Hazen *et al.* 2007).

SLCO1B1-KSM cRNA injected oocytes also had higher accumulation of the PIs compared to water injected controls. In addition to the PIs, concentrations of rilpivirine were also significantly higher in *SLCO1B1*-KSM cRNA injected oocytes than in water injected oocytes. However, in the presence of HSA, no difference in accumulation of rilpivirine was observed, whereas the PIs still accumulated higher in *SLCO1B1*-KSM cRNA injected oocytes. This suggests that rilpivirine is highly protein bound to HSA and is in agreement with the findings in Chapter 2; protein binding had more influence on the intracellular accumulation of rilpivirine than drug transport.

X. *laevis* oocytes were extracted using the collagenase treatment method for SLCO1A2 and SLCO1B1 uptake experiments. The platinum loop extraction method, which includes a collagenase treatment step prior to uptake experiments, was tested using *SLCO1B1* to compare with the collagenase treatment method to observe whether the extraction treatments altered accumulation of positive control substrates in *SLCO1B1*-KSM injected oocytes. For E3S, there was higher accumulation in collagenase extracted

oocytes, but the platinum loop extracted oocytes also had a large accumulation of E3S in *SLCO1B1*-KSM injected oocytes when compared to their respective water injected controls. For PGE2, there was higher accumulation in the oocytes extracted by platinum loop than the collagenase extracted oocytes. Interestingly, platinum extracted oocytes were more robust post-injection than collagenase treated oocytes, as many of the collagenase treated oocytes looked unhealthy at 4 days post-injection. Both the collagenase (Sacchi *et al.* 1995; Hagenbuch *et al.* 1996; Hammermann *et al.* 2001) and the platinum loop extraction methods (Sigel 1987; Hammermann *et al.* 2001; Boileau *et al.* 2002) have been used to extract oocytes and a third method, which requires the use of forceps, is used by some researchers (Sigel 2001). The advantage of using collagenase compared to the other methods is the ease of extraction and defolliculation of the oocytes. The use of forceps or the platinum loop is relatively labour intensive and requires a separate collagenase treatment prior to uptake experiments to remove the follicular membrane. However, the oocytes appear to survive for longer post-microinjection (personal observation).

SLCO1B3-KSM injected oocytes did not accumulate E3S, PGE2 or any of the antiretrovirals at 3 days post injection. A post-injection time course was performed to observe whether incubation time prior to uptake experiments increased the expression of *SLCO1B3* and hence accumulation of control substrates E3S or PGE2. At 4-6 days post-injection, the accumulation of E3S was higher than at day 3. The ability of *SLCO1B3* to transport the antiretrovirals was investigated by using oocytes at 5 days post-injection. SQV and rilpivirine accumulation was statistically higher in *SLCO1B3*-KSM injected oocytes than water injected controls whilst DRV and E3S showed a trend towards

increase. Other studies have shown that 3 days post injection and 1h incubation for uptake was sufficient to detect differences in accumulation of E3S in SLCO1A2 (Maeda *et al.* 2007), SLCO1B1 (Mahagita *et al.* 2007; Nakakariya *et al.* 2008) and SLCO1B3 expressed oocytes (Mahagita *et al.* 2007; Nakakariya *et al.* 2008). SLCO1B3 appears to transport similar antiretrovirals to SLCO1B1, as the PIs and rilpivirine showed increases in *SLCO1B1*-KSM as well as *SLCO1B3*-KSM injected oocytes. The effect of HSA on the accumulation of antiretrovirals by SLCO1B3 was inconclusive as the detection of many of the radiolabelled compounds including the positive control substrate, E3S, did not accumulate more in *SLCO1B3*-KSM injected oocytes than water injected control (data not shown).

The lower fold increases of E3S and the requirement of increased post-injection incubation time of *SLCO1B3*-KSM than *SLCO1B1*-KSM injected oocytes suggests either that the oocytes are not translating *SLCO1B3* into protein as efficiently as *SLCO1B1*, or that E3S is not as good a substrate for SLCO1B3 as for SLCO1B1. The amount of SLCO protein in the oocytes could be compared by Western blotting, but this would require specific antibodies for each SLCO transporter. Unfortunately, at present, there are no reliable commercially available antibodies for the SLCOs studied in this thesis.

SLCO3A1-KSM injected oocytes at 3 days post-injection did not have increased uptake of the control substrates E3S and PGE2 or any of the antiretrovirals. A time course for days post-injection was performed to observe whether increased incubation time would increase SLCO3A1 function, but no difference was observed between *SLCO3A1*-KSM and water injected oocytes at any of the time intervals. E3S, which was identified as a

substrate for several SLCOs, did not accumulate more in *SLCO3A1*-KSM injected oocytes, which was similar to observations made by Adachi *et al.* (2003). PGE2 was identified as a substrate for *SLCO3A1* and was demonstrated to have increased accumulation in *SLCO3A1*-KSM injected oocytes by 1.4–fold at 20nM (Huber *et al.* 2007) and 3.4-fold at 15nM (Adachi *et al.* 2003). Both studies conducted uptake experiments at 3 days post-injection. The lack of accumulation of PGE2 in *SLCO3A1*-KSM injected oocytes contradicts the observations made by Huber *et al.* (2007) and Adachi *et al.* (2003) where increases in accumulation were reported. However, the difference in fold-increase between these two studies varies and the study by Huber et al. (2007) showed that whilst increases in accumulation were detected, this was only a modest increase. To examine whether SLCO3A1 protein is present on the oocyte cell membrane, Western blotting could be applied, but antibodies for SLCO3A1 are to date, not commercially available.

As many PIs are boosted with ritonavir to improve the pharmacokinetic profile of the PIs, future studies should also evaluate the interactions between ritonavir and SLCOs, as ritonavir may inhibit influx transport.

The disadvantages of this type of assay include the variations in quality of oocytes and that they are relatively low-throughput and labour intensive (Sigel 1990; Markovich 2008). However, despite large variations in oocyte uptake, there were statistically significant differences between *SLCO1A2*-KSM, *SLCO1B1*-KSM and *SLCO1B3*-KSM injected oocytes uptake of E3S compared to their respective water injected controls. The issue of why albumin should have a marked effect on the uptake of rilpivirine is not clear, but it might relate to lowering the concentration of available drug for the transport

protein. Despite these limitations, the X. *laevis* model is a good model for evaluating influx transporters as it has very few endogenous transporters (Xia *et al.* 2007) and will readily express mammalian transporters which contain the Kozak consensus and are flanked by X. *laevis* 3' and 5' UTR.

In conclusion, SLCO1A2, SLCO1B1 and SLCO1B3 transport PIs and SLCO1B1 and SLCO1B3 transport rilpivirine in the absence of HSA. This suggests that intracellular accumulation of these drugs may be influenced by these transporters. This validates these genes for pharmacogenetic studies which may provide an insight into the impact of SLCOs on the pharmacokinetics of antiretrovirals. However, the importance of these SLCO transporters at basal levels of expression and their albility to alter pharmacokinetics of antiretrovirals has yet to be elucidated.

Chapter 5

Association between SLCO SNPs and lopinavir plasma concentrations

5.1 Introduction

Many synonymous and non-synonmyous SNPs for *SLCO1B1* have been identified and several have been found to alter function, with 521T>C and 388A>G being the best characterised. 521T>C and 388A>G are found at higher frequencies than other SNPs and are to be in linkage disequilibrium. 388A>G reduces the transport of rifampicin, but not other *SLCO1B1* substrates and has a high allele frequency in Caucasians (30%) and Africans (74%) (Tirona *et al.* 2001). 521T>C is located in the transmembrane region of SLCO1B1 and was shown to significantly lower expression of SLCO1B1 (Tirona *et al.* 2001). This SNP has been reported to have a large influence on uptake of compounds *in vitro* (Tirona *et al.* 2001; Kameyama *et al.* 2005) and also on the pharmacokinetics of statins, including atorvastatin (Lau *et al.* 2007), pravastatin (Niemi *et al.* 2006) and simvastatin (Pasanen *et al.* 2006). The frequency of this SNP is also high amongst Caucasians at 14% compared to Africans at 9% (Tirona *et al.* 2001).

467A>G, 1058T>C and 1964A>G SNPs have also been associated with reduced transport function of SLCO1B1 *in vitro*, but these SNPs are very rare (Tirona et al. 2001). The 1463G>C variant has been shown to reduce transport of estrone-3-sulphate (E3S). This SNP has an allele frequency of 9% in African-Americans, but was not detected in Caucasians (Tirona *et al.* 2001). In addition, the 578T>G variant is associated with significant defects in protein maturation and in transport function, but it was found in only 1 out of 81 liver samples (Michalski *et al.* 2002).

To date, 3 SNPs for *SLCO1B3* have been described, 1564G>T, 334T>G and 699G>A. 334T>G is in complete linkage disequilibrium with 699G>A (Tsujimoto *et al.* 2006)

and has an effect on the transport of digoxin, a SLCO1B3 substrate, although this was not statistically significant (Tsujimoto *et al.* 2008). However, a study by Smith *et al.* (2007), which showed that paclitaxel was a substrate for SLCO1B3 using the X *laevis* model, showed no association between 334T>G or 699G>A and paclitaxel pharmacokinetics in 475 individuals.

SLCO1A2 516A>C and 38T>C were identified along with 404A>T, 2003C>G, 559G>A and 382A>T (Lee *et al.* 2005). Of these SNPs, 516A>C, 404A>T and 2003C>G have an impact on the functional transport of SLCO1A2 substrates such as estrone-3-sulphate (E3S) (Lee *et al.* 2005). Using the X. *laevis* oocyte model, Badagnani *et al.* (2006) confirmed that 516A>C decreased accumulation of E3S and methatrexate whilst 38T>C increased the accumulation of these two compounds compared to wildtype SLCO1A2. 38T>C (11.1-16.3%) and 516A>C (1.9-5.3%) have been reported to be at higher frequencies in Caucasian populations than the other *SLCO1A2* SNPs, whilst 382A>T (0.5-1.3%) and 559G>A (1.5%) were higher in African and Hispanic ethnicities with 2003C>G observed in both African (3.7-4.4%) and Hispanic populations (1.0%) (Lee *et al.* 2005; Badagnani *et al.* 2006). 404A>T was not observed in the sample population by Lee *et al* (2005).

Therapeutic drug monitoring (TDM) is a strategy employed to measure drug plasma concentrations and is used to assess efficacy, toxicity and patient compliance to drug regimens (Duong *et al.* 2004). In Liverpool, there is a TDM program for antiretrovirals, which has appropriate retrospective consent for genetic analysis and hence provides a large sample population for pharmacogenetic studies. The disadvantages of using a TDM sample population include unknown ethnicity and different sampling times post-

dose. Despite these limitations, using a TDM cohort enables the use of a large sample population which would otherwise be difficult to recruit.

In Chapter 4, the ability of the SLCOs to transport antiretrovirals was explored and the PIs and rilpivirine were found to be substrates for SLCO1A2, SLCO1B1 and SLCO1B3. However, many PIs are co-administered with ritonavir and the effect of ritonavir on lopinavir (LPV) uptake, using the X. *laevis* model, was first ascertained. The effect of characterised SNPs, which are abundant in the Caucasian population, in SLCO1A2, SLCO1B1 and SLCO1B3 on the pharmacokinetics of LPV, the most commonly prescribed PI, was then investigated using the Liverpool TDM cohort.

5.2 Methods

5.2.1 Materials

TaqMan Reverse Transcription Reagents and TaqMan Gene Expression Assays were purchased from Applied Biosystems Inc. (Warrington, UK). Absolute QPCR Mix was purchased from ThermoFisherScientific (Loughborough, UK). All other chemicals were purchased from Sigma-Aldrich (Poole, UK).

5.2.2 Lopinavir uptake in the presence of ritonavir in the X. *laevis* oocyte model

X. *laevis* oocytes were extracted and injected as described in Chapter 4 (sections 4.2.3, 4.2.4, 4.2.5.1 and 4.2.6). At 3 days post injection, SLCO1B1-KSM and water injected oocytes were used in uptake experiments as described in Chapter 4 (section 4.2.7) with [^{3}H] LPV (1μM, 0.33μCi/ml) and a range of ritonavir concentrations (0-1μM).

5.2.3 Selection of plasma samples from the Liverpool TDM registry for SLCO genotyping

Ethics committee approval to genotype archived plasma blood samples without written, informed consent from individuals listed on the Liverpool TDM registry had previously been granted. Plasma samples were selected from 400 individuals that received lopinavir/ritonavir 400mg/100mg b.d. regimes, were aged above 18 years and had recorded lopinavir concentrations. 326/400 patients had plasma samples 10-14h post-

dose (designated Cmin) and 293/400 patients had plasma samples 2-6h post-dose (designated $C_{2\text{-}6}$). Exclusion criteria included pregnancy, undetectable plasma LPV concentrations (suggesting non-adherence to the regimes) and concomitant medications with: sodium valproate, carbamazepine, rifampicin (or any other TB treatment) and acid reducing agents. Prior to plasma sample analysis, all patient data were completely anonymised. Of the samples included in the analysis, 78% were male (4% unspecified), median age was 40 (range 19 to 64), median weight was 72 Kg (range 44 to 113) and median lopinavir concentration was 5072ng/ml (range 114 to 24432).

5.2.4 Plasma DNA extraction and SLCO genotyping

DNA was extracted from plasma (600 µL) using a GenElute Blood Genomic DNA kit (Sigma-Aldrich, Poole, UK), according to the manufacturer's instructions. Genotyping for the *SLCO1A2* 516A>C and 38T>C, *SLCO1B1* 521T>C SNP and *SLCO1B3* 334T>G SNPs were performed using a real-time qPCR based allelic discrimination assay. Polymerise chain reactions (PCR) were performed using a reaction volume of 25µl containing assay-specific primers (final conc. 0.5µM each primer), allele specific TaqMan MGB probes (0.1µM each probe), ABgene qPCR mix and 2 µl of the eluted sample genomic DNA solutions (100 µl). Thermal-cycling conditions consisted of 60 cycles of 95°C for 10 minutes, 92°C for 15 seconds and 60°C for 1 minute. Fluorescence, proportional to amplification, was measured using the Opticon 2 and Chromo4 real-time detector (Biorad, Hemel Hempstead, UK). All genotyping experiments were performed in duplicate and included no template controls and positive

controls for each of the possible genotypes. Genotype was only assigned when both duplicates were in agreement.

5.2.5 Statistical analysis

SNPs were tested to assess whether they were in Hardy-Weinburg equilibrium by Chi squared test of observed versus predicted genotype frequencies. The data set was tested for normality by Shapiro-Wilk. Genetic associations with LPV plasma concentrations were tested by Mann-Whitney and demographic associations were tested by Spearman's rank correlation coefficient on log transformed plasma concentrations. Multivariate analyses were also conducted by linear regression with backward subtraction using SPSS 16.

5.3 Results

5.3.1 Inhibition of SLCO1B1 transport by ritonavir

SLCO1B1-KSM cRNA injected oocytes had increased accumulation of both E3S and LPV compared to water injected oocytes. The addition of ritonavir (0-1000ng/ml) did not change the accumulation of E3S (Fig. 1a) or LPV (Fig. 1b) in *SLCO1B1*-KSM cRNA-injected or water-injected oocytes.

a)

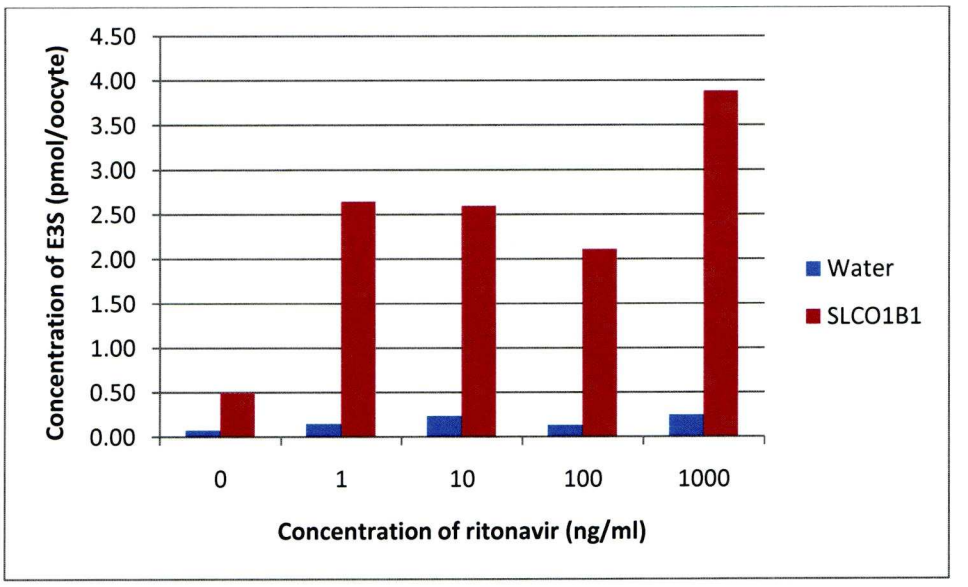

b)

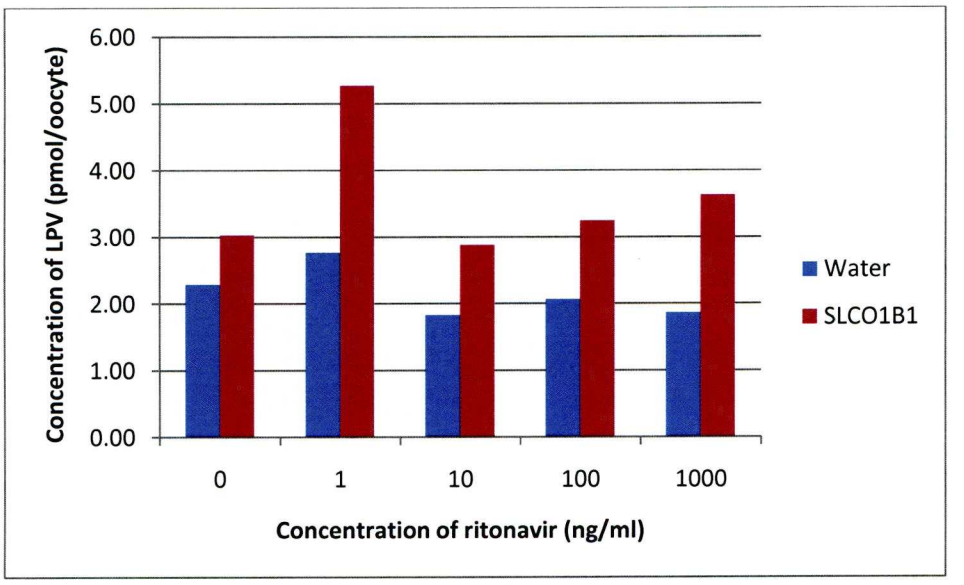

Fig. 1 Inhibition of a) E3S and b) LPV transport by ritonavir in SLCO1B1-KSM injected oocytes (n=1).

5.3.2 SLCO SNPs and association with lopinavir plasma concentrations

The frequencies of the minor alleles for *SLCO1A2* 38 (C), *SLCO1A2* 516 (C), *SLCO1B1* 521 (C) and *SLCO1B3* 334 (T) were 9%, 4%, 11% and 32% respectively. All SNPs were in Hardy-Weinburg equilibrium.

No significant associations were observed between *SLCO1A2* 38, *SLCO1A2* 516 and *SLCO1B3* 334 genotypes and LPV Cmin or $C_{2\text{-}6}$ (Fig. 2a-2f).

LPV Cmin was significantly higher in *SLCO1B1* 521C homozygotes (plasma concentration [range], 11141 [3409 - 19209] ng/ml) than in either heterozygotes (5353 [828 - 14615] ng/ml; p=0.03) or 521T homozygotes (4912 [114 - 35791] ng/ml; p=0.02; Fig. 2g). LPV $C_{2\text{-}6}$ was higher in *SLCO1B1* 521C homozygotes (9671 [3593 - 21399] ng/ml; p=0.13) and in heterozygotes (7514 [1617 - 17313] ng/ml; p=0.03) than in 521T homozygotes (6516 [312 -39894] ng/ml; Fig. 2h). Univariate and multivariate regression analyses are summarised in Table 1. For Cmin, the multivariate model had an adjusted R^2=0.068; F=10.7, p<0.001 and for $C_{2\text{-}6}$, the multivariate model had an adjusted R^2=0.062; F=7.6, p<0.001. *SLCO1B1* 521T>C was independently associated with LPV Cmin (15.6% higher for each allelic variant) and $C_{2\text{-}6}$ (13.9% for each allelic variant) when multivariate analysis was performed.

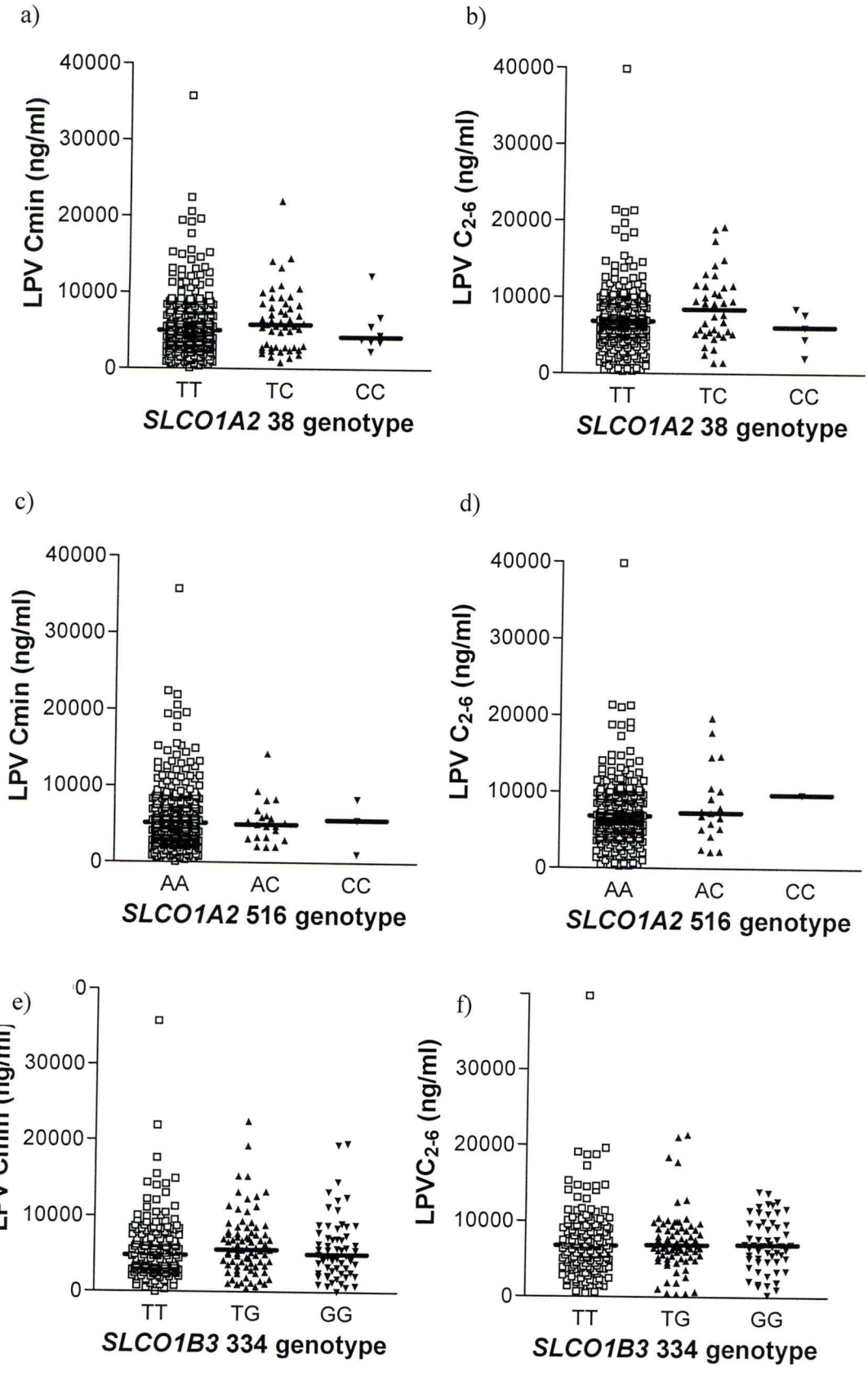
a)
LPV Cmin (ng/ml)
40000
30000
20000
10000
0
TT
TC
CC
SLCO1A2 38 genotype
b)
LPV C2-6 (ng/ml)
40000
30000
20000
10000
0
TT
TC
CC
SLCO1A2 38 genotype
c)
LPV Cmin (ng/ml)
40000
30000
20000
10000
0
AA
AC
CC
SLCO1A2 516 genotype
d)
LPV C2-6 (ng/ml)
40000
30000
20000
10000
0
AA
AC
CC
SLCO1A2 516 genotype
e)
LPV Cmin (ng/ml)
30000
20000
10000
0
TT
TG
GG
SLCO1B3 334 genotype
f)
LPVC2-6 (ng/ml)
30000
20000
10000
0
TT
TG
GG
SLCO1B3 334 genotype

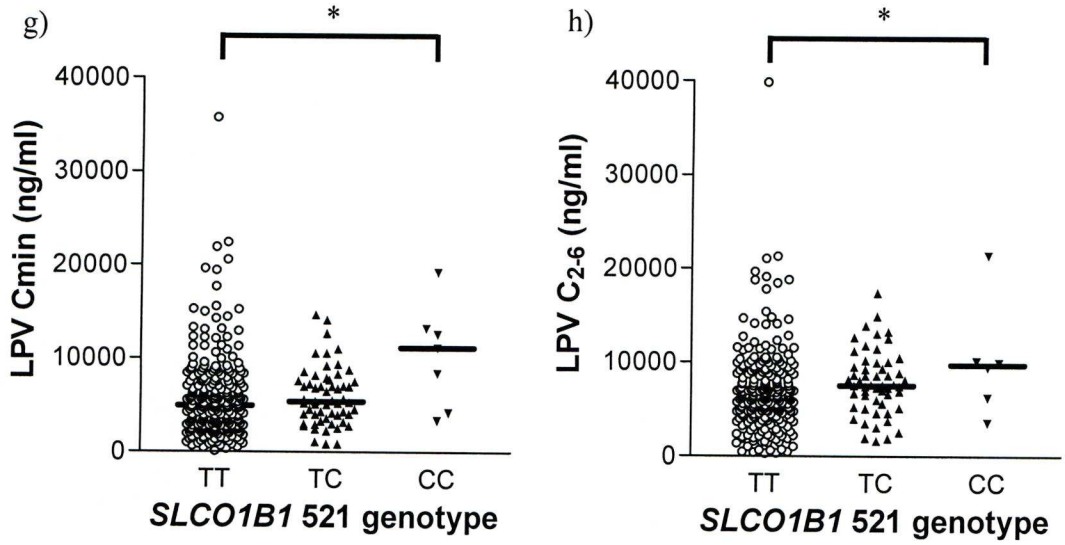

Fig. 2 Associations between SLCO genotypes and LPV Cmin and $C_{2\text{-}6}$ a) *SLCO1A2* 38 and Cmin, b) *SLCO1A2* 38 and $C_{2\text{-}6}$, c) *SLCO1A2* 516 and Cmin, d) *SLCO1A2* 516 and $C_{2\text{-}6}$, e) *SLCO1B3* 334 and Cmin, f) *SLCO1B3* 334 and $C_{2\text{-}6}$, g) *SLCO1B1* 521 and Cmin and h) *SLCO1B1* 521 and $C_{2\text{-}6}$. * $p<0.05$.

5.3.3 Demographic associations with lopinavir plasma concentrations

No significant associations were observed between age or gender with LPV plasma concentrations (Fig. 3a-3d). Body weight and co-administered PI were independently associated with LPV Cmin and $C_{2\text{-}6}$ in both univariate and multivariate analysis. Cmin was 10.3% lower for every 10kg increase in body weight (Fig 3e) and was also 25.9% higher in patients receiving an additional PI (Fig. 3g). An increase in body weight of 10kg lowered LPV plasma concentrations at $C_{2\text{-}6}$ by 6.9% (Fig. 3f) and co-administration with other PIs increased LPV $C_{2\text{-}6}$ plasma concentrations by 23.2% (Fig. 3h).

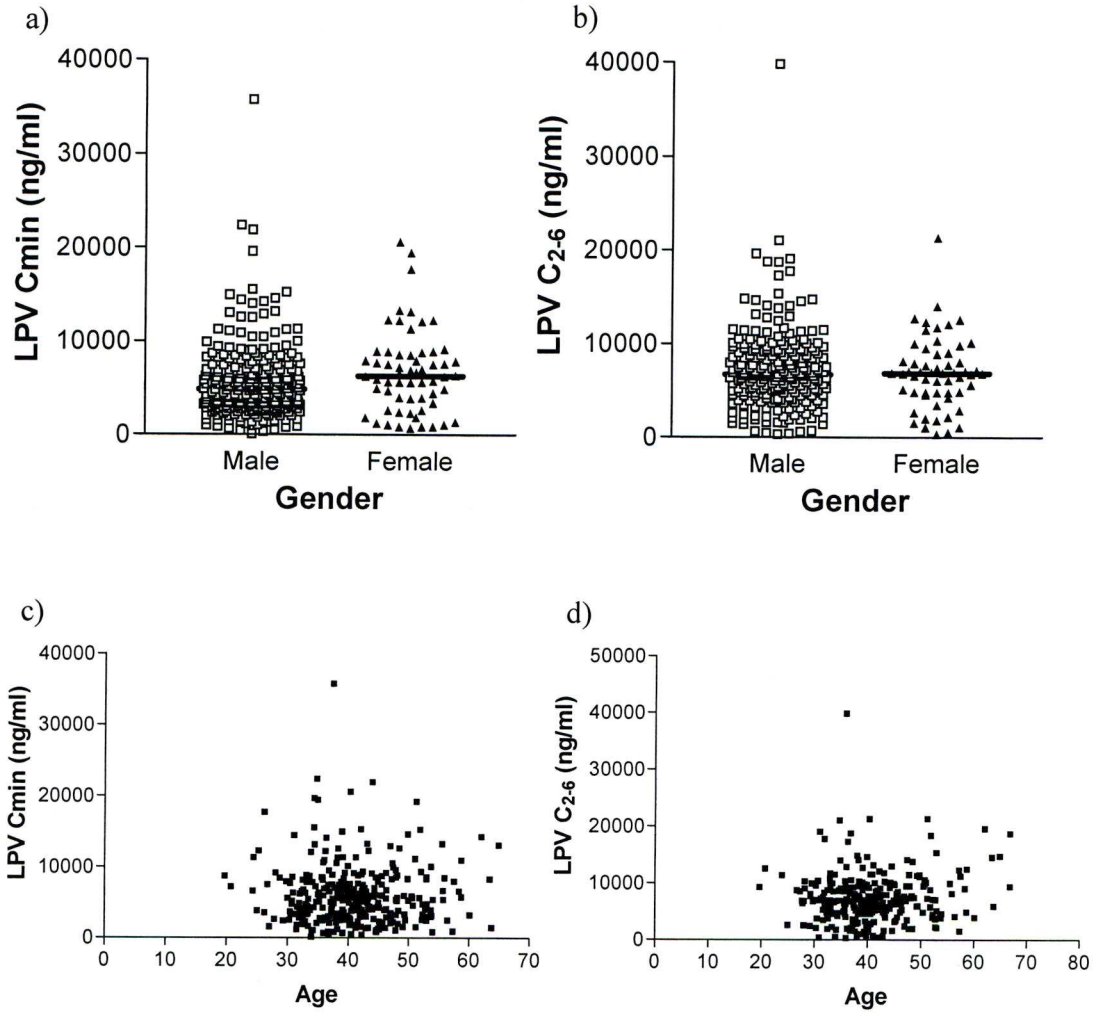

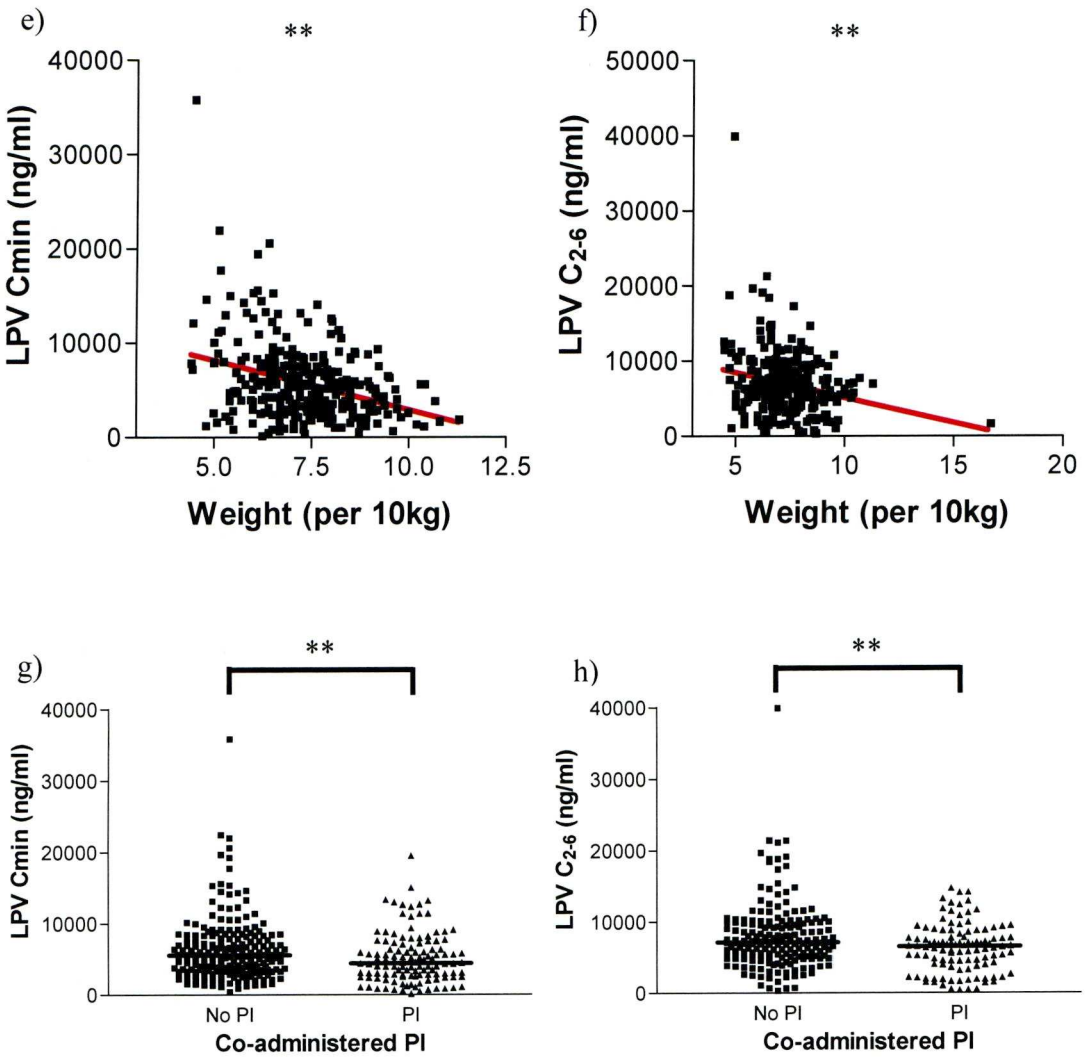

Fig. 3 Associations between population demographics and LPV Cmin and $C_{2\text{-}6}$ a) gender and Cmin, b) gender and $C_{2\text{-}6}$, c) weight and Cmin, d) weight and $C_{2\text{-}6}$, e) age and Cmin, f) age and $C_{2\text{-}6}$, g) co-administered PI and Cmin and h) co-administered PI and $C_{2\text{-}6}$. **$p \leq 0.01$

Table. 1 Multivariate analysis by best subset selection of factors influencing LPV plasma concentrations in the Liverpool TDM registry.

Independent Variable	Dependent variable	Univariate P (Effect size %)	Multivariate P (Effect size %)
SLCO1B1 521T>C	Cmin (ng/ml)	**0.025 (22.5)**	**0.046 (15.6)**
	$C_{2\text{-}6}$ (ng/ml)	**0.019 (23.1)**	**0.041 (13.9)**
SLCO1B3 334T>G	Cmin (ng/ml)	0.72	-
	$C_{2\text{-}6}$ (ng/ml)	0.98	-
SLCO1A2 38T>C	Cmin (ng/ml)	0.40	-
	$C_{2\text{-}6}$ (ng/ml)	0.25	-
SLCO1A2 516A>C	Cmin (ng/ml)	0.85	-
	$C_{2\text{-}6}$ (ng/ml)	0.24	-
Age	Cmin (ng/ml)	0.83	-
	$C_{2\text{-}6}$ (ng/ml)	0.20	-
Male Gender	Cmin (ng/ml)	0.25	-
	$C_{2\text{-}6}$ (ng/ml)	0.43	-
Body Weight (per 10kg)	Cmin (ng/ml)	**<0.001 (-14.9)**	**<0.001 (-10.3)**
	$C_{2\text{-}6}$ (ng/ml)	**0.003 (-9.1)**	**0.003 (-6.9)**
Coadministered PI	Cmin (ng/ml)	**0.001 (33.8)**	**0.001 (25.9)**
	$C_{2\text{-}6}$ (ng/ml)	**0.001 (31.7)**	**0.001 (23.2)**

5.4 Discussion

Many PIs are boosted with ritonavir and hence the effect of ritonavir on the transport of E3S, the paradigm control substrate, and LPV, the paradigm PI, was examined. Using the X. *laevis* oocyte model, no effect on E3S or LPV transport by SLCO1B1 was observed with increasing concentrations of ritonavir, up to 1μg/ml.

Genotyping from the Liverpool TDM plasma samples was performed in duplicate or triplicate where genotyping results were contradicting. This may be due to the low levels of DNA found in plasma samples (Lee *et al.* 2001), which may reduce the accuracy of genotyping by real-time PCR.

SLCO1B1 521C>T was found to be associated with LPV plasma concentrations at both Cmin and $C_{2\text{-}6}$. TT homozygotes had significantly lower LPV plasma concentrations than individuals with the CC or CT genotypes. This is consistent with other studies which found an association between 521C>T and statin plasma concentrations (Niemi *et al.* 2006; Pasanen *et al.* 2006; Lau *et al.* 2007). No correlations were observed between *SLCO1B3* 334T>G and LPV pharmacokinetics, which is consistent with data on this SNP and paclitaxel pharmacokinetics (Smith *et al.* 2007). There were also no associations observed between *SLCO1A2* 38T>C and 516A>C SNPs and LPV pharmacokinetics. Whilst this contradicts the *in vitro* studies by Badagnani *et al.* (2006) and Lee *at al.* (2005), little is known about the effect of these SNPs on *in vivo* pharmacokinetics. The lack of correlation between these SNPs and LPV pharmacokinetics warrants further investigation with other SLCO1A2 substrates, such as fexofenadine, to observe whether these results can be generalised. This would be

informative as to whether these candidate SNPs impact pharmacokinetics of other substrates or whether they only have an effect *in vitro*. It is also possible that this transporter may not be important for pharmacokinetics, but it may have a role in brain penetration, where it is found to be highly expressed.

From the demographic information available for the TDM cohort, body weight and co-administered PIs were the only variables which were significantly associated with changes in both LPV Cmin and $C_{2\text{-}6}$. The association with body weight is similar to studies which found a weak association between increasing body weight and decreases in saquinavir Cmax (Lotsch *et al.* 2007) and LPV Cmax (Oki *et al.* 2004). In another study, co-administration of LPV with atazanavir (ATV) was demonstrated to increase plasma concentration of both LPV and ATV (Ribera *et al.* 2006); however, co-administering LPV with other PIs is not currently common practice due to the availability of newer drugs (Ribera and Curran 2008).

To validate the effect of the polymorphisms or characterise novel SNPs on transporter affinity for substrates *in vitro*, the oocyte system may be used by injecting cRNA containing polymorphisms introduced by site-directed mutagenesis. Antibodies will be required to detect the expression of the mutated proteins, which is important for discerning whether a lack or reduced accumulation in the oocytes is due to the polymorphism or lack of expression. For transporters which currently do not have commercially available antibodies, the transporters can be His-tagged and detected using generic secondary antibodies.

This study shows that the *SLCO1B1* 521T>C SNP is associated with LPV pharmacokinetics; however, it is unlikely that it can be used as a genetic predictor of LPV pharmacokinetics. Whilst no correlations were observed between *SLCO1A2* or *SLCO1B3* SNPs and LPV plasma concentrations, LPV and other PIs are substrates for multiple SLCO transporters, hence a more comprehensive pharmacogenetic study combined with a haplotype analysis is required to fully characterize the impact of SLCO transporters on PI pharmacokinetics. However, population demographic factors such as body weight were also significantly associated with LPV pharmacokinetics. Due to the multi-factorial nature of variability in pharmacokinetics, developing personalized medicines and predictors of drug toxicity and efficacy still remains a challenge.

Chapter 6

Investigating the effect of siRNA knockdown of SLCO transporters in immortalised human cell lines

6.1 Introduction

Influx transporters, including SLCOs, are expressed in different tissues and at various levels. In the liver, SLCO1A2, SLCO1B1, SLCO1B3 and SLCO3A1 are expressed with higher levels of SLCO1B1 and SLCO1B3 (Tamai *et al.* 2000; Bleasby *et al.* 2006). However, in the intestine, SLCO1B1 and SLCO1B3 are not expressed and the expression of SLCO1A2 remains controversial (Lee *et al.* 2005; Bleasby *et al.* 2006; Hilgendorf *et al.* 2007). SLCO3A1 is expressed ubiquitously, with high levels of expression found in the blood mononuclear cells (Bleasby *et al.* 2006; Janneh *et al.* 2008). SLCO1A2 has varied expression with studies reporting expression in brain, intestine, kidney and lungs (Tamai *et al.* 2000; Lee *et al.* 2005; Bleasby *et al.* 2006). The SLCO transporters have overlapping substrate specificities and varied tissue distribution, which should be appreciated when considering drug distribution.

Cell lines are commonly used to observe the effect of basal levels of transport proteins on drugs and vice versa. Cell lines are also used for over-expression of target proteins by drug selection (Davey *et al.* 1996), or by transfection of plasmids containing the gene of interest (Bakos *et al.* 1998). Whilst cell models which over-express transport proteins are used to evaluate substrate specificity, this may not be an accurate representation of levels of expression or function in different tissues *in vivo*. Inhibitors of transporters are commonly used to ascertain the function of specific transporters but the limitations of this approach are the expression of various known and unknown transporters in the cell lines and also the lack of specificity of some inhibitors (as was observed in Chapter 2). Immortalised cell lines may not completely represent the expression levels of transporters present in their respective primary tissue counterparts (Hilgendorf *et al.*

2007), but they are similar and are easy to culture and manipulate compared to primary cells.

RNAi is a widely used approach for gene silencing to understand functions of specific proteins. There are two main methodologies for conducting RNAi knockdown studies, shRNA and siRNA. For stable knockdown of target genes, shRNA is commonly used, which involves cloning DNA into plasmids and transfection into cells (McCaffrey *et al.* 2002). These plasmids generate shRNA, which become siRNA after cleavage by dicer, a cellular enzyme (Preall and Sontheimer 2005). siRNA is used for transient knockdown and can be chemically synthesised. siRNA are short (20-25 nucleotides), double stranded RNA sequences which are complementary to, and bind to, the gene of interest (Elbashir *et al.* 2001; McCaffrey *et al.* 2002). This recruits cellular mechanisms to degrade the siRNA/gene complex and the reduction of gene specific mRNA consequently reduces the level of protein expression (Preall and Sontheimer 2005).

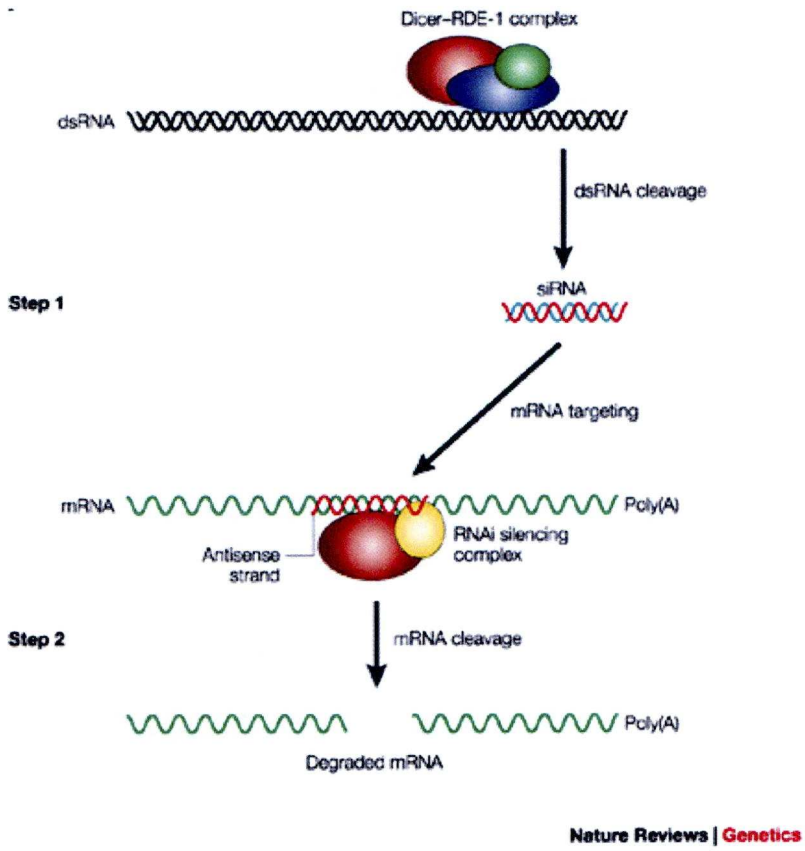

Fig. 1 Degradation of gene specific mRNA by siRNA (modified from McManus and Sharp 2002)

Introducing siRNA can also cause non-specific gene silencing (off-target effects) due to the incomplete complementarity of the siRNA with non-target genes (Jackson *et al.* 2003). This incomplete complementarity of siRNA also has a similar effect to microRNAs and has been reported to cause knock-up effects, especially of genes associated with the interferon response (Scacheri *et al.* 2004). The development of siRNA as a molecular tool for understanding the role of genes has improved, with recently designed siRNA having minimal off-target effects (Birmingham *et al.* 2006; Jackson *et al.* 2006). There are also different methodologies for RNAi delivery into

cells and the most commonly used approaches involve electroporation or cationic lipid reagents (Fedorov *et al.* 2005).

In the Chapter 4, protease inhibitors were found to be substrates for SLCO1A2, SLCO1B1 and SLCO1B3 in the X. *laevis* over-expression system. The aim of this chapter was to ascertain the importance of basal levels of SLCOs for protease inhibitors (PIs). However, due to time constraints it was only possible to conduct siRNA optimisation experiments and attempt validation using estrone-3-sulphate (E3S). This was conducted in Caco-2, HepG2, Huh7 and 293T human cell lines.

6.2 Methods

6.2.1 Materials

Brain, lung, liver, lymph, heart, pancreas, colon, kidney, adrenal and thymus total RNA was purchased from Stratagene (Cheshire, UK). Caco-2, 293T, Huh7 and HepG2 cell lines were purchased from ECACC (Salisbury, UK). SLCO1A2, SLCO1B1, SLCO1B3 and SLCO3A1 ON-TARGETplus SMARTpool were purchased from Perbio Science UK Ltd. (Northumberland, UK). Cell Line Nucleofector kit T and V were purchased from Amaxa AG (Koeln, Germany). Lipofectamine 2000 was purchased from Invitrogen (Paisley, UK). TaqMan Reverse Transcription Reagents and TaqMan Gene Expression Assays were purchased from Applied Biosystems (Warrington, UK). ABsolute QPCR mix was purchased from ThermoFisher Scientific (Loughborough, UK).

6.2.2 Cell culture

239T, Huh7 and HepG2 cells were routinely cultured in DMEM supplemented with 10% FCS and incubated (37°C with 5% CO_2). Caco-2 cells were cultured in DMEM supplemented with 15% FCS and incubated using the same conditions as above. For routine passaging, the cell lines were washed with HBSS (twice, 20mls) followed by trypsin treatment (2mls, 10-20mins incubation at 37°C) and deactivation (3mls DMEM with respective supplement). 239T were split 1:15, Caco-2 were split 1:3, Huh7 and HepG2 were split 1:6.

6.2.3 mRNA extraction and reverse transcription

A panel of tissue mRNA consisting of brain, lung, liver, lymph, heart, pancreas, colon, kidney, adrenal and thymus were used to analyse tissue distribution of SLCO1A2, SLCO1B1, SLCO1B3 and SLCO3A1. Tissue mRNA were reverse transcribed as described in Chapter 3.2.4, whilst mRNA from cell lines were extracted by treatment with TRI reagent and frozen (-20°C, overnight). After thawing, mRNA extraction and cDNA synthesis were conducted as described in Chapter 3.2.3 and 3.2.4, respectively.

6.2.4 Analysis of gene expression

cDNA was quantified by Nanodrop (Thermo Scientific) and normalised to 20ng/µl. The PCR reactions were assembled at room temperature and included ABSOLUTE PCR mastermix (12.5µl), respective primer and probe assay (1.25µl) and cDNA (40ng). Each sample was performed in duplicate in Opticon 2 and Chromo 4 Real-Time PCR machines (Biorad) to measure gene expression and the Opticon Monitor 3 software was used to analyse the data.

The C(t) values were taken and the δC(t) values were calculated (test C(t) values - β-actin C(t) values). δδC(t) values were then calculated from δC(t) values (test values were normalised to cells only control, test δC(t) - control δC(t)) and the relative expression was determined ($2^{-\delta\delta C(t)}$). The mean of the duplicates were calculated and the percentage knockdown levels were calculated (test/control mean relative expression × 100).

6.2.5 siRNA delivery by Nucleofection into cell lines

293T, Huh7, HepG2 and Caco-2 cells were grown to confluence. The cells were trypsinised, resuspended in DMEM with respective supplement and counted using the NucloCounter. Amaxa Nucleofection kits and programmes were used as described in the manufacturer's protocols. Supplement R was added to Solution T and V prior to resuspending the cells in the solutions (100µl). Nucleofector solution T was used for Caco-2 and Huh7, whilst solution V was used for HepG2 and HEK293T. Programme Q-001 was used for HEK293T, B-024 was used for Caco-2 and T-028 was used for Huh7 and HepG2 cells. For HEK293T, Huh7 and HepG2, 6×10^6 cells were used and for Caco-2 3×10^6 cells were used per transfection. For each cell line, SLCO1A2, SLCO1B1, SLCO1B3 and SLCO3A1, ON-TARGETplus SMARTpool siRNA (final concentration of 80nM) was used to knockdown gene expression. A cells-only control, mock transfection control, positive control and negative control (final concentration of 80nM) were also included. The positive control was human GAPDH ON-TARGETplus control pool siRNA and the negative control was human ON-TARGETplus Non-Targeting Pool. Each transfection was transferred (200µl) into 3 wells of a 48-well plate containing DMEM with respective supplement (750µl). Culture media was changed daily and cells were treated with TRI reagent (1ml) at 24, 48 and 72 hours post transfection.

6.2.6 siRNA delivery by Lipofectamine 2000 into cell lines

HepG2 and Caco-2 cells (5×10^4 cells, 400µl) were grown in 24 well plates 24 hours prior to transfection. SLCO1A2, SLCO1B3, SLCO1B1 and SLCO3A1 ON-TARGETplus SMARTpools (5-40pmol) were diluted with DMEM media supplemented with 10% FCS (50µl, 5mins, room temperature). Lipofectamine 2000 (0.5-1.5µl) was mixed with DMEM supplemented with 10% FCS (50µl, 10mins, room temperature) and subsequently added to the diluted siRNA and incubated to form siRNA complexes (20mins, room temperature). siRNA complexes (100µl) were then added to pre-plated cells. Media was replaced 24h post transfection and changed daily. Cells were collected into TRI reagent (800µl) 24h and 48h post transfection.

6.2.7 Cellular accumulation of E3S in SLCO knockdown cells

The optimal seeding density of HepG2 in 6 well plates was investigated to determine the seeding density for E3S uptake in SLCO knockdown HepG2 cells.

Subsequently, HepG2 cells were seeded (5×10^4 - 5×10^6 cells/well) and grown in 6-well plates (2.5ml DMEM supplemented with 10% FCS, incubated at 37°C with 5% CO_2, 48h). After incubation, HepG2 cells were trypsinised (500µl, 37°C) until cells detached. DMEM supplemented with 10% FCS (500µl) was then added and the trypsinised cells were placed into 1.5ml eppendorfs. The samples were centrifuged (2000rpm, 5mins), the supernatant was removed and the cells were resuspended in DMEM supplemented with 10% FCS (500µl). [3H] E3S (0.02µCi/ml, 500µl) was added to the cells and incubated (37°C, 20mins). Following incubation, cells were centrifuged (13,000 × g,

1min) and supernatant (100µl) was added to scintillation vials. The remaining supernatant was removed and ice cold Hank's balanced salt solution was used to wash the cell pellets. The cell pellets were centrifuged (13,000 × g, 1min) and washed a further 2 times. The cell pellets were solubilised in water (100µl) and transferred to scintillation vials. Scintillation fluid (4ml) was added to all the samples and counted by liquid scintillation spectroscopy. The cellular accumulation ratio (CAR) was calculated as described in Chapter 2 (2.2.5) and the average cell volume of HepG2 cells was assumed to be 1.2pl (Wehner *et al.* 2002).

HepG2 cells were trypsinised, counted and cultured in 6-well plates (2.5×10^5 cells, 2ml, overnight) prior to transfection. Lipofectamine 2000 was added to DMEM containing 10% FCS (7.5µl Lipofectamine 2000 per 250µl media, 5mins) and SLCO1B3 ON-TARGETplus smartPOOL siRNA was added to DMEM containing 10% FCS and upscaling was as per manufacturer's protocols (5µl of SLCO1B3 siRNA at 20µM per 250µl media, 5mins). Lipofectamine 2000 in media was subsequently added to SLCO1B3 siRNA in media (1:1) and incubated (20mins, room temperature). Media was added to a separate stock of Lipofectamine 2000 with media (1:1, 20mins, room temperature). Following the incubation period, media, Lipofectamine 2000 in media and Lipofectamine 2000 with SLCO1B3 siRNA in media was added to the pre-plated cells (500µl, 2.5ml total volume). At 48h and 72h post transfection, cells were trypsinised and used for uptake studies and treated with TRI reagent for subsequent mRNA extraction, reverse transcription and gene expression studies.

Extraction and reverse transcription was performed as described in 6.2.3 and gene expression was quantified as described in 6.2.4. Functional cell uptake studies were

performed by adding [^{3}H] E3S (0.02μCi/ml, 500μl) to trypsinised cells resuspended in DMEM media (500μl, 20mins, 37°C) and the subsequent methods for uptake were as described above.

6.2.8 Statistical analysis

The samples were tested for normality using the Shapiro-Wilk test and at least one of the data sets was not likely to be from a normal distribution; therefore, the Mann-Whitney U-test was used to test for statistical differences between the conditions.

6.3 Results

6.3.1 Expression of SLCOs in human tissues

The relative expression of SLCO1A2 mRNA was highest in the brain and with detectable levels in the kidney, lung and liver (Fig. 1a). SLCO1B1 was only detected in the liver (Fig. 1b) and SLCO1B3 was detected in the liver and the pancreas (Fig. 1c). SLCO3A1 had ubiquitous expression amongst the tissue samples tested (Fig. 1d).

a)

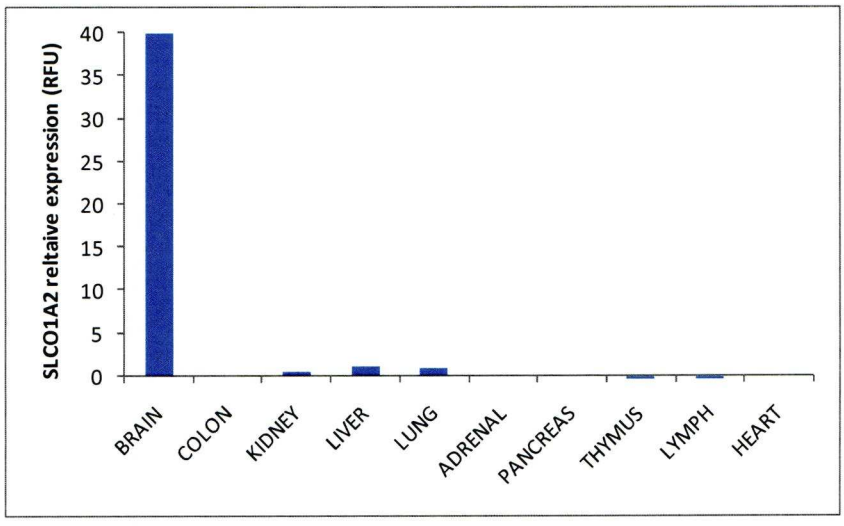

b)

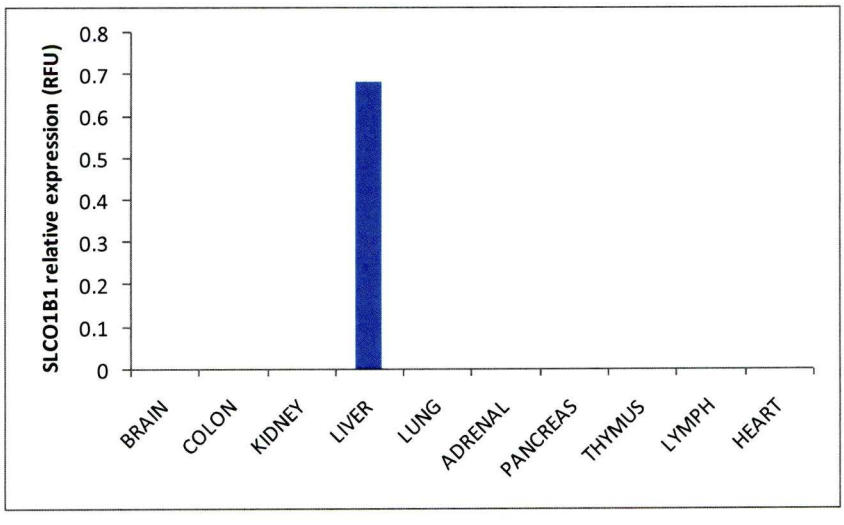

c)

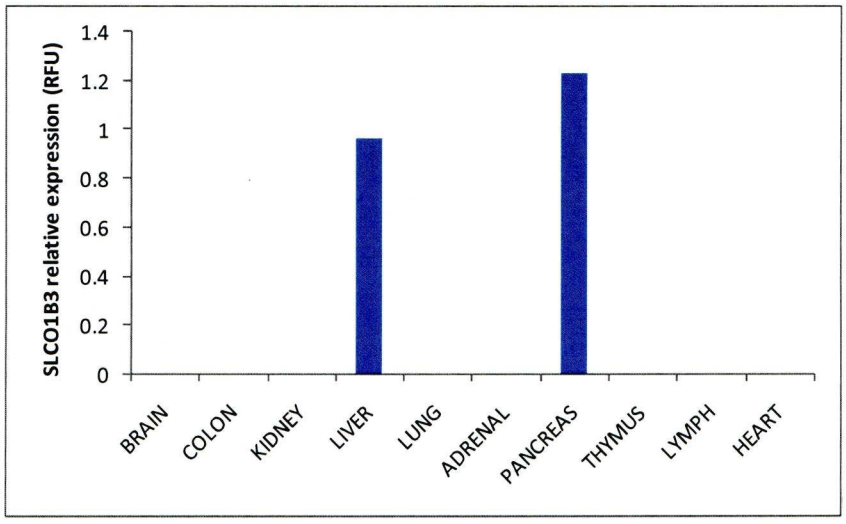

d)

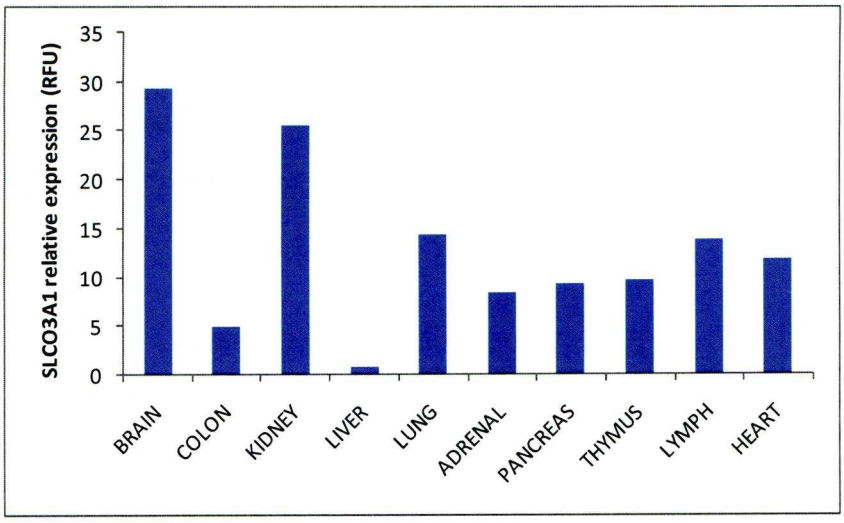

Fig. 2 The detection of a) SLCO1A2, b) SLCO1B1, c) SLCO1B3 and d) SLCO3A1 mRNA in a panel of tissues (n=1).

The relative expressions of SLCO1A2, SLCO1B1, SLCO1B3 and SLCO3A1 were assessed in Caco-2, Huh7, HepG2 and 293T cells and compared to their primary cell counterparts (colon, liver and kidney).

SLCO1B1 was not detected in colon or Caco-2, whereas SLCO1A2 was found to be expressed in Caco-2 cells and not in colon mRNA. SLCO1B3 was detected in colon but not in Caco-2 and relatively high expression of SLCO3A1 was detected in Caco-2 cells compared to colon (Fig. 3a).

In the liver, SLCO1A2, SLCO1B1, SLCO1B3 and SLCO3A1 were all detectable. However, Huh7 and HepG2, which are both hepatic cell lines, expressed different levels of SLCOs. Huh7 cells did not express detectable levels of SLCO1B1 and relatively lower levels of SLCO1B3 and SLCO3A1 compared to liver mRNA. SLCO1A2 was highly expressed in Huh7 cells compared to liver (Fig. 3b). SLCO1A2 and SLCO3A1 were not detectable in HepG2 cells and there were relatively lower levels of SLCO1B1 and SLCO1B3 compared to liver (Fig. 3c).

No SLCO1B1 or SLCO1B3 was detected in kidney mRNA or in 293T cells. SLCO1A2 and SLCO3A1 were detected in kidney mRNA and lower levels of these transporters were detected in 293T cells (Fig. 3d).

a)

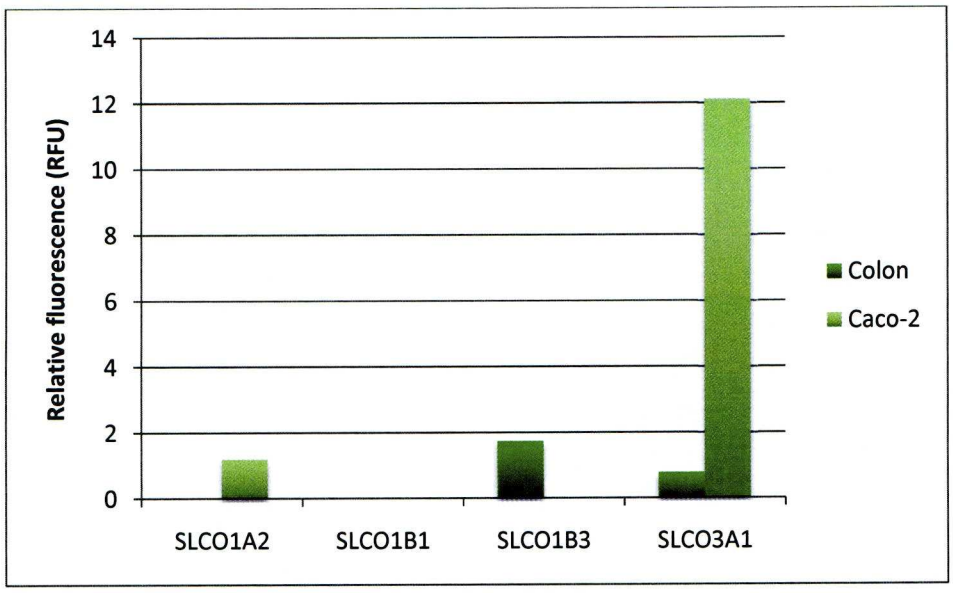
Relative fluorescence (RFU)
14
12
10
8
6
4
2
0
SLCO1A2
SLCO1B1
SLCO1B3
SLCO3A1
Colon
Caco-2

b)

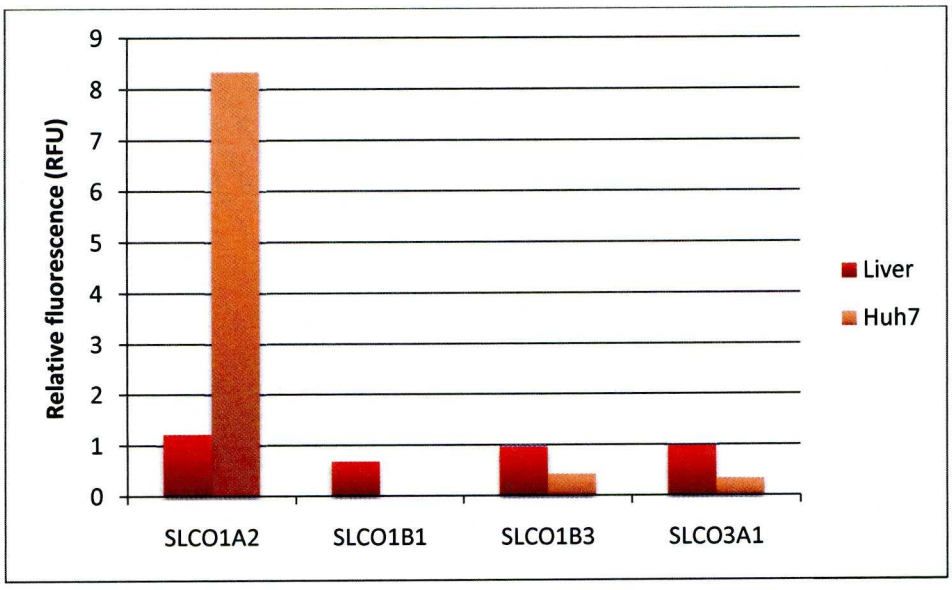
Relative fluorescence (RFU)
9
8
7
6
5
4
3
2
1
0
SLCO1A2
SLCO1B1
SLCO1B3
SLCO3A1
Liver
Huh7

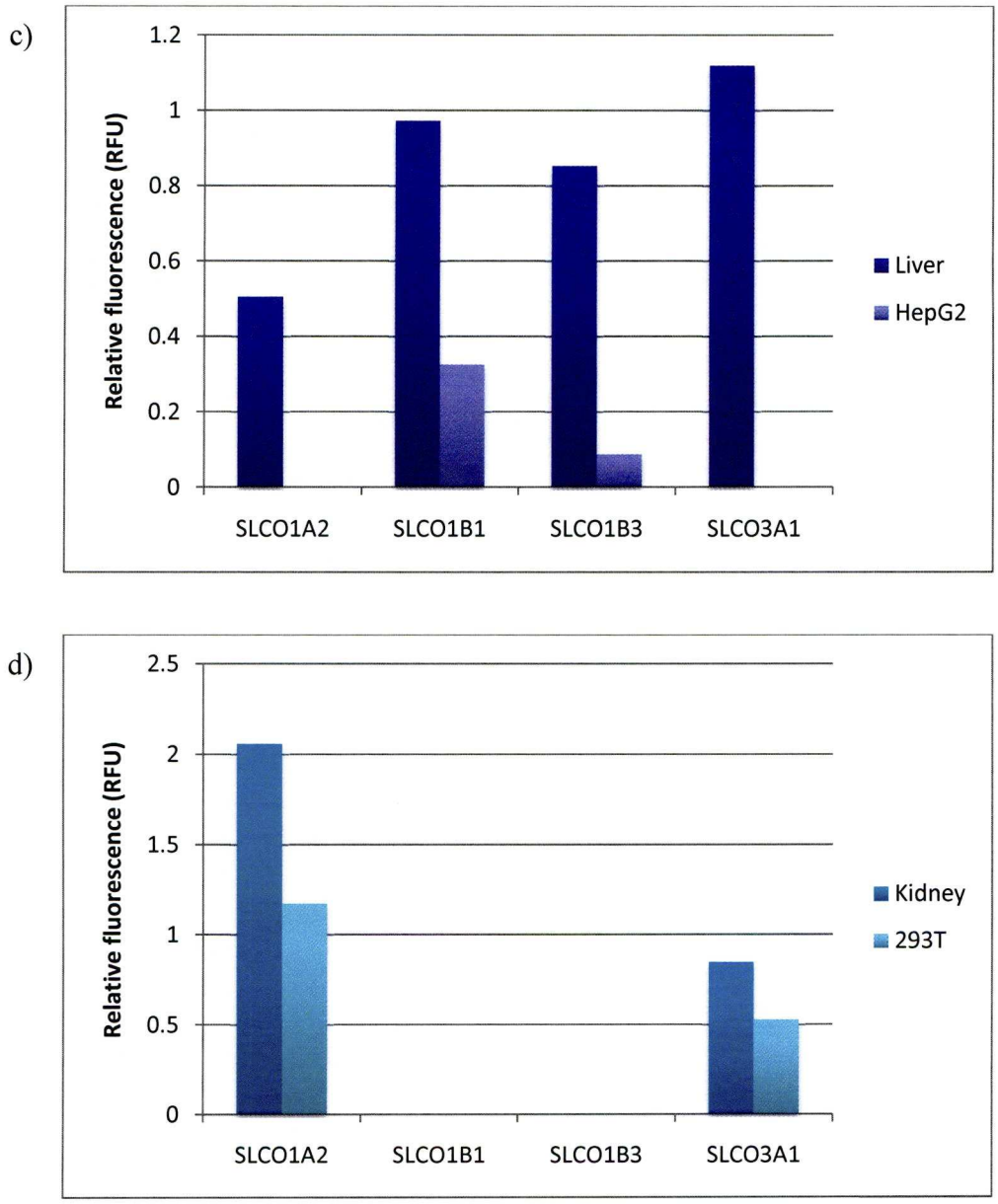

Fig. 3 Expression of SLCO1A2, SLCO1B1, SLCO1B3 and SLCO3A1 in cell lines compared to their tissue counterparts a) colon and Caco-2, b) liver and Huh7 c) liver and HepG2 and d) kidney and 293T (n=1).

6.3.2 Transfection of siRNA by Nucleofection

The TaqMan gene expression assay control, β-actin, was detected in all the cell lines, in every control (cells only) and in every test condition, and was comparable in each.

6.3.2.1 Caco-2 cells

Caco-2 cells had detectable knockdown of GAPDH after 24h (decrease of 94.8%), but this knockdown was not sustained at 48h and 72h post transfection (Fig. 4). SLCO1B1 and SLCO1B3 were not detected in the cell only control at 24h, 48h or 72h post transfection and SLCO1A2 and SLCO3A1 had inconsistent detection in cell only controls between the time points.

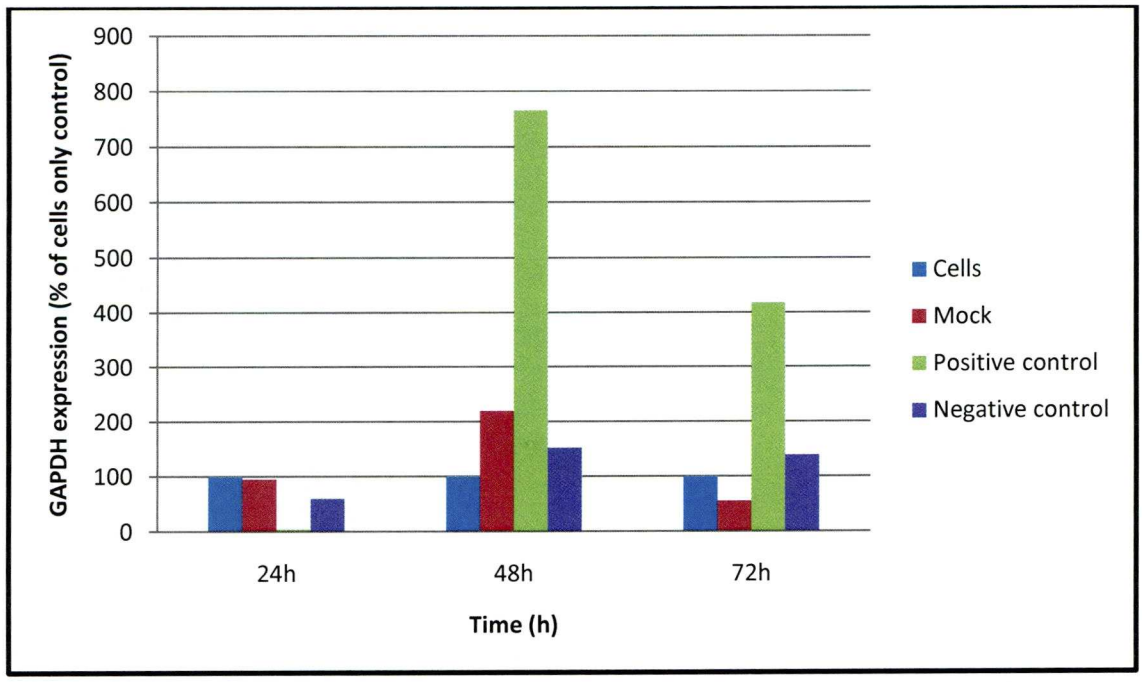

Fig. 4 GAPDH knockdown using Nucleofection with siRNA in Caco-2 cells (n=1)

6.3.2.2 HepG2 cells

HepG2 cells had detectable knockdown of GAPDH at 48h (decrease of 83.6%) and 72h (decrease of 85.2%) post-transfection (Fig. 5). SLCO1B1 was detected in the cell only control but no knockdown was observed at any of the time points. SLCO1B3 was detected in cell only controls, but was not detectable in siRNA-treated cells at 24h and 72h. At 48h, SLCO1B3 had detectable knockdown (decrease of 87.3%). Detection of SLCO1A2 and SLCO3A1 in the cell-only controls was inconsistent.

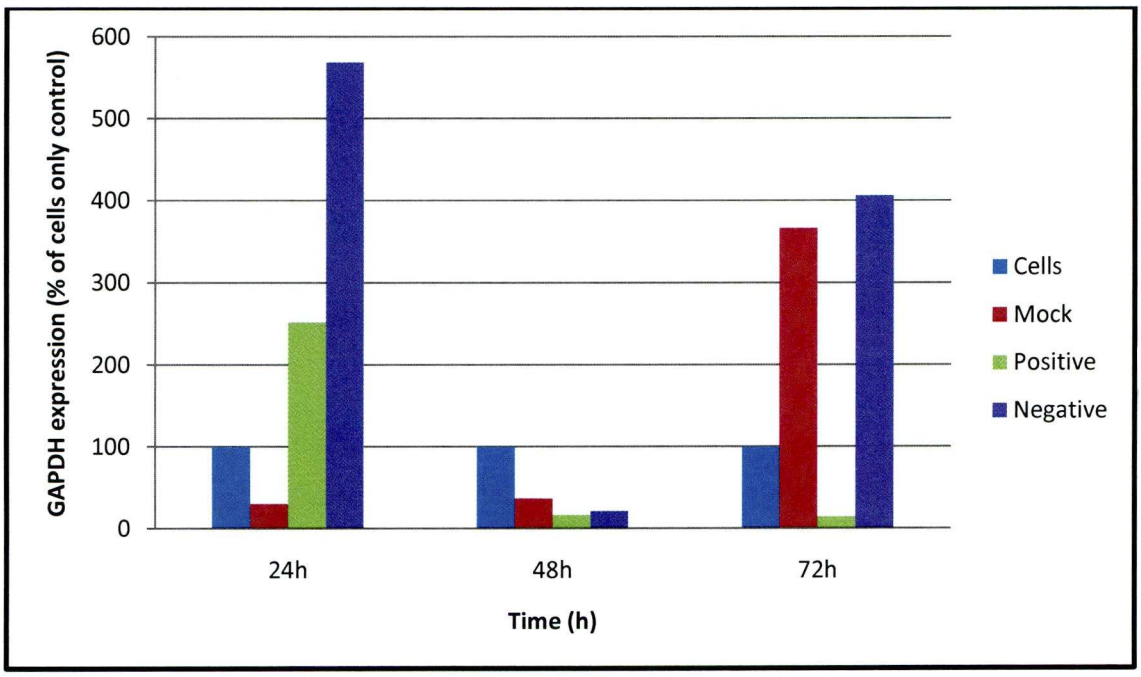

Fig. 5 GAPDH knockdown using Nucleofection with siRNA in HepG2 cells (n=1)

6.3.2.3 Huh7 cells

Huh7 cells had detectable knockdown of GAPDH at 24h (86.8%) and 48h (95.8%) post-transfection. At 72h, knockdown was still achieved (68.2%), but relatively more mRNA was detected compared to 24h and 48h time points (Fig. 6). SLCO1B1 and SLCO1B3 mRNA was present, but Nucleofection with respective siRNA did not decrease levels of expression at any of the time points. SLCO1A2 had detectable knockdown at 24h (55.9%) but detection in the cell-only control at 48h and 72h was inconsistent. SLCO3A1 mRNA detection was inconsistent.

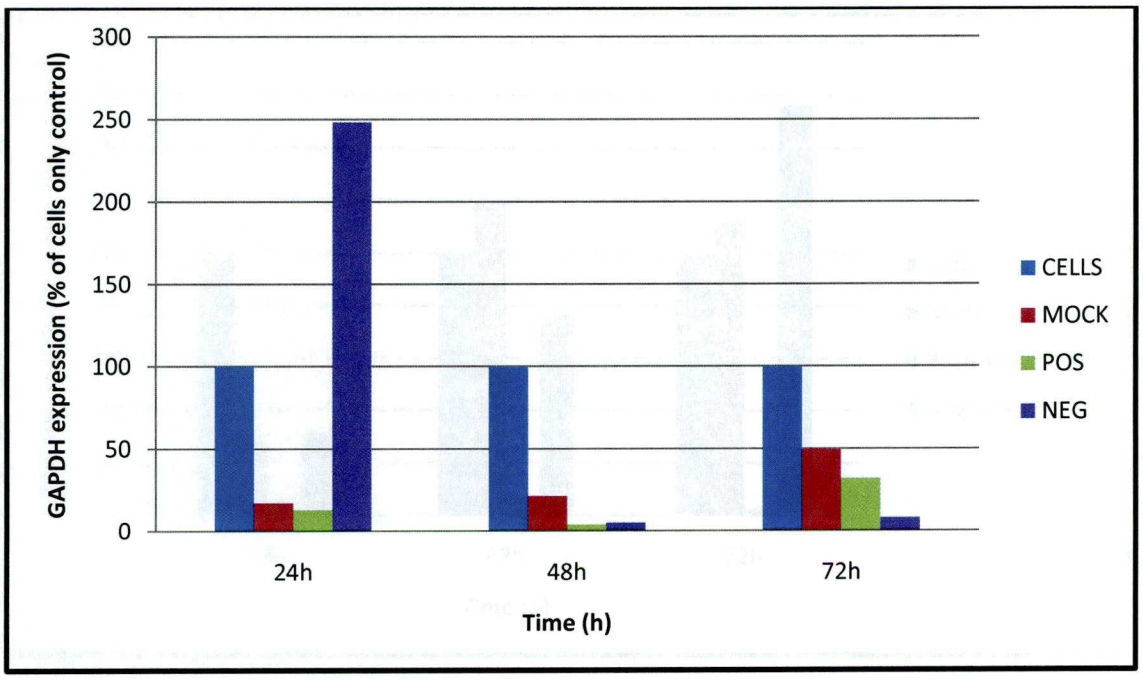

Fig. 6 GAPDH knockdown using Nucleofection with siRNA in Huh7 cells (n=1)

6.2.3.4 293T cells

293T cells had detectable and sustained knockdown of GAPDH at 24h (94.2%), 48h (97.5%) and 72h (97.4%, Fig. 7). No SLCO1B1 or SLCO1B3 was detected in 293T cells at any of the time points. SLCO1A2 and SLCO3A1 mRNA was detected in all the cell only controls. SLCO1A2 mRNA was detected, but no knockdown was observed at any of the time points. Detectable knockdown of SLCO3A1 was observed at the 24h time point (49.0%) and no detectable SLCO3A1 mRNA in SLCO3A1 siRNA-treated cells.

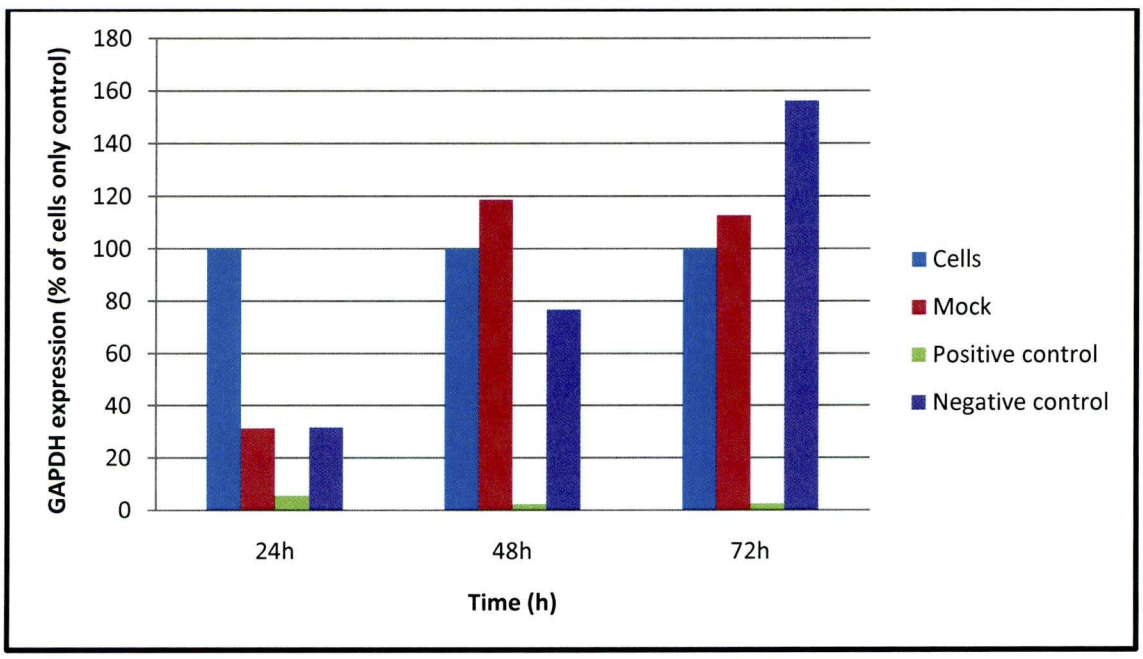

Fig. 7 GAPDH knockdown using Nucleofection with siRNA in 293T cells (n=1)

To observe the functional effect of siRNA knockdown by Nucleofection, uptake experiments using [^{3}H] E3S would be required. The uptake experiments require a much larger number of cells and several electroporations to be able to yield enough cells to

distinguish changes in CAR; therefore, further experiments using Nucleofection were not pursued.

6.3.3 Transfection of siRNA by Lipofectamine 2000

6.3.3.1 Caco-2 cells

The highest level of knockdown of GAPDH achieved in Caco-2 cells after 24h was with 2.5µl Lipofectamine 2000 and 40µl siRNA (76.3%). However, sustained knockdown of GAPDH in Caco-2 cells treated with Lipofectamine 2000 and siRNA was not achieved and conversely, many samples contained more GAPDH mRNA than untreated cells (Figure. 8a). SLCO1A2 knockdown at 24h was observed in a few of the treatment conditions (Lipofectamine 2000 + siRNA, % knockdown: 1.5µl + 5µl, 43.4%; 2µl + 5µl, 69.2%; 2µl + 40µl, 60.0%), with the highest level of knockdown achieved with 20µl siRNA and 1.5µl Lipofectamine 2000 (82.8%, Fig. 8b). However, of these samples, some had no detectable SLCO1A2 mRNA and others had no detectable knockdown at 48h. SLCO1B1 was not detected in cells only or treatment at any concentration of Lipofectamine 2000 and siRNA for any of the time points. SLCO1B3 mRNA was detected at all conditions at the 24h but not the 48h time point. Similar to GAPDH and SLCO1A2, SLCO3A1 had detectable knockdown at several treatment conditions (Lipofectamine 2000 + siRNA, 2.5µl + 5µl, 85.7%; 2µl + 10µl, 57.8%; 2.5µl + 10µl, 71.6%; 1.5µl + 20µl, 69.1%; 2µl + 20µl, 58.8%; and1.5µl + 40µl, 59.1%, Fig. 8c), but at 48h, mRNA levels in many samples were higher than cells alone and a few samples had no detectable mRNA.

a)

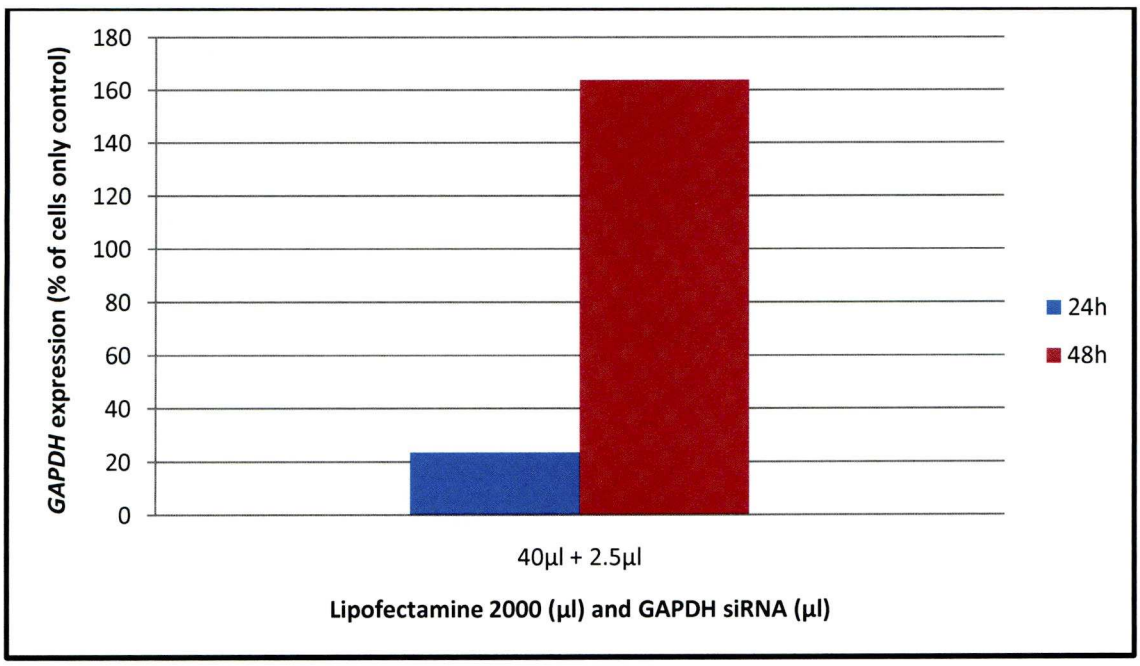
180
160
140
120
100
80
60
40
20
0
GAPDH expression (% of cells only control)
24h
48h
40µl + 2.5µl
Lipofectamine 2000 (µl) and GAPDH siRNA (µl)

b)

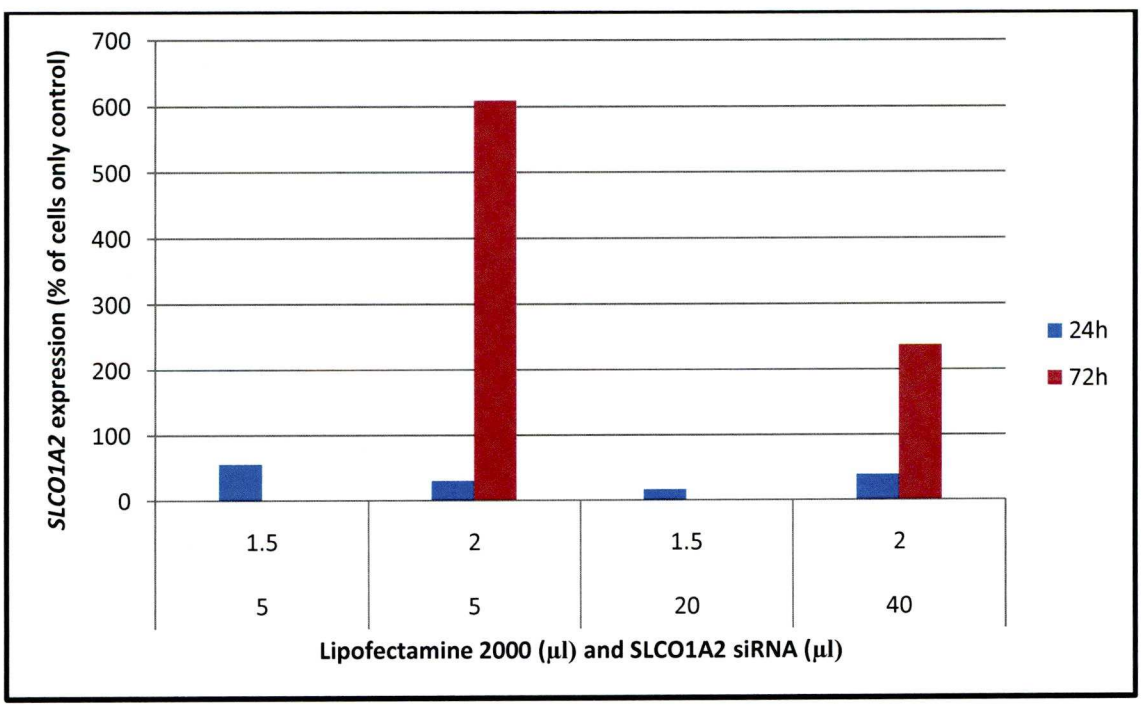
700
600
500
400
300
200
100
0
SLCO1A2 expression (% of cells only control)
24h
72h
1.5
5
2
5
1.5
20
2
40
Lipofectamine 2000 (µl) and SLCO1A2 siRNA (µl)

c)

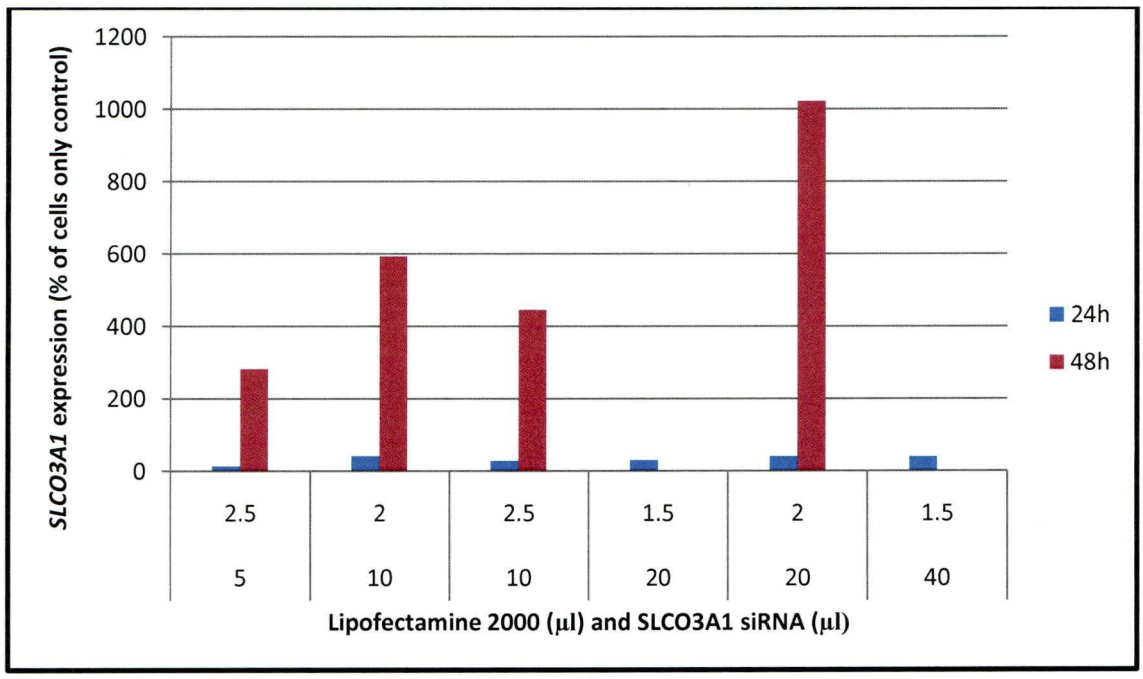

Fig. 8 Knockdown of a) GAPDH, b) SLCO1A2 and c) SLCO3A1 using lipofectamine 2000 (x-axis, top row) with siRNA (x-axis, bottom row) in Caco-2 cells (n=1).

6.3.3.2 HepG2 cells

GAPDH was knocked down in Lipofectamine and siRNA-treated HepG2 cells (1.5µl + 10µl, 52.1%; 0.5µl + 20µl, 41.6%; 1µl + 40µl, 50%) and in a few of these conditions, this knockdown was sustainable at 48h post transfection (1.5µl + 10µl, 45%; 0.5µl + 20µl, not detectable, 1µl + 40µl, 82.0%; Fig. 9a). SLCO1A2 mRNA was not detectable in untreated or any treated samples. SLCO1B1 was detected (1µl + 20µl, 6.4%, Fig. 9b) at 24h post-transfection and with the same Lipofectamine and siRNA concentrations, further knockdown was observed at 48h (99.4%). At 24h post-transfection, many SLCO1B3 samples contained more SLCO1B3 mRNA than cell-only controls, whilst

some had no detectable mRNA. However, knockdown at 24h post transfection was detected in one of the SLCO1B3 siRNA-treated samples (Lipofectamine 1.5µl + siRNA 20µl, 52.4%) and with the same condition, this knockdown was sustained at 48h (1.5µl + 20µl, 99.6%; Fig. 9c). Two conditions were identified to have knockdown of SLCO3A1 after 24h post transfection (0.5µl + 10µl, 15.3%; and 0.5µl + 20µl, 53.7%; Fig. 9d) and at 48h, no SLCO3A1 mRNA was detected.

a)

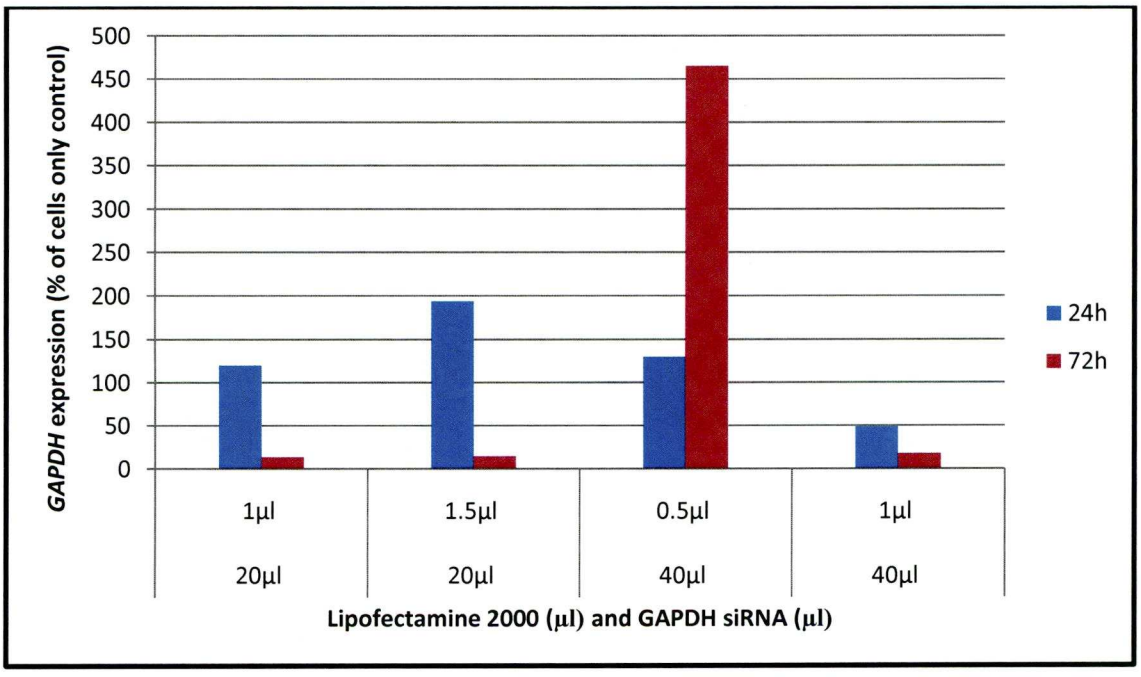

b)

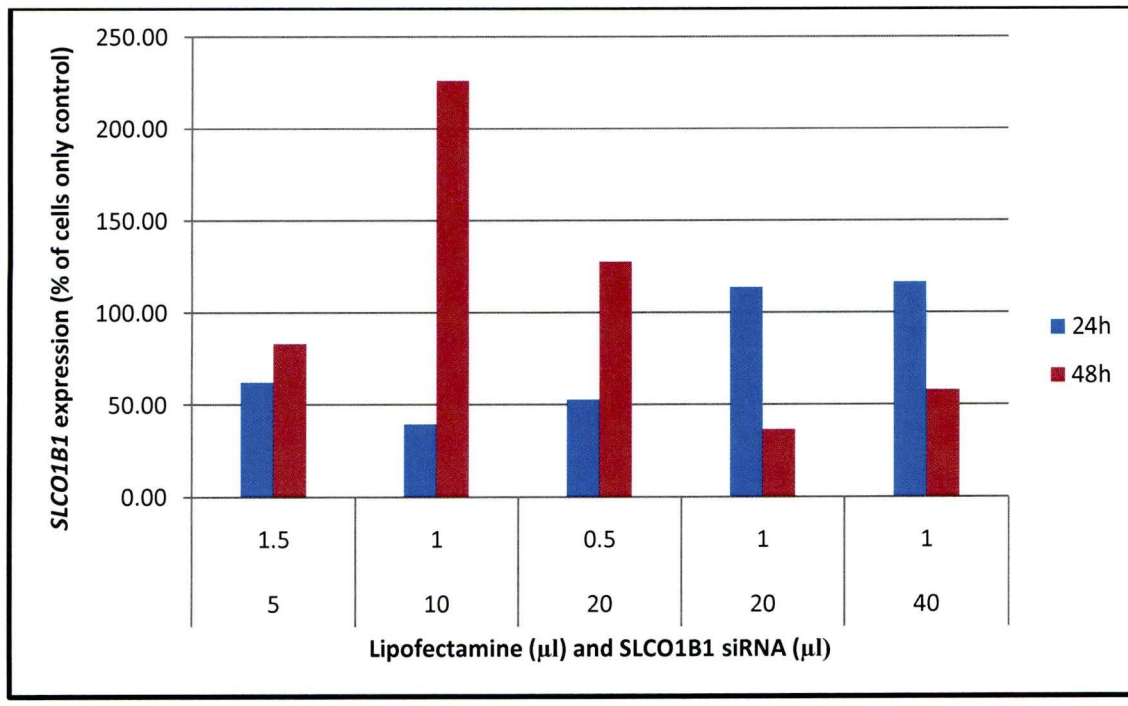
250.00
200.00
150.00
100.00
50.00
0.00
SLCO1B1 expression (% of cells only control)
24h
48h
1.5
5
1
10
0.5
20
1
20
1
40
Lipofectamine (µl) and SLCO1B1 siRNA (µl)

c)

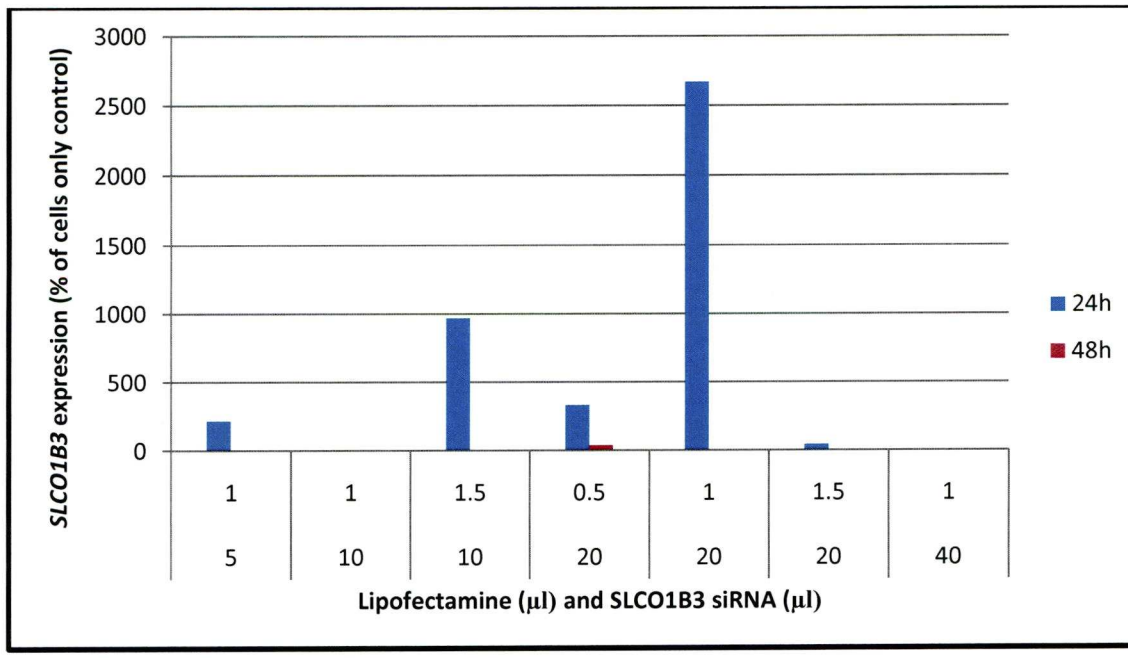
3000
2500
2000
1500
1000
500
0
SLCO1B3 expression (% of cells only control)
24h
48h
1
5
1
10
1.5
10
0.5
20
1
20
1.5
20
1
40
Lipofectamine (µl) and SLCO1B3 siRNA (µl)

d)

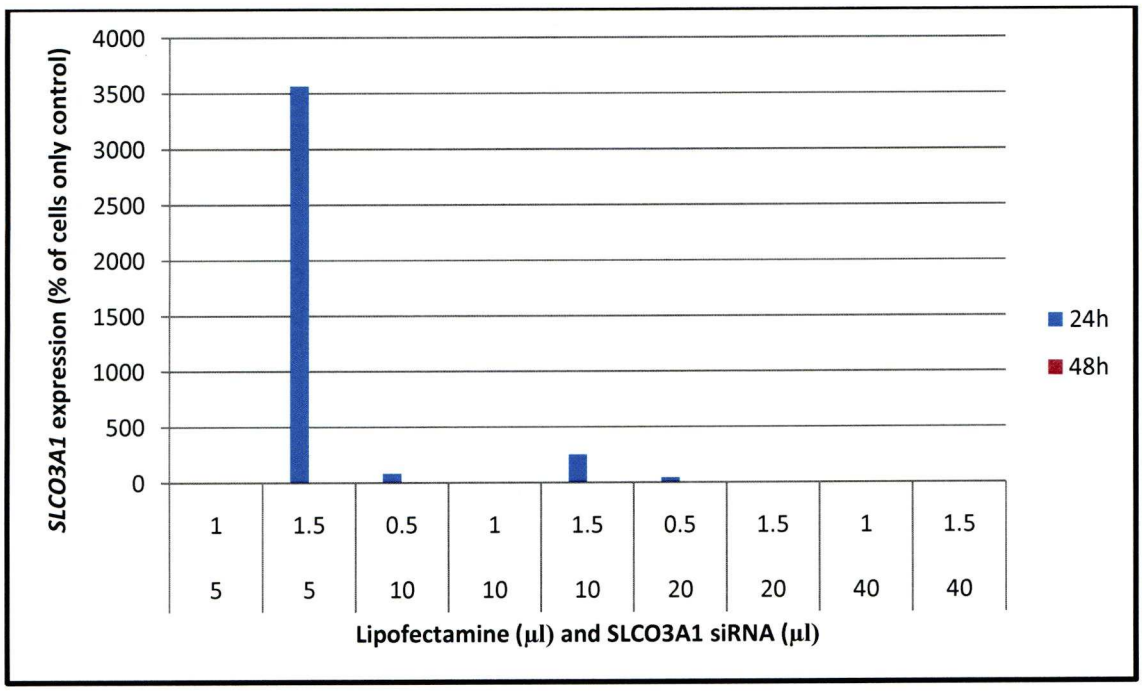

Fig. 9 Knockdown of a) GAPDH, b) SLCO1B1, c) SLCO1B3 and d) SLCO3A1 using Lipofectamine (x-axis, bottom row) with siRNA (x-axis, top row) in HepG2 cells (n=1).

The most reproducible results were with Lipofectamine 1.5µl + siRNA 20µl and hence this condition was used for analysis with [^{3}H] E3S.

6.3.4 Optimisation of HepG2 seeding for [^{3}H] E3S uptake

HepG2 cells had detectable [^{3}H] E3S in all seeding conditions with uptake increasing in a cell number dependent manner. Adequate detection was observed starting from 1.5×10^5 cells (Fig. 10). Optimisation of siRNA knockdown was based upon 2.5×10^5 and this cell density had adequate detection of [^{3}H] E3S.

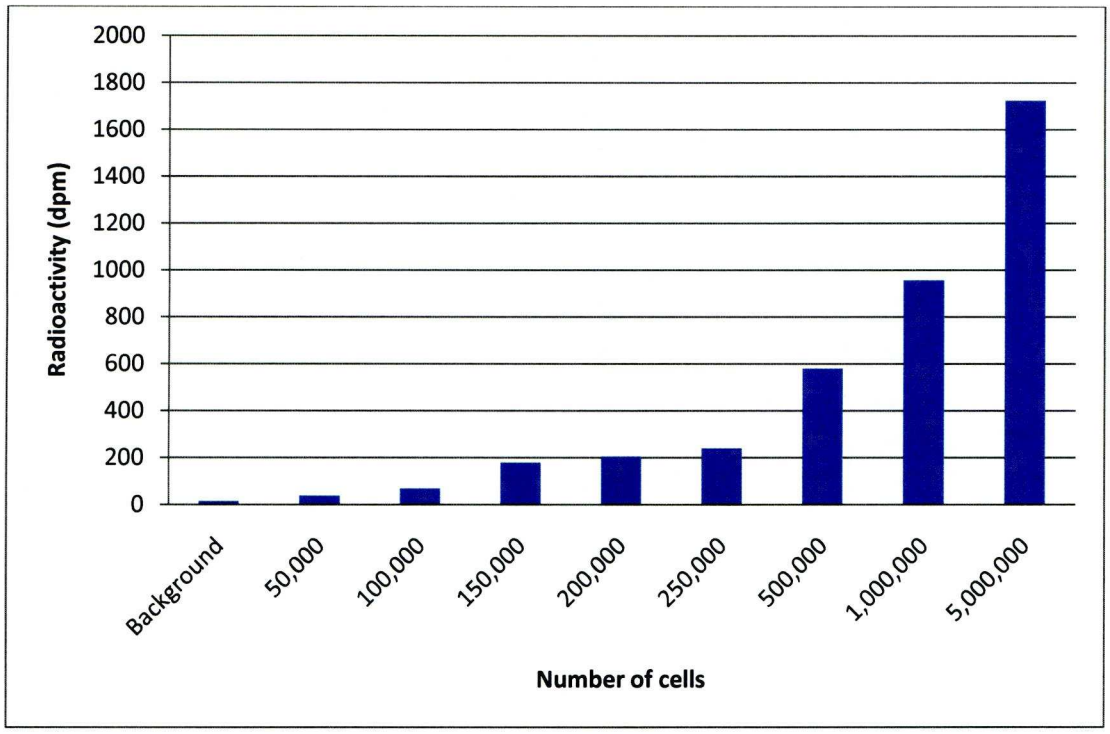

Fig. 10 Uptake of [^{3}H] E3S in varying seeding densities of HepG2 cells (n=1).

6.3.5 Uptake of [^{3}H]-E3S in SLCO1B3 knockdown HepG2 cells

At 48h post transfection, there was no difference in [^{3}H] E3S accumulation between HepG2 cells only or cells incubated with Lipofectamine 2000 (7.5µl). There was a trend towards an increase in radioactivity in cells incubated with Lipofectamine 2000 (7.5µl) and SLCO1B3 siRNA (100µl) compared to cells-only control, but this was not significant. At 72h post transfection, there was a trend towards a decrease in radioactivity in cells incubated with Lipofectamine 2000 only and in cells incubated with Lipofectamine 2000 with SLCO1B3 siRNA compared to cells-only control, but this was also not significant (Fig. 11a).

At the mRNA level, there were no observable differences between the three conditions at either 48h or 72h post transfection (Fig. 11b).

a)

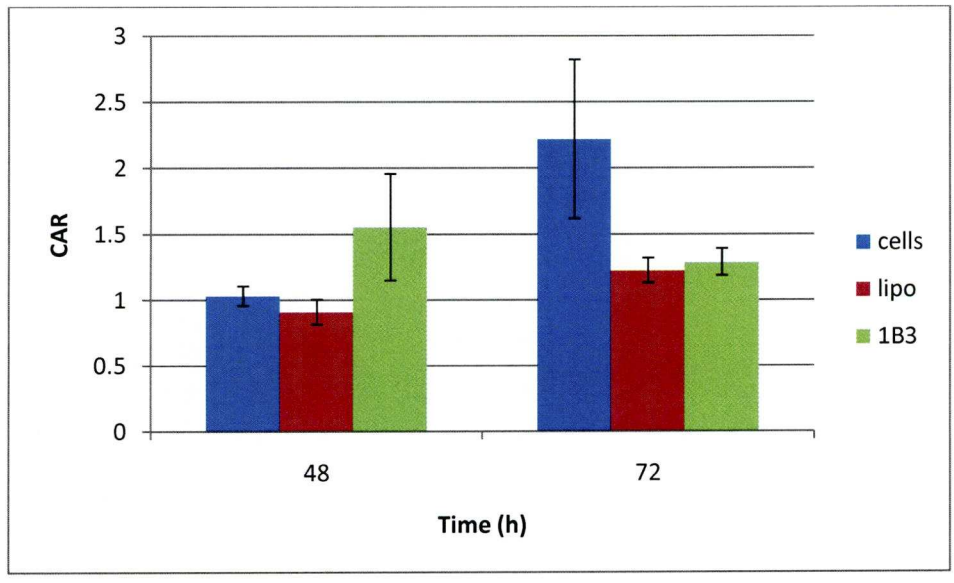

b)

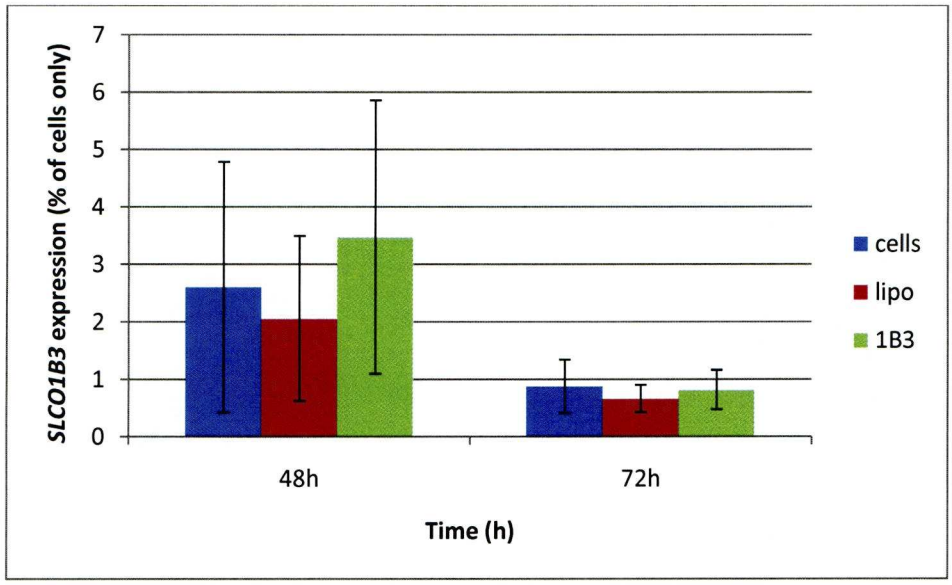

Fig. 11 a) Uptake of [^{3}H]-E3S in SLCO1B3 knockdown HepG2 cells at 48h and 72h post transfection and initially seeded at 2.5×10^5 cells (n=3) and b) mRNA levels of SLCO1B3 in HepG2 cells at 48h and 72h post transfection of siRNA and initially seeded at 2.5×10^5 cells (n=3).

6.4 Discussion

HepG2, Huh7, Caco-2 and 293T cells are commonly used cell lines as models for hepatic, intestinal and renal cells. RNAi is a widely used approach for knockdown of various genes including those involved in drug transport and metabolism (Yu 2007).

Consistent with the literature, SLCO1B1 and SLCO1B3 were not expressed in Caco-2 cells (Hilgendorf *et al.* 2007). SLCO1B1 and SLCO1B3 were also reported not to be detected in HepG2 (Cui *et al.* 2003), but expression of both transporters in HepG2 was detectable in this study, which was consistent with the findings by Hilgendorf *et al.* (2007). SLCO1B3 but not SLCO1B1 was detected in Huh7 cells. This differs from hepatocytes, which were found to contain high levels of SLCO1B1 and SLCO1B3 mRNA. Neither SLCO1B1 nor SLCO1B3 were detected; whereas, levels of SLCO1A2 and SLCO3A1 mRNA were detected in 293T cells, which was similar to their primary cell counterparts. SLCO1A2 and SLCO3A1 were inconsistently detected in Caco-2, HepG2 cells and Huh7 cells. This suggests that immortalized cell lines are, in general, not good representatives of their primary cell counterparts for influx transporters. However, cell lines are easier to culture and manipulate, and several studies have used these cell lines to observe influx transport by transfecting plasmids with the influx transporters of interest (Tamai *et al.* 2000; Jung *et al.* 2001; Vavricka *et al.* 2004).

Nucleofection (electroporation) and Lipofectamine (cationic lipid reagents) are common methods of nucleic acid delivery. Different cells have been reported to respond to the methods of delivery with different efficiencies (Gresch *et al.* 2004; Ghartey-Tagoe *et al.* 2006) and hence both methods have been tested. Lipofectamine allows easier scaling of

experiments, as the ratio of the reagents (Lipofectamine, siRNA and number of cells) determines the efficiency of transfection (Hawley-Nelson *et al.* 2008). However, several factors which determine the transfection efficiency of Lipofectamine, including the dilution ratio, seeding density and Lipofectamine/siRNA incubation time, have been described (Dalby *et al.* 2004). Amaxa has optimized nucleofection protocols for many commonly used cell lines and is easy to operate, but does not scale up for larger transfections and hence requires separate, smaller transfections. Interestingly, a study comparing the effects of lipid based reagents and electroporation showed upregulation of non-target genes by both methods, with relatively more non-target genes upregulated using lipid based reagents (Fedorov *et al.* 2005).

In the Nucleofection experiments, the GAPDH knockdown was observed in all of the cell lines; however, with the test conditions, only SLCO3A1 knockdown was observed in 293T cells. This may be due to the abundance of GAPDH in all the cell lines, whereas the SLCO transporters may be expressed in much lower levels, making knockdown difficult to detect. Up-scaling uptake experiments require a larger number of cells and would require several separate electroporations per sample; therefore, SLCO3A1 knockdown in 293T cells were not investigated further.

The Lipofectamine transfections in Caco-2 cells did not knockdown GAPDH, the endogenous control. This suggests that Caco-2 cells are difficult to transfect, which is consistent with a study by Cryan *et al.* (2003). In HepG2 cells, GAPDH and SLCO1B3 mRNA knockdown using Lipofectamine appeared to be consistent between the 24h and 48h post-transfection time points. E3S uptake in SLCO1B3 knockdown HepG2 cells (transfection condition, 2.5µl SLCO1B3 siRNA + 1.5µl Lipofectamine) was measured

to observe whether SLCO1B3 was knocked down. No significant difference was observed between SLCO1B3 siRNA with Lipofectamine-treated cells and Lipofectamine-treated cells only.

The inability to reproduce the knockdown in SLCO1B3 mRNA in the scaled up transfections for E3S uptake, along with the inconsistent detection of other SLCOs suggest that the SLCOs are not as abundant as GAPDH, increasing the difficulty in detecting knockdown of mRNA. This suggests that the SLCOs in general are not highly expressed in cell lines at basal level and supports observations by Hilgendorf *et al.* (2007) that cell lines do not truly reflect the levels of influx transporters compared to their primary cell counterparts. However, the report also showed levels of efflux transporters were a better representation of primary cell basal levels than influx transporters. Levels of protein were not measured as currently there are no reliable and commercially available antibodies for specific SLCO transporters.

Due to time constraints it was only possible to conduct optimisation experiments. Whilst the results obtained are preliminary, there were several conclusions that could be drawn. The detection of SLCO mRNA was inconsistent amongst Caco-2 and Huh7 cells. Transfections with Nucleofection would not have yielded enough cells for functional analysis and hence Lipofectamine 2000 was chosen for these experiments. The knockdown of SLCOs in cell lines using Lipofectamine 2000 was also inconsistent as the scaling-up of the Lipofectamine 2000 transfections did not reproduce the observed effects of mRNA knockdown in the preliminary experiments and had no observable effect on SLCO1B3 activity. RNAi is a useful technique to understand gene function and has been used to evaluate transporters, albeit efflux (Yu 2007). The use of

primary cells, which have higher levels of influx transporters despite being harder to transfect (Gresch *et al.* 2004; Tahvanainen *et al.* 2006), may be more appropriate for analyzing the role of influx transporters using RNAi.

Chapter 7
General Discussion

With continuing improvements to antiretroviral therapy, living with HIV has changed from being a life threatening disease to a chronic illness. However, due to the high mutation rate of HIV, viral resistance is a persistent problem and hence there is a continual need for new therapeutic compounds in existing and new drug classes. Recently licensed antiretrovirals such as raltegravir (Iwamoto *et al.* 2008) and darunavir (Rittweger and Arasteh 2007) have improved pharmacokinetic and toxicity profiles, but viral resistance has already been reported for these compounds (Cooper *et al.* 2008; Mitsuya *et al.* 2007). To limit the risks of viral resistance and to formulate effective regimens, the mechanisms which govern their virologic and immunologic response in addition to their pharmacokinetics need to be well characterised.

There are many factors which can impact on the efficacy and toxicity of antiretrovirals and other xenobiotics. These factors include drug-drug interactions within the antiretroviral regimen and/or concomitant drugs for other illnesses, age, weight, transport and metabolism. The interactions between these factors are outlined in Fig. 1. Research into each of the factors that contribute to the clinical outcome of antiretroviral therapy is progressing. The focus of this thesis was to examine the effect of drug transport on cellular accumulation and observe the impact of polymorphisms in SLCO transporters on lopinavir (LPV) pharmacokinetics.

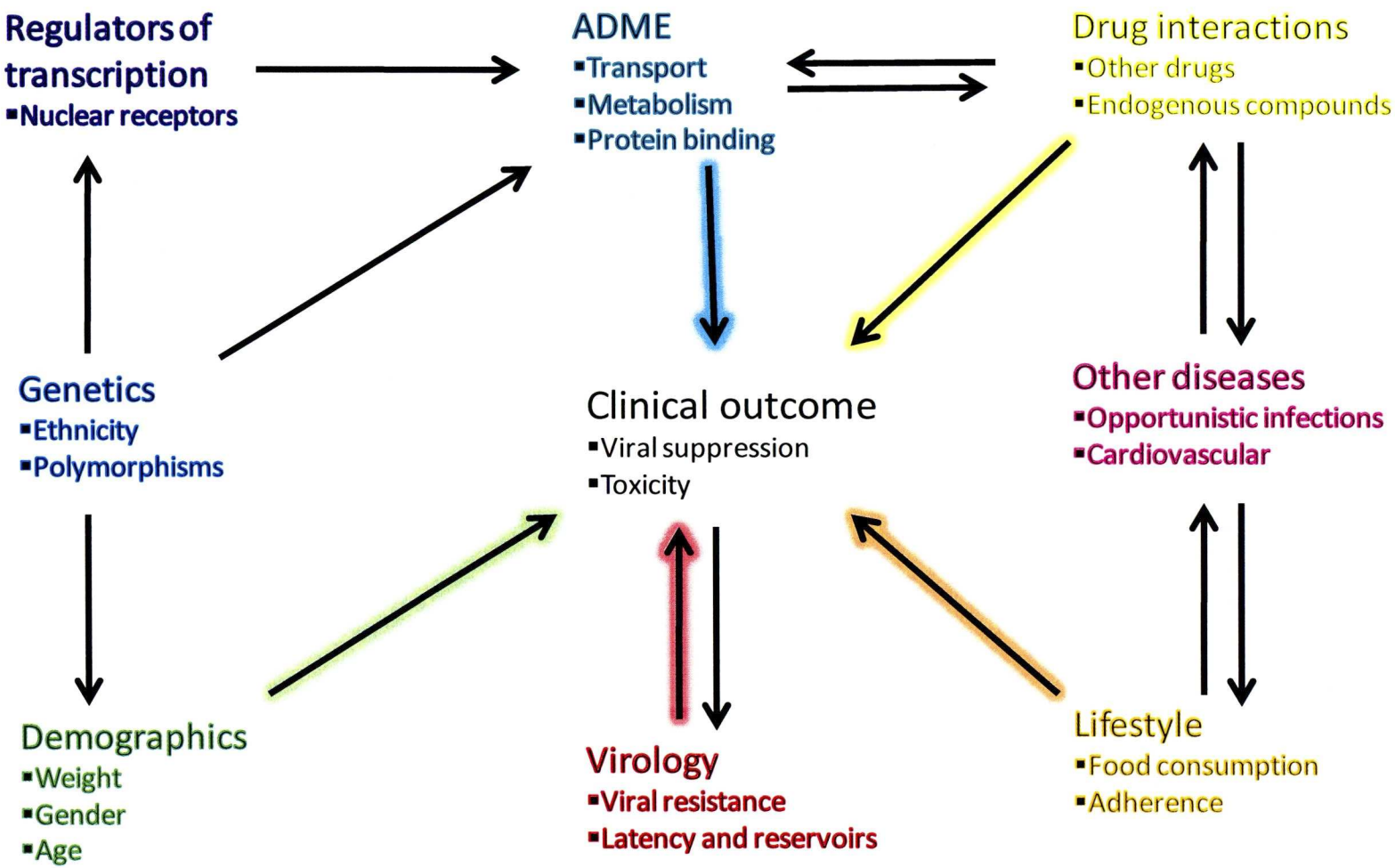

Fig.1 The interactions between factors which may contribute to the clinical outcome of antiretrovirals therapy.

Since the discovery and characterisation of ABCB1, the study of transporters and their influence on the pharmacokinetics of pharmacological compounds has been a major focus. In antiretroviral therapy, many protease inhibitors (PIs) are substrates of ABCB1 and some are also substrates for ABCC1 and ABCC2 (Huisman *et al.* 2002; Janneh *et al.* 2007). Darunavir (DRV), which is the most recently licensed PI, is also a substrate for ABCB1 (Chapter 2). There is increasing awareness that other transporters with different tissue distributions and substrate specificities are important determinants of variability in pharmacokinetics of endo- and xenobiotics.

The role of the SLCO transporters is currently being investigated, with various xenobiotics being characterised for substrate specificity (Hirano *et al.* 2004; Lee *et al.* 2005). The specificity for antiretrovirals was investigated in Chapter 4 and many PIs were demonstrated to be substrates of SLCO1A2, SLCO1B1 and SLCO1B3, which implicates these transporters in the distribution of PIs. SLCO1B1 and SLCO1B3 are hepatic influx transporters known to influence systemic exposure to many drugs. SLCO1A2 is expressed in the brain (Lee *et al.* 2005) and hence may have a role in transporting substrates across the blood-brain barrier, where latent viral reservoirs reside (Blankson 2006). There are other transporters in the SLCO subfamily and also within the general SLC family, with different expression, distribution and substrate specificities. Research into these transporters is sparse, although this is increasing, which will further our understanding of their roles for antiretrovirals and other xenobiotics.

The non-nucleoside reverse transcriptase inhibitors (NNRTIs) are not transported by ABCB1 (Dirson *et al.* 2006; Storch *et al.* 2007). Rilpivirine is an NNRTI in early development, which has been shown to have properties different to other NNRTIs. This

compound was shown not to be transported by ABCB1 (Chapter 2), but was demonstrated to be a substrate for SLCO1B1 and SLCO1B3 in the absence of human serum albumin (HSA), whereas neither efavirenz nor nevirapine were shown to be substrates for any of the SLCO transporters (Chapter 4). The lack of substrate specificity of SLCO1B1 and SLCO1B3 for rilpivirine in the presence of HSA may be due to the high affinity protein binding, thereby lowering the amount of available rilpivirine.

Many antiretrovirals have been characterised and exhibit high affinity for protein binding. PIs bind primarily to α_1-acid-glycoprotein and NNRTIs to HSA (Boffito *et al.* 2003). The concentration of human serum albumin (HSA), the most abundant serum protein, has an impact on the cellular concentration of efavirenz and rilpivirine in Chapter 2, with rilpivirine exhibiting a high affinity for protein binding. This suggests that HSA concentration may have a more important role in determining the pharmacokinetics of NNRTIs than cellular transport.

In this thesis, several *in vitro* models have been used to determine cellular transport. The CEM and MDCKII models are well established models for assessing ABCB1 and ABCC transporters (Davey *et al.* 1996; Bakos *et al.* 1998). They are relatively easy to manipulate and culture, but the limitations include unknown effects of other transporters within the model. For the CEM model, over-expression of ABCB1 in CEM_{VBL} cells was generated by drug selection so other tranporters in CEM cells may also be up- or down-regulated and for the MDCKII model, there is inherent expression of canine transporters. In this thesis, the X. *laevis* oocyte model was developed for analysis of influx transporters as they contain few endogenous transporters, but the model was relatively variable and labour intensive (Sigel 1990). Whilst these models may not be a true

representation of the *in vivo* environment, they serve as useful tools for observing the mechanisms which govern cellular accumulation and offer an insight into individual components of drug absorption and distribution. However, to understand the clinical importance of transporters, metabolising enzymes and their regulators, their effects must also be observed and characterised in the human population.

The study of pharmacogenomics is increasing, with several large studies investigating the effects of transport, metabolism and also regulators of transcription of genes on the pharmacokinetics of antiretrovirals. Several functional polymorphisms have been identified with varying strength of associations. Within the field of antiretrovirals, the *HLA-B*5701* SNP had the strongest association with hypersensitivity and has led to a change in clinical practice in the use of abacavir (Mallal *et al.* 2008). In Chapter 5, the *SLCO1B1 521 T>C* genotype was associated with altered lopinavir (LPV) plasma concentrations using the Liverpool TDM cohort, but other factors such as weight and co-administered PIs were also associated. Moreover, there are a large number of polymorphisms within each transporter, metabolism enzyme and the regulators of transcription and each polymorphism has a varying degree of effect on their respective genes; this increases the complexity of using genetic variation as a predictor of pharmacokinetics. Due to the number of possible genes which may have an effect on the pharmacokinetics of antiretrovirals (and other xenobiotics), the use of pharmacogenomics in a clinical setting requires multiloci genotyping and haplotype analyses to predict clinical outcome.

There are two general approaches for identifying candidate polymorphisms for pharmacogenomic analyses. The first is a whole genome approach, which requires

analysing genetic databases for polymorphisms and testing these polymophisms for associations with changes in pharmacokinetics of a given xenobiotic in a sample population. The second involves identifying a mechanism which affects cellular concentrations and validating these findings in a clinical scenario. The former method is subject to an increased risk of false positives. These risks may be minimised by using statistical corrections, but this may reduce the strength of the associations leading to a risk of false negative, and hence large sample populations are required.

The strongest pharmacogenomic studies are prospective studies, which need to be designed with clear strata and stringent sampling methods to identify associations. This requires recruitment and follow-up of volunteers specific to the study and prospective ethics committee approval. Whilst retrospective studies such as those that use TDM cohorts may contain missing data or inaccurate sampling strategies, they provide access to a large resource of readily available genomic material (in the form of plasma or whole blood) with matched pharmacokinetic and demographic data. Since samples are anonymised, retrospective ethics approval can also be sought for these studies and the advantage of using such cohorts is the time-effectiveness of obtaining samples as active recruitment of volunteers is not required.

The findings in this thesis have contributed to the understanding of pharmacogenetic variability of commonly used anti-retrovirals, firstly by identifying protease inhibitors as substrates for SLCOs in the oocyte expression system and secondly by observing an effect of *SLCO1B1 521 T>C* genotype on LPV plasma concentrations. Further studies to determine the effects of SLCO SNPs in a larger pharmacogenetic study in combination with novel transporter SNPs or with other mediators of antitretroviral pharmacokinetics

– such as metabolism enzymes – in human populations may lead to better understanding of the overall pharmacogenetics of antiretrovirals. In depth pharmacogenetic studies may lead to personalised medicine for HIV patients and improve the effectiveness of regimens and clinical outcome.

To conclude, HIV therapy has improved since the introduction of the first anti-HIV agent, zidovudine, with patients having treatment options, living longer and with reduced adverse reactions to treatment. With new drugs in new classes and potentially different modes of administration (e.g. rilpivirine given by intramuscular injection once a month, Woodfall, 2008, for HIV patients is encouraging. However, there are still many challenges facing the goal of personalised medicine as there are many factors which influence the efficacy of antiretrovirals. Research into analysing these factors (Fig. 1) independently and their effects in concert are progressing. This thesis has contributed to our understanding of pharmacokinetic variability and this in turn will ultimately translate to improvement in patient outcome.

References

Abbott, Pharmaceuticals. (2008). "Kaletra product insert."

Abe, T., M. Kakyo, et al. (1999). "Identification of a novel gene family encoding human liver-specific organic anion transporter LST-1." J Biol Chem **274**(24): 17159-63.

Abe, T., M. Unno, et al. (2001). "LST-2, a human liver-specific organic anion transporter, determines methotrexate sensitivity in gastrointestinal cancers." Gastroenterology **120**(7): 1689-99.

Adachi, H., T. Suzuki, et al. (2003). "Molecular characterization of human and rat organic anion transporter OATP-D." Am J Physiol Renal Physiol **285**(6): F1188-97.

Agarwal, S., D. Pal, et al. (2007). "Both P-gp and MRP2 mediate transport of Lopinavir, a protease inhibitor." Int J Pharm **339**(1-2): 139-47.

Almond, L. M., D. Edirisinghe, et al. (2005). "Intracellular and plasma pharmacokinetics of nevirapine in human immunodeficiency virus-infected individuals." Clin Pharmacol Ther **78**(2): 132-42.

Almond, L. M., P. G. Hoggard, et al. (2005). "Intracellular and plasma pharmacokinetics of efavirenz in HIV-infected individuals." J Antimicrob Chemother **56**(4): 738-44.

Anderson, C. M., V. Ganapathy, et al. (2008). "Human solute carrier SLC6A14 is the beta-alanine carrier." J Physiol **586**(Pt 17): 4061-7.

Applebaum, A. J., M. A. Richardson, et al. (2009). "Gender and Other Psychosocial Factors as Predictors of Adherence to Highly Active Antiretroviral Therapy (HAART) in Adults with Comorbid HIV/AIDS, Psychiatric and Substance-related Disorder." AIDS Behav **13**(1): 60-5.

Arasteh, K., N. Clumeck, et al. (2005). "TMC114/ritonavir substitution for protease inhibitor(s) in a non-suppressive antiretroviral regimen: a 14-day proof-of-principle trial." Aids **19**(9): 943-7.

Arendt, G., D. de Nocker, et al. (2007). "Neuropsychiatric side effects of efavirenz therapy." Expert Opin Drug Saf **6**(2): 147-54.

Autran, B., G. Carcelain, et al. (1997). "Positive effects of combined antiretroviral therapy on CD4+ T cell homeostasis and function in advanced HIV disease." Science **277**(5322): 112-6.

Bacheler, L., S. Jeffrey, et al. (2001). "Genotypic correlates of phenotypic resistance to efavirenz in virus isolates from patients failing nonnucleoside reverse transcriptase inhibitor therapy." J Virol **75**(11): 4999-5008.

Badagnani, I., R. A. Castro, et al. (2006). "Interaction of methotrexate with organic-anion transporting polypeptide 1A2 and its genetic variants." J Pharmacol Exp Ther **318**(2): 521-9.

Bakos, E., R. Evers, et al. (2000). "Interactions of the human multidrug resistance proteins MRP1 and MRP2 with organic anions." Mol Pharmacol **57**(4): 760-8.

Bakos, E., R. Evers, et al. (1998). "Functional multidrug resistance protein (MRP1) lacking the N-terminal transmembrane domain." J Biol Chem **273**(48): 32167-75.

Barre-Sinoussi, F., J. C. Chermann, et al. (1983). "Isolation of a T-lymphotropic retrovirus from a patient at risk for acquired immune deficiency syndrome (AIDS)." Science **220**(4599): 868-71.

Batt, A. M., J. Magdalou, et al. (1994). "Drug metabolizing enzymes related to laboratory medicine: cytochromes P-450 and UDP-glucuronosyltransferases." Clin Chim Acta **226**(2): 171-90.

Beck, E. J., M. Bowlby, et al. (2002). "Remodelling inactivation gating of Kv4 channels by KChIP1, a small-molecular-weight calcium-binding protein." J Physiol **538**(Pt 3): 691-706.

Beck, W. T., T. J. Mueller, et al. (1979). "Altered surface membrane glycoproteins in Vinca alkaloid-resistant human leukemic lymphoblasts." Cancer Res **39**(6 Pt 1): 2070-6.

Beers, P. (2006). Merck Manual of Diagnostic and Therapy.

Berger, E. A., P. M. Murphy, et al. (1999). "Chemokine receptors as HIV-1 coreceptors: roles in viral entry, tropism, and disease." Annu Rev Immunol **17**: 657-700.

Berry, N., K. Ariyoshi, et al. (1998). "Low peripheral blood viral HIV-2 RNA in individuals with high CD4 percentage differentiates HIV-2 from HIV-1 infection." J Hum Virol **1**(7): 457-68.

Bilello, J. A., P. A. Bilello, et al. (1996). "Human serum alpha 1 acid glycoprotein reduces uptake, intracellular concentration, and antiviral activity of A-80987, an inhibitor of the human immunodeficiency virus type 1 protease." Antimicrob Agents Chemother **40**(6): 1491-7.

Birmingham, A., E. M. Anderson, et al. (2006). "3' UTR seed matches, but not overall identity, are associated with RNAi off-targets." Nat Methods **3**(3): 199-204.

Blankson, J. N. (2006). "Viral reservoirs and HIV-specific immunity." Curr Opin HIV AIDS **1**(2): 147-51.

Bleasby, K., J. C. Castle, et al. (2006). "Expression profiles of 50 xenobiotic transporter genes in humans and pre-clinical species: a resource for investigations into drug disposition." Xenobiotica **36**(10-11): 963-88.

Boehringer-Ingelheim, I. (1999). "Viramune product insert."

Boffito, M., D. J. Back, et al. (2003). "Protein binding in antiretroviral therapies." AIDS Res Hum Retroviruses **19**(9): 825-35.

Boileau, A. J., R. Baur, et al. (2002). "The relative amount of cRNA coding for gamma2 subunits affects stimulation by benzodiazepines in GABA(A) receptors expressed in Xenopus oocytes." Neuropharmacology **43**(4): 695-700.

Bristol-Myers-Squibb. (2008). "Sustiva product insert."

Busti, A. J., A. M. Bain, et al. (2008). "Effects of atazanavir/ritonavir or fosamprenavir/ritonavir on the pharmacokinetics of rosuvastatin." J Cardiovasc Pharmacol **51**(6): 605-10.

Calmy, A., B. Hirschel, et al. (2007). "Clinical update: adverse effects of antiretroviral therapy." Lancet **370**(9581): 12-4.

Caron, M., C. Vigouroux, et al. (2009). "Antiretroviral-Related Adipocyte Dysfunction and Lipodystrophy in HIV-Infected Patients: Alteration of the PPARgamma-Dependent Pathways." PPAR Res **2009**: 507141.

Carr, A., K. Samaras, et al. (1998). "A syndrome of peripheral lipodystrophy, hyperlipidaemia and insulin resistance in patients receiving HIV protease inhibitors." Aids **12**(7): F51-8.

Cattori, V., B. Hagenbuch, et al. (2000). "Identification of organic anion transporting polypeptide 4 (Oatp4) as a major full-length isoform of the liver-specific transporter-1 (rlst-1) in rat liver." FEBS Lett **474**(2-3): 242-5.

Chakrabarti, R. and C. E. Schutt (2001). "The enhancement of PCR amplification by low molecular-weight sulfones." Gene **274**(1-2): 293-8.

Chandler, B., M. Detsika, et al. (2007). "Factors impacting the expression of membrane-bound proteins in lymphocytes from HIV-positive subjects." J Antimicrob Chemother **60**(3): 685-9.

Chandler, B., M. Detsika, et al. (2007). "Effect of transporter modulation on the emergence of nelfinavir resistance in vitro." Antivir Ther **12**(5): 831-4.

Chen, Z. S., E. Hopper-Borge, et al. (2003). "Characterization of the transport properties of human multidrug resistance protein 7 (MRP7, ABCC10)." Mol Pharmacol **63**(2): 351-8.

Chesney, M. A. (2000). "Factors affecting adherence to antiretroviral therapy." Clin Infect Dis **30 Suppl 2**: S171-6.

Chinn, L. W. and D. L. Kroetz (2007). "ABCB1 pharmacogenetics: progress, pitfalls, and promise." Clin Pharmacol Ther **81**(2): 265-9.

Choo, E. F., B. Leake, et al. (2000). "Pharmacological inhibition of P-glycoprotein transport enhances the distribution of HIV-1 protease inhibitors into brain and testes." Drug Metab Dispos **28**(6): 655-60.

Clavel, F., D. Guetard, et al. (1986). "Isolation of a new human retrovirus from West African patients with AIDS." Science **233**(4761): 343-6.

Coffin, J. M. (1995). "HIV population dynamics in vivo: implications for genetic variation, pathogenesis, and therapy." Science **267**(5197): 483-9.

Cooper, D. A., R. T. Steigbigel, et al. (2008). "Subgroup and resistance analyses of raltegravir for resistant HIV-1 infection." N Engl J Med **359**(4): 355-65.

Cordon-Cardo, C., J. P. O'Brien, et al. (1989). "Multidrug-resistance gene (P-glycoprotein) is expressed by endothelial cells at blood-brain barrier sites." Proc Natl Acad Sci U S A **86**(2): 695-8.

Crowe, S. M. and S. Sonza (2000). "HIV-1 can be recovered from a variety of cells including peripheral blood monocytes of patients receiving highly active antiretroviral therapy: a further obstacle to eradication." J Leukoc Biol **68**(3): 345-50.

Crum, N. F., R. H. Riffenburgh, et al. (2006). "Comparisons of causes of death and mortality rates among HIV-infected persons: analysis of the pre-, early, and late HAART (highly active antiretroviral therapy) eras." J Acquir Immune Defic Syndr **41**(2): 194-200.

Cryan, S. A. and C. M. O'Driscoll (2003). "Mechanistic studies on nonviral gene delivery to the intestine using in vitro differentiated cell culture models and an in vivo rat intestinal loop." Pharm Res **20**(4): 569-75.

Cui, Y., J. Konig, et al. (2003). "Detection of the human organic anion transporters SLC21A6 (OATP2) and SLC21A8 (OATP8) in liver and hepatocellular carcinoma." Lab Invest **83**(4): 527-38.

Curtin, N. J. and D. P. Turner (1999). "Dipyridamole-mediated reversal of multidrug resistance in MRP over-expressing human lung carcinoma cells in vitro." Eur J Cancer **35**(6): 1020-6.

Dalby, B., S. Cates, et al. (2004). "Advanced transfection with Lipofectamine 2000 reagent: primary neurons, siRNA, and high-throughput applications." Methods **33**(2): 95-103.

Danielson, P. B. (2002). "The cytochrome P450 superfamily: biochemistry, evolution and drug metabolism in humans." Curr Drug Metab **3**(6): 561-97.

Davey, M. W., R. M. Hargrave, et al. (1996). "Comparison of drug accumulation in P-glycoprotein-expressing and MRP-expressing human leukaemia cells." Leuk Res **20**(8): 657-64.

De Clercq, E. (2008). "Emerging antiviral drugs." Expert Opin Emerg Drugs **13**(3): 393-416.

De Meyer, S., H. Azijn, et al. (2005). "TMC114, a novel human immunodeficiency virus type 1 protease inhibitor active against protease inhibitor-resistant viruses, including a broad range of clinical isolates." Antimicrob Agents Chemother **49**(6): 2314-21.

Dirson, G., C. Fernandez, et al. (2006). "Efavirenz does not interact with the ABCB1 transporter at the blood-brain barrier." Pharm Res **23**(7): 1525-32.

Dorr, P., M. Westby, et al. (2005). "Maraviroc (UK-427,857), a potent, orally bioavailable, and selective small-molecule inhibitor of chemokine receptor CCR5 with broad-spectrum anti-human immunodeficiency virus type 1 activity." Antimicrob Agents Chemother **49**(11): 4721-32.

Duong, M., A. Golzi, et al. (2004). "Usefulness of therapeutic drug monitoring of antiretrovirals in routine clinical practice." HIV Clin Trials **5**(4): 216-23.

Elbashir, S. M., J. Harborth, et al. (2001). "Duplexes of 21-nucleotide RNAs mediate RNA interference in cultured mammalian cells." Nature **411**(6836): 494-8.

Eloranta, J. J., P. J. Meier, et al. (2005). "Coordinate transcriptional regulation of transport and metabolism." Methods Enzymol **400**: 511-30.

Erickson, D. A., G. Mather, et al. (1999). "Characterization of the in vitro biotransformation of the HIV-1 reverse transcriptase inhibitor nevirapine by human hepatic cytochromes P-450." Drug Metab Dispos **27**(12): 1488-95.

Este, J. A. and A. Telenti (2007). "HIV entry inhibitors." Lancet **370**(9581): 81-8.

Falcone, D. and D. W. Andrews (1991). "Both the 5' untranslated region and the sequences surrounding the start site contribute to efficient initiation of translation in vitro." Mol Cell Biol **11**(5): 2656-64.

Fedorov, Y., A. King, et al. (2005). "Different delivery methods-different expression profiles." Nat Methods **2**(4): 241.

Fellay, J., C. Marzolini, et al. (2002). "Response to antiretroviral treatment in HIV-1-infected individuals with allelic variants of the multidrug resistance transporter 1: a pharmacogenetics study." Lancet **359**(9300): 30-6.

Ferraro, T. N. and R. J. Buono (2005). "The relationship between the pharmacology of antiepileptic drugs and human gene variation: an overview." Epilepsy Behav **7**(1): 18-36.

Ford, J., E. R. Meaden, et al. (2003). "Effect of protease inhibitor-containing regimens on lymphocyte multidrug resistance transporter expression." J Antimicrob Chemother **52**(3): 354-8.

Francis, P., J. J. Chung, et al. (2000). "Functional impairment of lens aquaporin in two families with dominantly inherited cataracts." Hum Mol Genet **9**(15): 2329-34.

Freed, E. O. (2001). "HIV-1 replication." Somat Cell Mol Genet **26**(1-6): 13-33.

Fujino, H., T. Saito, et al. (2005). "Transporter-mediated influx and efflux mechanisms of pitavastatin, a new inhibitor of HMG-CoA reductase." J Pharm Pharmacol **57**(10): 1305-11.

Gallant, J. E. (2004). "Protease-inhibitor boosting in the treatment-experienced patient." AIDS Rev **6**(4): 226-33.

Gallay, P., T. Hope, et al. (1997). "HIV-1 infection of nondividing cells through the recognition of integrase by the importin/karyopherin pathway." Proc Natl Acad Sci U S A **94**(18): 9825-30.

Gazzard, B. G. (2008). "British HIV Association Guidelines for the treatment of HIV-1-infected adults with antiretroviral therapy 2008." HIV Med **9**(8): 563-608.

Geeraert, L., G. Kraus, et al. (2008). "Hide-and-seek: the challenge of viral persistence in HIV-1 infection." Annu Rev Med **59**: 487-501.

Gether, U., P. H. Andersen, et al. (2006). "Neurotransmitter transporters: molecular function of important drug targets." Trends Pharmacol Sci **27**(7): 375-83.

Geyer, J., T. Wilke, et al. (2006). "The solute carrier family SLC10: more than a family of bile acid transporters regarding function and phylogenetic relationships." Naunyn Schmiedebergs Arch Pharmacol **372**(6): 413-31.

Ghartey-Tagoe, E. B., B. A. Babbin, et al. (2006). "Plasmid DNA and siRNA transfection of intestinal epithelial monolayers by electroporation." Int J Pharm **315**(1-2): 122-33.

Gilead Sciences, (2009). "Coporate Overview." Retrieved 21/01/09, 2009, from http://www.gilead.com/corporate_overview.

Goebel, F., A. Yakovlev, et al. (2006). "Short-term antiviral activity of TMC278--a novel NNRTI--in treatment-naive HIV-1-infected subjects." Aids **20**(13): 1721-6.

Gresch, O., F. B. Engel, et al. (2004). "New non-viral method for gene transfer into primary cells." Methods **33**(2): 151-63.

Groschel, B., J. Cinatl, et al. (1997). "Viral and cellular factors for resistance against antiretroviral agents." Intervirology **40**(5-6): 400-7.

Grube, M., K. Kock, et al. (2006). "Organic anion transporting polypeptide 2B1 is a high-affinity transporter for atorvastatin and is expressed in the human heart." Clin Pharmacol Ther **80**(6): 607-20.

Guengerich, F. P., L. M. Distlerath, et al. (1986). "Human-liver cytochromes P-450 involved in polymorphisms of drug oxidation." Xenobiotica **16**(5): 367-78.

Haas, D. W., H. J. Ribaudo, et al. (2004). "Pharmacogenetics of efavirenz and central nervous system side effects: an Adult AIDS Clinical Trials Group study." Aids **18**(18): 2391-400.

Haas, D. W., L. M. Smeaton, et al. (2005). "Pharmacogenetics of long-term responses to antiretroviral regimens containing Efavirenz and/or Nelfinavir: an Adult Aids Clinical Trials Group Study." J Infect Dis **192**(11): 1931-42.

Hagenbuch, B. and C. Gui (2008). "Xenobiotic transporters of the human organic anion transporting polypeptides (OATP) family." Xenobiotica **38**(7-8): 778-801.

Hagenbuch, B., B. F. Scharschmidt, et al. (1996). "Effect of antisense oligonucleotides on the expression of hepatocellular bile acid and organic anion uptake systems in Xenopus laevis oocytes." Biochem J **316 (Pt 3)**: 901-4.

Hammer, S. M., J. J. Eron, Jr., et al. (2008). "Antiretroviral treatment of adult HIV infection: 2008 recommendations of the International AIDS Society-USA panel." JAMA **300**(5): 555-70.

Hammermann, R., C. Stichnote, et al. (2001). "Inhibition of nitric oxide synthase abrogates lipopolysaccharides-induced up-regulation of L-arginine uptake in rat alveolar macrophages." Br J Pharmacol **133**(3): 379-86.

Hawley-Nelson, P., V. Ciccarone, et al. (2008). "Transfection of cultured eukaryotic cells using cationic lipid reagents." Curr Protoc Mol Biol **Chapter 9**: Unit 9 4.

Hazen, R., R. Harvey, et al. (2007). "In vitro antiviral activity of the novel, tyrosyl-based human immunodeficiency virus (HIV) type 1 protease inhibitor brecanavir (GW640385) in combination with other antiretrovirals and against a panel of protease inhibitor-resistant HIV." Antimicrob Agents Chemother **51**(9): 3147-54.

Hearps, A. C. and D. A. Jans (2006). "HIV-1 integrase is capable of targeting DNA to the nucleus via an importin alpha/beta-dependent mechanism." Biochem J **398**(3): 475-84.

Hediger, M. A., M. F. Romero, et al. (2004). "The ABCs of solute carriers: physiological, pathological and therapeutic implications of human membrane transport proteinsIntroduction." Pflugers Arch **447**(5): 465-8.

Hilgendorf, C., G. Ahlin, et al. (2007). "Expression of thirty-six drug transporter genes in human intestine, liver, kidney, and organotypic cell lines." Drug Metab Dispos **35**(8): 1333-40.

Hirano, M., K. Maeda, et al. (2004). "Contribution of OATP2 (OATP1B1) and OATP8 (OATP1B3) to the hepatic uptake of pitavastatin in humans." J Pharmacol Exp Ther **311**(1): 139-46.

Hoetelmans, R. M. (1998). "Sanctuary sites in HIV-1 infection." Antivir Ther **3 Suppl 4**: 13-7.

Hoffmeyer, S., O. Burk, et al. (2000). "Functional polymorphisms of the human multidrug-resistance gene: multiple sequence variations and correlation of one allele with P-glycoprotein expression and activity in vivo." Proc Natl Acad Sci U S A **97**(7): 3473-8.

Hoggard, P. G. and A. Owen (2003). "The mechanisms that control intracellular penetration of the HIV protease inhibitors." J Antimicrob Chemother **51**(3): 493-6.

Horio, M., K. V. Chin, et al. (1989). "Transepithelial transport of drugs by the multidrug transporter in cultured Madin-Darby canine kidney cell epithelia." J Biol Chem **264**(25): 14880-4.

Hsiang, B., Y. Zhu, et al. (1999). "A novel human hepatic organic anion transporting polypeptide (OATP2). Identification of a liver-specific human organic anion transporting polypeptide and identification of rat and human hydroxymethylglutaryl-CoA reductase inhibitor transporters." J Biol Chem **274**(52): 37161-8.

Hube, F., P. Reverdiau, et al. (2005). "Improved PCR method for amplification of GC-rich DNA sequences." Mol Biotechnol **31**(1): 81-4.

Huber, R. D., B. Gao, et al. (2007). "Characterization of two splice variants of human organic anion transporting polypeptide 3A1 isolated from human brain." Am J Physiol Cell Physiol **292**(2): C795-806.

Huisman, M. T., J. W. Smit, et al. (2002). "Multidrug resistance protein 2 (MRP2) transports HIV protease inhibitors, and transport can be enhanced by other drugs." Aids **16**(17): 2295-301.

Invitrogen. (2004). "TA Cloning Kit Dual Promoter (pCRII)."

Ito, K., H. Suzuki, et al. (2005). "Apical/basolateral surface expression of drug transporters and its role in vectorial drug transport." Pharm Res **22**(10): 1559-77.

Iwamoto, M., L. A. Wenning, et al. (2008). "Safety, tolerability, and pharmacokinetics of raltegravir after single and multiple doses in healthy subjects." Clin Pharmacol Ther **83**(2): 293-9.

Jackson, A. L., S. R. Bartz, et al. (2003). "Expression profiling reveals off-target gene regulation by RNAi." Nat Biotechnol **21**(6): 635-7.

Jackson, A. L., J. Burchard, et al. (2006). "Position-specific chemical modification of siRNAs reduces "off-target" transcript silencing." Rna **12**(7): 1197-205.

Jaffe, H. W., D. J. Bregman, et al. (1983). "Acquired immune deficiency syndrome in the United States: the first 1,000 cases." J Infect Dis **148**(2): 339-45.

Janneh, O., R. C. Hartkoorn, et al. (2008). "Cultured CD4T cells and primary human lymphocytes express hOATPs: intracellular accumulation of saquinavir and lopinavir." Br J Pharmacol **155**(6): 875-83.

Janneh, O., E. Jones, et al. (2007). "Inhibition of P-glycoprotein and multidrug resistance-associated proteins modulates the intracellular concentration of lopinavir in cultured CD4 T cells and primary human lymphocytes." J Antimicrob Chemother **60**(5): 987-93.

Janneh, O., A. Owen, et al. (2005). "Modulation of the intracellular accumulation of saquinavir in peripheral blood mononuclear cells by inhibitors of MRP1, MRP2, P-gp and BCRP." Aids **19**(18): 2097-102.

Jones, K., P. G. Bray, et al. (2001). "P-Glycoprotein and transporter MRP1 reduce HIV protease inhibitor uptake in CD4 cells: potential for accelerated viral drug resistance?" Aids **15**(11): 1353-8.

Jones, K., P. G. Hoggard, et al. (2001). "Effect of alpha1-acid glycoprotein on the intracellular accumulation of the HIV protease inhibitors saquinavir, ritonavir and indinavir in vitro." Br J Clin Pharmacol **51**(1): 99-102.

Jones, K., P. G. Hoggard, et al. (2001). "Differences in the intracellular accumulation of HIV protease inhibitors in vitro and the effect of active transport." Aids **15**(6): 675-81.

Juliano, R. L. and V. Ling (1976). "A surface glycoprotein modulating drug permeability in Chinese hamster ovary cell mutants." Biochim Biophys Acta **455**(1): 152-62.

Jung, D., B. Hagenbuch, et al. (2001). "Characterization of the human OATP-C (SLC21A6) gene promoter and regulation of liver-specific OATP genes by hepatocyte nuclear factor 1 alpha." J Biol Chem **276**(40): 37206-14.

Kahle, K. T., K. J. Staley, et al. (2008). "Roles of the cation-chloride cotransporters in neurological disease." Nat Clin Pract Neurol **4**(9): 490-503.

Kakizaki, S., Y. Yamazaki, et al. (2008). "New insights on the xenobiotic-sensing nuclear receptors in liver diseases--CAR and PXR." Curr Drug Metab **9**(7): 614-21.

Kalkut, G. (2005). "Antiretroviral therapy: an update for the non-AIDS specialist." Curr Opin Oncol **17**(5): 479-84.

Kameyama, Y., K. Yamashita, et al. (2005). "Functional characterization of SLCO1B1 (OATP-C) variants, SLCO1B1*5, SLCO1B1*15 and SLCO1B1*15+C1007G, by using transient expression systems of HeLa and HEK293 cells." Pharmacogenet Genomics **15**(7): 513-22.

Kassahun, K., I. McIntosh, et al. (2007). "Metabolism and disposition in humans of raltegravir (MK-0518), an anti-AIDS drug targeting the human

immunodeficiency virus 1 integrase enzyme." Drug Metab Dispos **35**(9): 1657-63.

Kempf, D. J., K. C. Marsh, et al. (1997). "Pharmacokinetic enhancement of inhibitors of the human immunodeficiency virus protease by coadministration with ritonavir." Antimicrob Agents Chemother **41**(3): 654-60.

Kim, R. B., B. F. Leake, et al. (2001). "Identification of functionally variant MDR1 alleles among European Americans and African Americans." Clin Pharmacol Ther **70**(2): 189-99.

Kimchi-Sarfaty, C., J. M. Oh, et al. (2007). "A "silent" polymorphism in the MDR1 gene changes substrate specificity." Science **315**(5811): 525-8.

King, J. R. and E. P. Acosta (2006). "Tipranavir : A Novel Nonpeptidic Protease Inhibitor of HIV." Clin Pharmacokinet **45**(7): 665-82.

King, N. M., M. Prabu-Jeyabalan, et al. (2004). "Structural and thermodynamic basis for the binding of TMC114, a next-generation human immunodeficiency virus type 1 protease inhibitor." J Virol **78**(21): 12012-21.

Kiser, J. J., J. G. Gerber, et al. (2008). "Drug/Drug interaction between lopinavir/ritonavir and rosuvastatin in healthy volunteers." J Acquir Immune Defic Syndr **47**(5): 570-8.

Klokouzas, A., C. P. Wu, et al. (2003). "cGMP and glutathione-conjugate transport in human erythrocytes." Eur J Biochem **270**(18): 3696-708.

Kobayashi, K., Y. Yamanaka, et al. (2005). "Identification of HMG-CoA reductase inhibitors as activators for human, mouse and rat constitutive androstane receptor." Drug Metab Dispos **33**(7): 924-9.

Koepsell, H., K. Lips, et al. (2007). "Polyspecific organic cation transporters: structure, function, physiological roles, and biopharmaceutical implications." Pharm Res **24**(7): 1227-51.

Kolars, J. C., P. Schmiedlin-Ren, et al. (1992). "Identification of rifampin-inducible P450IIIA4 (CYP3A4) in human small bowel enterocytes." J Clin Invest **90**(5): 1871-8.

Komoroski, B., N. Vachharajani, et al. (2009). "Dapagliflozin, a Novel SGLT2 Inhibitor, Induces Dose-Dependent Glucosuria in Healthy Subjects." Clin Pharmacol Ther.

Konig, J., Y. Cui, et al. (2000). "Localization and genomic organization of a new hepatocellular organic anion transporting polypeptide." J Biol Chem **275**(30): 23161-8.

Konya, A., A. Andor, et al. (2006). "Inhibition of the MDR1 transporter by new phenothiazine derivatives." Biochem Biophys Res Commun **346**(1): 45-50.

Kopplow, K., K. Letschert, et al. (2005). "Human hepatobiliary transport of organic anions analyzed by quadruple-transfected cells." Mol Pharmacol **68**(4): 1031-8.

Kozak, M. (1987). "An analysis of 5'-noncoding sequences from 699 vertebrate messenger RNAs." Nucleic Acids Res **15**(20): 8125-48.

Kullak-Ublick, G. A., M. G. Ismair, et al. (2001). "Organic anion-transporting polypeptide B (OATP-B) and its functional comparison with three other OATPs of human liver." Gastroenterology **120**(2): 525-33.

Kwan, W., Hartkoorn, R., Salcedo-Sora, E., Bray, P., Khoo, S., Back, D., Owen, A (2008). Determining the substrate specificities of SLCO1A2 and SLCO1B1 for antiretroviral drugs. 9th International Workshop on Clinical Pharmacology of HIV Therapy, New Orleans, USA.

la Porte, C. J., Y. Li, et al. (2007). "The effect of ABCB1 polymorphism on the pharmacokinetics of saquinavir alone and in combination with ritonavir." Clin Pharmacol Ther **82**(4): 389-95.

Lau, Y. Y., Y. Huang, et al. (2007). "effect of OATP1B transporter inhibition on the pharmacokinetics of atorvastatin in healthy volunteers." Clin Pharmacol Ther **81**(2): 194-204.

Lee, L. M., J. M. Karon, et al. (2001). "Survival after AIDS diagnosis in adolescents and adults during the treatment era, United States, 1984-1997." Jama **285**(10): 1308-15.

Lee, T. H., L. Montalvo, et al. (2001). "Quantitation of genomic DNA in plasma and serum samples: higher concentrations of genomic DNA found in serum than in plasma." Transfusion **41**(2): 276-82.

Lee, W., H. Glaeser, et al. (2005). "Polymorphisms in human organic anion-transporting polypeptide 1A2 (OATP1A2): implications for altered drug disposition and central nervous system drug entry." J Biol Chem **280**(10): 9610-7.

Lefebvre, E. and C. A. Schiffer (2008). "Resilience to resistance of HIV-1 protease inhibitors: profile of darunavir." AIDS Rev **10**(3): 131-42.

Leier, I., J. Hummel-Eisenbeiss, et al. (2000). "ATP-dependent para-aminohippurate transport by apical multidrug resistance protein MRP2." Kidney Int **57**(4): 1636-42.

Leslie, E. M., R. G. Deeley, et al. (2001). "Toxicological relevance of the multidrug resistance protein 1, MRP1 (ABCC1) and related transporters." Toxicology **167**(1): 3-23.

Letschert, K., H. Faulstich, et al. (2006). "Molecular characterization and inhibition of amanitin uptake into human hepatocytes." Toxicol Sci **91**(1): 140-9.

Letschert, K., D. Keppler, et al. (2004). "Mutations in the SLCO1B3 gene affecting the substrate specificity of the hepatocellular uptake transporter OATP1B3 (OATP8)." Pharmacogenetics **14**(7): 441-52.

Lew, J. L., A. Zhao, et al. (2004). "The farnesoid X receptor controls gene expression in a ligand- and promoter-selective fashion." J Biol Chem **279**(10): 8856-61.

Liao, W. and G. Ning (2006). "Knockdown of apolipoprotein B, an atherogenic apolipoprotein, in HepG2 cells by lentivirus-mediated siRNA." Biochem Biophys Res Commun **344**(2): 478-83.

Lim, Y. P. and J. D. Huang (2008). "Interplay of pregnane X receptor with other nuclear receptors on gene regulation." Drug Metab Pharmacokinet **23**(1): 14-21.

Liu, S., H. Lu, et al. (2005). "Different from the HIV fusion inhibitor C34, the anti-HIV drug Fuzeon (T-20) inhibits HIV-1 entry by targeting multiple sites in gp41 and gp120." J Biol Chem **280**(12): 11259-73.

Lotsch, J., S. Harder, et al. (2007). "Association of saquinavir plasma concentrations with side effects but not with antiretroviral outcome in patients infected with protease inhibitor-susceptible human immunodeficiency virus type 1." Antimicrob Agents Chemother **51**(9): 3264-72.

Lucia, M. B., A. Savarino, et al. (2005). "Role of lymphocyte multidrug resistance protein 1 in HIV infection: expression, function, and consequences of inhibition." J Acquir Immune Defic Syndr **40**(3): 257-66.

Maeda, T., K. Takahashi, et al. (2007). "Identification of influx transporter for the quinolone antibacterial agent levofloxacin." Mol Pharm **4**(1): 85-94.

Mahagita, C., S. M. Grassl, et al. (2007). "Human organic anion transporter 1B1 and 1B3 function as bidirectional carriers and do not mediate GSH-bile acid cotransport." Am J Physiol Gastrointest Liver Physiol **293**(1): G271-8.

Mallal, S., D. Nolan, et al. (2002). "Association between presence of HLA-B*5701, HLA-DR7, and HLA-DQ3 and hypersensitivity to HIV-1 reverse-transcriptase inhibitor abacavir." Lancet **359**(9308): 727-32.

Mallal, S., E. Phillips, et al. (2008). "HLA-B*5701 screening for hypersensitivity to abacavir." N Engl J Med **358**(6): 568-79.

Markovich, D. (2008). "Expression cloning and radiotracer uptakes in Xenopus laevis oocytes." Nat Protoc **3**(12): 1975-80.

Martin, D. E., K. Salzwedel, et al. (2008). "Bevirimat: a novel maturation inhibitor for the treatment of HIV-1 infection." Antivir Chem Chemother **19**(3): 107-13.

Martin-Romero, C., J. Santos-Alvarez, et al. (2000). "Human leptin enhances activation and proliferation of human circulating T lymphocytes." Cell Immunol **199**(1): 15-24.

Maubon, N., M. Le Vee, et al. (2007). "Analysis of drug transporter expression in human intestinal Caco-2 cells by real-time PCR." Fundam Clin Pharmacol **21**(6): 659-63.

McCaffrey, A. P., L. Meuse, et al. (2002). "RNA interference in adult mice." Nature **418**(6893): 38-9.

McNaught AD, W. A. (1997). IUPAC. Compendium of Chemical Terminology. Oxford, Blackwell Scientific Publications.

Mehlotra, R. K., M. J. Bockarie, et al. (2007). "CYP2B6 983T>C polymorphism is prevalent in West Africa but absent in Papua New Guinea: implications for HIV/AIDS treatment." Br J Clin Pharmacol **64**(3): 391-5.

Merry, C., M. G. Barry, et al. (1997). "Saquinavir pharmacokinetics alone and in combination with ritonavir in HIV-infected patients." Aids **11**(4): F29-33.

Meyer zu Schwabedissen, H. E., R. G. Tirona, et al. (2008). "Interplay between the nuclear receptor pregnane X receptor and the uptake transporter organic anion transporter polypeptide 1A2 selectively enhances estrogen effects in breast cancer." Cancer Res **68**(22): 9338-47.

Michalski, C., Y. Cui, et al. (2002). "A naturally occurring mutation in the SLC21A6 gene causing impaired membrane localization of the hepatocyte uptake transporter." J Biol Chem **277**(45): 43058-63.

Mikkaichi, T., T. Suzuki, et al. (2004). "The organic anion transporter (OATP) family." Drug Metab Pharmacokinet **19**(3): 171-9.

Mistry, P., A. J. Stewart, et al. (2001). "In vitro and in vivo reversal of P-glycoprotein-mediated multidrug resistance by a novel potent modulator, XR9576." Cancer Res **61**(2): 749-58.

Mitsuya, Y., T. F. Liu, et al. (2007). "Prevalence of darunavir resistance-associated mutations: patterns of occurrence and association with past treatment." J Infect Dis **196**(8): 1177-9.

Mordant, C., B. Schmitt, et al. (2007). "Synthesis of novel diarylpyrimidine analogues of TMC278 and their antiviral activity against HIV-1 wild-type and mutant strains." Eur J Med Chem **42**(5): 567-79.

Moreno, S., B. Hernandez, et al. (2006). "Antiretroviral therapy in AIDS patients with tuberculosis." AIDS Rev **8**(3): 115-24.

Mosmann, T. (1983). "Rapid colorimetric assay for cellular growth and survival: application to proliferation and cytotoxicity assays." J Immunol Methods **65**(1-2): 55-63.

Moyle, G. J. and D. Back (2001). "Principles and practice of HIV-protease inhibitor pharmacoenhancement." HIV Med **2**(2): 105-13.

Mukwaya, G., T. MacGregor, et al. (2005). "Interaction of ritonavir-boosted tipranavir with loperamide does not result in loperamide-associated neurologic side effects in healthy volunteers." Antimicrob Agents Chemother **49**(12): 4903-10.

Nakakariya, M., T. Shimada, et al. (2008). "Identification and species similarity of OATP transporters responsible for hepatic uptake of beta-lactam antibiotics." Drug Metab Pharmacokinet **23**(5): 347-55.

Nascimbeni, M., C. Lamotte, et al. (1999). "Kinetics of antiviral activity and intracellular pharmacokinetics of human immunodeficiency virus type 1 protease inhibitors in tissue culture." Antimicrob Agents Chemother **43**(11): 2629-34.

Nielsen, M. H., F. S. Pedersen, et al. (2005). "Molecular strategies to inhibit HIV-1 replication." Retrovirology **2**: 10.

Niemi, M., M. K. Pasanen, et al. (2006). "SLCO1B1 polymorphism and sex affect the pharmacokinetics of pravastatin but not fluvastatin." Clin Pharmacol Ther **80**(4): 356-66.

Nigam, S. K., K. T. Bush, et al. (2007). "Drug and toxicant handling by the OAT organic anion transporters in the kidney and other tissues." Nat Clin Pract Nephrol **3**(8): 443-8.

Oki, T., Y. Usami, et al. (2004). "Pharmacokinetics of lopinavir after administration of Kaletra in healthy Japanese volunteers." Biol Pharm Bull **27**(2): 261-5.

Owen, A., B. Chandler, et al. (2004). "Functional correlation of P-glycoprotein expression and genotype with expression of the human immunodeficiency virus type 1 coreceptor CXCR4." J Virol **78**(21): 12022-9.

Pal, D. and A. K. Mitra (2006). "MDR- and CYP3A4-mediated drug-drug interactions." J Neuroimmune Pharmacol **1**(3): 323-39.

Pasanen, M. K., M. Neuvonen, et al. (2006). "SLCO1B1 polymorphism markedly affects the pharmacokinetics of simvastatin acid." Pharmacogenet Genomics **16**(12): 873-9.

Pascussi, J. M., S. Gerbal-Chaloin, et al. (2008). "The tangle of nuclear receptors that controls xenobiotic metabolism and transport: crosstalk and consequences." Annu Rev Pharmacol Toxicol **48**: 1-32.

Pereira, E., M. N. Borrel, et al. (1994). "Non-competitive inhibition of P-glycoprotein-associated efflux of THP-adriamycin by verapamil in living K562 leukemia cells." Biochim Biophys Acta **1225**(2): 209-16.

Philpott, S. M. (2003). "HIV-1 coreceptor usage, transmission, and disease progression." Curr HIV Res **1**(2): 217-27.

Poppe, S. M., D. E. Slade, et al. (1997). "Antiviral activity of the dihydropyrone PNU-140690, a new nonpeptidic human immunodeficiency virus protease inhibitor." Antimicrob Agents Chemother **41**(5): 1058-63.

Preall, J. B. and E. J. Sontheimer (2005). "RNAi: RISC gets loaded." Cell **123**(4): 543-5.

Preston, G. M., T. P. Carroll, et al. (1992). "Appearance of water channels in Xenopus oocytes expressing red cell CHIP28 protein." Science **256**(5055): 385-7.

Pulido, F., R. Delgado, et al. (2008). "Long-term (4 years) efficacy of lopinavir/ritonavir monotherapy for maintenance of HIV suppression." J Antimicrob Chemother **61**(6): 1359-61.

Qazi, N. A., J. F. Morlese, et al. (2002). "Lopinavir/ritonavir (ABT-378/r)." Expert Opin Pharmacother **3**(3): 315-27.

Ray, A. S., T. Cihlar, et al. (2006). Mechanism of Active Tubular Secretion of Tenofovir and Potential for a Renal Drug-Drug Interaction with HIV Protease Inhibitors. 7th International Workshop on Clinical Pharmacology of HIV Therapy. Lisbon, Portugal.

Ribera, E., C. Azuaje, et al. (2006). "Atazanavir and lopinavir/ritonavir: pharmacokinetics, safety and efficacy of a promising double-boosted protease inhibitor regimen." AIDS **20**(8): 1131-9.

Ribera, E. and A. Curran (2008). "Double-boosted protease inhibitor antiretroviral regimens: what role?" Drugs **68**(16): 2257-67.

Rittweger, M. and K. Arasteh (2007). "Clinical pharmacokinetics of darunavir." Clin Pharmacokinet **46**(9): 739-56.

Rivero, A., J. A. Mira, et al. (2007). "Liver toxicity induced by non-nucleoside reverse transcriptase inhibitors." J Antimicrob Chemother **59**(3): 342-6.

Riviere J. E., Papich M. G. (2009) Veterinary Pharmacology and Therapeutics

Roche, P. (2007). "Invirase product insert."

Sacchi, V. F., C. Perego, et al. (1995). "Functional characterization of leucine transport induced in Xenopus laevis oocytes injected with mRNA isolated from midguts of lepidopteran larvae (Philosamia cynthia)." J Exp Biol **198**(Pt 4): 961-6.

Saitoh, A., A. D. Hull, et al. (2005). "Myelomeningocele in an infant with intrauterine exposure to efavirenz." J Perinatol **25**(8): 555-6.

Sakaeda, T., T. Nakamura, et al. (2003). "Pharmacogenetics of MDR1 and its impact on the pharmacokinetics and pharmacodynamics of drugs." Pharmacogenomics **4**(4): 397-410.

Sala-Rabanal, M., D. D. Loo, et al. (2008). "Molecular mechanism of dipeptide and drug transport by the human renal H+/oligopeptide cotransporter hPEPT2." Am J Physiol Renal Physiol **294**(6): F1422-32.

Samson, M., F. Libert, et al. (1996). "Resistance to HIV-1 infection in caucasian individuals bearing mutant alleles of the CCR-5 chemokine receptor gene." Nature **382**(6593): 722-5.

Scacheri, P. C., O. Rozenblatt-Rosen, et al. (2004). "Short interfering RNAs can induce unexpected and divergent changes in the levels of untargeted proteins in mammalian cells." Proc Natl Acad Sci U S A **101**(7): 1892-7.

Schellens, J. H., M. M. Malingre, et al. (2000). "Modulation of oral bioavailability of anticancer drugs: from mouse to man." Eur J Pharm Sci **12**(2): 103-10.

Schneck, D. W., B. K. Birmingham, et al. (2004). "The effect of gemfibrozil on the pharmacokinetics of rosuvastatin." Clin Pharmacol Ther **75**(5): 455-63.

Seden, K., D. Back, et al. (2009). "Antiretroviral drug interactions: often unrecognized, frequently unavoidable, sometimes unmanageable" J Antimicrob. Chemother. **64**(1): 5-8

Seelamgari, A., A. Maddukuri, et al. (2004). "Role of viral regulatory and accessory proteins in HIV-1 replication." Front Biosci **9**: 2388-413.

Seminari, E., A. Castagna, et al. (2008). "Etravirine for the treatment of HIV infection." Expert Rev Anti Infect Ther **6**(4): 427-33.

Sharom, F. J. (2008). "ABC multidrug transporters: structure, function and role in chemoresistance." Pharmacogenomics **9**(1): 105-27.

Sheehy, A. M., N. C. Gaddis, et al. (2002). "Isolation of a human gene that inhibits HIV-1 infection and is suppressed by the viral Vif protein." Nature **418**(6898): 646-50.

Siccardi, M., A. D'Avolio, et al. (2008). "Association of a single-nucleotide polymorphism in the pregnane X receptor (PXR 63396C-->T) with reduced concentrations of unboosted atazanavir." Clin Infect Dis **47**(9): 1222-5.

Sigel, E. (1987). "Properties of single sodium channels translated by Xenopus oocytes after injection with messenger ribonucleic acid." J Physiol **386**: 73-90.

Sigel, E. (1990). "Use of Xenopus oocytes for the functional expression of plasma membrane proteins." J Membr Biol **117**(3): 201-21.

Sigel, E. (2001). Microinjection into Xenopus laevis oocytes, Wiley-Blackwell.

Siliciano, J. D., J. Kajdas, et al. (2003). "Long-term follow-up studies confirm the stability of the latent reservoir for HIV-1 in resting CD4+ T cells." Nat Med **9**(6): 727-8.

Skinner-Adams, T. S., J. S. McCarthy, et al. (2008). "HIV and malaria co-infection: interactions and consequences of chemotherapy." Trends Parasitol **24**(6): 264-71.

Smith, N. F., S. Marsh, et al. (2007). "Variants in the SLCO1B3 gene: interethnic distribution and association with paclitaxel pharmacokinetics." Clin Pharmacol Ther **81**(1): 76-82.

Sprecher, S., G. Soumenkoff, et al. (1986). "Vertical transmission of HIV in 15-week fetus." Lancet **2**(8501): 288-9.

Staszewski, S., C. Katlama, et al. (1998). "A dose-ranging study to evaluate the safety and efficacy of abacavir alone or in combination with zidovudine and lamivudine in antiretroviral treatment-naive subjects." Aids **12**(16): F197-202.

Stohr, W., D. Back, et al. (2008). "Factors influencing efavirenz and nevirapine plasma concentration: effect of ethnicity, weight and co-medication." Antivir Ther **13**(5): 675-85.

Storch, C. H., D. Theile, et al. (2007). "Comparison of the inhibitory activity of anti-HIV drugs on P-glycoprotein." Biochem Pharmacol **73**(10): 1573-81.

Störmer E., von Moltke L. L., et al. (2004). "Differential Modulation of P-Glycoprotein Expression and Activity by Non-Nucleoside HIV-1 Reverse Transcriptase Inhibitors in Cell Culture" Pharm Res. 19(7): 1038-1045

St-Pierre, M. V., B. Hagenbuch, et al. (2002). "Characterization of an organic anion-transporting polypeptide (OATP-B) in human placenta." J Clin Endocrinol Metab **87**(4): 1856-63.

Su, Y., X. Zhang, et al. (2004). "Human organic anion-transporting polypeptide OATP-A (SLC21A3) acts in concert with P-glycoprotein and multidrug resistance protein 2 in the vectorial transport of Saquinavir in Hep G2 cells." Mol Pharm **1**(1): 49-56.

Sugiura, T., Y. Kato, et al. (2006). "Role of SLC xenobiotic transporters and their regulatory mechanisms PDZ proteins in drug delivery and disposition." J Control Release **116**(2): 238-46.

Sulkowski, M. S., D. L. Thomas, et al. (2000). "Hepatotoxicity associated with antiretroviral therapy in adults infected with human immunodeficiency virus and the role of hepatitis C or B virus infection." Jama **283**(1): 74-80.

Summa, V., A. Petrocchi, et al. (2008). "Discovery of raltegravir, a potent, selective orally bioavailable HIV-integrase inhibitor for the treatment of HIV-AIDS infection." J Med Chem **51**(18): 5843-55.

Tahvanainen, J., M. Pykalainen, et al. (2006). "Enrichment of nucleofected primary human CD4+ T cells: a novel and efficient method for studying gene function

and role in human primary T helper cell differentiation." J Immunol Methods **310**(1-2): 30-9.

Tamai, I., J. Nezu, et al. (2000). "Molecular identification and characterization of novel members of the human organic anion transporter (OATP) family." Biochem Biophys Res Commun **273**(1): 251-60.

Teng, S. and M. Piquette-Miller (2008). "Regulation of transporters by nuclear hormone receptors: implications during inflammation." Mol Pharm **5**(1): 67-76.

Thiebaut, F., T. Tsuruo, et al. (1987). "Cellular localization of the multidrug-resistance gene product P-glycoprotein in normal human tissues." Proc Natl Acad Sci U S A **84**(21): 7735-8.

Thiry, L., S. Sprecher-Goldberger, et al. (1985). "Isolation of AIDS virus from cell-free breast milk of three healthy virus carriers." Lancet **2**(8460): 891-2.

Tibotec, P. (2006). "Prezista product insert."

Tirona, R. G., B. F. Leake, et al. (2001). "Polymorphisms in OATP-C: identification of multiple allelic variants associated with altered transport activity among European- and African-Americans." J Biol Chem **276**(38): 35669-75.

Tirona, R. G., B. F. Leake, et al. (2003). "Human organic anion transporting polypeptide-C (SLC21A6) is a major determinant of rifampin-mediated pregnane X receptor activation." J Pharmacol Exp Ther **304**(1): 223-8.

Tong, L., T. K. Phan, et al. (2007). "Effects of human immunodeficiency virus protease inhibitors on the intestinal absorption of tenofovir disoproxil fumarate in vitro." Antimicrob Agents Chemother **51**(10): 3498-504.

Toyoda, Y., Y. Hagiya, et al. (2008). "MRP class of human ATP binding cassette (ABC) transporters: historical background and new research directions." Xenobiotica **38**(7-8): 833-62.

Traunecker, H. C., M. C. Stevens, et al. (1999). "The acridonecarboxamide GF120918 potently reverses P-glycoprotein-mediated resistance in human sarcoma MES-Dx5 cells." Br J Cancer **81**(6): 942-51.

Tsujimoto, M., Y. Dan, et al. (2008). "Influence of SLCO1B3 gene polymorphism on the pharmacokinetics of digoxin in terminal renal failure." Drug Metab Pharmacokinet **23**(6): 406-11.

Turgut-Balik, D., V. C. Celik, et al. (2005). "Overcoming cloning problems by staining agarose gels with crystal violet instead of ethidium bromide in lactate dehydrogenase gene from Plasmodium vivax and Plasmodium falciparum." Acta Biol Hung **56**(3-4): 389-97.

Turner, D., J. M. Schapiro, et al. (2004). "The influence of protease inhibitor resistance profiles on selection of HIV therapy in treatment-naive patients." Antivir Ther **9**(3): 301-14.

Urquhart, B. L., R. G. Tirona, et al. (2007). "Nuclear receptors and the regulation of drug-metabolizing enzymes and drug transporters: implications for interindividual variability in response to drugs." J Clin Pharmacol **47**(5): 566-78.

Utoguchi, N., G. A. Chandorkar, et al. (2000). "Functional expression of P-glycoprotein in primary cultures of human cytotrophoblasts and BeWo cells." Reprod Toxicol **14**(3): 217-24.

Vavricka, S. R., D. Jung, et al. (2004). "The human organic anion transporting polypeptide 8 (SLCO1B3) gene is transcriptionally repressed by hepatocyte nuclear factor 3beta in hepatocellular carcinoma." J Hepatol **40**(2): 212-8.

Vavricka, S. R., J. Van Montfoort, et al. (2002). "Interactions of rifamycin SV and rifampicin with organic anion uptake systems of human liver." Hepatology **36**(1): 164-72.

Very, A. A., F. Gaymard, et al. (1995). "Expression of a cloned plant K+ channel in Xenopus oocytes: analysis of macroscopic currents." Plant J **7**(2): 321-32.

Virkki, L. V., C. Franke, et al. (2002). "Cloning and functional characterization of a novel aquaporin from Xenopus laevis oocytes." J Biol Chem **277**(43): 40610-6.

von Hentig, N. (2007). "Lopinavir/ritonavir: appraisal of its use in HIV therapy." Drugs Today (Barc) **43**(4): 221-47.

Wacher, V. J., C. Y. Wu, et al. (1995). "Overlapping substrate specificities and tissue distribution of cytochrome P450 3A and P-glycoprotein: implications for drug delivery and activity in cancer chemotherapy." Mol Carcinog **13**(3): 129-34.

Wain-Hobson, S. (1996). "HIV. One on one meets two." Nature **384**(6605): 117-8.

Wang, Y. M., W. B. Dyer, et al. (2000). "Molecular evidence for drug-induced compartmentalization of HIV-1 quasispecies in a patient with periodic changes to HAART." Aids **14**(15): 2265-72.

Ward, B. A., J. C. Gorski, et al. (2003). "The cytochrome P450 2B6 (CYP2B6) is the main catalyst of efavirenz primary and secondary metabolism: implication for HIV/AIDS therapy and utility of efavirenz as a substrate marker of CYP2B6 catalytic activity." J Pharmacol Exp Ther **306**(1): 287-300.

Wehner, F., P. Lawonn, et al. (2002). "Ionic mechanisms of regulatory volume increase (RVI) in the human hepatoma cell-line HepG2." Pflugers Arch **443**(5-6): 779-90.

Weiss, J., J. Rose, et al. (2007). "Modulation of human BCRP (ABCG2) activity by anti-HIV drugs." J Antimicrob Chemother **59**(2): 238-45.

Whitcomb, J. M., N. T. Parkin, et al. (2003). "Broad nucleoside reverse-transcriptase inhibitor cross-resistance in human immunodeficiency virus type 1 clinical isolates." J Infect Dis **188**(7): 992-1000.

WHO (2007). HIV/AIDS TREATMENT AND CARE Clinical protocols for the WHO European Region.

Wild, C. T., D. C. Shugars, et al. (1994). "Peptides corresponding to a predictive alpha-helical domain of human immunodeficiency virus type 1 gp41 are potent inhibitors of virus infection." Proc Natl Acad Sci U S A **91**(21): 9770-4.

Wilhelm, J. E., R. D. Vale, et al. (2000). "Coordinate control of translation and localization of Vg1 mRNA in Xenopus oocytes." Proc Natl Acad Sci U S A **97**(24): 13132-7.

Williams, G. C., A. Liu, et al. (2002). "Direct evidence that saquinavir is transported by multidrug resistance-associated protein (MRP1) and canalicular multispecific organic anion transporter (MRP2)." Antimicrob Agents Chemother **46**(11): 3456-62.

Winship, P. R. (1989). "An improved method for directly sequencing PCR amplified material using dimethyl sulphoxide." Nucleic Acids Res **17**(3): 1266.

Wong, K. H., K. C. Chan, et al. (2004). "Delayed progression to death and to AIDS in a Hong Kong cohort of patients with advanced HIV type 1 disease during the era of highly active antiretroviral therapy." Clin Infect Dis **39**(6): 853-60.

Woodfall, B. (2008). Drug discovery and investigational compounds in development at Tibotec, a division of Janssen Cilag. HIV Clin Trials.

Wright, S. H. (2005). "Role of organic cation transporters in the renal handling of therapeutic agents and xenobiotics." Toxicol Appl Pharmacol **204**(3): 309-19.

Wyen, C., H. Hendra, et al. (2008). "Impact of CYP2B6 983T>C polymorphism on non-nucleoside reverse transcriptase inhibitor plasma concentrations in HIV-infected patients." J Antimicrob Chemother **61**(4): 914-8.

Xia, C. Q., M. N. Milton, et al. (2007). "Evaluation of drug-transporter interactions using in vitro and in vivo models." Curr Drug Metab **8**(4): 341-63.

Yu, A. M. (2007). "Small interfering RNA in drug metabolism and transport." Curr Drug Metab **8**(7): 700-8.

Zhang, L., J. M. Strong et al (2006). "Scientific Perspectives on Drug Transporters and Their Role in Drug Interactions" Mol Pharm. **3**(1): 62-69

Zhang, X. Q., R. T. Schooley, et al. (1999). "The effect of increasing alpha1-acid glycoprotein concentration on the antiviral efficacy of human immunodeficiency virus protease inhibitors." J Infect Dis **180**(6): 1833-7.

Zhou, S., E. Chan, et al. (2005). "Drug bioactivation, covalent binding to target proteins and toxicity relevance." Drug Metab Rev **37**(1): 41-213.